The role of epithelial cells and fibroblasts in the pathogenesis of chronic rhinosinusitis.

Stephen Ball

Doctor of Philosophy

Institutes of Cellular Medicine and Health & Society

September 2016

Abstract

Background

Chronic rhinosinusitis without nasal polyps (CRSsNP) is a heterogeneous condition with common symptoms, clinical and radiological findings. CRSsNP is typified by inflammation of the sinonasal epithelium and development of fibrosis, yet its precise pathophysiology remains elusive. Recently stromal cells have been shown to act like immune effector cells in orchestrating chronic inflammation. Histological analysis of tissue biopsies from patients with CRSsNP demonstrates recruitment of circulating inflammatory cells, though the precise role of structural cells such as epithelial and fibroblast cells in CRSsNP remains to be discovered.

Aims

1. (a) Recruit phenotyped cohorts of control & CRSsNP participants.

(b) Characterise recruited CRSsNP participants' tissue samples and isolated epithelial & fibroblast cells.

2. Assay the sinonasal environment to determine any association between, infection, inflammation and remodelling.

3. Identify clusters of genes differentially expressed in CRSsNP & control participants.

Methods

Cohorts of healthy control and CRSsNP participants were recruited. Matched tissue biopsy, epithelial and fibroblast cells were harvested together with clinical, radiological, microbiological and mucosal swab data. Tissue and cellular samples were characterised to confirm their identity and disease status. The sinonasal environment was characterised from mucosal swabs and analysed for a range of 40 human disease biomarkers. Transcriptome analysis was performed using microarrays and RNA sequencing with downstream bioinformatics investigation of the data.

Results

47 age and sex matched CRSsNP and control participants were recruited, differing significantly in symptom and radiological scores. Histological analysis of tissue biopsy specimens was consistent with CRSsNP and control samples. Matched epithelial and fibroblast cells were generated. Assay of the sinonasal microenvironment identified 13 discriminant mediators separating CRSsNP samples from controls using a novel, non-invasive technique. Transcriptomics identified 239 differentially expressed genes in CRSsNP tissue biopsy samples. Cellular samples differed significantly from their matched tissue biopsies.

Conclusions

This thesis characterises a cohort of tightly defined CRSsNP patients and healthy controls to investigate the potential role of epithelial and fibroblast cells in CRSsNP. Transcriptomics has demonstrated clusters of genes upregulated in CRSsNP, however changes were not consistent in matched cellular samples questioning the validity of cellular models in CRSsNP. Additionally, a straightforward, non-invasive measure of the CRSsNP cytokine profile has been demonstrated. The mediators identified in these assays could potentially be developed as biomarkers of sinonasal inflammation as an adjunct in patient management.

Acknowledgements

I would firstly like to acknowledge the kind help and assistance of the patient participants involved in this thesis – it certainly would not have been possible without their contribution. Next I'd like to thank my supervisors, Professors Janet Wilson, Derek Mann and Andrew Fisher - and all my colleagues for their tuition and guidance throughout my fellowship. The Wellcome Trust must also be acknowledged for providing me the opportunity with this clinical research training fellowship funding. However, most of all I'd like to thank my wife Sarah and my children Emily and Matthew for supporting me throughout and making me smile!

Contents

List of figures

List of tables

List of abbreviations

ATCC - American type culture collection

bFGF - basic fibroblast growth factor

BAFF - B cell activating-factor

BEGM - basal epithelial growth medium

BLyS - B lymphocyte stimulator

CD - cluster of differentiation

CLR - C-type lectin receptors

CRS – chronic rhinosinusitis

CRSsNP - chronic rhinosinusitis without nasal polyps

CRSwNP - chronic rhinosinusitis with nasal polyps

CSE - cigarette smoke extract

CT – computerised tomogram

DAMPs - damage associated molecular patterns

DMEM - Dulbecco's modified Eagle's medium

dsRNA – double stranded ribonucleic acid

ECACC - European collection of cell cultures

EDTA – ethylene diamine tetra acetic acid

ELISA - enzyme-linked immunosorbent assay

EMEM - Eagle's minimum essential medium

EPOS – European position paper on rhinosinusitis and nasal polyps

FCS - foetal calf serum

FESS - functional endoscopic sinus surgery

GAPDH - Glyceraldehyde 3-phosphate dehydrogenase

GCP-2 - granulocyte chemotactic protein-2

GRO-a - growth related oncogene

ICAM - intercellular adhesion molecules

IFN-γ - interferon gamma

IL – interleukin

JNK - c-Jun N-terminal kinases

LPS - Lipopolysaccharide

MCP-4 - monocyte chemotactic protein-4

M-CSF - macrophage colony-stimulating factor

MIP - macrophage inflammatory protein

NFE2L3 - nuclear factor erythroid-derived 2-like 3

NOD - nucleotide-binding oligomerization domain

PAMPs - pathogen associated molecular patterns

PDGF - platelet-derived growth factor

PI3K -phosphatidylinositide 3-kinase

PlGF -Placental growth factor

Poly I:C - polyinosinic-polycytidylic acid

PNECs - primary nasal epithelial cells

PNFs – primary nasal fibroblasts

PRRs - pathogen recognition receptors

RAGE - receptor for advanced glycation end-products

RANKL - receptor activator of nuclear factor κB ligand

RANTES -regulated on activation normal T cell expressed and secreted

RLRs - RIG-I-like receptors

RT-PCR - reverse transcription polymerase chain reaction

SAA - serum amyloid A

sFlt-1- soluble Fms-like tyrosine kinase 1

TARC - thymus and activation-regulated chemokine

TGF-β - transforming growth factor β

Th – T helper cell

TLR - Toll-like receptor

TNF-α - tissue necrosis factor α

VCAM-1 - vascular cell adhesion molecule 1

VEGF - vascular endothelial growth factor

1 Background

1.1 Anatomy of the paranasal sinuses

The paranasal sinuses consist of three paired and one unpaired air filled spaces within the bones of the skull, namely the maxillary, frontal, ethmoid and sphenoid sinuses (Figure 1). All four sinuses are located around the nasal cavity into which they drain. The sinuses are lined by pseudostratified ciliated epithelium with goblet cells, which produce mucus along with the sub-epithelial mucus glands to keep the sinuses clear (Figure 2). The paranasal sinuses collectively humidify and warm inspired air on its passage to the lungs, increase the resonance of speech, reduce the weight of the skull and serve as protective crumple zones in facial and head trauma (Dalgorf and Harvey, 2013). Human paranasal sinuses develop from the viscerocranium, the origins of the maxillary sinus are seen after the 10th week of embryonic life and the sinuses continue to develop into adolescence.

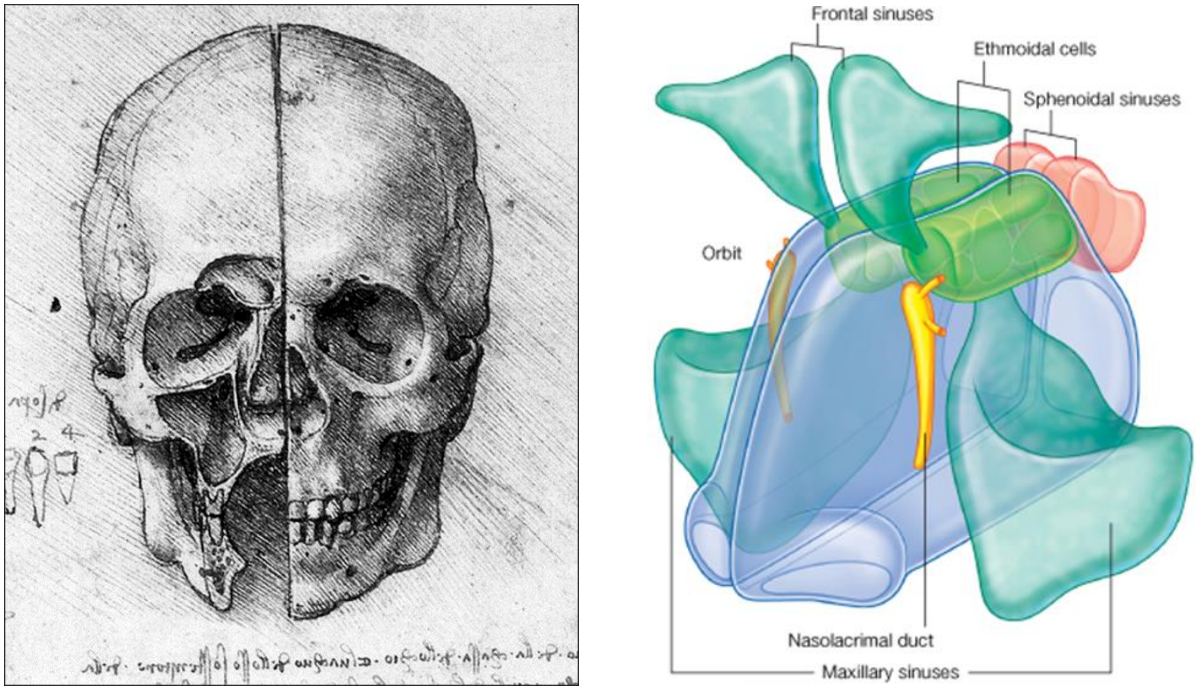

(a) (b)

Figure 1. Anatomy of the paranasal sinuses. (a) Leonardo da Vinci's depiction of a skull. The right side of the skull has been sectioned to demonstrate the frontal and maxillary sinuses. The close proximity of the sinuses, orbit and dentition is shown as infections of these anatomical areas had significant morbidity and mortality in the pre-antibiotic era. Image taken from (Mavrodi and Paraskevas, 2013). (b) Schematic illustration of the paranasal sinuses. Image adapted from (Drake, 2014).

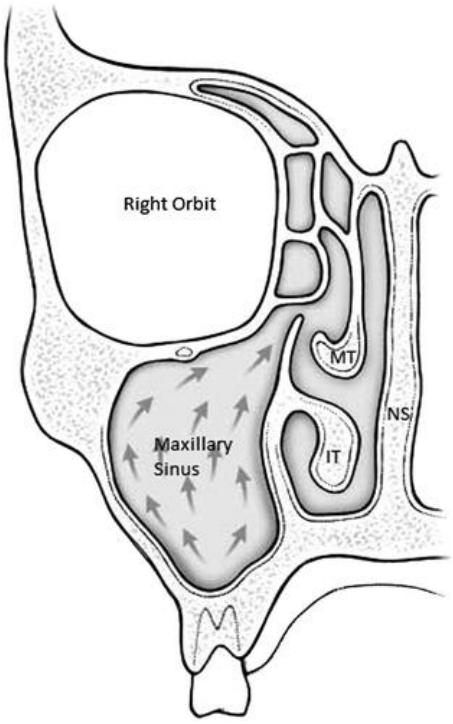

Figure 2. Mucociliary clearance of the paranasal sinuses. Here the mucociliary pathway for the maxillary sinus is shown from its most inferior dependent part along the walls of the sinus to the nasal cavity via its ostium. IT = inferior turbinate, MT = middle turbinate, NS = nasal septum. Image taken from (Suh and Kennedy, 2011)

1.2 Rhinosinusitis

Rhinosinusitis refers to inflammation of the nose and paranasal sinuses resulting in the production of symptoms. Rhinosinusitis is a more appropriate term than sinusitis as inflammation of the nose and paranasal sinuses coexist and are concurrent in most individuals (Fokkens et al., 2012). Infection typically spreads from the nasal cavities to the sinuses and in the rare cases where infection may originate in the sinus, it will spread retrogradely into the nose.

Rhinosinusitis is temporarily categorised into acute rhinosinusitis, with symptoms lasting less than four weeks and chronic rhinosinusitis with symptoms in excess of 12 weeks. The overwhelming majority of rhinosinusitis episodes worldwide are short-lived acute viral infections, however the chronic form causes significant patient morbidity and as a result consumes vast amount of health resources (section 1.3.1.).

Acute rhinosinusitis typically is caused by respiratory viruses such as *Rhinovirus, Influenza A* and *B, Respiratory Syncytial Virus, Parainfluenza, Adenovirus* and *Human metapneumovirus*.

An acute episode of viral rhinosinusitis usually has maximal symptoms after a few days and is resolved within a week. Acute bacterial rhinosinusitis is much less common and typically follows a viral rhinosinusitis, with an initial reduction in symptoms and a second more severe peak of symptoms - referred to as a 'double sickening' with associated fever, mucopurulent secretions and raised serum inflammatory markers (Figure 3).

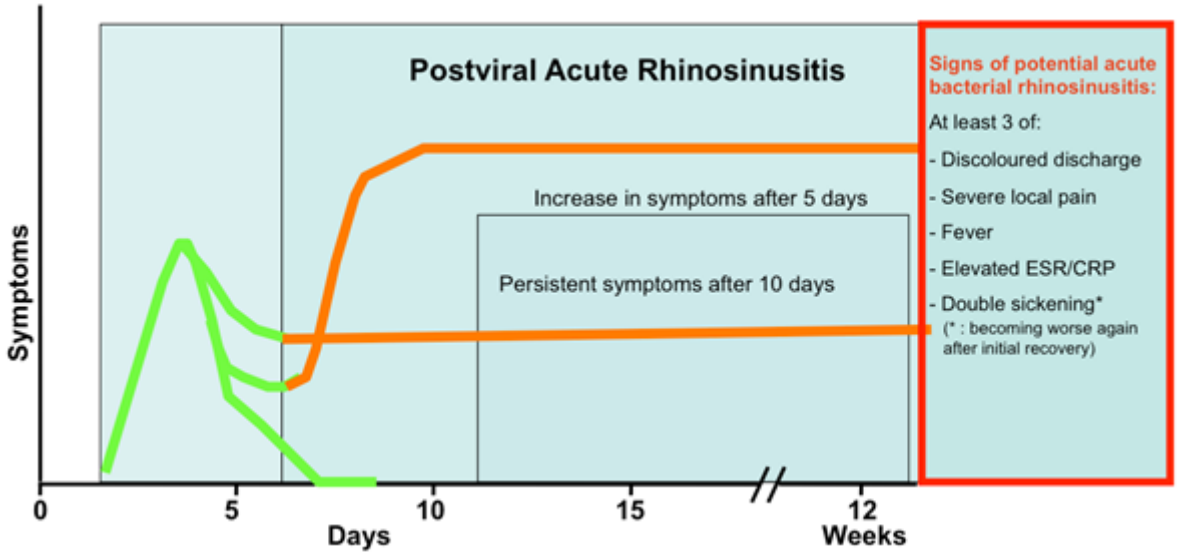

Figure 3. Acute viral versus bacterial rhinosinusitis. A second peak in symptoms or 'double sickening' together with mucopurulent nasal secretions, fever and raised serum inflammatory markers is typical of an acute bacterial rhinosinusitis. Image adapted from (Fokkens et al., 2012).

1.3 Chronic rhinosinusitis

The clinical and research definition of chronic rhinosinusitis (CRS) is an inflammation of the nose and paranasal sinuses that is present for more than 12 weeks (Fokkens et al., 2012). Chronic rhinosinusitis is not regarded simply as a prolonged episode of acute rhinosinusitis although its pathophysiology remains elusive. However, it is currently best described as a dysfunctional host-environment interaction occurring in the nose and paranasal sinuses. CRS is presently phenotyped into chronic rhinosinusitis without nasal polyps (CRSsNP) and chronic rhinosinusitis with nasal polyps (CRSwNP). Historically, CRSsNP was thought to be a result of a severe or incompletely treated acute rhinosinusitis and CRSwNP due to severe atopy, though these hypotheses have now been superseded by advances in our understanding of CRS pathophysiology (section 1.3.6).

1.3.1 Epidemiology

The nose is the first point of contact between environmental microbes, pollutants, allergens and the respiratory system, and it is therefore not surprising that rhinosinusitis is so common. Epidemiological data indicate that the prevalence of CRS in the general population is approximately 12% (Meltzer et al., 2004, Hastan et al., 2011) and greater than chronic back pain or diabetes (DiabetesUK, 2015) with annual healthcare costs in excess of $22 billion in the United States (Smith et al., 2015). In 2014 the direct healthcare costs in the US were estimated to be between $6.9 and $9.9 billion, having risen from $5.8 billion in the late 1990's (Ray et al., 1999), with indirect costs of $13 billion. The high cost of treatment reflects the vast number of affected individuals, chronicity of symptoms and the percentage of patients who are refractory to current maximal medical management (Lal et al., 2009) and thus require surgical intervention (Fokkens et al., 2012). CRS is one of our commonest medical conditions and the fifth most common indication for antibiotic prescription (McCaig and Hughes, 1995). Patients with CRS have been shown to have significantly impaired quality of life, with some patient reported outcome scores ranking as highly as COPD or angina (Soler et al., 2011).

The current standard maximal medical therapy culminates in systemic antibiotics and steroids, yet failure rates remain high. Thus there are approximately 500,000 sinus surgical procedures per year (Owings and Kozak, 1998). UK figures from clinical coding of hospital episode statistics HESONLINE (2015) shows in the order of 60,000 secondary care diagnoses and 15,000 associated sinus surgery procedures, meaning approximately one in four people elects to have surgical treatment. Surgical intervention is effective in the short term, but often the disease process recurs (Hopkins et al., 2009b). Such statistics for surgical therapy illustrate that our current medical therapies, either alone or combined with surgery are not effective. This is not surprising, given that the basic disease mechanisms and pathogenesis of CRS are not understood (Van Crombruggen et al., 2011).

1.3.2 Diagnosis

Diagnosis of CRS is currently made from patients symptoms with corroborative evidence identified from endoscopic sino-nasal assessment combined with computerised tomography (CT) scanning. A pan-European consensus document has been published to standardise the diagnosis and management approach for CRS. This collaborative, evidence based position paper is currently in its third revision (Fokkens et al., 2012) and seeks to standardise current clinical knowledge of CRS and help set the agenda for research based on the deficiencies in understanding of sinusitis.

Diagnosis of CRS is currently defined as an inflammation of the nose and paranasal sinuses of at least 12 weeks duration of:

1. two or more symptoms, one of which should be nasal blockage or nasal discharge
2. either facial pain/pressure or loss of smell
3. corroborative changes in the endoscopic assessment or CT scan

In addition there are a number of related general symptoms associated with CRS such as irritation of the larynx, pharynx and trachea - sometimes causing cough, ear pain and pressure and generalised fatigue, however at present these distant symptoms do not form part of the main diagnostic criteria and can be subject to other influences such as gender (Ference et al., 2015).

The overall severity of CRS can be estimated using a variety of patient reported outcome measures, such as the well validated Sino-nasal Outcome Test-22 (SNOT-22) questionnaire (Hopkins et al., 2009a, Morley and Sharp, 2006, Piccirillo et al., 2002) which generates a severity score between 0-110 and can be stratified between mild (8-20), moderate (>20-50) and severe (>50) (Toma and Hopkins, 2016). The Lund-Mackay radiological severity score (Lund and Mackay, 1993) is calculated based on the degree of sinus opacification on CT scan and gives a score between 0-24 (Table 1).

Anatomical sinus group/drainage pathway	Right side	Left side
Frontal sinus	0/1/2	0/1/2
Maxillary sinus	0/1/2	0/1/2
Anterior ethmoid sinuses	0/1/2	0/1/2
Posterior ethmoid sinuses	0/1/2	0/1/2
Sphenoid sinuses	0/1/2	0/1/2
Ostiomeatal complex	0/2	0/2

Table 1. Lund-Mackay scoring system for degree of sinus involvement. Points are accrued for the degree of opacification of each sinus group (0 = normal, 1 = partly opacified, 2 = completely opacified) and the important drainage pathway of the ostiomeatal unit (0 = unaffected, 2 = opacified). A combined score between 0-24 is generated from the sinus groups bilaterally.

1.3.3 Classification

The current literature defines CRS as a disease of the nasal and paranasal sinus mucosa present for more than 12 weeks with mucosal changes that vary from inflammatory remodelling to the formation of nasal polyps (Fokkens et al., 2012). It represents a spectrum of diseases with a common end result of chronic sinonasal inflammation and fibrotic airway remodelling. CRS is subtyped principally by the presence or absence of nasal polyps on examination of the nose either by direct inspection, endoscopic assessment and sometimes supplemented by CT imaging (Figure 4). The aetiopathogenesis of CRS is, however, poorly understood. It is classified as sinonasal inflammation, but is currently defined only by symptomatology rather than specific cellular or histological appearances. The symptoms are often attributable to changes in sinonasal mucosa, mucus or mucociliary clearance leading to sinonasal ostial blockage and impaired function.

Histological assessment of polypoid and non-polypoid tissue specimens demonstrates that they represent differing disease pathologies. Chronic rhinosinusitis without nasal polyps (CRSsNP) is characterised by sinonasal fibrosis, basement membrane thickening, epithelial damage, mononuclear cell infiltration and goblet cell hyperplasia (Kou et al., 2012). Chronic

rhinosinusitis with nasal polyps (CRSwNP) is characterised by basement membrane thickening, epithelial damage, stromal oedema and pseudocyst formation (Bachert et al., 2000, Kou et al., 2012). The basement membrane thickening is the end result of a dense fibrotic response typified by accumulation of fibronectin and type I, III and V collagens (Pawankar and Nonaka, 2007). Both diseases also have a differing T helper cell profile and cytokine signature. CRSsNP has been shown to be predominantly a Th1 inflammatory environment with type 1 interferon gamma (IFN-γ) as the predominant cytokine along with the pro-fibrotic transforming growth factor β (TGF- β). In contrast CRSwNP is associated with a Th2 and IL-5 predominant inflammatory environment (Van Crombruggen et al., 2011).

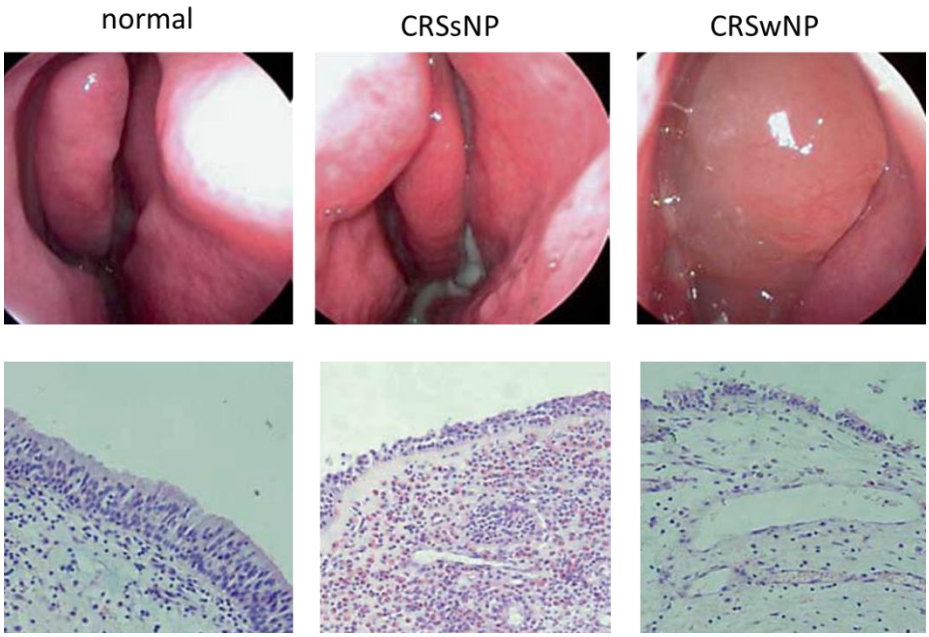

Figure 4. Endoscopic photographs of normal nasal cavity mucosa. CRS without nasal polyps (CRSsNP) and CRS with polyps (CRSwNP). Accompanying each photograph, H&E stained sections illustrate differing disease histopathology. CRSsNP demonstrates epithelial cell loss, fibrosis and immune cell chemotaxis. CRSwNP shows sub-epithelial oedema, pseudocyst formation and absence of fibrosis. Image adapted from (Kou et al., 2012).

In addition to the well-established phenotypes of polypoid and non-polypoid CRS, various sub-phenotypes or endotypes have been proposed in an attempt to further sub-categorise the two heterogeneous polyp/non-polypoid groupings (Akdis et al., 2013, Tomassen et al., 2016). Such sub-classification is greatly needed to help our understanding of CRS, however no doubt due to their novelty their use is not yet widespread.

1.3.4 Current treatments

Chronic rhinosinusitis is principally managed using medical therapy, with surgical procedures reserved for cases that fail to respond to pharmacological management. A percentage of patients are not responsive to a combination of medical and surgical treatments and have been termed 'difficult to treat' rhinosinusitis (Fokkens et al., 2012).

1.3.4.1 Medical

Current maximal medical therapy comprises corticosteroids either intranasal, systemic or both in combination with antibiotics and nasal irrigation (Dubin et al., 2007). Corticosteroids have been shown to reduce the amounts of chemotactic cytokines produced from the nasal mucosa (Mullol et al., 2000, Xaubet et al., 2001) and reduce eosinophil viability and activation (Mullol et al., 1997, Mullol et al., 1995). Corticosteroids act via intracellular glucocorticoid receptors, promoting an increase in anti-inflammatory cytokines including interleukin 10 (IL-10) and negative regulation of pro-inflammatory cytokines such as tissue necrosis factor α (TNF-α) and interferon-γ (IFN-γ). Corticosteroids can be delivered either systemically or topically, with the topical route preferred to minimise the side effect from systemic absorption. The main drawback to the topical route is the varied penetration of drug delivery to the nose & sinuses in the presence of obstructive nasal disease (Harvey et al., 2008, Grobler et al., 2008), however their use is supported by level 1 evidence from multiple published randomised controlled trials (Fokkens et al., 2012). Antibiotics are frequently used to treat CRS in both primary and secondary care. Short term antibiotics currently do not have any substantial evidence to support their use, with the exception of proven, culture positive exacerbations. The use of long term antibiotics attracted significant interest following the increased survival of patients with diffuse pan bronchiolitis treated with erythromycin who were observed to achieve CRS symptom resolution (Nagai et al., 1991, Kudoh et al., 1998). Macrolide antibiotics have been shown to possess anti-inflammatory effects at lower dosage than conventionally used for their anti-infective properties. Unfortunately, despite the initial promise, a recent Cochrane review has found little evidence of their efficacy in CRS (Head et al., 2016). However, it is worth noting that only five randomised controlled trials could be included in this review, each with small cohorts between 43 to 79 participants therefore further evidence on the efficacy of antibiotics in CRS is required (Bewick et al., 2016). Nasal irrigation with either iso or hypertonic saline solution can be topically applied and its use is widespread. The lack of

drugs and hence side effects in saline irrigation, makes it a popular choice among patients and physicians, however a recent Cochrane review has questioned the evidence for its use (Chong et al., 2016).

Due to the lack of medical treatment evidence base for efficacy in CRS, pharmacological treatment has remained essentially unchanged over a time that has seen significant developments in the surgical management of CRS. Medical therapy has also been relatively static over the last couple of decades in which time other chronic inflammatory conditions such as inflammatory bowel disease and rheumatoid arthritis have seen biological therapies revolutionise their treatments and patient outcomes. To improve CRS management, similar, contemporary medical advances are required and are currently in their infancy such as the biological therapies dupilumab (monoclonal anti IL-4 & IL-13 Th2 cytokine inhibitor) (Bachert et al., 2016), mepolizumab (monoclonal anti IL-5) (Gevaert et al., 2011) and omalizumab (monoclonal anti IgE) (Pauwels et al., 2015, Gevaert et al., 2013). There is currently an unmet need for further clinical trials of medical therapy for CRS.

1.3.4.2 Surgical

Within secondary care CRS is often found to be refractory to current pharmacological treatment with antibiotics and corticosteroids, leaving many patients facing the choice of surgery or persistent symptoms. Failure of medical therapy typically results in patients having functional endoscopic sinus surgery (FESS) to resect diseased tissue, ventilate affected sinus groups and provide access for topical medical therapy. Since its original description by Messerklinger in the 1980s (Messerklinger) FESS has become a widely accepted treatment for CRS. As with any surgical procedure it is not without complications; including bleeding, ocular complications or a leakage of cerebrospinal fluid. FESS is a time consuming and expensive intervention whose high disease recurrence may require frequent re-operation (Hopkins et al., 2009b).

Advances in endoscopic surgical equipment, image guidance systems, surgical procedures and anaesthesia have improved the surgical management of CRS - with robotic surgery on the horizon. However effective surgery is in the short-term, there remains a relatively high disease recurrence rate (Hopkins et al., 2009b). Patients with post-surgical CRS recurrence face a frustrating cycle of revisiting previously failed medical and surgical interventions. A current evidence based summary of the management of CRS is shown in Figure 5. The lack

of medical treatment options is, however, not surprising when we consider the pathogenesis of CRS is not understood.

1.3.5 Physiology of the sinuses

Mucociliary clearance is essential to the maintenance of normal paranasal sinus physiology and health. Paranasal sinuses are lined with respiratory pseudostratified ciliated epithelium with goblet cells, which together produce the mucus and then transports it with any trapped material posteriorly to the pharynx where it is swallowed. The rate of mucociliary clearance is controlled by a combination of anatomical factors of the sinuses, biochemical components of the constituent mucus and physiological parameters. The physiological factors co-ordinate the mucus volume produced and the rate of ciliary clearance. In health there are between 50 to 200 cilia per epithelial cell, each measuring approximately 5µm long. Under normal conditions ciliary beat frequency varies from 9 to 15Hz which propels the mucus to the nasopharynx at approximately 3 to 25mm/min (Cohen, 2006). This can be measured by a saccharin transit test, placing sweet tasting saccharin at the tip of the nose and asking the subject how long it takes to taste. Cilia consist of a typical '9+2' axoneme of microtubules, that when stimulated by ATP cause the dynein arms of the microtubules to move against one another and produce ciliary movement. Cilia insert into the basal membrane in an organised orientation so they all beat in the same direction and efficiently transport mucus. The ciliary beat frequency can be altered by both temperature, mechanical, hormonal and autonomic stimuli in an attempt to clear particulate matter trapped within the mucus. Unlike the lower airways where coughing can be used in combination with mucociliary clearance, the paranasal sinuses rely exclusively on mucociliary clearance to maintain their normal health.

.

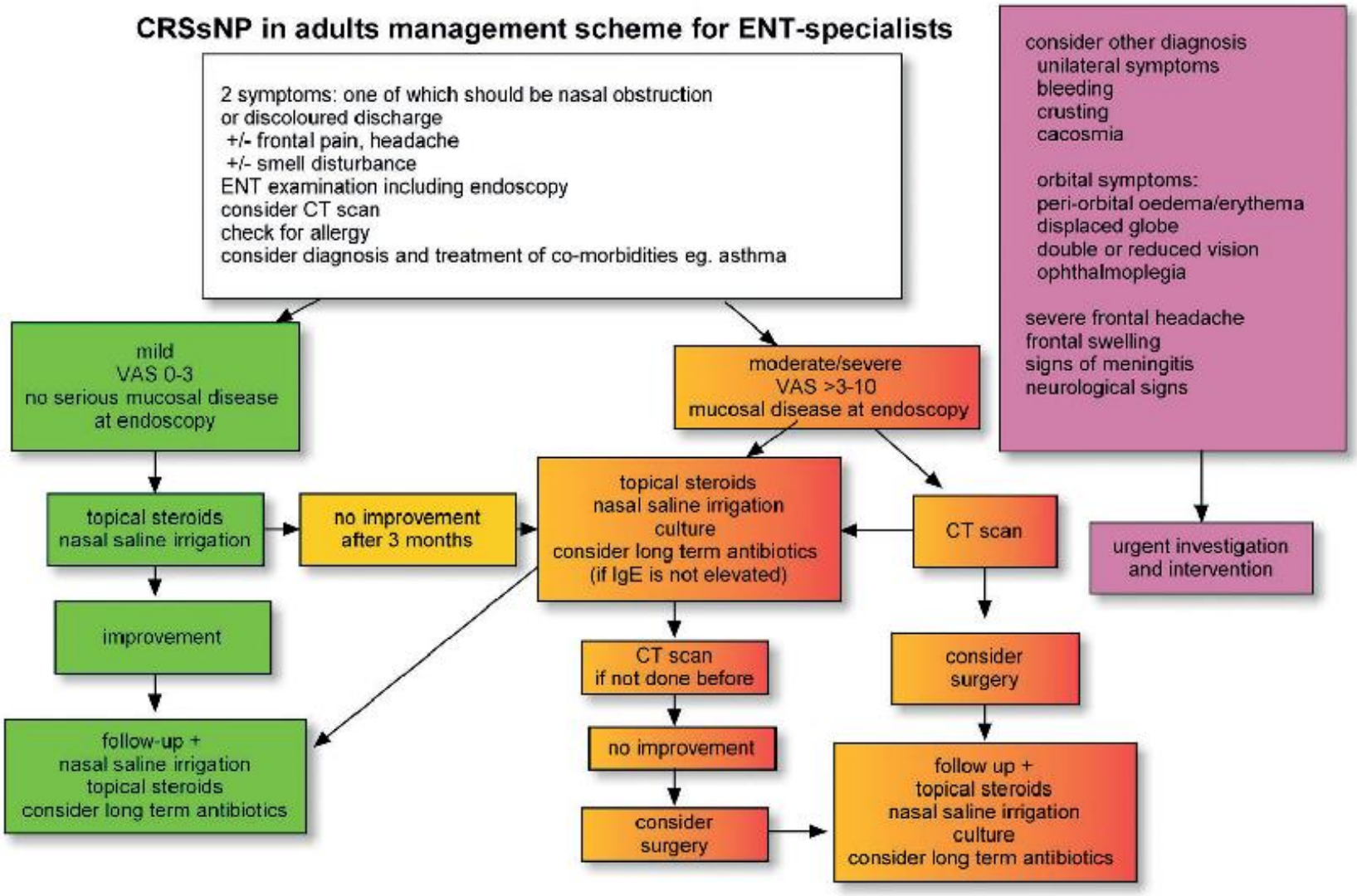

Figure 5. 2012 European position paper on sinusitis (EPOS) CRS diagnosis and treatment algorithm. Figure taken from (Fokkens et al., 2012)

1.3.6 Pathophysiology of chronic rhinosinusitis

Globally, the majority of rhinitis or sinusitis episodes constitute acute disease, and as such are usually self-limiting or respond to simple medical intervention. The pathophysiology of acute sinus inflammation is well documented. However, it is not clear why CRS develops with its persistent inflammatory response, sinonasal airway remodelling and chronic disease symptoms. Multiple studies have demonstrated that the CRS sino-nasal tract does not demonstrate a significantly altered microbial flora (section 1.3.6.1). Similarly, it has been shown that CRS is not typically the result from a specific host immune deficiency.

The first significant attempt to address the pathophysiology of CRS was the fungal hypothesis, suggesting CRS was due to a disproportionate immune response to Alternaria species of fungi (Ponikau et al., 1999, Sasama et al., 2005, Hamilos and Lund, 2004). Numerous trials of antifungal therapy failed to corroborate the fungal hypothesis and this hypothesis has now been rejected. Similarly, alterations in the leukotriene/prostaglandin axis have been hypothesised, but are not substantiated by the lack of response to leukotriene inhibitors. Specifically for CRSwNP a 'staphylococcal superantigen hypothesis' has been proposed suggesting staphylococcal exotoxins drive a Th2 inflammatory response in combination with eosinophil and mast cell recruitment (Bachert et al., 2003). However, superantigen effects have only been demonstrated in fewer than half of all CRSwNP patients, suggesting that superantigens may potentiate nasal polyps rather than be a direct cause (Van Crombruggen et al., 2011). The 'innate immune barrier hypothesis' suggested defects in the innate immune barriers such as Toll-like receptors (TLRs) permit increased microbial stimulation and an accentuated immune response resulting in the phenotype of CRS (Kern et al., 2008, Ooi et al., 2008, van Drunen et al., 2012, Lane, 2009, Zhang et al., 2013). However the 'innate immune barrier hypothesis' does not explain the different phenotypes of CRSsNP and CRSwNP and the observed differences in their T helper cytokines. Finally following the observations of biofilms in periodontal disease (Ohlrich et al., 2009), the 'biofilm hypothesis' suggests that in CRS bacteria organise themselves within biofilms to evade host defence mechanisms and therefore promote persistent inflammation (Foreman et al., 2012, Boase et al., 2013b).

Resection of diseased surgical specimens from appropriately consenting patients in FESS procedures provides a valuable source of tissue for further investigation. Histological analysis of CRS specimens has so far identified inflammatory cells, inflammatory cytokine

signatures and airway remodelling, though the precise pathophysiological mechanisms that cause the persistent, exaggerated sinonasal inflammation remain unclear. This lack of disease understanding may perhaps explain the high proportion of patients refractory to current conventional pharmacological therapy. The position of the sinonasal tract makes it highly accessible to the delivery of topical medical therapy. As a result there are tremendous translational research opportunities to develop better topical nasal anti-inflammatory approaches to treat this large patient population and hence reduce the number of operative procedures.

Considerable, organised, international effort has gone into investigating the pathophysiology of CRS and our understanding of local sinonasal and upper airway immune mechanisms has greatly increased. However, no one unifying molecular mechanism or pathway has been identified. Therefore, CRS is still considered to be multifactorial, reflecting the numerous hypotheses and disease associations which have so far been described.

1.3.6.1 Microbiology

Historically the paranasal sinuses were thought to represent a sterile environment until Brook's landmark publication (Brook, 1981), the first of many on the microbiology of the paranasal sinuses. Early hypotheses from conventional, culture based assays suggested that CRS was due to the colonisation of the sinuses of CRS patients with more isolates of bacterial strains and possibly more pathogenic species including anaerobes than in healthy sinuses (Brook et al., 1996, Aral et al., 2003) (Brook, 2005). More recent molecular techniques to study the microbiome (all of the microbial genes present) have allowed a more definitive understanding of the microbiology of the sinonasal cavities than traditional culture methods. Microbiome studies from a number of authors have not shown significant differences in the microbial environment of CRS patients compared to healthy controls (Aurora et al., 2013) (Ramakrishnan et al., 2016, Ramakrishnan et al., 2013, Wilson and Hamilos, 2014). As a result there is nowadays less emphasis on a 'pathogen driven hypothesis'.

Current literature suggests that CRS may be the result of activation of abnormal pro-inflammatory and fibrotic responses to numerous inhaled particles and ubiquitous pathogens that may constitute normal sinonasal flora (Van Crombruggen et al., 2011). In health, epithelia of the sinonasal airway are able to clear inhaled particles and organisms and to produce appropriate defensive immune responses to pathogens, yet maintain immunological tolerance of commensal flora. The epithelium of the sinonasal airway has a

series of membrane bound and intracellular Pathogen Recognition Receptors (PRRs) including the Toll-like receptor (TLR), Nucleotide-binding oligomerization domain (NOD) receptors, RIG-I-like receptors (RLRs) and C-type lectin receptors (CLRs) (Takeuchi and Akira, 2010) capable of recognising conserved universal microbial motifs including Pathogen Associated Molecular Patterns (PAMPs) and endogenous Damage Associated Molecular Patterns (DAMPs) or alarmins (see below). A number of reports of the expression of TLRs in sinonasal mucosa in general agree that all TLRs are expressed in both healthy controls CRSwNP patients and CRSsNP patients (Ramanathan et al., 2007, Vandermeer et al., 2004). In both CRSsNP and CRSwNP, receptor for advanced glycation end-products (RAGE) receptors have been reported to be expressed at lower levels than in healthy sinonasal and upper airway mucosa (Van Crombruggen et al., 2012).

1.3.6.2 Alarmins

Alarmins or DAMPs constitute a variety of intracellular molecules and extra cellular matrix elements released following cellular injury that cause inflammation. Their release from cells undergoing non-programmed cell death has the ultimate aim of restoring cellular and tissue architecture by inflammatory and reparative mechanisms. Alarmins typically signal through activation of TLRs, RAGE and related PRRs (Piccinini and Midwood, 2010). Sino-nasal cells are subject to a whole variety of different stimuli that may result in cellular injury and release of alarmins due to their location at the entrance to the respiratory tract and the many thousands of litres of air per day that pass over their surface.

Numerous DAMPs have been studied in the sinonasal passages. Altered protein amounts or RNA expression have been summarised in Van Crombruggen's review (2013), Table 2.

DAMP	CRSsNP	CRSwNP	Receptors
S100A8/A9		↓	TLR4, CD36, RAGE
S100A7		↓	RAGE
Surfactant protein A & D	↑	↑	TLR2 & TLR4
Eosinophil-derived neurotoxin	↑		TLR2
Fibronectin		↑	TLR4
Galectins		↑	TLR2
Tenascin-C		↑	TLR4 & CD36
B-defensins 2 & 3	↔		TLR1, TLR2 & TLR4

Table 2. Summary of known altered expression of damage associated molecular pattern (DAMPs) in CRSsNP and CRSwNP. Adapted from (Van Crombruggen et al., 2013).

1.3.6.3 Airway remodelling

Irreversible airway remodelling and a progression from normal to disease is accepted in lower airways disease pathophysiology, for example asthma (Lazarus, 2006). Similar mechanisms are gaining popularity in understanding CRS (Bassiouni et al., 2013, Bassiouni et al., 2012). The end result of CRS airway remodelling is shown, with typical clinical and histological appearances (Figure 4), however the precise mechanisms underpinning these changes remain unknown. From the published literature to date it is clear that CRS represents a spectrum of diseases with similar clinical symptoms, but differing pathophysiology (Van Crombruggen et al., 2012). The mechanisms of CRS without polyps (CRSsNP) and CRS with nasal polyps (CRSwNP) represent differing diseases within the overall umbrella of CRS (Figure 6).

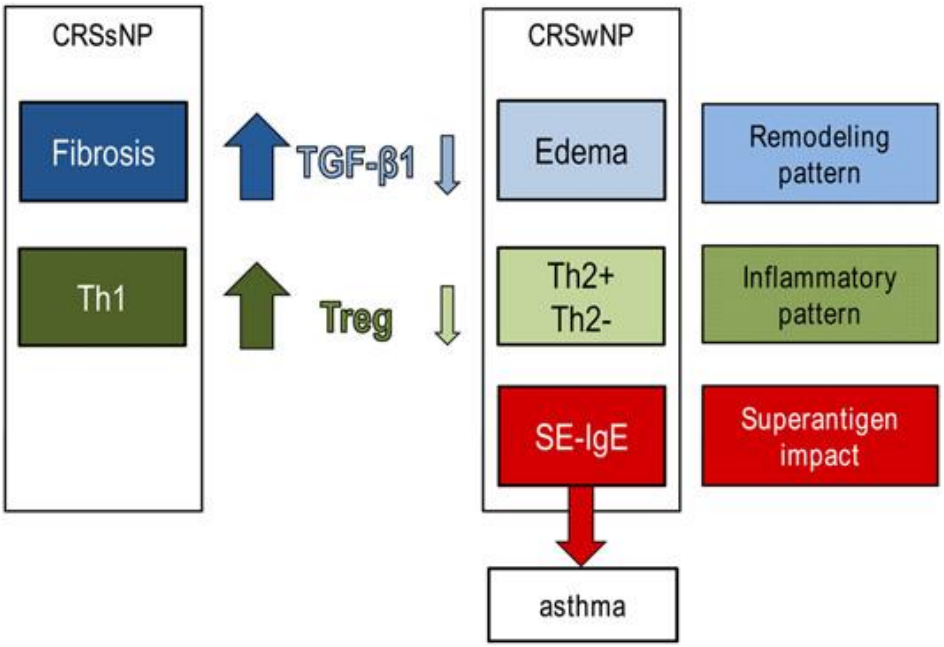

Figure 6. CRS phenotypes and their proposed pathophysiologies. Different inflammatory T-cell signatures and remodelling patterns are suggested. CRS without nasal polyps (CRSsNP) and with polyps (CRSwNP). Th1 = T_H1 predominant cytokine pattern. Th2+ =IL-5 positive, T_H2 predominant signature; Th2- =IL-5 negative, T_H2 predominant signature. SE-IgE =IgE antibodies to *S. aureus* enterotoxins. Figure adapted from (Van Crombruggen et al., 2011).

1.3.6.3.1 Early fibrosis

Pivotal to the development of this thesis was the observation of early fibrosis and airway remodelling in the development of CRS (Van Bruaene et al., 2012). Van Bruaene et al. compared sinonasal mucosal samples from nine patients with early CRSsNP, defined as symptomatic bilateral endoscopic disease with persistent changes on CT scanning refractory to maximal medical therapy (Fokkens et al., 2012). Sinonasal mucosa from the maxillary sinus, ethmoid sinus, uncinate process, inferior and middle turbinate was compared between CRSsNP and healthy controls. The mucosal samples were analysed for Th1 inflammatory cytokines, neutrophil activity and fibrotic airway remodelling by collagen deposition, Tissue Growth Factor-β (TGF-β) and its receptors at both the RNA and protein level. Sinonasal fibrotic mucosal remodelling was observed, with significantly upregulated TGF-β throughout CRSsNP sinus biopsies compared to those of healthy controls, whilst no differences in inflammatory cytokines or neutrophil activity were seen. This novel observation suggested that fibrotic airway remodelling preceded the inflammatory response typical of CRSsNP. Although contrary to the then prevailing consensus of the of CRSsNP

natural history, subsequent clinical evidence has shown that a window of opportunity exists for effective surgical treatment of CRS following failure of medical therapy (Hopkins et al., 2015b, Hopkins et al., 2015a). A combination of these observations together with relevant observations in the fibrosis literature (section 1.3.7) led me to study the fibroblast in CRSsNP in more detail for this thesis.

The sinonasal airway epithelium has a unique position in the upper airway, sampling and filtering all the inhaled particles and microorganisms. Consequently the epithelial cells are subject to a variety of environmental and infective stimuli that can cause damage, release of intracellular alarmins and potentiate the inflammatory load. The epithelial cells sit directly upon a network of fibroblasts within the lamina propria, yet the roles of the sensing nasal epithelium and underlying fibroblast cells have not been conclusively investigated, regardless of the fact that sinonasal airway fibrosis may precede overt inflammation and forms an end stage of the disease process.

1.3.7 Fibroblasts role in inflammation

The body is not afflicted with generalised inflammation in CRS sufferers. Thus it is evident that the mal-regulation of inflammatory pathways is local rather than systemic. Indeed, chronic inflammation has two defining features; chronicity and tissue specificity e.g. dermatitis, colitis, nephritis and so on. What is it then that could be orchestrating such specific, tissue-tropic inflammation within the sinonasal tract? Recent research highlights the role of stromal cells in the generation and persistence of chronic inflammation (Naylor et al., 2013). Rather than simply being scaffolding or matrix generating cells on which organs are built, stromal cells such as fibroblasts and osteocytes have their own immunological function. Also, stromal cells from various tissues are significantly different, for example fibroblasts from inflamed skin have a completely different appearance, immunological profile and function to fibroblasts from arthritic joints. These epigenetic changes have been shown stable through generations both *in vivo* and *in vitro* (Polyak and Weinberg, 2009). It is suggested that rather than being innocent bystanders, stromal cells actually co-ordinate tissue-specific chronic inflammation, directing immune cell activation (Figure 7). This hypothesis could readily apply to the paranasal sinuses, where epithelial cells reside alongside fibroblasts within a complex bony honeycomb. Recent early-CRS publications

suggest an increase in sinonasal fibroblasts and of collagen deposition precedes local inflammation (Van Bruaene et al., 2012) rather than the other way round. The initiator of fibroblast recruitment and expansion is suggested to be due to upregulation of tissue growth factor β (TGF-β), a key cytokine in wound healing and repair. This novel concept opposes the traditional concept that fibrosis and airway remodelling result from epithelial injury.

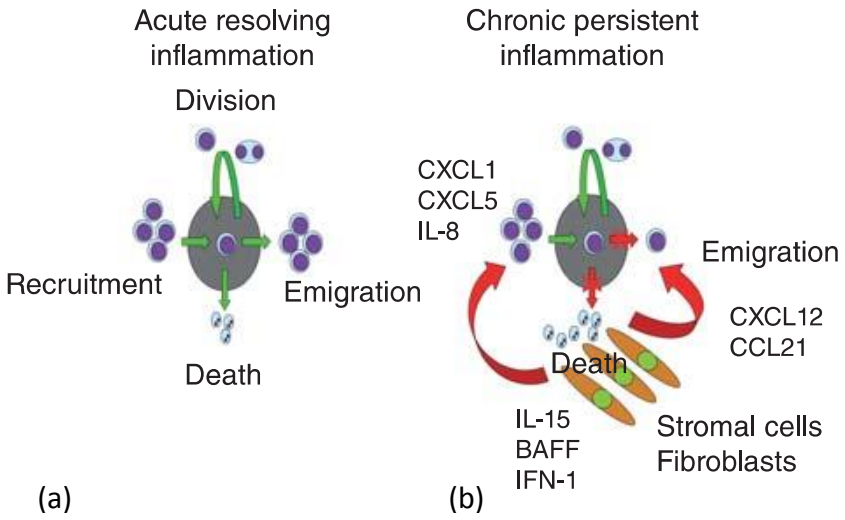

Figure 7. Control of immune cell accumulation. (a) Normal health; division and recruitment are balanced by emigration and death. (b) Chronic inflammation; an imbalance of recruitment, death and emigration of immune cells. Stromal cells can influence this via the production of cytokines and chemokines e.g. interferons (IFN), interleukins (IL), B cell activating-factor (BAFF), and chemokines (CCl and CXC). Image adapted from (Naylor et al., 2013)

1.3.8 Fibroblasts in chronic rhinosinusitis

Examination of sinonasal tissue sections from CRS patients and healthy controls demonstrates a marked difference in their tissue architecture. CRS patients undergo airway remodelling with epithelial damage and an influx of multiple immune cell types including neutrophils, eosinophils, T-cells and macrophages. This inflammatory infiltrate is localised alongside fibroblasts in the lamina propria underneath the epithelial surface. At present there no therapeutic approaches to target the fibroblast in upper airway pathology. Within this section I will present the results of a review article (Ball et al., 2016) of the current understanding of the role of the fibroblast in sinonasal disease with and without nasal polyposis (Figure 8) and how it could potentially be a focus for development of future CRS-specific therapeutics.

1.3.8.1 Chronic rhinosinusitis without nasal polyps

Due to the plentiful supply of excised nasal polyp tissue, most sinonasal fibroblast investigations have been performed on cells from nasal polyps. However, nasal fibroblasts can also be readily isolated from non-polypoid tissue, a feature that has been successfully exploited in a variety of investigations. Thus far the clear distinction between the clinical phenotypes of polypoid and non-polypoid CRS has not been mirrored by distinct cellular differences in phenotype and function of their respective CRS fibroblasts. This is no doubt due to the novelty of the fibroblast driven upper airway inflammation hypothesis, however we do know fibroblasts have a number of roles in both CRS with and without polyps. The sections below review the current understanding of fibroblast involvement in non-polypoid CRS.

1.3.8.1.1 Cell receptors and inflammatory signalling in nasal fibroblasts

The sinonasal mucosa is exposed to a great range of pathogens, especially respiratory viruses. Fibroblasts compose a dense sub-mucosal layer of the sinonasal passages and no doubt convey an important protective role from the many common viral infections. Takahashi et al (2006) investigated the effects of a synthetic dsRNA viral analogue, Poly I:C, on chemokines, type 1 interferons, Th1 cytokines and pro-inflammatory cytokines in nasal mucosal fibroblasts. They first confirmed the presence of TLRs on nasal fibroblasts, identifying high levels of TLR 3, 4 and 9. TLRs 1, 2, 5 and 6 were also detected but only at low levels whilst TLR 7, 8 and 10 were found not to be expressed. Poly I:C signals via TLR-3 and expression of this receptor was increased fivefold following Poly I:C treatment. A

significant release of the chemokines IL-8 and RANTES and small amounts of type I interferon IFN-β were also observed following poly I:C treatment. RANTES is a potent chemo attractant for a number of immune cells including monocytes, eosinophils, lymphocytes and basophils. In the sinonasal environment it has been shown that fibroblasts and not epithelial cells are the source of RANTES (Maune et al., 1996). Release of eotaxin, IL-1β, TNF-α, IFN-α, IFN-γ and IL-12 was assessed by ELISA but could not be detected following nasal fibroblast stimulation. Maune et al. also confirmed the signalling pathway for production of nasal fibroblast derived IL-8 and RANTES was by JNK and PI3 kinase. In addition, p38 MAP kinase was important for IL-8 production. Therefore Takahashi et al propose Poly I:C, like viruses clinically, are potent and selective stimuli for nasal fibroblast derived IL-8 and RANTES, but not Th1 cytokines, pro-inflammatory cytokines or eotaxin. Therefore more precise profiling of sinonasal viral infection associated chemokines may offer new pharmacological targets to block cellular inflammation in the nasal and sinus cavities.

1.3.8.1.2 Nasal fibroblast derived cytokines & chemokines

Kouzaki et al investigated the role in CRS of platelet-derived growth factor (PDGF) (2009), a proliferative and pro-fibrotic cytokine with emerging roles in renal, hepatic, respiratory and other inflammatory and fibrotic organ pathologies. Using immunohistochemical techniques they localised PDGF in CRS patients to inflammatory, epithelial, glandular and vascular endothelial cells. Increased expression of PDGF receptors was found in CRS submucosal fibroblasts. The authors suggest that in CRS, local PDGF production may be important in promoting sinonasal fibrosis.

Nonaka et al. (2010b) analysed the ability of nasal and respiratory tract fibroblasts to amplify inflammatory cell infiltration via chemokine production. They measured the ability of fibroblasts to produce thymus and activation-regulated chemokine (TARC), a Th2 chemokine. Co-stimulation with either TNF-α and poly I:C or Th2 cytokines was found to induce a substantial TARC release. Nasal fibroblasts may therefore be an additional source of chemokines, amplifying viral and Th2 induced airway disease.

Oyer et al. (2013) studied the role of leukocyte adhesion molecules VCAM and ICAM to attract neutrophils and eosinophils by nasal fibroblasts. Levels of nasal fibroblast VCAM and ICAM were measured by flow cytometry. They found that both ICAM and VCAM nasal fibroblast expression were elevated in CRS. Additionally, *in vitro* treatment with TNF-α and IFN-γ further increased ICAM, while treatment with TNF-α and IL-4 increased VCAM. From

these observations they suggest that CRS has higher levels of leukocyte adhesion molecules, and the effect is amplified by the CRS inflammatory cytokine environment.

In summary fibroblasts in chronic rhinosinusitis without nasal polyps emerge as important sensors of the sinonasal environment, able to monitor and respond to the upper airway environment through expression of a variety of pattern recognition receptors. Dependent on their precise environmental milieu, nasal fibroblasts are able to produce a variety of pro-inflammatory cytokines and chemokines to amplify the local inflammatory response.

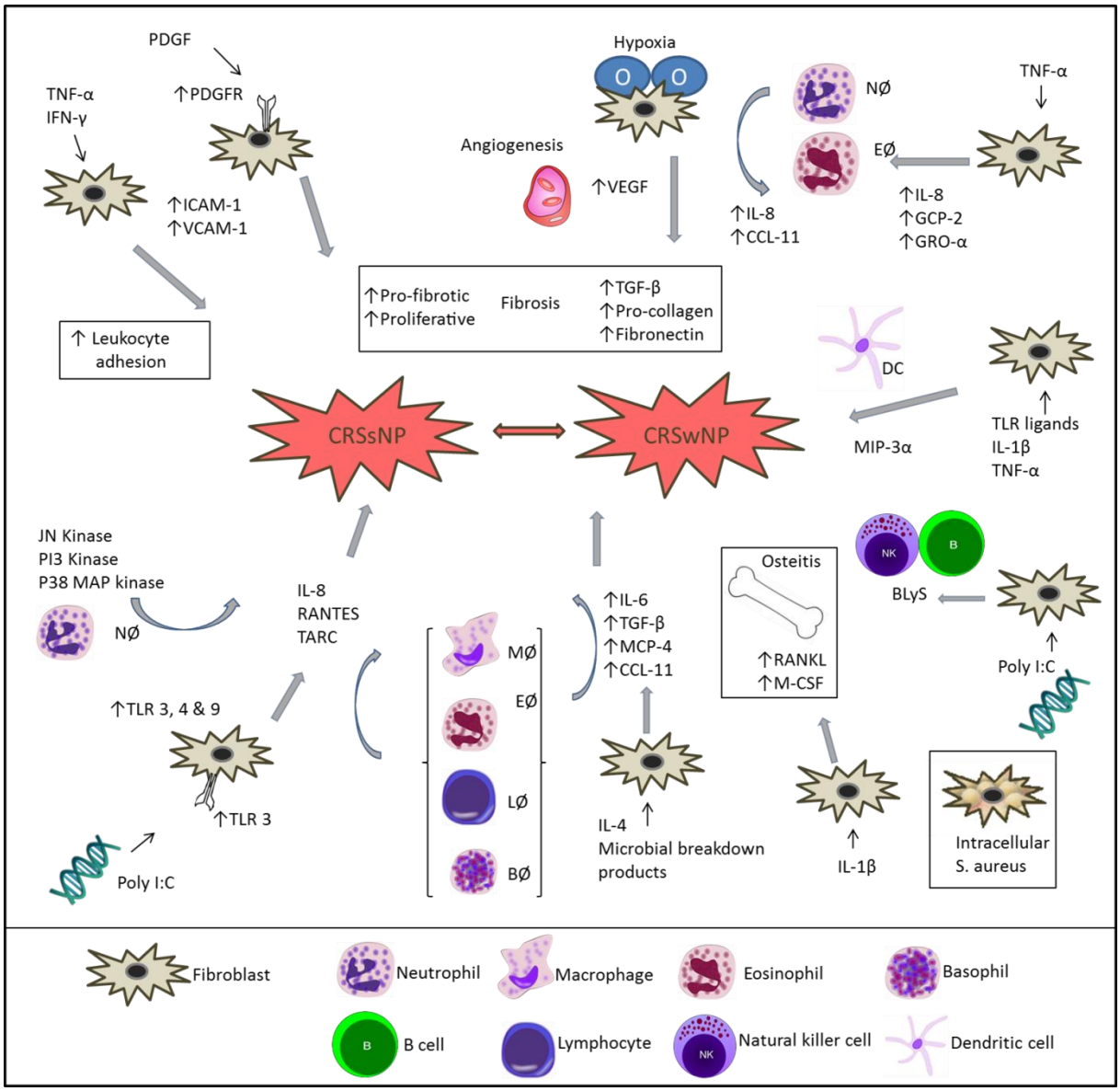

Figure 8. Summary of the current inflammatory and fibrotic roles of the fibroblast in CRS with polyposis (CRSwNP) and without (CRSsNP). Sinonasal fibroblasts have a wide range of chemotactic, inflammatory, and pro-fibrotic roles in the pathophysiology of chronic rhinosinusitis.

BLyS, B-lymphocyte stimulator; CCL-11, C-C motif chemokine-11; DC, dendritic cell; GCP-2, granulocyte chemotactic protein-2; GRO-a, growth related oncogene a; ICAM, intercellular adhesion molecule; IFN, interferon; MCP-4, monocyte chemotactic protein-4; MIP-3a, macrophage inflammatory protein-3a; NK, natural killer; PDGF, platelet-derived growth factor; PDGFR, platelet derived growth factor receptor; PI, phosphatidylinositol; TGF, transforming growth factor; TLR, Toll-like receptor; TNF, tumour necrosis factor; VEGF, vascular endothelial growth factor. Image taken from (Ball et al., 2016).

1.3.8.2 Chronic rhinosinusitis with nasal polyps

Fibroblasts have been shown to contribute to the development of nasal polyps, providing extracellular matrix proteins including collagens, fibronectin and vimentin to the nasal polyp architecture. In addition to a pro-fibrotic role fibroblasts have additionally been suggested to have inflammatory actions which may be important in the development and persistence of nasal polyps. Most CRS fibroblast investigations to date have been based around *in vitro* cellular cultures of primary human nasal fibroblasts, since animal models of sinonasal disease do not presently sufficiently resemble CRS (Kara, 2004).

1.3.8.2.1 Hypoxia driven inflammation

Mucosal inflammation and swelling cause ostial sinus blockage in CRSwNP, reducing sinuses' capacity to ventilate normally. Such processes may create an environment with reduced oxygen tension. In hepatic fibrosis and many similar conditions hypoxia results in an infiltration of inflammatory cells and subsequent cytokine release. Early et al. (2007) investigated the role of reduced oxygen concentrations on fibroblasts isolated from nasal polyps. Nasal polyp fibroblast hypoxia increased vascular endothelial growth factor (VEGF), transforming growth factor β (TGF-β), interleukin 8 (IL-8) and C-C motif chemokine-11 (CCL-11) involved in eosinophil recruitment. Importantly, hypoxia also resulted in airway remodelling with a significant up-regulation of fibroblast derived intracellular pro-collagen and fibronectin. Shun et al. (2011) and Sun et al. (2005) replicated the stimulation of IL-8 and VEGF by nasal polyp fibroblast hypoxia, suggesting they prime the sinonasal environment for neutrophil infiltration and angiogenesis.

1.3.8.2.2 Fibroblast – osteitis crosstalk

Inflammation and remodelling of the bony paranasal sinus cavities or osteitis has been observed as a factor in CRS pathophysiology. In CRS the histological and radiological appearances of the ethmoid sinus bone demonstrate fibrosis, new bone formation, inflammatory infiltrates and increased bone turnover, similar to skeletal osteomyelitis (Kennedy et al., 1998). Park & colleagues (2007) investigated whether CRS inflammation stimulates nasal fibroblasts to function in a manner similar to osteoblasts and disrupt the normal paranasal sinus bone homeostasis. They found that the pro-inflammatory cytokine interleukin-1β (IL-1β) stimulated nasal polyp fibroblasts to express receptor activator of nuclear factor κB ligand (RANKL) and macrophage colony-stimulating factor (M-CSF), key regulators of osteoclastogenesis. Paranasal fibroblasts reside in a densely packed lamina

propria directly in contact with paranasal sinus bone and periosteum. Through this close anatomical relationship it appears that fibroblasts can influence the environment of the paranasal sinus bony labyrinth. Whether or not inflammation/osteitis of the sinus bony architecture acts as a reservoir to drive persistence of chronic mucosal inflammation is currently a subject of much debate (Georgalas et al., 2010, Sacks et al., 2013, Videler et al., 2011, Leung et al., 2016, Snidvongs et al., 2014).

1.3.8.2.3 Nasal polyp fibroblasts as a source of cytokines

Nasal polyposis is characterised by a chronic Th2 cytokine dominant environment. Nasal and airway fibroblasts may be a major source of such Th2 cytokines (Tremblay GM, 1995, Nonaka et al., 1999, Nonaka et al., 2010b). Nonaka et al. investigated whether either the Th2 cytokine IL-4 or microbial breakdown products stimulated nasal polyp fibroblasts to produce the C-C chemokine MCP-4 (Nonaka et al., 2007). MCP-4 is a potent chemokine for eosinophils, monocytes and lymphocytes which are important immune cells in the nasal polyp (Cauna et al., 1972, Nonaka et al., 1995). They assessed the contribution of IL-4 to fibroblast mediated inflammation in nasal polyposis by evaluating the presence of IL-4 and pro-inflammatory lipid receptors on nasal polyp fibroblasts. From this they identified IL-4 receptors are present on nasal fibroblasts and that fibroblasts stimulated by IL-4 up regulate amounts of IL-6, CCL-11, MCP-4 & TGF-β1. The authors suggest that nasal fibroblasts contribute to ongoing inflammatory processes in nasal polyps, producing an environment to drive nasal polyp growth by releasing pro inflammatory IL-6 and pro fibrotic TGF-β which may work together in an autocrine fashion (Steinke et al., 2004).

1.3.8.2.4 Nasal polyp fibroblast chemotaxis of airway immune cells

Neutrophilic infiltrate of nasal mucosa in CRS is readily identified histologically. Presence of neutrophils suggests that during the development of CRS, neutrophil chemokines are generated. Rudack & colleagues (2002) isolated nasal polyp fibroblasts and treated them with TNF-α. Neutrophil chemokines were measured by ELISA and mRNA expression with biological chemotactic activity identified by three step high performance liquid chromatography. They identified that IL-8, Granulocyte chemotactic protein-2 (GCP-2) and growth-related oncogene α (GRO-α) were induced by pro-inflammatory stimuli, with the most significant neutrophil chemotactic activity resulting from IL-8. GRO-α contributed to neutrophil chemotaxis and GCP-2 represented a co-stimulatory chemokine from human nasal polyp fibroblasts. The secretion of IL-8 from CRS sinonasal fibroblasts also suggests

that once neutrophils have been attracted, they will themselves produce further IL-8 amplifying the inflammatory process. Subsequently, neutrophils will release further interleukins 1 and 6, interferon-γ (IFN-γ) and TNF-α to contribute to the chemotaxis and activation of additional immune cells.

Dendritic cells are critical mediators of antigen surveillance and presentation and can help to amplify adaptive immune responses. They are present in upper airway diseases including CRSwNP, though their regulation in CRS is not yet clear. Nonaka et al (2010c) investigated the role of Macrophage inflammatory protein-3α (MIP-3α), a known migratory factor for immature dendritic cells in nasal polyp fibroblasts. Nasal polyp fibroblasts cultured with Toll-like receptor (TLR) 2, 3, 4, 5 ligands, IL-1β, and TNF-α induced MIP-3α expression, as quantified by mRNA on real time RT-PCR and ELISA measurement of protein levels. They discuss the fact that fibroblasts make up 47% of the cells present in nasal polyps (Jordana M, 1995), and since the proportion of activated fibroblasts is higher in nasal polyps, they may well represent a critical source of inflammatory mediators. The researchers further propose that nasal polyp fibroblasts may contribute to dendritic cell recruitment by TLR and pro inflammatory cytokine induced production of MIP-3α.

1.3.8.2.5 Nasal polyp fibroblast interactions with the adaptive immune system

Recruitment and activation of B cells to sites of upper airway inflammation will engage the humoral immunity of the adaptive immune system. B lymphocyte stimulator (BLyS) has potent stimulatory activity on B cells and their subsequent immune responses. Yamada & colleagues (2010) examined BLyS expression in human nasal polyp fibroblasts. They identified that BLyS was present in nasal polyp fibroblasts and its expression was markedly induced by the viral TLR analogue Poly I:C in a dose dependent manner. BLyS is an important survival factor for lymphocytes - increasing B-cell, CD4 positive T-cell and natural killer cell activity (Shan et al., 2006). BLyS is targeted therapeutically in patients with systemic lupus erythematosus with the monoclonal antibody belimumab. The finding that BLyS is overexpressed in nasal polyp tissue may allow future therapeutic trials of similar agents in nasal polyposis.

1.3.8.2.6 Intracellular nasal polyp fibroblast *Staphylococcus aureus*

Staphylococcus aureus is one of the major pathogens in CRS with nasal polyps, and is thought to produce exotoxins that act as superantigens in polyp formation (Bachert et al., 2007). Persistence of *Staphylococcus aureus* may be a factor in the chronicity of nasal polyp inflammation. The potential for *S. aureus* to reside intracellularly, thus being protected from extracellular host defence mechanisms is likely to promote nasal persistence. It has been established that fibronectin binding proteins on the fibroblast surface facilitate intracellular human *S. aureus* invasion via its associated receptor integrin $\alpha_5\beta_1$ (Alexander and Hudson, 2001). Following internalisation, *S. aureus* is capable of inducing pro-inflammatory cytokines to exacerbate the disease microenvironment. Clement et al. (2005) identified invasion of *S. aureus* into fibroblast and myofibroblastic cells of CRS patients nasal mucosa by confocal scanning microscopy. Clusters of greater than ten intracellular *Staphylococcus aureus* organisms were frequently seen intracellularly encapsulated within a ring of α smooth muscle actin.

In summary, the fibroblast in chronic sinusitis with nasal polyposis appears to have multiple roles, especially in regard to airway remodelling, immune cell chemotaxis and contributing directly to the inflammatory milieu, all hallmarks of nasal polyp formation.

The understanding of chronic rhinosinusitis disease pathophysiology is certainly increasing following concerted international effort, though is by no means complete. The large burden of CRS disease requires more effective therapy and only by understanding the disease mechanisms can progress with new therapies become a reality. The potentially paradigm changing role for fibrosis early in the disease appears to be somewhat supported by investigation of registries of clinical patient outcome data for patients who have had delayed surgery for CRS after medical therapy has failed. The role of fibrosis and the fibroblast in CRS therefore merits further study.

1.4 Approaches to investigating nasal cells in chronic rhinosinusitis

A number of different techniques will be employed in this thesis to investigate nasal cells including fibroblasts and will be described in the following sections. The use of transcriptome analysis within chapter 5 is introduced here.

1.4.1 Transcriptome analysis

The transcriptome is the sum of all RNA within cells, tissues or an organism. It differs from the genome (DNA) which remains fairly static. The transcriptome reflects all the genes that are actively being expressed at a point in time, therefore will vary with environment or disease conditions. Knowledge of the transcriptome is a very useful way to analyse the molecular make up of cells and tissues, to interpret functional elements of the genome and to help understand disease. Study of the transcriptome has been made possible with advances in powerful nucleic acid sequencing technology, in part driven by the Human Genome Project. High throughput sequencing technology dramatically reduced the time, and hence cost, resulting in the phrase 'next generation sequencing'. Within this thesis I will use both microarrays and next generation RNA sequencing to investigate the transcriptome of sinonasal tissue biopsies and isolated cells from CRS patients and healthy controls.

1.4.1.1 Microarrays

Microarrays have been available for transcriptome research for a few decades, with evolving complexity and range of targets. Microarrays utilise a series of known single stranded DNA probes hybridised onto a solid chip surface. The DNA being investigated is labelled with a fluorophore and if it hybridises with one of the known complementary probes it fluoresces a specific colour which can be measured following stimulation with a laser (Figure 9). The raw data produced consist of the fluorescence intensities for all the hybridised probes, which are then background corrected and normalised. This is facilitated by a number of in built control probes within the array. The background corrected, normalised data is then suitable for further downstream bioinformatics analysis. Microarrays often contain many tens of thousands of DNA probes so a single sample can be interrogated for many genes at a time. However, samples can only be investigated for the known DNA probes on the chip rather than all the possible nucleic acids within the sample.

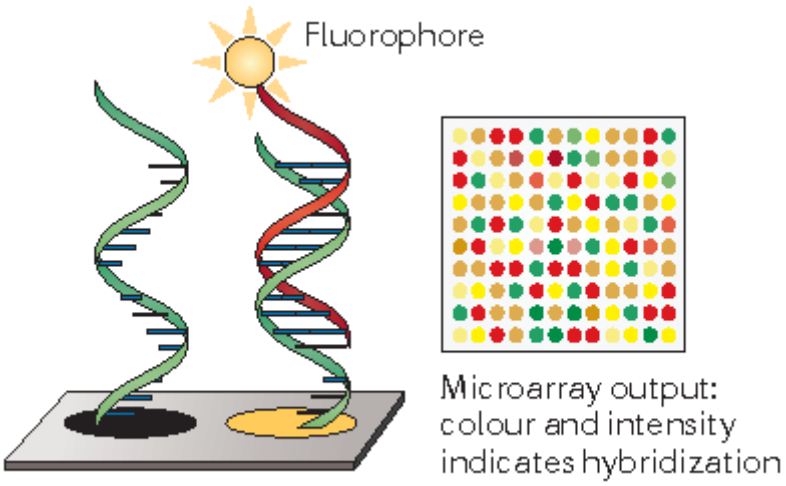

Figure 9. Schematic illustration of a microarray. Known DNA probes are attached to a microarray chip (green DNA strand). Complementary DNA labelled with a fluorophore within the sample can hybridise to the probes (red strand). Following a series of washing steps hybridised probes can be stimulated with a laser and the fluorescence measured for down stream bioinformatics analysis. Image adapted from (Goodwin et al., 2016).

1.4.1.2 RNA sequencing

RNA sequencing is a more recent and sophisticated form of transcriptome analysis. In comparison to microarray technology, RNA sequencing directly determines all the complementary DNA sequences in a sample. Historically this was performed by the much slower, more expensive and non-quantitative Sanger dideoxy sequencing method developed in the 1970s which was the mainstay of sequencing technology for nearly 40 years (Sanger et al., 1977). RNA sequencing first involves the generation or libraries from the RNA by fragmenting into short read segments with adaptors attached to each end. The fragments are then amplified many times and bound to a template with adaptors. The template concentration and localisation are directed by patterned flow cells to control and increase the cluster density of amplified fragments. The sequencing is then determined by synthesis; complementary fluorophore labelled nucleotides then bind to the fragments which are read following excitation with lasers. The fluorophores are then cleaved from the newly synthesised DNA strand and the process is repeated sequentially until all of the fragments have been synthesised and read (Figure 10). Once sequencing has been completed, all the reads are aligned to a reference genome with information provided about the genes present and their expression level available for further bioinformatics analysis.

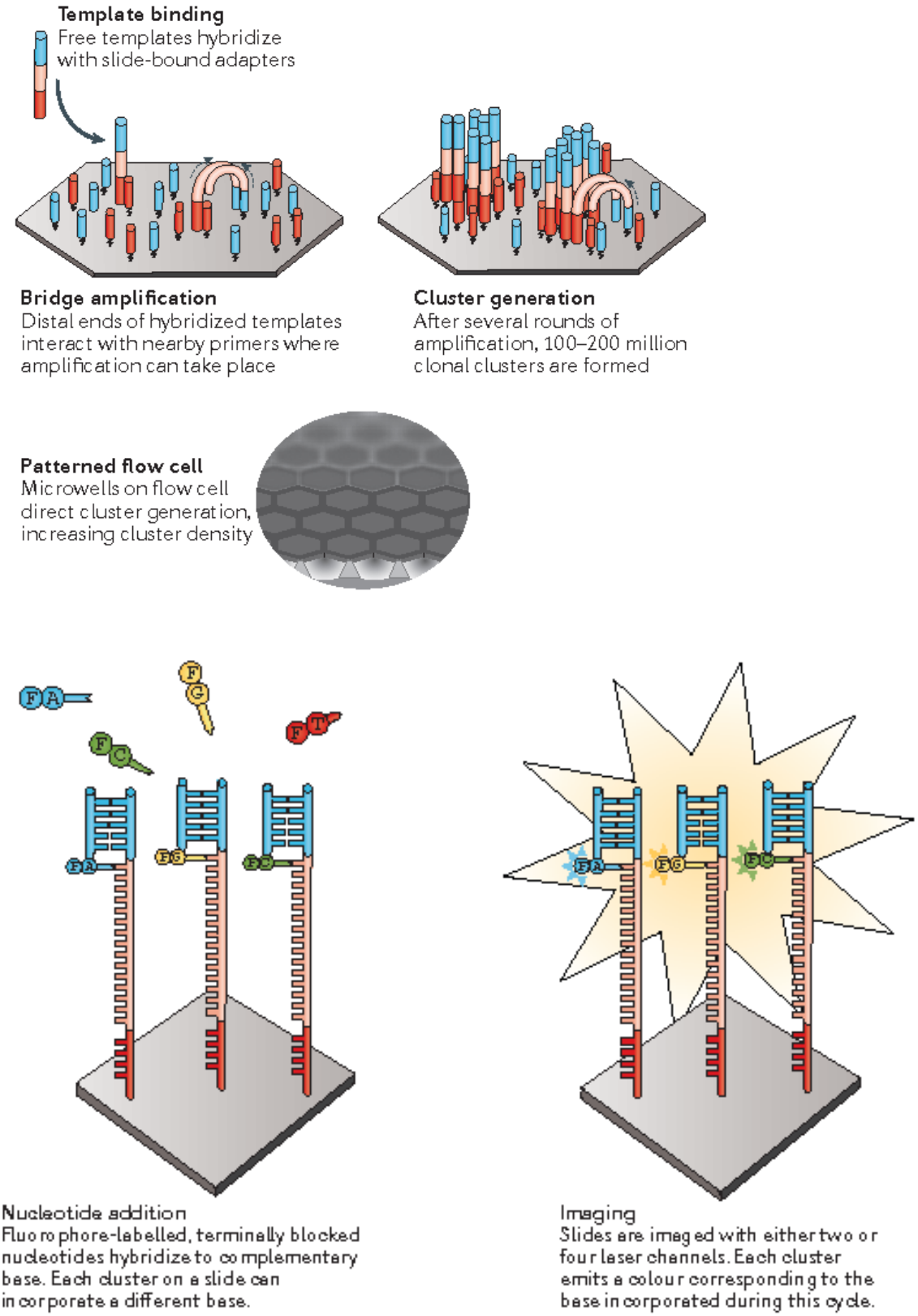

Figure 10. Schematic illustration of RNA sequencing. RNA samples are first fragmented into short read segments with adaptors attached to either end, amplified and bound to a flow cell. The short fragments are synthesised with fluorophore labelled nucleotides which are read sequentialy following stimulation with a laser. The process is repeated till the sequence and amounts of all the fragments is known. Image adapted from (Goodwin et al., 2016)

1.5 Hypothesis, aims and objectives

1.5.1 Hypotheses

The pathophysiology of chronic rhinosinusitis without nasal polyps (CRSsNP) is in part due to key differences in tissue structural cells such as epithelial and fibroblast cells. Further, epithelial and fibroblast cells contribute to the pathophysiology of CRSsNP by driving the inflammatory and fibrotic environment of CRSsNP. Nasal epithelial cells and fibroblasts will be significantly different between healthy control and CRSsNP participants in terms of their cytological appearance, behaviour and transcriptome and be useful models representative of their parent tissues for the study of CRSsNP.

1.5.2 Aims

1(a). Recruit phenotyped cohorts of control & CRSsNP participants.

1(b). Characterise recruited CRSsNP participants' tissue samples and isolated epithelial & fibroblast cells.

2. Assay the sinonasal environment to determine any associations among infection, inflammation and remodelling.

3. Identify clusters of genes differentially expressed in CRSsNP & control participants.

1.5.3 Objectives

1. Recruit a cohort of well phenotyped CRSsNP patients and controls from the Newcastle Hospitals. Patients will be phenotyped on the basis of a) quantification of symptoms by patient reported outcome measures, b) radiologically by CT scans and c) histologically.

2. Isolate and characterise patient derived primary nasal epithelial cells and primary nasal fibroblasts by tinctorial, immunohistochemical and electron microscopy and compare these cellular observations to their associated participant tissue biopsies.

3. Characterise the environment of the sino-nasal cavities by measurement of inflammatory cytokines, known human disease biomarkers and microbial species present by mucosal lining fluid analysis, sandwich and multiplex ELISA and quantitative RT-PCR.

4. Characterise the transcriptome of CRSsNP tissue biopsies and isolated primary epithelial and fibroblast cells using microarrays and RNA sequencing.

2 General laboratory methods

2.1 Tissue culture

2.1.1 Primary cell culture

All tissue culture work was performed within sterile class II laminar flow hoods in a dedicated tissue culture lab. Harvested primary nasal epithelial cells (PNECs) were isolated from their cytology brushes and centrifuged at 400g for 4 minutes to pellet cells. PNECs were then re-suspended in 15ml of Lonza basal epithelial growth (BEGM) media (BEGM BulletKit CC-3171 & CC-4175) at 37˚C. PNECs were then placed into 75ml submerged tissue culture flasks (Greiner Bio-One, Germany) that had been coated with 0.5% collagen I (Nutacon Purecol, Netherlands) to facilitate adherence. Once in tissue culture flasks, PNECs were viewed with a phase contrast microscope (Nikon, Japan) and motile cilia could be seen for 72 hours until ciliated cells were lost and adherent basal cells were seen confirming harvest of viable epithelial cells. Cells were grown in a tissue culture incubator enriched with 5% CO2 at 37˚C until confluent at passage zero (P0). Once confluent, PNECs were trypsinised with 2ml 0.25% trypsin EDTA (T4049, Sigma UK) for approximately 5 minutes then re-suspended in cell culture media prior to use in experiments or frozen down to build up an archive of primary patient-derived PNECs. All samples were stored in a biobank in accordance with the Human Tissue Act (HTA reference: 12195)

Primary nasal fibroblasts (PNFs) were directly isolated from sinonasal biopsy samples using an outgrowth technique. Resected biopsy specimens were dissected into 1-2mm tissue fragments whilst still in media and then placed in a scored 10cm vented petri dish to aid cell adherence. On top of each 1-2mm tissue fragment one drop of Sigma high glucose Dulbecco's Modified Eagle's Medium (DMEM) media (DMEM 5671, Sigma) with 100iu/ml penicillin/streptomycin (P0781, Sigma), 50ml foetal calf serum (FCS) (F9665, Sigma), 2mM L-Glutamine (G7513, Sigma) and 5ml Amphotericin B (A2942, Sigma) was added for 24 hours. Following the first 24 hour incubation with minimal media to aid adherence, a further 10ml of media was added to the petri dish. As soon as islands of fibroblast cells were observed to be proliferating out from the tissue fragments, PNFs were trypsinised and seeded in 75ml tissue culture flasks and grown to passage 1 (P1). Once confluent, cells were trypsinised for either experimentation or freezing as part of the study archive.

Cells in culture were maintained with media changes every 2-3 days. In addition to growth in culture flasks, cells were cultured for microscopy on 13mm coverslips (collagen coated for PNECs) inserted into a 24 well culture plate using the same culture conditions.

Primary human lung fibroblasts were isolated and cultured using the same methodology as described for nasal fibroblasts. Primary human lung fibroblasts were kindly donated via a related lung transplantation project within our group's laboratories, with appropriate research governance approvals co-ordinated by my supervisor Professor Fisher.

2.1.2 Cell line culture

Searches for commercially available cell lines were performed using the online catalogues of the American Type Culture Collection (ATCC) and European Collection of Cell Cultures (ECACC) using the search terms nose, sinus and human. Searches identified only one appropriate cell line, RPMI 2650 which was purchased and grown in standard laboratory cell culture conditions as detailed above. A vial of $2x10^6$ cells was cultured as per the supplier's instructions (ATCC) in Sigma Eagle's Minimum Essential Medium (EMEM) (M2279, Sigma) with supplemental 1% non-essential amino acids (7145, Sigma), 100iu/ml penicillin/streptomycin (P0781, Sigma), 50ml foetal calf serum (FCS) (F9665, Sigma) and 2mM L-Glutamine (G7513, Sigma). Cells were supplied at P26 and were amplified in T175 tissue culture flasks to generate sufficient cell numbers for the required experiments. Cells were grown as submerged monolayer cultures in tissue culture flasks for stimulation experiments and on 13mm circular coverslips for imaging.

2.1.3 Cell viability

Cell viability was assessed either by propidium iodide (P4170, Sigma, UK) flow cytometry or automated cell counting of trypan blue (T8154, Sigma) stained cells with an EVE cell counter (NanoEnTek, USA). For flow cytometry cells were washed in phosphate buffered saline (PBS) (D8537, Sigma), re-suspended in phenol free minimum essential medium (MEM) (51145, Sigma) with 10µl propidium iodide added prior to running samples on a 3 laser BD FACS CantoII instrument as per manufacturer's instructions.

2.1.4 Freezing & archiving cultured cells

Cells were trypsinised with 0.25% primary cell trypsin-EDTA and re-suspended in their respective media. Cells were then centrifuged at 400g for 4 minutes and the supernatant was removed. The cells were then re-suspended in cell freezing medium (C6164, Sigma UK) at $1x10^6$ cells/ml as determined by cell counting with an automated cell counter (EVE, NanoEnTek, USA). Cells were cooled at 1°C per minute to -80°C in a Mr. Frosty cell freezer (C1562, Sigma UK) and then transferred to archived liquid nitrogen storage.

2.2 Epithelial cell treatments

Confluent monolayers of cultured PNECs were stimulated with a number of CRS disease relevant stimuli. Cells were grown in 24 well tissue culture plates and stimuli were applied for 24 hours at which point cells were harvested and their viability was measured using propidium iodide (P4170, Sigma, UK) flow cytometry. The media was collected to determine the relative amounts of inflammatory cytokine & alarmin release from the stimulated cells. Cells were cultured with a six -point dose range of stimulants; diesel exhaust particles from 0-100µg/ml, cigarette smoke extract 0-100% solution (see below for protocol), hydrogen peroxide solution 0-10mM (16911, Sigma UK), whole cell lysates of laboratory reference strains of *Pseudomonas aeruginosa* and patient derived *Haemophilus influenza* 0-100µl/ml and thapsigargin 0-100µM (T9033, Sigma, UK). Dose ranges were identified from previous work on airway epithelial cells within our laboratory (Suwara et al., 2014).

2.2.1 Cigarette smoke extract preparation

Cigarette smoke produced from one University of Kentucky reference research grade cigarette was drawn through 25ml of Lonza BEGM basal epithelial growth media over 2-3 minutes with a vacuum pump in a fume hood. The media containing cigarette smoke extract (CSE) was then sterile filtered using a 0.2 µm pore size Minisart filter and designated 100% CSE. CSE was diluted to concentrations as required for stimulation experiments, with Lonza BEGM basal epithelial growth media. Once prepared, CSE was immediately used for cell treatments to prevent degradation.

2.2.2 Bacterial whole cell lysates

Whole cell lysates of *Pseudomonas aeruginosa* lab reference strain PA01 and a patient derived *Haemophilus influenza* (kindly supplied by Dr Liz Moisey) were generated by streaking out bacteria on to brain, heart infusion (BHI) media (LM1135, Oxoid, UK) agar plates and incubated at 37˚C overnight to form colonies. Colonies were then scraped off the agar and re-suspended to an even solution in PBS to a bacterial optical density standard of 0.2 at 600nm. The suspension was sonicated for 3 cycles on ice using a Branson Sonifier 150 (Sigma) and placed on ice. A one hour incubation with 200µg/ml of DNase II at 37˚C, then 1mg/ml proteinase K incubation for 2 hours at 60˚C was performed, followed by boiling at 100˚C for 20 minutes to inactivate proteinase K. Lysates were confirmed rather than live bacteria by re-streaking on BHI agar plates overnight to demonstrate the absence of colony formation.

2.3 Fibroblast treatments

Confluent monolayers of cultured PNFs were stimulated with a range of recombinant human alarmin proteins to determine their inflammatory response. PNFs were cultured in 6-well tissue culture plates and, once confluent, serum starved for 24 hours in modified Eagle's medium (M4526, Sigma UK). Human recombinant alarmins were added for 24 hours' incubation using doses determined from previous work within our laboratory (Suwara et al., 2014); IL-1α (200-LA, R&D Systems) and IL-1β (201-LB, R&D Systems) 125pg/ml & 500pg/ml, HMGB-1 50ng/ml & 200ng/ml (1690-HM, R&D Systems), LPS (L2630, Sigma) and Poly I:C (P1530, Sigma) 5µg/ml & 20µg/ml. After 24 hours in culture, the media was harvested, centrifuged at 600g for 5 minutes to pellet any debris and the supernatants stored at -80^{o}C prior to analysis by ELISA. Adherent PNFs were trypsinised and their RNA was extracted using a NucleoSpin RNA extraction kit (Machery-Nagel, Germany) as described below.

2.4 RPMI 2650 cell line treatments

Monolayers of PNECs and RPMI 2650 cells approaching confluence were stimulated with CRSsNP disease relevant pro-inflammatory ligands: TNF-α 1ng/ml, 5ng/ml, 10 ng/ml (T0157, Sigma), Lipopolysaccharide (LPS) 0.1μg/ml, 1 μg/ml, 10 μg/ml (L2630, Sigma), Polyinosinic:polycytidylic acid (Poly I:C) 50 μg/ml, a synthetic viral analogue (P9582, Sigma) and TGF-β 5ng/ml (T7924, Sigma) for 3 and 24 hours to determine if the cells were able to mount appropriate inflammatory responses. Untreated control cells without inflammatory ligands were cultured in parallel. Standard curves were performed as internal controls to ensure reproducibility between experiments. All cells were treated with identical conditions in triplicate repeats from the same batch of inflammatory ligands. Following stimulation, the conditioned media was harvested and the inflammatory response measured by the amount of IL-8 released into the culture media. Quantification was by sandwich ELISA for IL-8 protein as per manufacturer's instructions (DY208, R&D systems).

2.5 Macrophage conditioned media

Conditioned media from cultured macrophages (THP-1 cell line and peripheral blood mononuclear cell isolation) were kindly provided by Dr Lee Borthwick & David Dixon. Briefly, THP-1 cells were cultured in complete RPMI 1640 media till confluence, then polarised for 48 hours in RPMI 1640 with 10ng/ml IFN-γ (R&D Systems, 285-IF-100) and 1μg/ml LPS (Sigma, L2880) for M1 macrophages or 2ng/ml of IL-13 (R&D systems, 213-ILB-025) and 2ng/ml IL-4 (R&D systems, 204-IL-010) for M2 macrophages. After 8 hours, polarised cells were then washed and RPMI 1640 media was incubated for 24 hours to generate conditioned media. Peripheral blood mononuclear cells were isolated from consenting volunteers (NRES REC reference: 12/NE/0121) using gradient centrifugation with Percoll (17-5445-01, GE Healthcare). Monocytes were separated from peripheral blood mononuclear cells by CD14 MicroBead magnetic separation (Miltenyi Biotec) following manufacturer's instructions. Primary human monocytes were subsequently cultured in Lonza X-Vivo-10 primary media (BE04-743Q, Lonza) and polarised as for THP-1 cells, with the appropriate X-Vivo-10 primary cell media.

Conditioned media from M0, M1 and M2 polarised macrophages as above was incubated with cultures of primary nasal fibroblasts to investigate the effect of interleukin (IL) 1α and IL-1β blockage with blocking antibodies; IL-1 α (R&D systems, AF-280-NA), IL-1β (R&D

systems, AF-201-NA) and IL-1 receptor antagonist (R&D systems, 280-RA) following the protocol developed in our laboratory by Suwara et al. (2014).

2.6 Reverse transcription polymerase chain reaction

2.6.1 RNA extraction from cultured cells

RNA was extracted from confluent cells using a NucleoSpin RNA extraction kit (Machery-Nagel, Germany) as per manufacturer's instructions. The optional DNase I digestion step was included. The concentration in ng/µl and purity by absorbance at 260/280nm and 260/230nm of isolated RNA were determined using a nanodrop 2000 spectrophotometer (Thermoscientific, USA). Samples were kept on ice throughout and stored at -80˚C.

2.6.2 RNA extraction from tissue biopsies

RNA extraction from tissue biopsy samples was performed with Life technologies RecoverAll Total Nucleic Acid Isolation Kit (Ambion, USA) as per manufacturer's instructions. Tissue biopsy samples were homogenised in a bead homogeniser (Qiagen TissueLyser II, Netherlands) for two cycles of 2 minutes at 30Hz. Both the protease digestion and DNase I digestion step were performed. The quality and concentration of isolated RNA was assessed with a nanodrop 2000 spectrophotometer as above.

2.6.3 qRT-PCR

Quantitative RT-PCR was used to measure relative levels of gene expression using the standard ΔΔCt (cycle threshold) method; ΔΔCt= 2^(Ct of reference gene – Ct of candidate gene). cDNA was reverse transcribed from isolated RNA samples using the BIORAD iScript cDNA synthesis kit as per manufacturer's instructions. 10ng of cDNA template was used per qRT-PCR reaction using SYBR Green JumpStart Taq Ready Mix on an Applied Biosystems 7500 Real-Time PCR System for 35 cycles. 1µl of forward and reverse primers were supplied by Eurofins per reaction. PCRs were performed in triplicate repeats with a no template or mRNA negative control. Expression levels of mRNA were normalised to those of healthy controls for relative mRNA expression data. Products formed in the qRT-PCR reactions were verified by 2% agarose gel electrophoresis and compared to a 100 base pair ladder.

2.6.3.1 Primers

Gene	Forward primer	Reverse primer
GAPDH	GAGTCAACGGATTTGGTCGT	GACAAGCTTCCCGTTCTCAG
SAA	CAGACAAATACTTCCATGCT	ATTGTGTACCCTCCCCC
TARC	ACTGCTCCAGGGATGCCATCGTTTTT	ACAAGGGGATGGGATCTCCCTCACTG
VCAM1	GGCAGAGTACGCAAACACTT	GGCTGTAGCTCCCCGTTAG
Eotaxin-3	AACTCCGAAACAATTGTACTCAGCTG	GTAACTCTGGGAGGAAACACCCTCTCC
CCL2	GGCTAAACTCATCCATACTGT	GCACTGAGATCTTCCTATTGGTGAA
CCL4	CCAAACCAAAAGAAGCAAGC	AGAAACAGTGACAGTGGACC
CCL17	ACTGCTCCAGGGATGCCATCGTTTTT	ACAAGGGGATGGGATCTCCCTCACTG
IL-6	TACCCCCAGGAGAAGATT	AAGGTTCAGGTTGTTTTC
PlGF	CAGAGGTGGAAGTGGTACCCTTCC	CGGATCTTTAGGAGCTGCATGGTGAC
sFLT-1	ACAATCAGAGGTGAGCACTGCAA	TCCGAGCCTGAAAGTTAGCAA
SFRP4	GCCAACTTTGGCAACGTATC	GTGGACACTGGCAAGAAGAA
IFI27	TGCCTCGGGCAGCCT	TTGGTCAATCCGGAGAGTCC
TNFRSF19	TTGGTCAATCCGGAGAGTCC	GCCACATTCCTTAGACAACTCC
LOX	AAAACCAAGGGACATCAGA	GGCTAAACTCATCCATACTGT
SULF1	AACATTGCTAAGCGTCAT	CACTCGGACAGTGGTAGG
ITGB1	CACTCGGACAGTGGTAGG	CCCCTGATCTTAATCGCAAA
GAGE5	CCCCTGATCTTAATCGCAAA	TTCACCTCCTCTGGATTTGG
NFE2L3	TCCCAGCATGAGGAAAATGA	TTCTGCCTCCCAGTCAGGTTT

Table 3. RT-PCR primers.

2.7 Cell staining

Cells grown on 13mm coverslips were washed twice in PBS, fixed in 4% paraformaldehyde for 10 minutes and then washed with PBS. Glycine (100mM) was added to quench any remaining paraformaldehyde. Cells were permeabilised in 0.1% Triton-X100 (T8787, Sigma) in PBS for 30 minutes, washed twice in PBS 0.2% Tween 20 (P1379, Sigma) and once further in PBS. Cells were then either stained with H&E to assess cellular morphology or using immunocytochemical techniques for epithelial and mesenchymal markers. Primary antibodies were incubated at 4^{o}C overnight as follows: rabbit anti-human cytokeratin 17 (Abcam ab53707), mouse anti-human cytokeratin 19 (Abcam ab52625), mouse anti-human

pancytokeratin (ab6401) mouse anti-human E-cadherin (ab15148), rabbit anti-human vimentin (Abcam ab92547), rabbit anti-human α smooth muscle actin (Abcam ab5694) and rabbit anti-human fibronectin (Sigma F3648). Fluorophore-conjugated secondary antibodies at 1:100 dilution in 5% bovine serum albumin PBS-0.2% Tween 20 were incubated for 90 minutes in the dark: goat anti-mouse FITC conjugated (Sigma F2012) and goat anti-rabbit TRITC conjugated (Sigma T6778). Negative controls were performed with secondary only antibodies and matched IgG isotype negative controls to identify if there was non-specific binding or background auto fluorescence. Coverslips were mounted on slides with DAPI Vectashield (H1200, Vector USA) and images were captured with a Nikon A1 confocal microscope on a Nikon Eclipse NI-E upright stand running Nikon Elements 4.30.02, with a x20 0.75Na Plan Apo lens.

2.8 Enzyme linked immunosorbent assay (ELISA)

Sandwich ELISA kits were used to quantify amounts of cytokines released from stimulated cultures of PNECs & PNFs. A 96 well format ELISA kit was used to measure the amount of cytokines as per manufacturer's instructions (R&D systems). The amount of cytokine present was read by the optical densities at 450nm and calculated relative to a known standard curve on a Multiskan FC spectrophotometer (Thermoscientific, USA).

2.9 Statistical analysis

Statistical analysis of experimental results was mainly performed using the non-parametric Mann Whitney U test with a significance level of $p<0.05$ unless otherwise stated, since due to the relatively small sample sizes a normal distribution could not be assumed. Statistical analysis of the bioinformatics data is presented in their respective results chapters. Graphical data are presented visually as the mean, with standard error of the mean.

3 Results - Participant recruitment & sample characterisation

3.1 Specific aims & objectives

The specific aims & objectives for this phase of research were to recruit a well phenotyped cohort of research patient participants with non-polypoid chronic rhinosinusitis (CRSsNP) and a cohort of healthy control volunteers as sources for appropriate tissue and cells for further study. I aimed to establish matched patient and control epithelial and fibroblast cells with functional data on their differential responses to disease relevant stimuli. The samples were further used in studies to analyse the sinonasal environment in CRSsNP and comprehensively characterise the RNA transcriptome.

3.2 Scientific rationale for experimental approach

Chronic rhinosinusitis is a heterogeneous condition with an as yet unknown pathophysiology. There are two distinct subtypes, those with and those without nasal polyps and it has been postulated that there will be an as yet undefined emerging number of endotypes or sub-phenotypes. Analysis of patients with CRS requires careful prior phenotyping to ensure similar patients are being studied to draw meaningful conclusions. I triangulated my participant phenotyping according to

1. Endoscopic appearance in terms of presence/absence of nasal polyps

2. Symptom severity from patient reported outcome measure score

3. Radiological appearance on cross sectional CT scanning scores.

Data concerning the microbiological environment were also collected as the resident flora has an impact on the local sinonasal tissues. The tissue biopsies collected and cells isolated underwent confirmatory histological and electron microscopic examination. Isolated cells were also stimulated with a number of disease relevant stimuli to confirm their viability and functional responsiveness.

3.3 Methods

3.3.1 Research Governance approvals

A research protocol, patient information sheets, patient invitation letters & consent forms were produced and submitted to the Sunderland office of the National Research Ethics Service (NRES) together with the standard accompanying documents. National Institute of Health Research (NIHR) Good Clinical Practice (GCP) training and assessment for consenting research participants was completed.

Ethical approval for the project was granted from the Sunderland office of the NRES, REC reference 13/NE/0099. Newcastle Hospitals NHS Foundation Trust R&D project approval was given, reference 6487. Caldicott approval was granted from the Newcastle Hospitals Information Governance Officer, reference 6487 (2520). Research participants were successfully recruited to the study to allow investigation of human tissue biopsies, primary sinonasal cells and mucosal samples with the required research governance details stored in the study master file. The project is registered on the NIHR Clinical Research Network UKCRN ID: 14335.

3.3.2 Participant recruitment

Participants undergoing elective operations for chronic rhinosinusitis according to the EPOS 2012 international consensus document (Fokkens et al., 2012) were invited to participate in the study. Control participants undergoing elective operations that use the nose as an access route, for example for non-functioning pituitary gland surgery, in the absence of sinusitis symptoms or clinical findings were also invited to participate. Participants were non-allergic based on their clinical history, were invited for definitive skin prick testing and free of corticosteroids via all routes for the preceding two weeks. Standardised patient letters of invitation and participant information sheets were sent in advance of admission for operation to the Freeman Hospital ENT surgery department. On the day of admission I discussed the study and addressed any questions raised by potential participants. Those who agreed to participate in the study signed a consent form. The original was inserted into the study master file, with a copy given to the participant and one filed in the patient's hospital notes. Recruited participants completed the well validated patient reported outcome measure to quantify their sinonasal symptoms; Sinonasal outcome test 22 (SNOT-22 - see appendix for questionnaires) (Hopkins et al., 2009a). Once collected, participants'

cells, samples and data were given a unique study identifier to preserve confidentiality & anonymity prior to transport to the laboratory. All samples were stored in a HTA approved biobank reference: 12195. The same participant samples were used for each of the results chapters presented in the thesis.

3.3.3 Microbiological samples

Once enrolled in the study, patient participants proceeded to surgery as per the routine clinical practice. Following induction of general anaesthesia and prior to their operative procedure, a conventional microbiological swab was taken of the middle meatus, an anatomically important and constant landmark of the paranasal sinuses for standard culture and sensitivity. A viral swab was also taken from a cohort of twenty of the recruited participants to collect viral nucleic acids for molecular detection of respiratory viruses; *Influenza A, Influenza B, Rhinovirus, Respiratory Syncytial Virus, Parainfluenza 1-4, Adenovirus* and *Human metapneumovirus*. Using the same swab sample, molecular detection of common respiratory pathogens *Streptococcus pneumoniae, Chlamydia pneumoniae, Bordetella pertussis, Haemophilus influenza* and *Mycoplasma pneumoniae* was performed. Unfortunately it was not possible as part of this assay to investigate for the presence of *Staphylococcus aureus at this stage.* Samples were analysed by quantitative real time PCR and processed by the clinical diagnostic standard Public Health England Molecular laboratory, Royal Victoria Infirmary, Newcastle upon Tyne.

3.3.4 Primary cell harvesting

Having obtained microbiological and mucosal lining fluid analysis samples, I harvested primary nasal epithelial cells (PNECs). This was performed by gentle passage of a multipurpose cytology brush as in (Figure 11) (CellPath UK, M467). Cells were harvested from the middle meatus, the principal drainage area of the most commonly affected CRS sinuses and an anatomically consistent landmark. Cytology brushings were then placed in 15ml Falcon tubes containing Lonza BEGM cell culture media (Lonza UK, CC-3171 & CC-4175) and transported to the research laboratory.

(a)

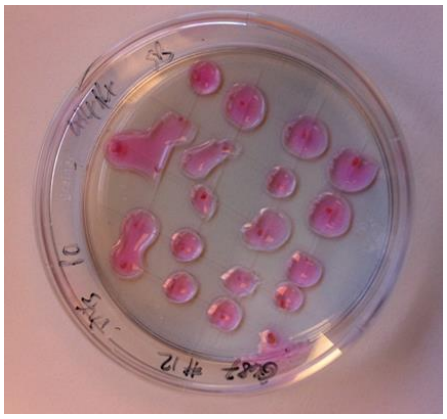

(b)

Figure 11. (a) Cytology brush for harvesting primary nasal epithelial cells. (b) Tissue biopsy fragments cut into 1-2mm size pieces on a cross-scored petri dish with a drop of media for the first 24 hours to generate primary nasal fibroblasts.

Primary nasal fibroblasts (PNFs) were harvested from small (2-5mm) research tissue biopsies from the uncinate process, a consistent anatomical landmark within the middle meatus. The uncinate process is usually resected and discarded as clinical waste during functional endoscopic surgery (FESS) for CRS. The resected uncinate processes were kept in physiological saline until the operation was complete (approximately 45 minutes). Once the surgeon was satisfied that they could be disposed of and not required for clinical histological examination they were collected for research. Samples were transported to the laboratory in Sigma high glucose DMEM media (DMEM 5671, Sigma UK) with 100iu/ml penicillin/streptomycin (P0781, Sigma UK), 50ml fetal calf serum (FCS) (F9665, Sigma UK), 2mM L-Glutamine (G7513, Sigma UK) and 5ml Amphotericin B (A2942, Sigma UK).

3.3.5 Biopsy sample processing and archiving

Surgically resected tissue biopsy specimens were processed to yield multiple sample types from the each patient with matched clinical and symptom data. A portion of tissue was fixed in formaldehyde to allow generation of paraffin embedded tissue sections for histology. A portion was stored in RNAlater and stored at -80^{o}C to allow RNA isolation from tissue biopsies. A further portion of tissue was frozen to allow the subsequent extraction and analysis of protein content.

3.3.6 Electron microscopy

3.3.6.1 Scanning electron microscopy

Samples were fixed overnight in 2% glutaraldehyde in Sorenson's phosphate buffer at 4°C, rinsed in several changes of phosphate buffered saline then dehydrated through a graded series of ethanol from 25% to 100% ethanol for a minimum of 30 minutes. Once in 100% ethanol, final dehydration was carried out by critical-point drying with carbon dioxide using a Baltec Critical Point Dryer. Samples were mounted on an aluminium stub with Achesons Silver ElectroDag. Mounted samples were coated with 15nm gold using a Polaron SEM Coating Unit and examined with a Tescan Vega LMU scanning electron microscope.

3.3.6.2 Transmission electron microscopy

Samples were fixed in 2% glutaraldehyde in 0.1M sodium cacodylate buffer at 4°C overnight, rinsed in several changes of phosphate buffered saline then a secondary fixation was completed with 1% osmium tetroxide in water for 1 hour. Samples were then dehydrated using graded acetone - 25%, 50%, 75% 100% acetone for a minimum of 30 minutes. Dehydrated samples were processed by impregnating with 25% resin in acetone, 50% resin in acetone, 75% resin in acetone then 100% resin for minimum of 3 changes over 24hrs. Samples were then embedded in 100% resin at 60°C for 24-36 hrs.

Semi-thin survey sections of 0.5µm were cut and stained with 1% toluidine blue in 1% borax to check for an appropriate region of interest. Relevant ultrathin sections (70 nm) were then cut using a diamond knife on a Reichert ultra microtome or a Leica EM UC7 ultra microtome. The sections were stretched with chloroform to eliminate compression and picked up on Pioloform-filmed copper grids. Grids were stained on a Leica EM AC20 automatic staining machine using 2% aqueous Uranyl Acetate and 3% Lead Citrate. Sections were examined using a Philips CM 100 Compustage (FEI) Transmission Electron Microscope and digital images are collected using an AMT CCD camera (Deben), Electron Microscopy Research Services, Newcastle University.

3.3.7 Tinctorial staining of biopsy samples

Paraffin embedded tissue sections of biopsy specimens were stained using haematoxylin and eosin staining to demonstrate tissue architecture. Sections were dewaxed in xylene for 5 minutes, rehydrated through graded alcohols and washed in water until slides were clear. Sections were then stained with freshly filtered Harris Haematoxylin for 1-2 min and washed in running tap water for 2- 3 minutes. Eosin Y was applied as a counterstain for 2 minutes and slides were washed to remove excess eosin then dehydrated through graduated xylene and mounted in DPX (06522, Sigma, UK).

Picro Sirius red staining was used to determine the histological visualization of collagen I and III fibres within the tissue biopsies. Paraffin sections were dewaxed in xylene then rehydrated and washed with water. Sections were treated with 0.2% phosphor molybdic acid, washed in distilled water and incubated with Picro Sirius red in the dark for two hours. They were then washed in 0.01% hydrochloric acid, dehydrated in increasing concentrations of ethanol followed by xylene and mounted in pertex mounting medium.

Sections were also stained with picro Mallory trichrome to demonstrate the presence of collagen deposition within tissue biopsies. Paraffin sections were dewaxed in xylene then rehydrated and washed with water. Nuclei were stained in Celestine Blue for 10 minutes followed by Haematoxylin for 10 minutes and washed in tap water. Picro orange staining was applied for 1 - 2 minutes, washed in tap water then stained with acid fuchsin for 2 minutes. Sections were rinsed in 2% acetic acid, differentiated in red differentiator and washed in tap water. Aniline blue stain was applied for 2 minutes, followed by a further 2% acetic acid rinse, dehydrated through graduated alcohols and mounted in DPX.

3.3.8 Immunohistochemical staining of biopsy samples

Paraffin embedded tissue sections were stained using antibodies to determine the composition of the resident immune cells. Neutrophils were stained with anti-neutrophil elastase, T-cells with anti CD3, monocytes and macrophages with anti CD68 and eosinophils with Sirius red carried out by the department of cellular pathology, Royal Victoria Infirmary, Newcastle upon Tyne.

3.3.9 Fluorescent immunohistochemical staining of biopsies and cells

Paraffin embedded tissue sections were dewaxed in xylene twice for 5 minutes, followed by two 5 minute incubations in 100% and 70% alcohol. Antigen retrieval was performed in 10mM EDTA at pH8 in a microwave at 700W for 15 minutes. Samples were allowed to cool and then non-specific binding was blocked with 5% BSA in PBS-0.2% Tween 20 (P1379, Sigma UK). Sections were incubated overnight with primary antibodies at 4^{o}C and then washed three times in PBS-Tween 20. Fluorophore secondary antibodies were then incubated for 90 minutes in the dark alongside a series of secondary only controls. Following three further PBS-Tween 20 washes sections were mounted with DAPI Vectashield (H1200, Vector USA). Images were captured with a Nikon A1 confocal microscope on a Nikon Eclipse NI-E upright stand running Nikon Elements 4.30.02, with a x20 0.75Na Plan Apo lens.

Cells grown on coverslips were fixed in 4% paraformaldehyde for 10 minutes and then washed with 1x phosphate buffered saline (PBS). 500µl 100mM glycine was added to quench any remaining paraformaldehyde. Cells were then permeabilised in 0.1% Triton-X100 (T8787, Sigma UK) in 1x PBS for 30 minutes and washed twice in PBS-0.2% Tween 20 (P1379, Sigma UK) and once further in 1xPBS. Cells were blocked with 5% bovine serum albumin (BSA) (A7906, Sigma UK) for 60 minutes to reduce non-specific binding. Primary antibodies were incubated at 4^{o}C overnight and then washed three times in PBS-Tween20. Fluorophore-conjugated secondary antibodies at 1:100 dilution were incubated for 90 minutes in the dark. The negative controls were incubated only with secondary antibodies to identify any non-specific binding or background auto fluorescence. After five washes with PBS-Tween20 cells were mounted on slides in DAPI Vectashield and images captured.

3.4 Results

3.4.1 Participant recruitment and clinical data

A cohort of 47 age and sex matched patient participants were recruited to enter the study (Table 4). Twenty five of the participants had a diagnosis of chronic rhinosinusitis without nasal polyps refractory to maximal medical management, defined as at least 3 months treatment with topical +/- systemic corticosteroids and antibiotics. Twenty two were healthy control volunteers having no sinusitis symptoms, radiological CT scan or endoscopic findings of sinonasal disease having had no previous surgical treatment. All patients had no specific history of allergy and were invited for skin prick testing. Assessment with transmission electron microscopy excluded a diagnosis of primary ciliary dyskinesia base on the typical '9+2' axoneme. The sinonasal patient reported outcome measure symptom scores of the two groups were significantly different ($p<0.0001$) as illustrated in Figure 12(a). The calculated Lund Mackay radiological CT scan scores were also significantly different ($p<0.0001$) between the control and chronic sinusitis cohorts as shown in Figure 12(b).

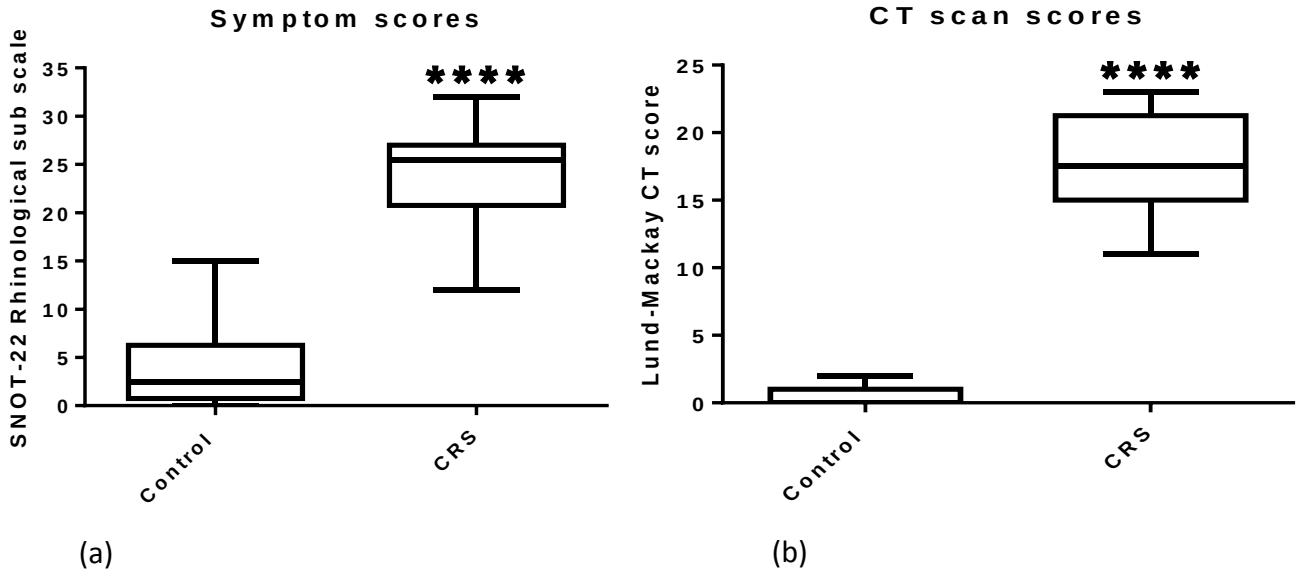

Figure 12. (a) Patient reported outcome measures of sinonasal symptoms (SNOT-22 questionnaire) in healthy control volunteers and chronic sinusitis patient participants without nasal polyps (CRSsNP). **** = $p<0.0001$.

(b) Lund Mackay CT scan scores in healthy control volunteers and chronic sinusitis patient participants without nasal polyps (CRSsNP). **** = $p<0.0001$ (n=47).

Patient ID	CRS / Control	Age	Sex
6487#1	Control	***35***	F
6487#2	CRS	***48***	F
6487#3	Control	***65***	M
6487#4	CRS	***64***	F
6487#5	Control	***68***	F
6487#6	Control	***52***	M
6487#7	CRS	***71***	M
6487#8	Control	***71***	M
6487#9	CRS	***62***	F
6487#10	CRS	***44***	F
6487#11	CRS	***59***	M
6487#12	CRS	***63***	M
6487#13	Control	***64***	M
6487#14	CRS	***68***	M
6487#15	CRS	***37***	F
6487#16	Control	***59***	M
6487#17	CRS	***40***	M
6487#18	control	***36***	M
6487#19	CRS	***53***	M
6487#20	CRS	***43***	F
6487#21	control	***68***	F
6487#22	CRS	***69***	M
6487#23	CRS	***40***	F
6487#24	CRS	***66***	M
6487#25	control	***43***	F
6487#26	CRS	***69***	F
6487#27	control	***43***	F
6487#28	CRS	***73***	F
6487#29	Control	***73***	F
6487#30	Control	***60***	F
6487#31	Control	***43***	M
6487#32	CRS	***41***	M
6487#33	Control	***90***	F
6487#34	Control	***26***	F
6487#35	CRS	***48***	F
6487#36	Control	***31***	M
6487#37	Control	***63***	M
6487#38	Control	***67***	M
6487#39	CRS	***73***	M
6487#40	Control	***77***	M
6487#41	CRS	***46***	F
6487#42	Control	***73***	M
6487#43	CRS	***57***	M
6487#44	CRS	***64***	F
6487#45	CRS	***63***	F
6487#46	CRS	***25***	F
6487#47	Control	***69***	M

Table 4. Table detailing recruited participant's demographic data

3.4.2 Microbiological data

Analysis of recruited control participants' sinonasal microbiological environment by conventional culture identified clinically significant growth (*Staphylococcus aureus*) in only one. *Staphylococcus aureus* was identified from three of the chronic rhinosinusitis patient participants. There were no polymicrobial isolates on conventional culture. A molecular analysis was performed on 20 of the participants. This included multiplex RT-PCR for both bacterial and viral pathogens. *Streptococcus pneumoniae* and *Haemophilus influenza* were found in seven individuals, six in the rhinosinusitis cohort. There was no evidence of *Influenza A, Influenza B, Rhinovirus, Respiratory Syncytial Virus, Parainfluenza 1-4, Adenovirus* and *Human metapneumovirus*.

3.4.3 Histological characterisation

Haematoxylin and eosin staining of healthy control samples confirmed the typical healthy appearance of ciliated sinonasal pseudostratified epithelium (Figure 13ii(a)). Serial sections immunostained for the presence of inflammatory cells (Figure 13ii (b-e)) show minimal evidence of either neutrophils with neutrophil elastase, T-cells with CD3, macrophages and monocytes with CD68 or eosinophils with Sirius red.

Sections from participants with CRSsNP appeared markedly different. Figure 13i(a) shows the typical non-polypoid appearances of epithelial cell damage and loss of cilia, combined with inflammatory cell recruitment and basement membrane thickening. Immunohistochemical analysis of the recruited immune cells demonstrates a mixed inflammatory infiltrate of neutrophils, T-cells, macrophages and monocytes and eosinophils.

Sections were also stained for fibrosis with Picro Sirius. CRSsNP participants showed a dense thick band of staining at the level of the basement membrane consistent with increased deposition of a matrix of collagens 1 and 3 (Figure 14 (a+b)). The increased deposition of collagen 1 and 3 is visible immediately below an epithelial layer with the typical disease appearances of epithelial and cilial loss. Healthy control patient participants in contrast show much less mucosal basement membrane collagen deposition and an intact ciliated pseudostratified epithelial layer (Figure 14 (c+d)).

Tinctorial staining with Picro Mallory trichrome highlights the CRSsNP appearances of connective tissue deposition and immune cell recruitment. Figure 14(e) shows a low power view through the uncinate process with the bony component stained clear red. The overlying mucosa is better visualised in higher magnification in Figure 14(f+g) where the typical features of epithelial and cilial loss are again demonstrated, combined with basement membrane thickening and immune cell recruitment.

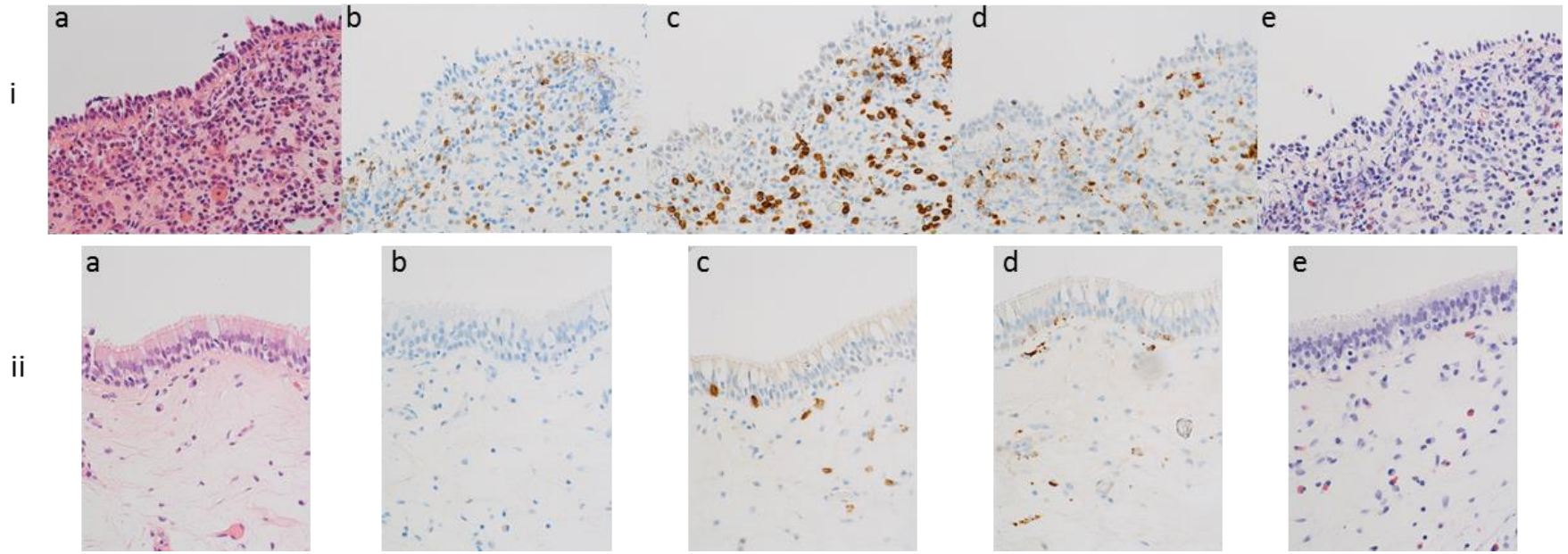

Figure 13. Immunohistochemical analysis of immune cell infiltration and distribution in chronic rhinosinusitis (panel i) and healthy control participants (panel ii).

(a) H&E stained tissue section, panel (i) demonstrates typical pathological findings in chronic rhinosinusitis; epithelial cell loss, infiltration of immune cells in the fibroblast rich lamina propria and basement membrane thickening, panel (ii) shows the normal healthy sinonasal pseudostratified epithelium. Immunohistochemical staining for (b) neutrophils with neutrophil elastase, (c) T-cells with CD3, (d) macrophages and monocytes with CD68 (e) eosinophils with Sirius red, magnification x40 (n=30).

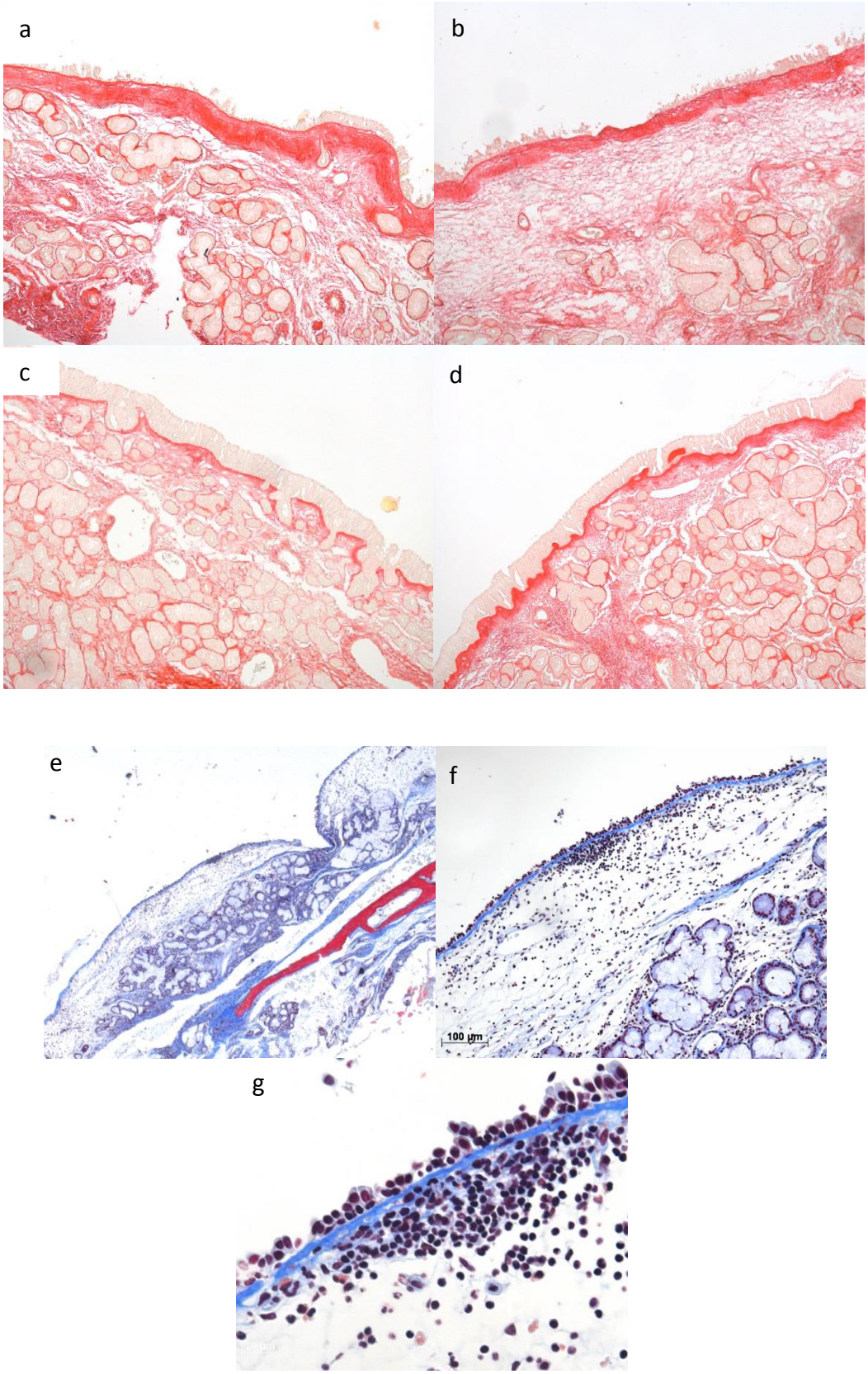

Figure 14. Tinctorial staining of chronic rhinosinusitis without nasal polyposis (CRSsNP) and healthy control participant tissue biopsies. (a+b) Picro Sirius red staining of CRSsNP participant sections (c+d) Picro Sirius red staining of healthy control participant tissue sections. Magnification x20. (e-g) Picro Mallory trichrome staining of CRSsNP participant tissue section. Magnification x10(e) x20 (f) x40 (g) (n=10)

3.4.4 Tissue biopsy electron microscopy

The ultrastructural epithelial health and integrity was first investigated with scanning electron microscopy. Control samples (Figure 15 (a+c)) show low power images of a healthy pseudostratified epithelium with a dense network of intact cilia. CRSsNP samples (Figure 15 (b+d)) show the predicted marked epithelial and cilial loss, together with airway remodelling and deposition of fibrotic matrix. When viewed in higher power magnification such as Figure 15(d) x10 000 or Figure 16(b) x35 100, a few remaining epithelial cells with damaged, shortened cilia are visible in stark contrast to the high power views of healthy ciliated epithelial cells (Figure 16 (a)).

Transmission electron microscopy was also performed. Figure 17(a) shows the intact epithelium of a healthy control participant with the notable features of a continuous epithelial layer and abundant cilia, some of which are cut in longitudinal section and others in cross section. Below the apical epithelial layer mitochondria can be seen to supply the large amounts of energy required by the motile cilia. Figure 17(b) demonstrates a high power magnification (x64 000) through a cross section of healthy control participant cilia with the distinctive '9+2' axoneme. Figure 18(a+b) shows the dense epithelial covering of cilia and abundant mitochondria below the apical membrane for their supply of energy. When the transmission electron microscopy images are compared to the chronic rhinosinusitis without nasal polyposis participants there are quite significant differences. Figure 19 demonstrates the loss of epithelial cells and cilia. Figure 20 shows that there are still some isolated clusters of cilia, which is best demonstrated in Figure 20b, however the epithelium has an unhealthy looking appearance with formation of multiple vesicles and unhealthy looking mitochondria.

Figure 21 compares the mucosal glands between healthy control participants and those with non-polypoid chronic rhinosinusitis. The healthy control tissue mucosal glands in Figure 21(a) show regular healthy columnar epithelial cells. The mucosal glands from diseased tissue in Figure 21(b) do not share the same regular, healthy appearance with increased vesicle formation and abundant mucous typical of chronic rhinosinusitis.

Control **CRS**

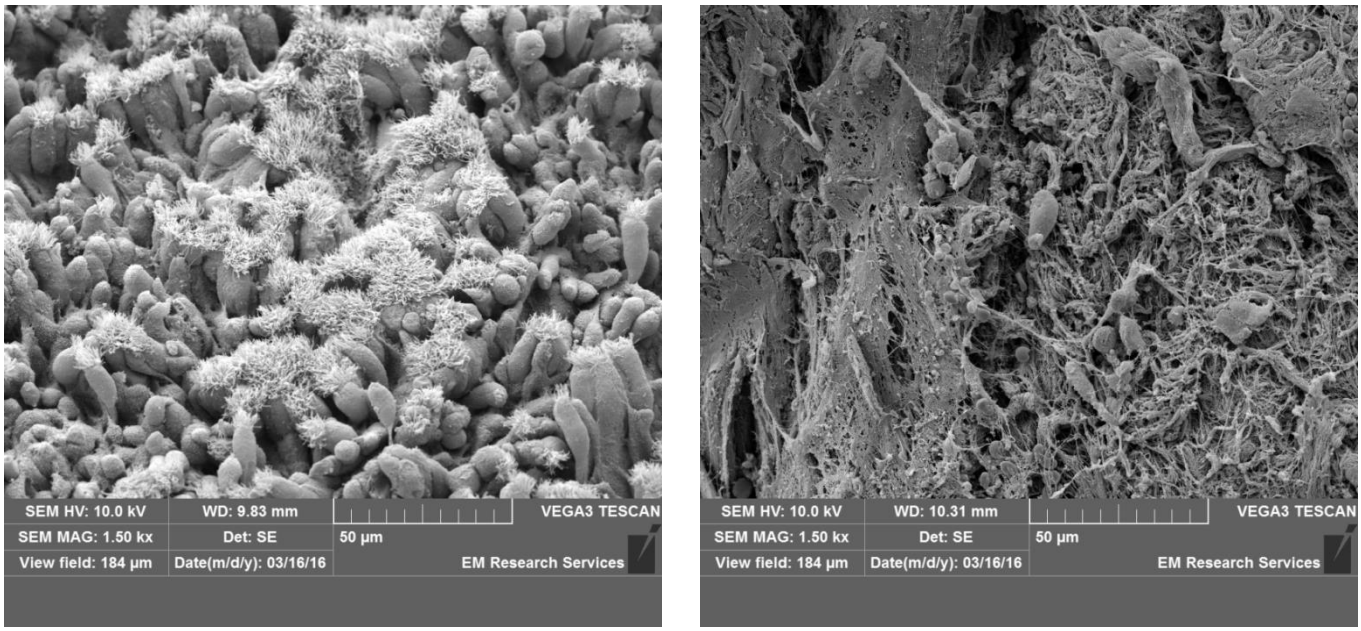

(a) (b)

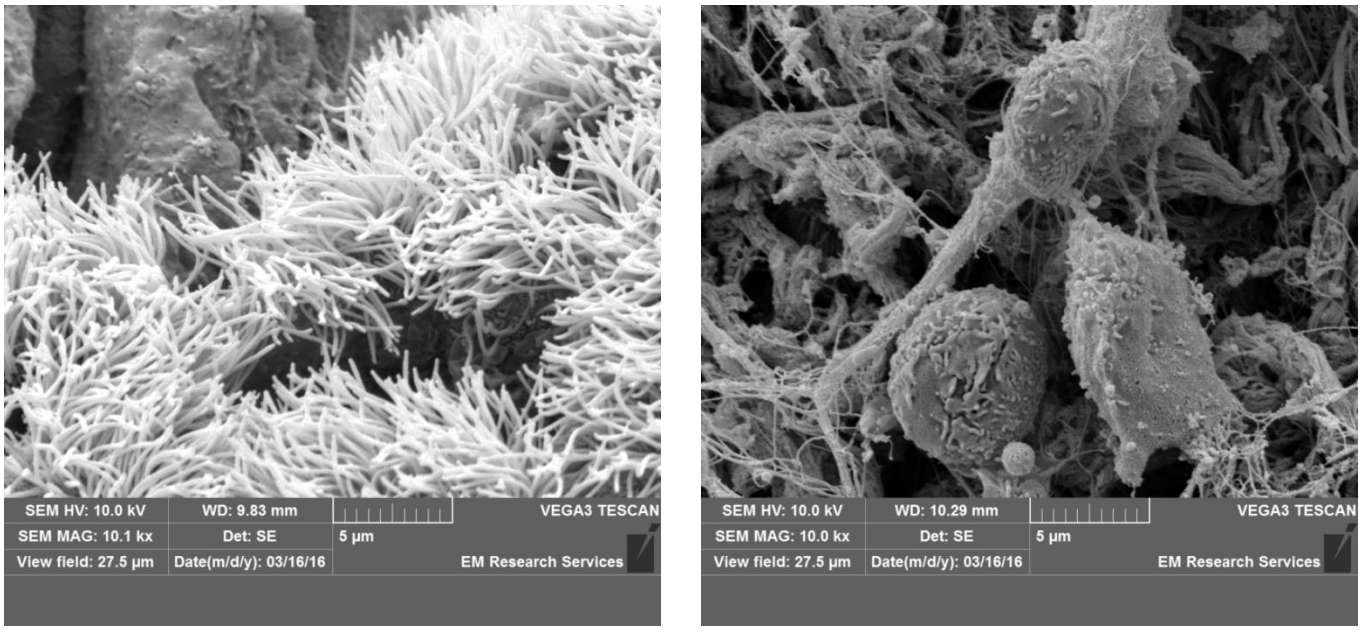

(c) (d)

Figure 15. Scanning electron microscopy images of study participants healthy sinonasal mucosal tissue biopsy samples and chronic rhinosinusitis without nasal polyps (CRSsNP) samples. Compared to healthy control mucosa CRSsNP samples demonstrate the typical appearances of loss of cilia and epithelial cells and airway remodelling. Magnifications; panels (a+b) 1500x, panels (c+d) 10 000x (n=6).

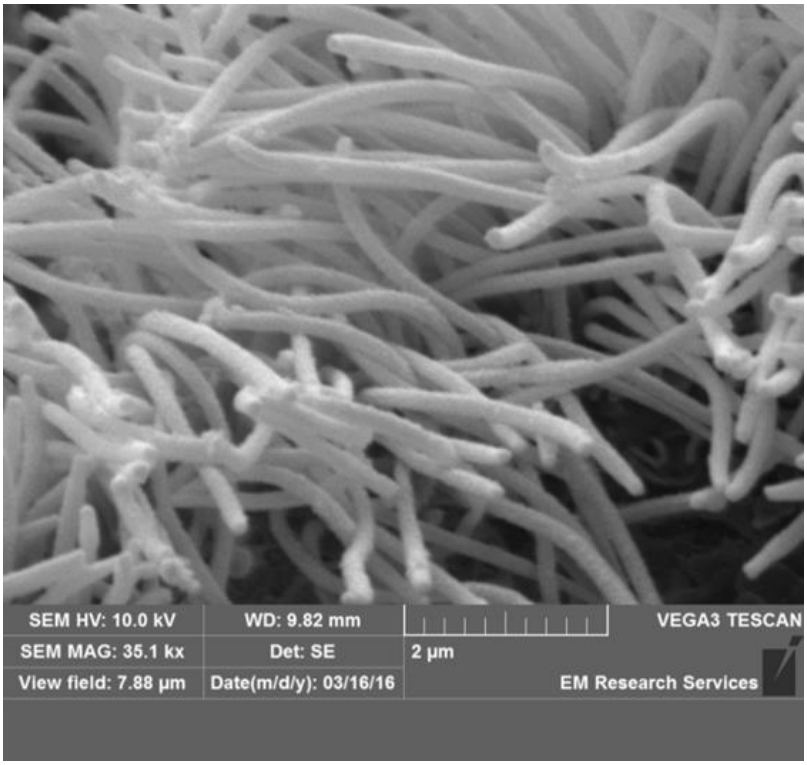

(a)

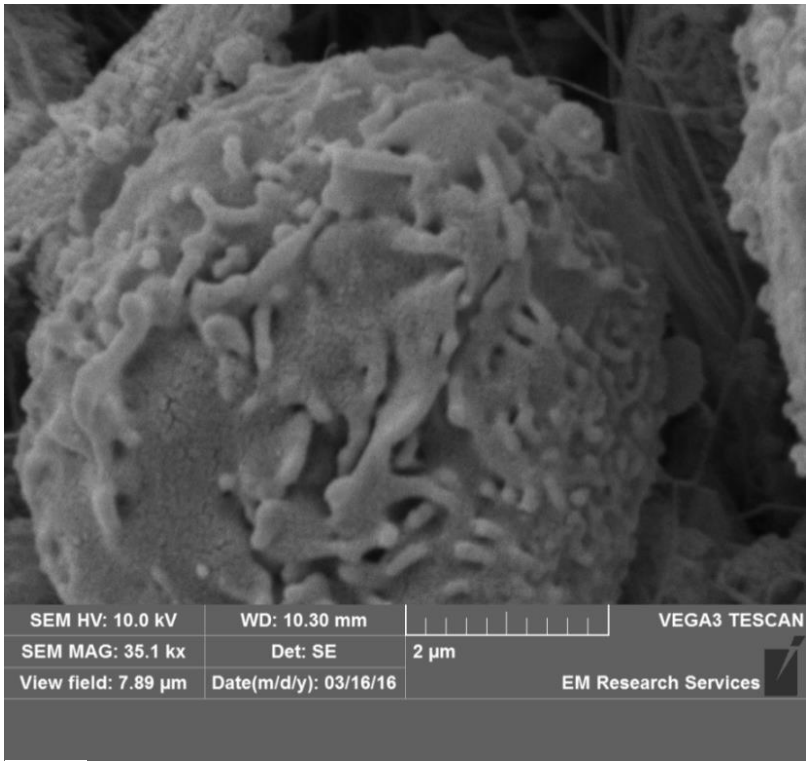

(b)

Figure 16. High power scanning electron microscopy images show (a) healthy sinonasal mucosa with cilia arising from their associated epithelial cells. (b) Chronic rhinosinusitis images demonstrate epithelial remodelling with loss of cilia. Magnification 35 100x (n=6).

(a)

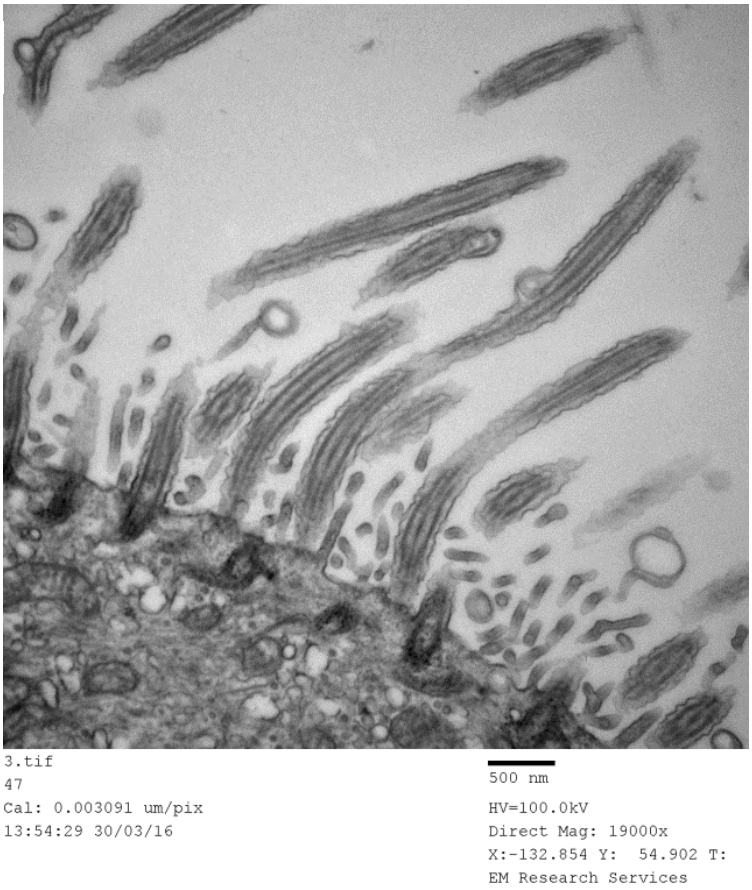

(b)

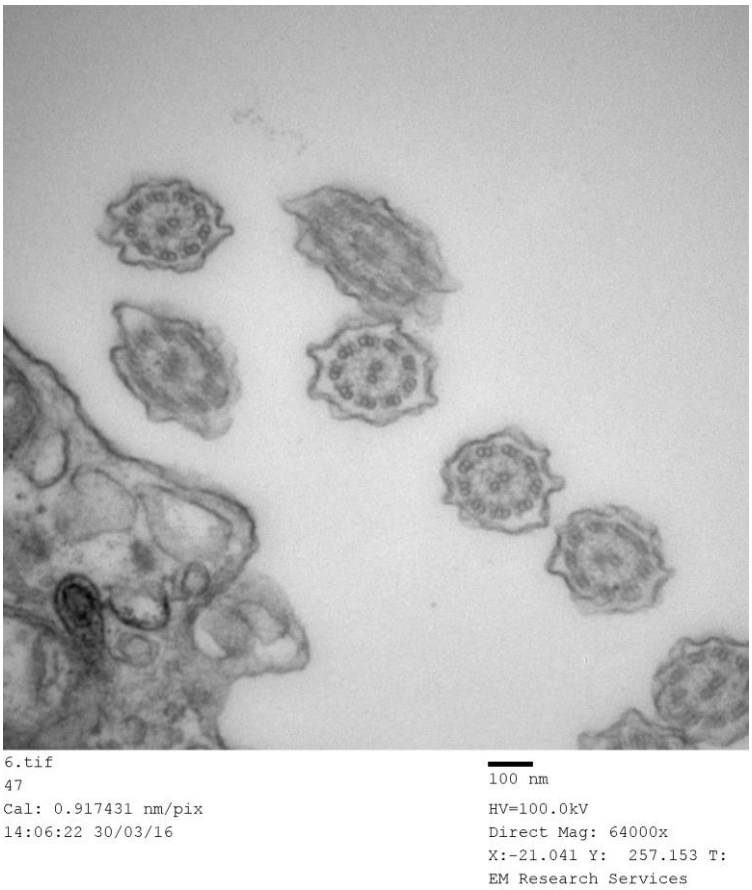

Figure 17. Transmission electron microscopy images acquired from healthy control volunteers. (a) shows longitudinal sections of the sinonasal cilia arising from the epithelial surface. Magnification 19 000x. There are also some areas within the image where the cilia have been cut in cross section. (b) shows cross sections through the healthy cilia with the distinctive 9+2 axoneme pattern. Magnification 64 000x (n=6).

(a)

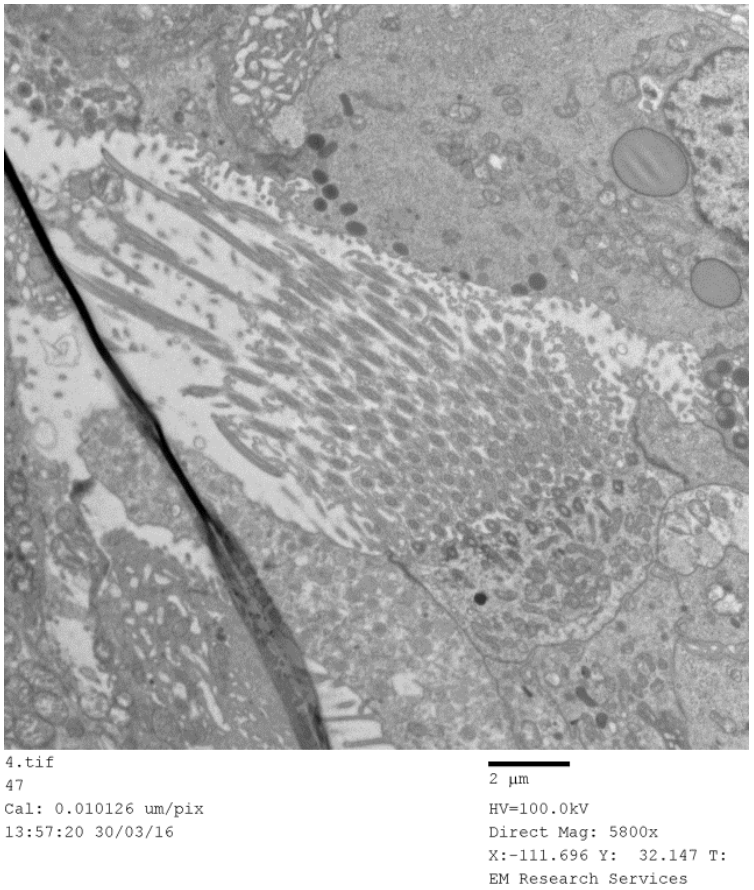

(b)

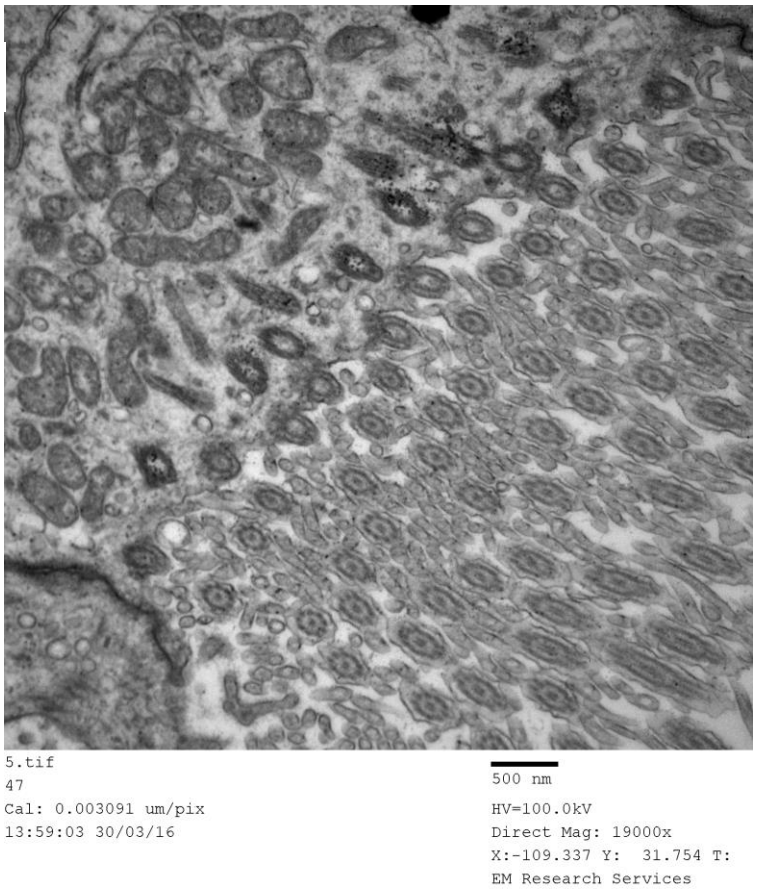

Figure 18. Transmission electron microscopy images acquired from healthy control participants demonstrating abundant cilia arising from the epithelial surface (a+b). Note the numerous mitochondria to provide the energy for the dynein motor domains for motion. Magnification 5800x (a) 19 000x (b) (n=6)

(a)

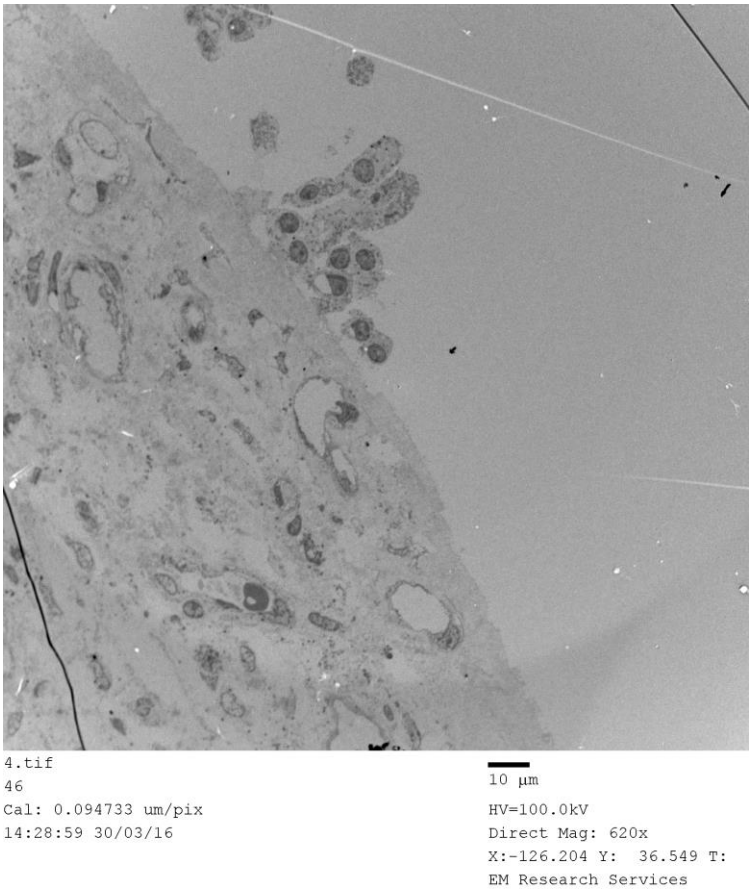

(b)

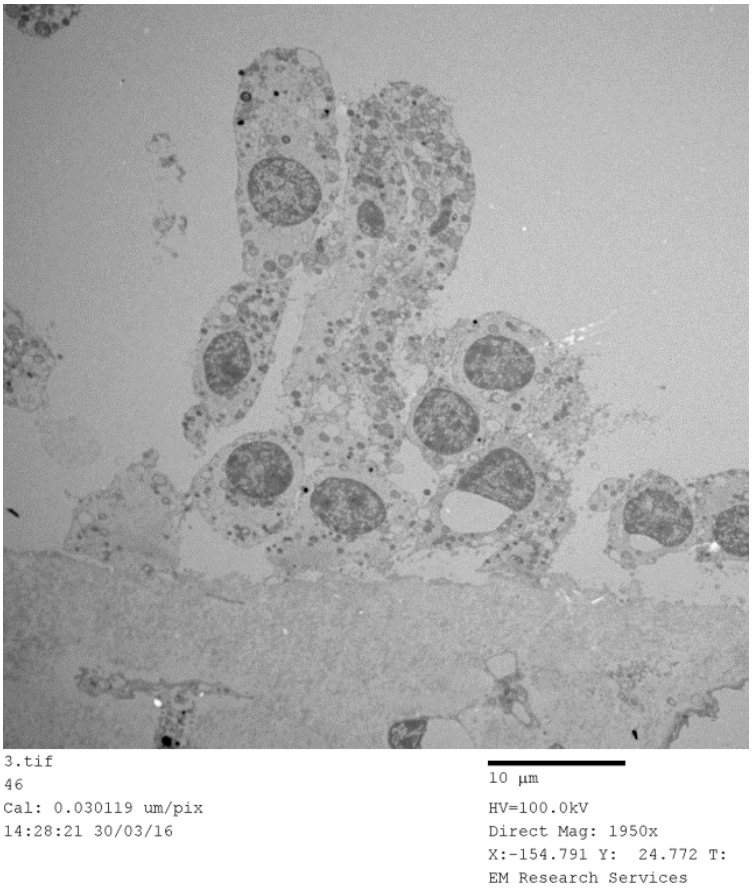

Figure 19. Transmission electron microscopy images captured from chronic rhinosinusitis without nasal polyposis patient participants. Micrographs detail the loss of epithelial cells and cilia present in the tissue biopsies (a+b). Magnification 620x (a) 1950x (b).(n=6)

(a)

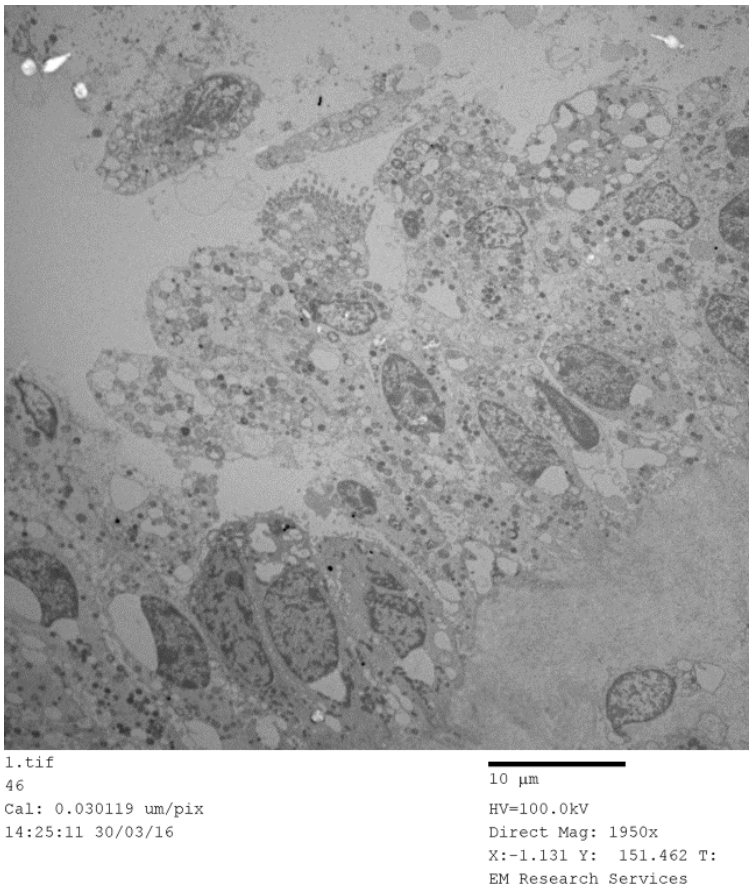

(b)

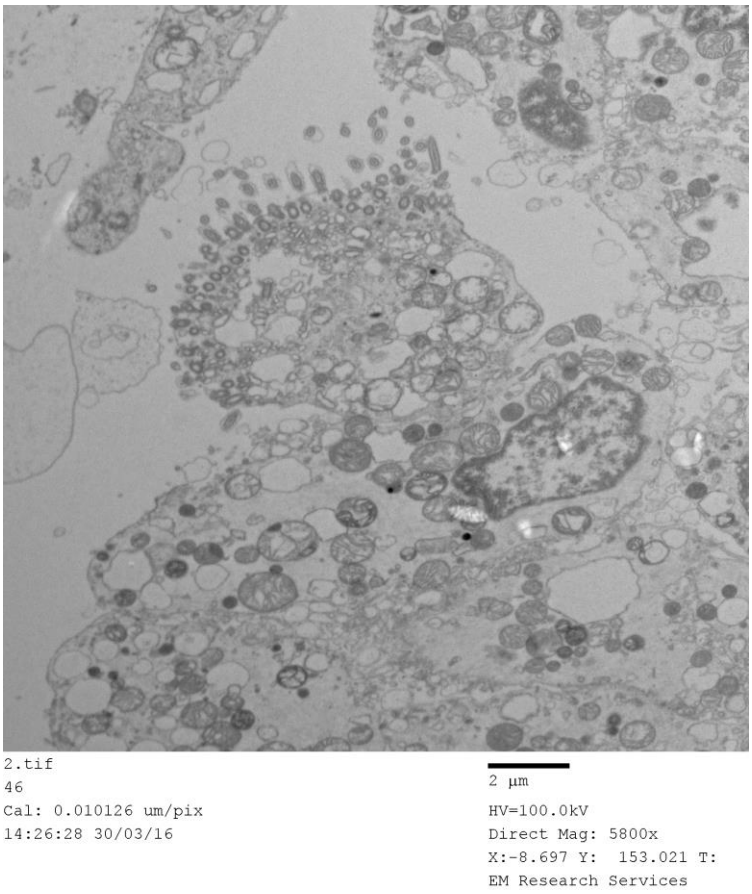

Figure 20. Transmission electron micrograph images acquired from chronic rhinosinusitis without nasal polyposis patient participants. Images show some areas of preserved cilia on a pseudostratified epithelium. Surrounding this there is marked loss of cilia upon an unhealthy epithelial layer. Magnification 1950x (a) 5800x (b) (n=6)

(a)

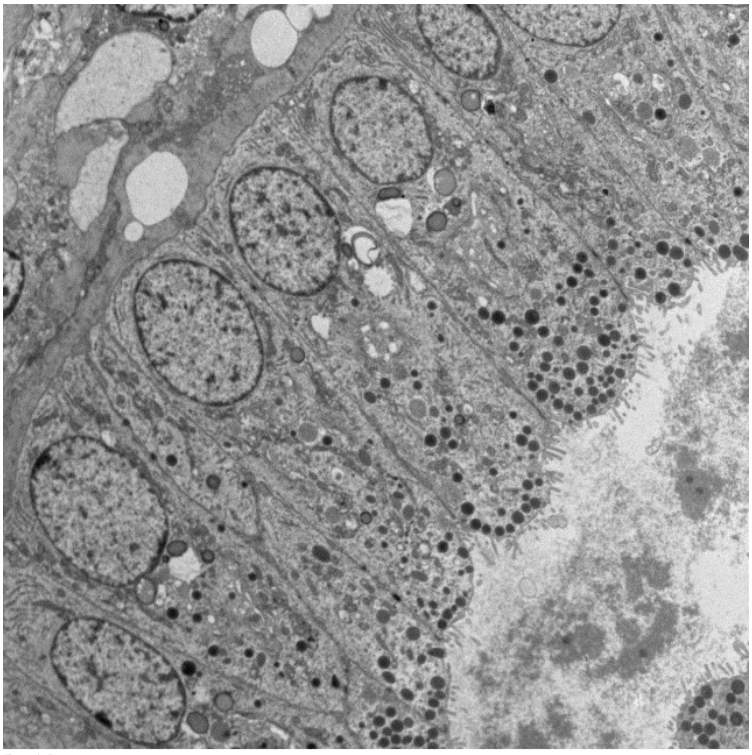

(b)

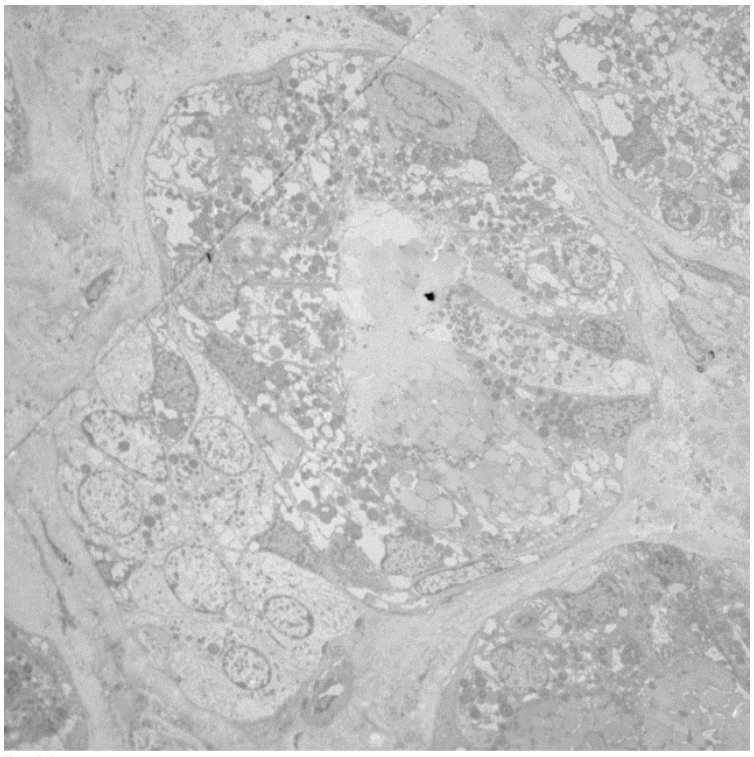

Figure 21 Transmission electron micrograph images captured of mucosal glands from healthy control volunteers (a) magnification 3400x and chronic rhinosinusitis without nasal polyposis (CRSsNP) patient participants (b) magnification 1450x. (a) shows a normal healthy glandular appearance in contrast to the images in CRSsNP (b).(n=6)

3.4.5 Tissue biopsy immunohistochemistry

Antibody staining methods were optimised prior to fluorescent immunohistochemistry. A range of epithelial and mesenchymal markers was used to complement the previous observations. A combination of epithelial marker antibodies is shown on healthy control samples in Figure 22 with their associated control samples. Figure 22(b-d) shows strong staining of the epithelial layer of the mucosal biopsy with cytokeratin 17 as identified by the TRITC red. There is an intact pseudostratified epithelial layer with nuclei counterstained in blue with DAPI. Figure 22(d) is dual stained for β-tubulin conjugated with FITC green and demonstrates an intact cilial layer to the epithelium. The cilial staining is also demonstrated with FITC green in isolation in Figure 22(g). The integrity of the epithelial layer is further confirmed by the presence of E-cadherin in Figure 22(e+f) where there is strong staining of the epithelial cells. The presence of E-cadherin confirms it is a healthy pseudostratified epithelium with the formation of tight junctions. There is also staining of E-cadherin below the epithelial layer in the lamina propria which is consistent with the columnar epithelial cells which line the sinonasal mucous glands.

Staining of tissue sections using mesenchymal antibodies as markers of fibroblasts is shown in Figure 23. Figure 23(a) is a control image and (b-d) are triple stained with FITC green for E-cadherin, TRITC red for vimentin, fibronectin and α-smooth muscle actin respectively and all sections have a blue DAPI as a nuclear counterstain. Sections show strong TRITC red staining for the mesenchymal markers in the lamina propria where fibroblasts typically reside underneath the basement membrane of the epithelial layer. Sitting within the areas of TRITC red conjugated mesenchymal staining are the mucous glands staining green from the E-cadherin proteins within the columnar epithelium.

The combination of epithelial and mesenchymal markers shown can be used to characterise the differences between mucosal tissue biopsies in health and CRSsNP. Figure 24 compares the epithelial staining in health and disease, the intact ciliated pseudostratified epithelium seen in health is not seen in CRSsNP. The epithelial stains seen in CRSsNP tissue sections highlight the epithelial damage, loss of tight junctions and loss of cilia. Figure 25 compares the mesenchymal marker expression between healthy control biopsy sections and those from chronic rhinosinusitis without nasal polyposis. In CRSsNP there is an increased staining of TRITC red conjugated mesenchymal markers vimentin, fibronectin and α-smooth muscle actin when compared to healthy control participant biopsies. Tissue sections have been

counterstained with FITC green conjugated E-cadherin and blue DAPI nuclear stain to aid orientation and comparison.

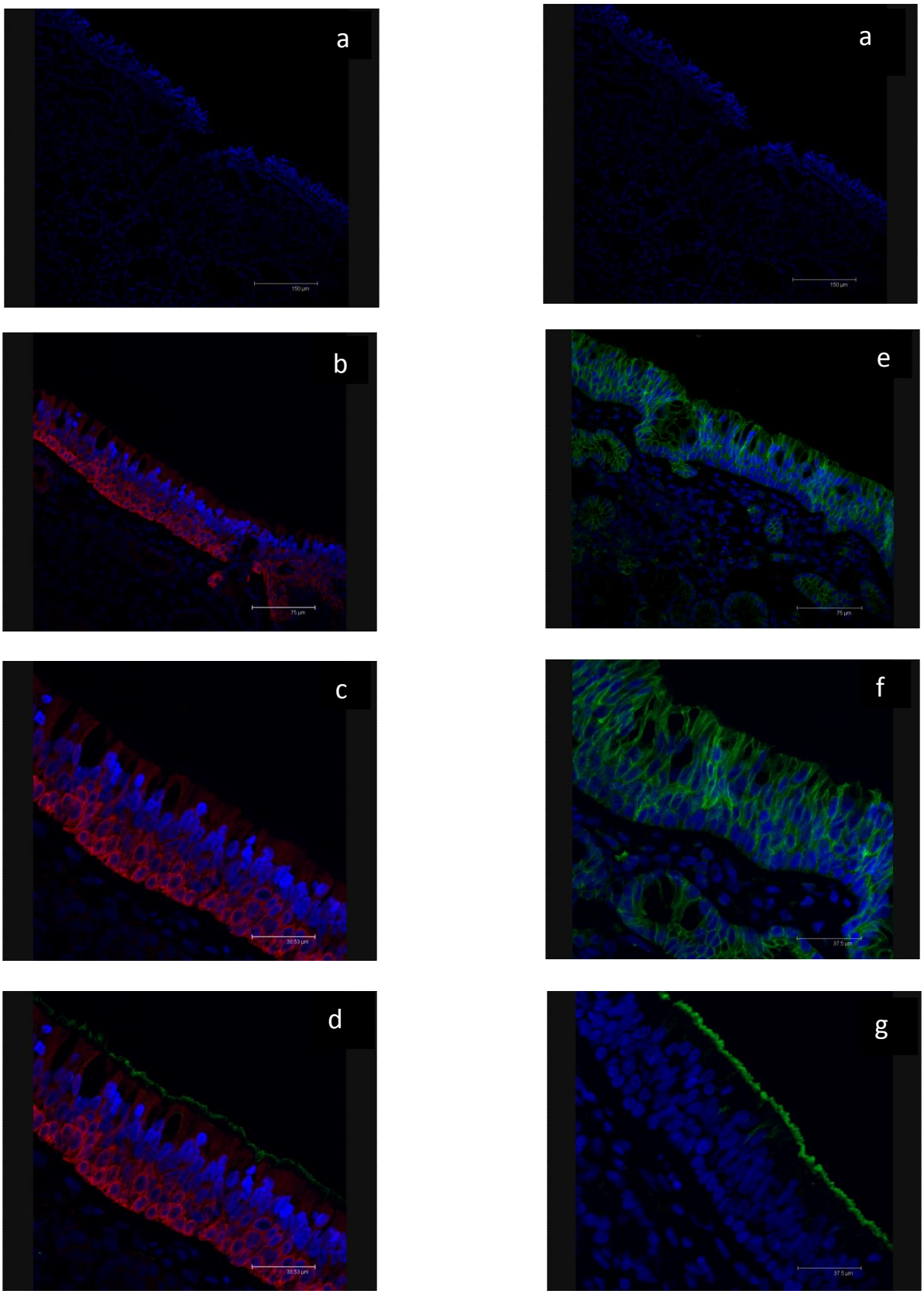

Figure 22. Epithelial marker staining of normal healthy sinonasal tissue (a) no primary antibody control with FITC & TRITC secondary antibodies. (b) Cytokeratin 17 TRITC red x40 magnification (c) x80 magnification (d) x80 magnification with cilial β-tubulin FITC green staining. (e) Epithelial cadherin FITC green x 40 magnification (f) x 80 magnification. (g) β-tubulin FITC green staining x 80 magnification. All images counterstained with blue DAPI nuclear stain (n=12).

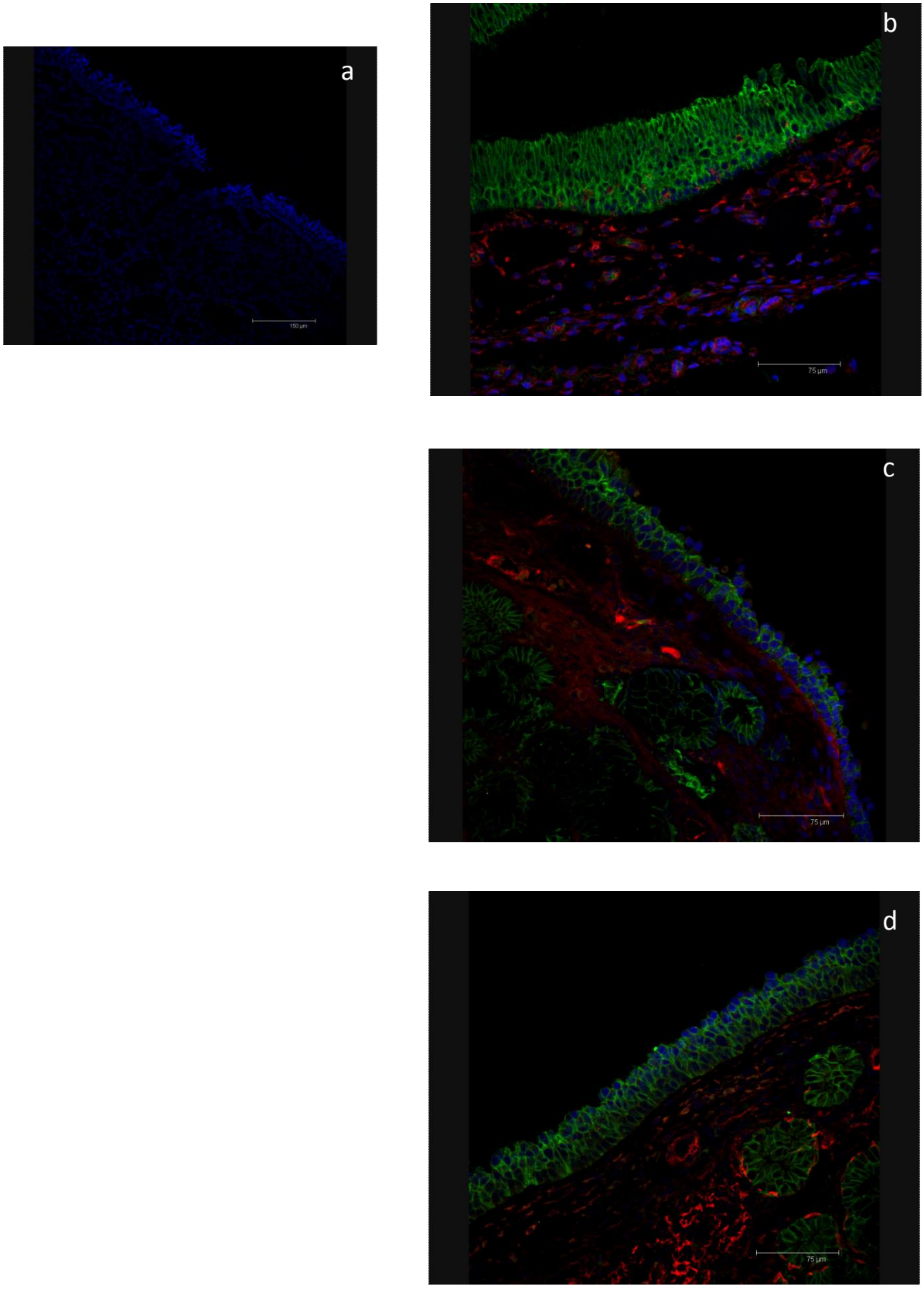

Figure 23. Fibroblast marker staining of sinonasal tissue sections (a) no primary antibody control with FITC & TRITC secondary antibodies. (b) vimentin TRITC red magnification x40 (c) fibronectin TRITC red magnification x40 (d) α-smooth muscle actin TRITC red magnification x40. All images counterstained with green FITC epithelial cadherin and blue DAPI nuclear stain (n=12).

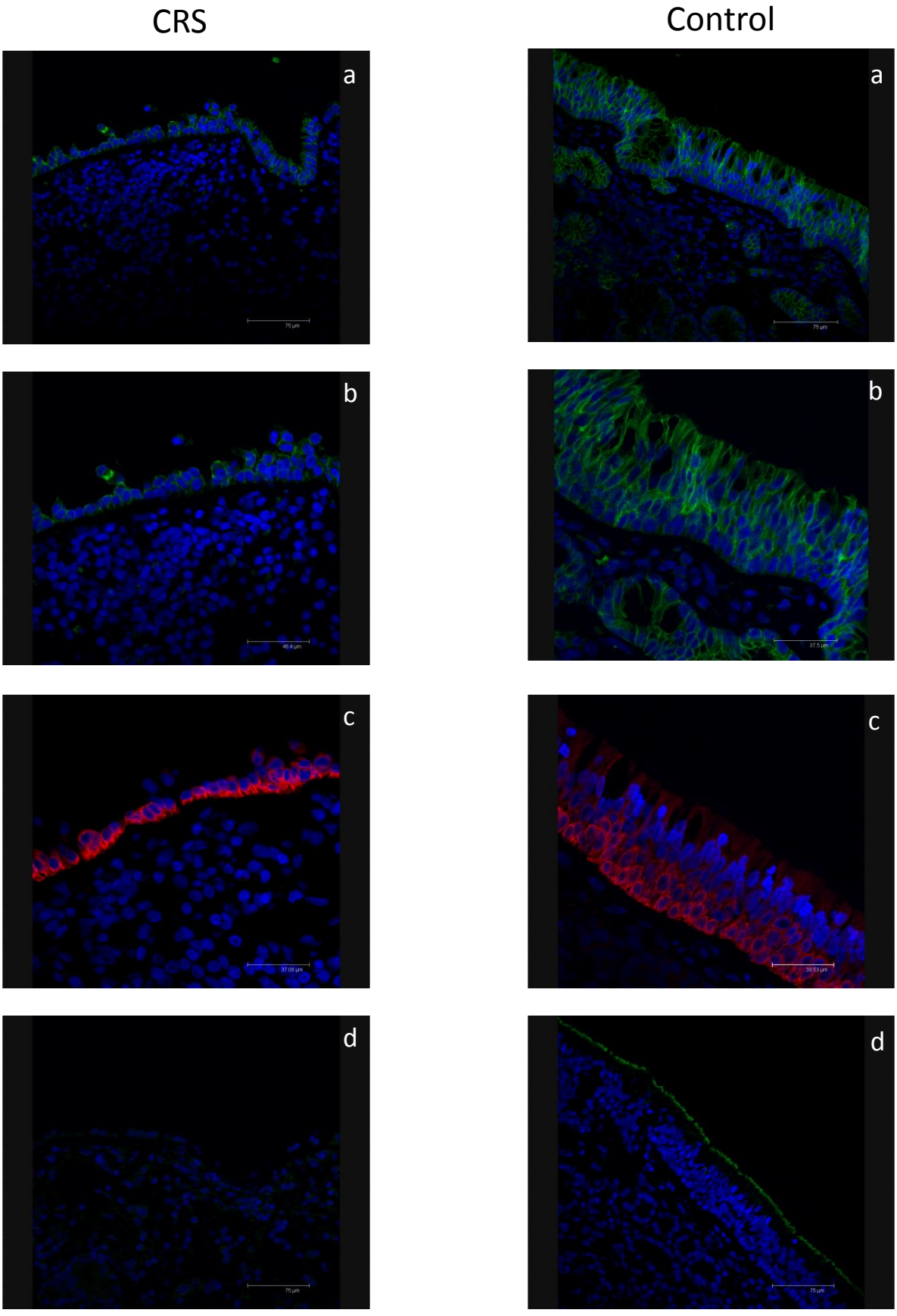

Figure 24. Epithelial marker staining of CRS & normal healthy sinonasal tissue (a) Epithelial cadherin FITC green x 40 magnification (b) x 80 magnification. (c) Cytokeratin 17 TRITC red x80 magnification (d) Cilial β-tubulin FITC green staining x 40 magnification. All images counterstained with blue DAPI nuclear stain (n=12).

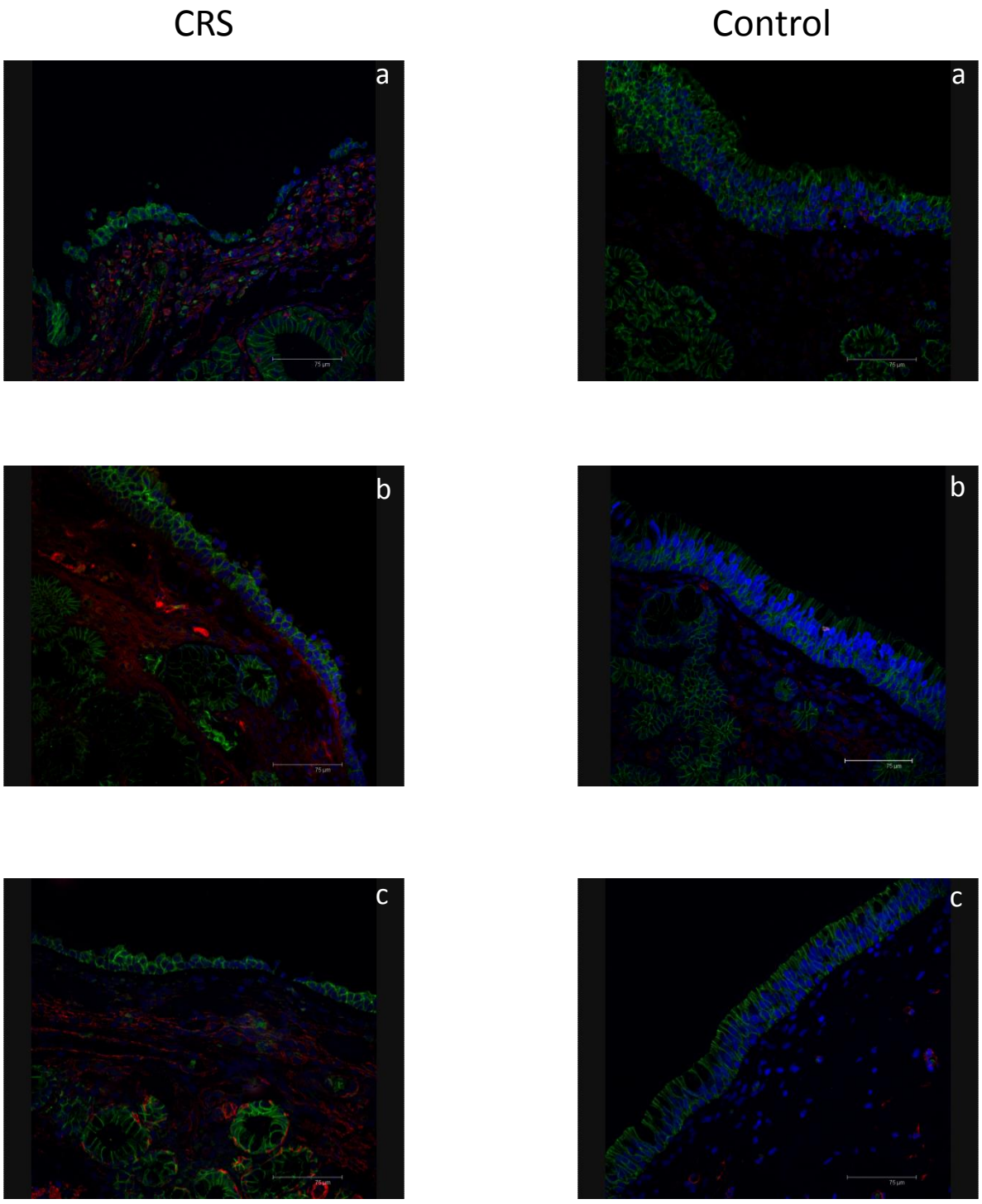

Figure 25. Fibroblast marker staining of CRS & normal healthy sinonasal tissue (a) Vimentin TRITC red x40, epithelial cadherin FITC green magnification x40 (b) fibronectin TRITC red , epithelial cadherin FITC green magnification x40 (c) α-smooth muscle actin TRITC red x40, epithelial cadherin FITC green magnification x40. All images counterstained with green FITC epithelial cadherin and blue DAPI nuclear stain (n=12).

3.4.6 Cytology

Patient derived primary cells were isolated from all participants' tissue biopsies and cytological brushings. The cells were then characterised by H+E and immunocytochemistry.

Upon taking a cytological brushing for epithelial cells a smear was prepared and fixed for immediate analysis (Figure 26). Haematoxylin and eosin staining of these cells confirms ciliated nasal epithelial cells as Figure 26(a). Immunocytochemical staining was performed using the conjugated fluorescent antibody panel described in Section 3.3.9. Figure 26(b+c) show examples of individual and clustered pseudostratified ciliated epithelial cells. Figure 26(d) shows a phase contrast microscopy image of the same fluorescent immunocytochemically stained epithelial cell.

When epithelial cells were grown in culture they were further characterised as in Figure 27. The H+E sections show a confluent monolayer of cells with an epithelial appearance. These cells were then characterised with a panel of epithelial stains (Figure 27 (b-d)). Positive staining for the epithelial markers TRITC conjugated cytokeratin 17 red, FITC conjugated cytokeratin 19 green, FITC conjugated pan-cytokeratin green and FITC conjugated E-cadherin is shown. The strongest staining for E-cadherin is seen where cells are confluent in small clusters and forming adherent junctions as would be expected. The panel in Figure 27(g-i) shows a negative control and negative staining for the mesenchymal markers TRITC conjugated vimentin red, TRITC conjugated Fibronectin red, TRITC conjugated αSMA red with blue DAPI nuclear counterstain.

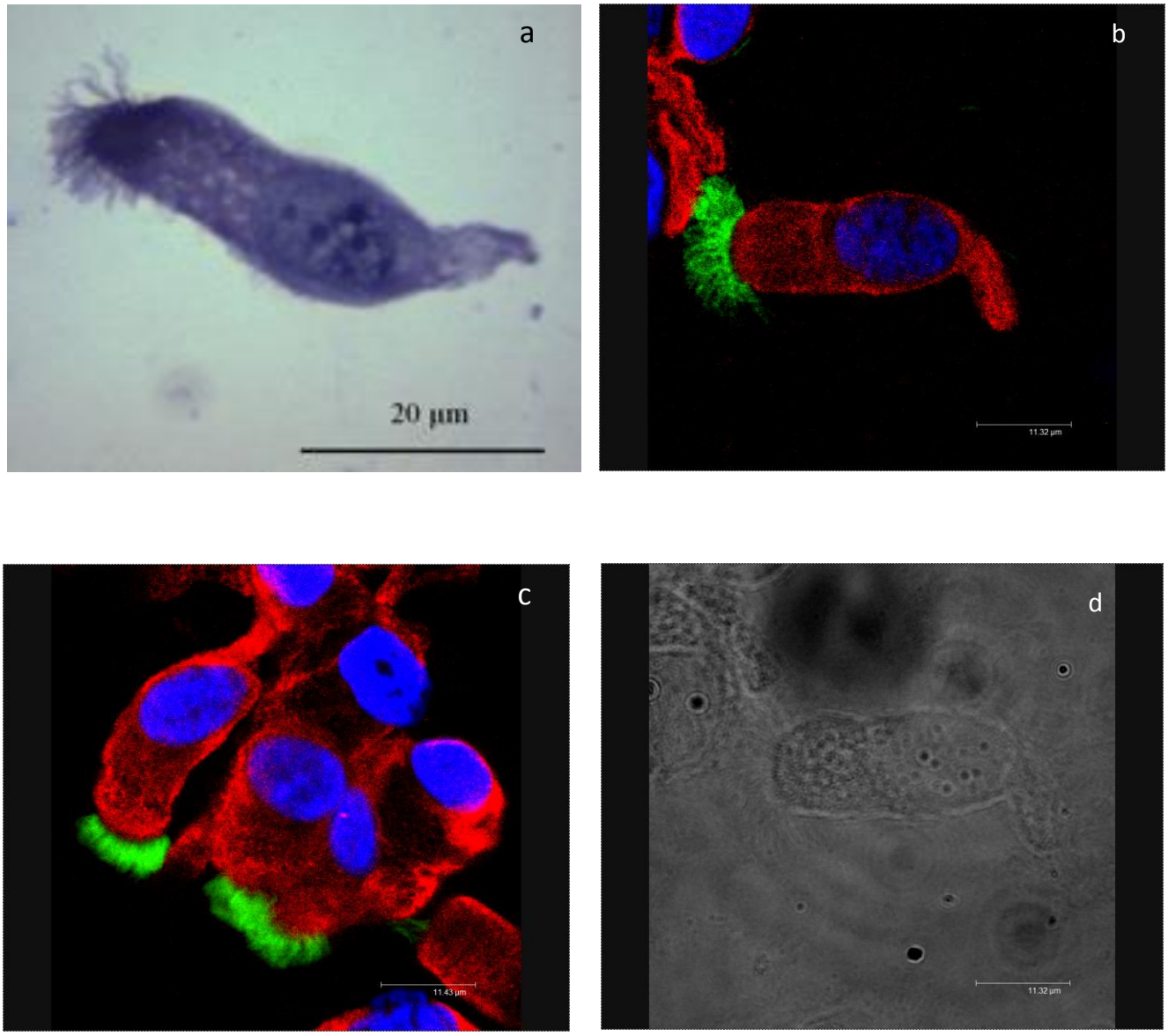

Figure 26. Epithelial sinonasal cells stained after brush harvesting with (a) haematoxylin and eosin, magnification x 20. (b+c) cells immunostained with FITC conjugated β-tubulin to stain cilia green and TRITC conjugated cytokeratin 17 red stain, sections counterstained with DAPI showing the nuclei in blue. (d) phase contrast image of the same view of (b) magnification x63 (n=5).

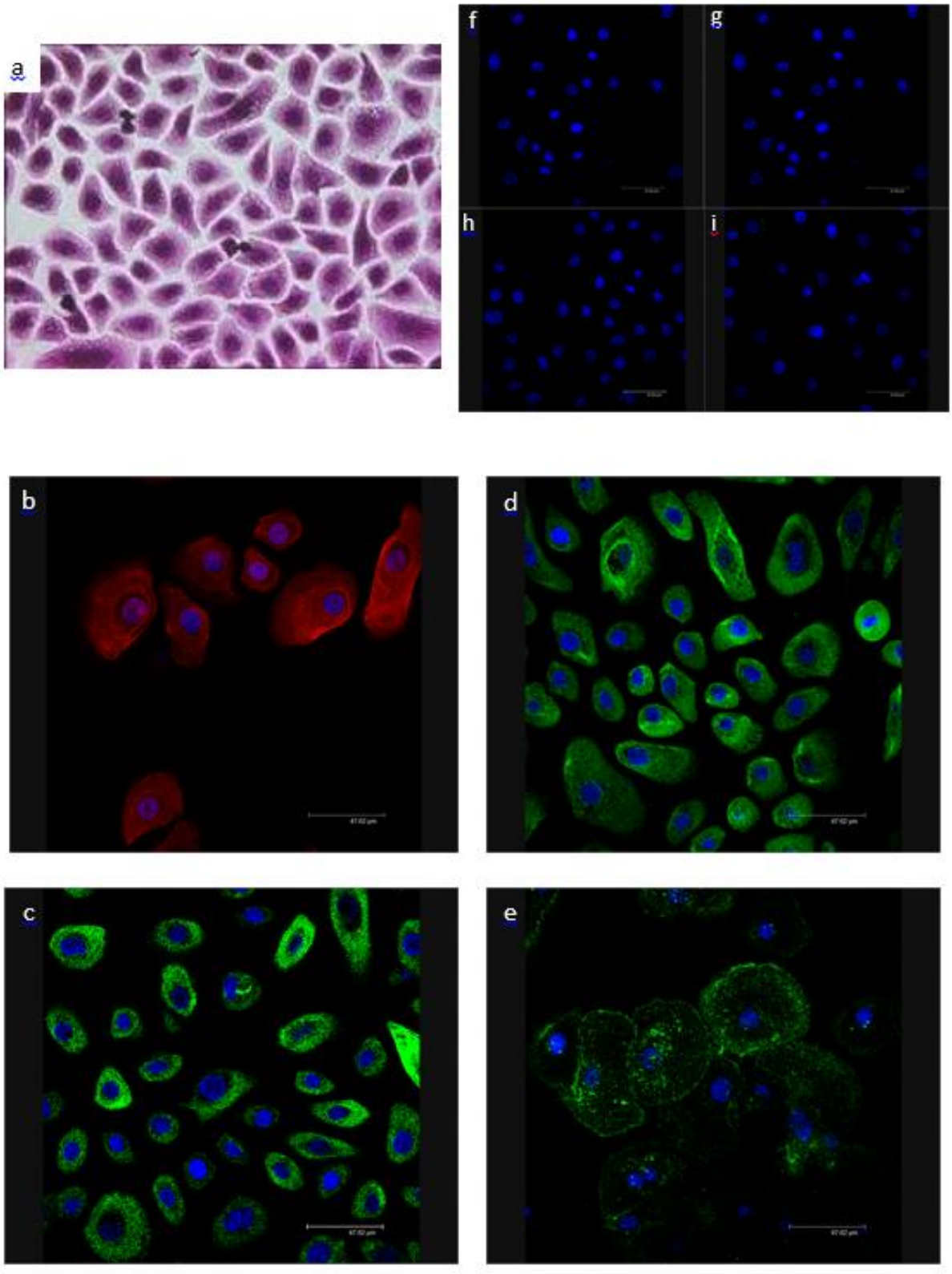

Figure 27. Cultured PNECs stained with (a) H&E, magnification x40. (b) TRITC conjugated cytokeratin 17 red, (c) FITC conjugated cytokeratin 19 green (d) FITC conjugated pan-cytokeratin green (e) FITC conjugated E-cadherin (f) secondary antibody only negative control (g) TRITC conjugated vimentin red, (h) TRITC conjugated Fibronectin red (i) TRITC conjugated αSMA red (b-i) magnification x63 with blue DAPI nuclear stain (n=12).

3.4.7 Primary epithelial cell electron microscopy

In addition to the tinctorial and immunocytochemical characterisation, isolated primary nasal epithelial cells (PNECs) were further analysed using scanning and transmission electron microscopy. Scanning electron microscopy images acquired from cultures of PNECs demonstrated monolayers of cells with an epithelial like appearance and the formation of cilial structures (Figure 28).

The same cells were visualised in culture with transmission electron microscopy. To image cells with transmission electron microscopy they have to be grown on transwell filter inserts to allow the supporting medium to be cut in cross section for processing. This explains the appearance of a white/grey membrane under the cells basolateral surface. Figure 29 demonstrates the transmission electron microscopy images between chronic sinusitis without nasal polyp participant derived primary cells and those from healthy control participants. The most striking differences between the cells are the presence of cilial like structures on the healthy control cells in Figure 29(a) and their relative absence in panel (b). In addition to this the healthy control cells would form pseudostratified epithelial cultures as in Figure 30 with a covering of cilial like structures, whereas the cells derived from CRSsNP participants would not.

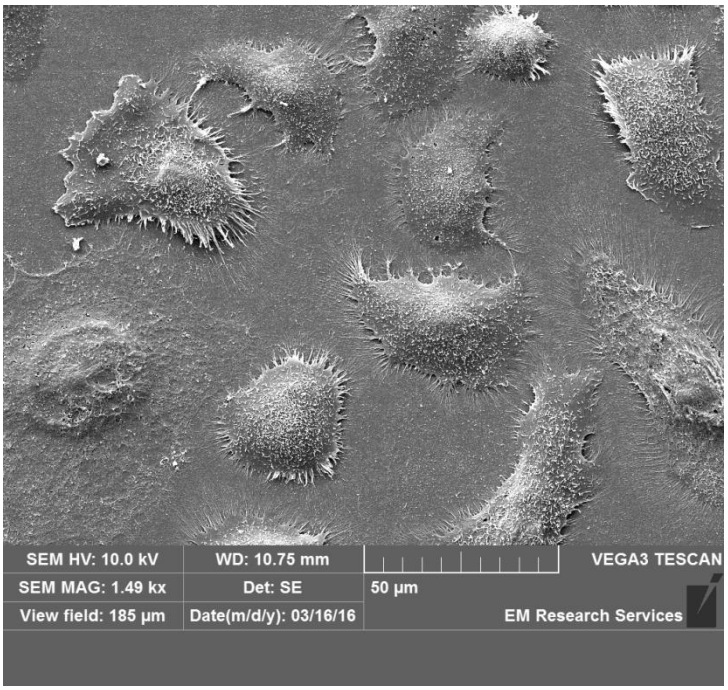

(a)

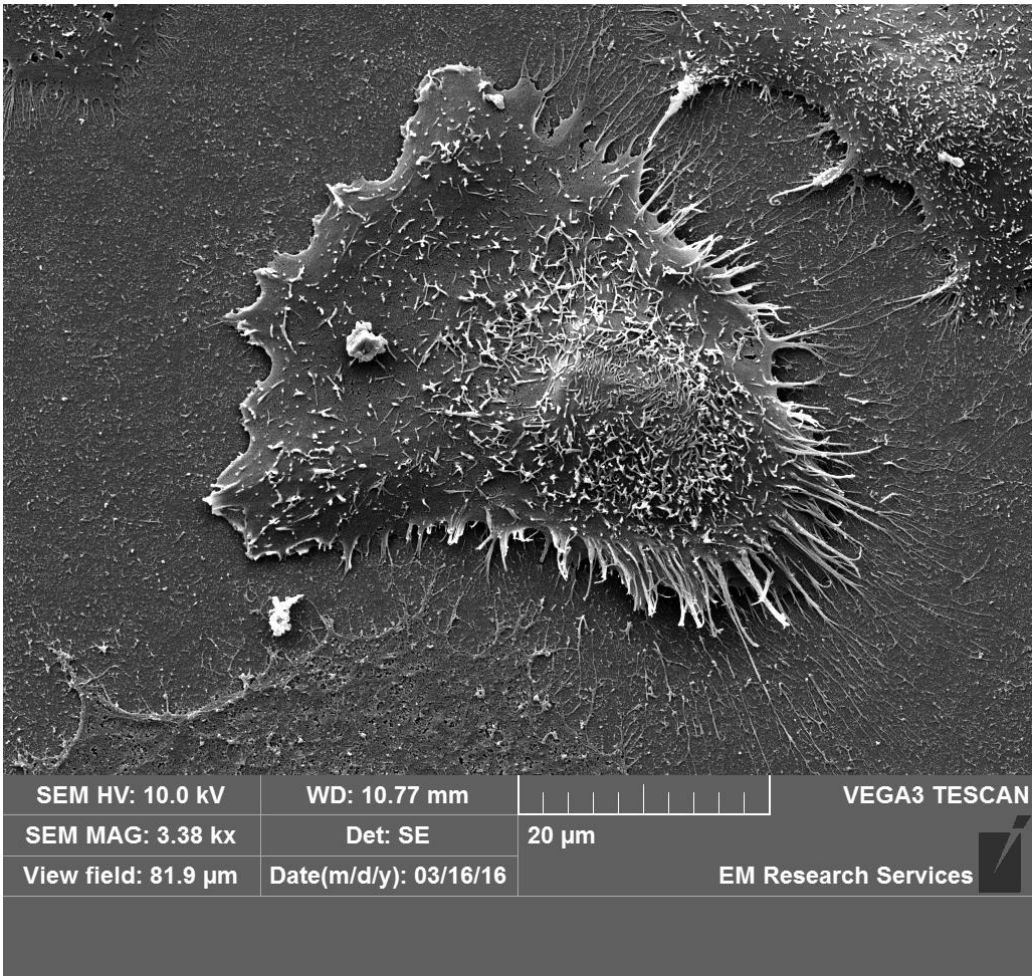

(b)

Figure 28. Scanning electron microscopy images acquired from cultured primary nasal epithelial cells. Magnification x1490 (a) x3380 (b) (n=6)

(a)

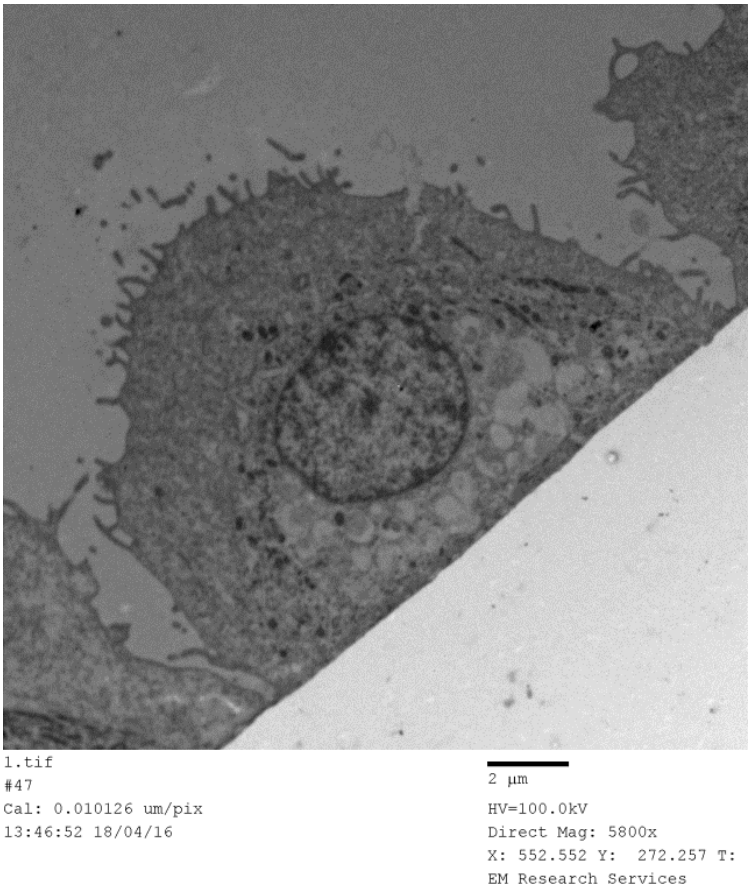

(b)

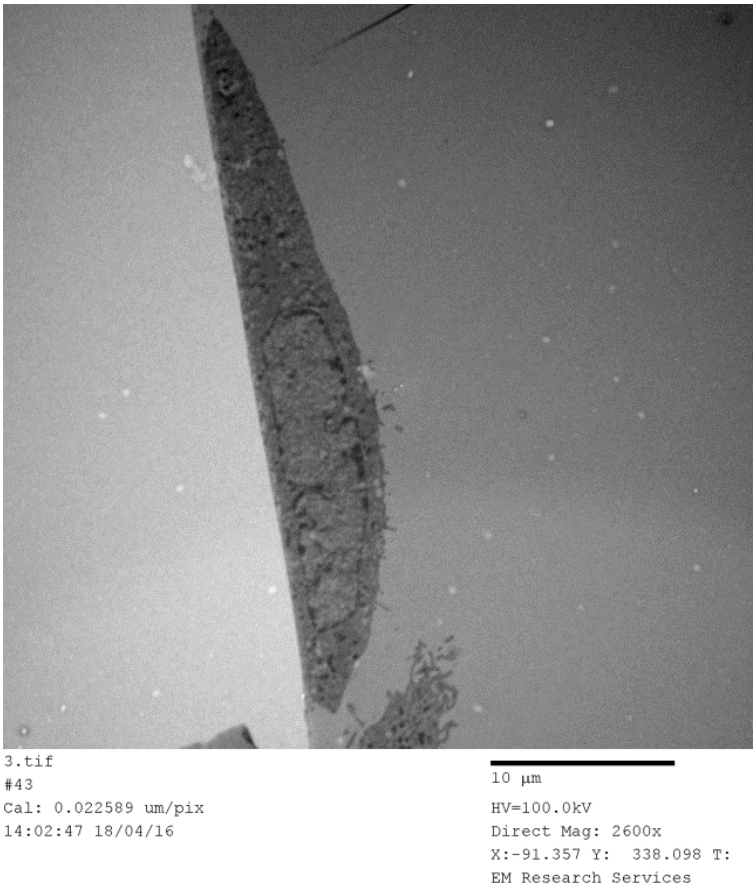

Figure 29. Transmission electron microscopy images acquired from (a) healthy control cultures of primary nasal epithelial cells and (b) chronic rhinosinusitis without nasal polyposis. Magnification x5800 (a) x3400 (b) (n=6).

(a)

(b)

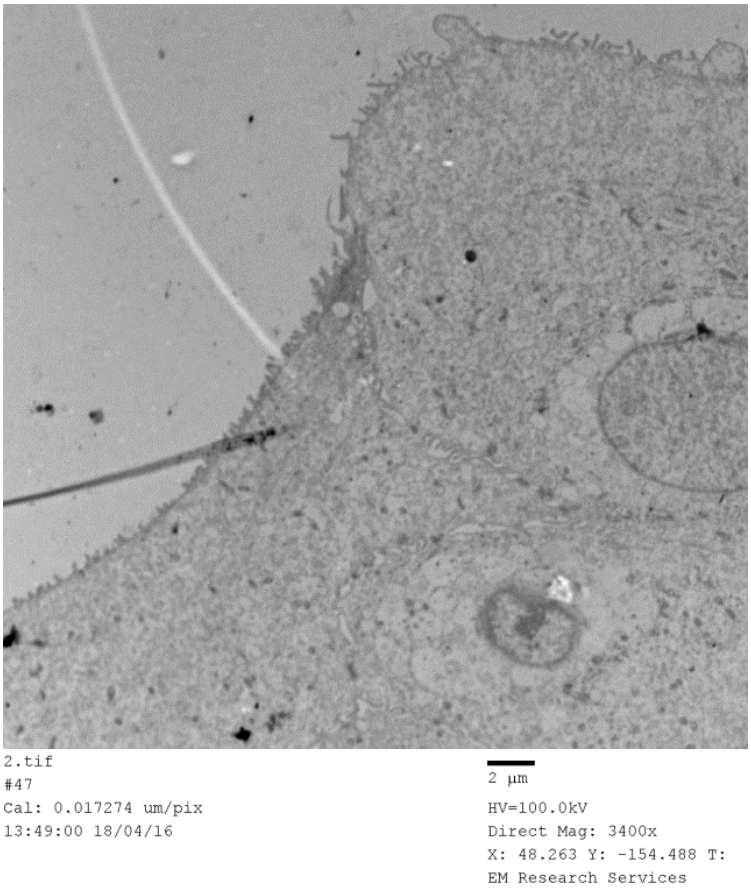

Figure 30. Transmission electron microscopy images captured from healthy control cultures of primary nasal epithelial cells showing formation of a pseudostratified epithelium and presence of cilia. Magnification x1950 (a) x3400(b) (n=6).

3.4.8 RPMI 2650 commercial cell line

The isolated primary nasal epithelial cells were compared with a commercially available sinonasal epithelial cell line, RPMI 2650, purchased from the American Type Culture Collection (ATCC) www.atcc.org/. The morphological appearance of RPMI 2650 cells and response to some common cytokines and inflammatory ligands was compared to the isolated patient-derived primary cells to see if they could be used as substitutes in certain experiments due to their ready availability and inherent reproducibility.

When grown in culture the RPMI 2650 cell line did not grow in confluent monolayers, but instead in isolated stacked clusters (Figure 31 (a)). Using the same panel of fluorescent conjugated antibodies as the primary cells and tissue biopsies demonstrated a low expression of epithelial cytokeratin 17, an atypical staining pattern for E-cadherin and positive mesenchymal staining with vimentin. Taken together these immunocytochemical appearances are not consistent with a pure epithelial cell line.

To characterise RPMI 2650 cells their response to common inflammatory ligands, cytokines and growth factors was compared to primary epithelial cells as a screen. I then measured the IL-8 inflammatory response to co-culture for three and twenty four hours with lipopolysaccharide (LPS) as a bacterial ligand, tumour necrosis factor-α (TNF-α) as an inflammatory cytokine, Polyinosinic:polycytidylic acid (Poly I:C) as a viral ligand and tissue growth factor –β (TGF-β) as a pro-fibrotic growth factor As shown in Figure 31(e-h) primary nasal epithelial cells produced a statistically significant ($p<0.05$ - $p<0.0001$) dose dependent response, whereas RPMI 2650 cell lines did not show any response at either 3 or 24 hours. Following these results it was decided not to pursue the epithelial cell line any further and the results were published to alert other researchers in the field (Ball et al., 2015).

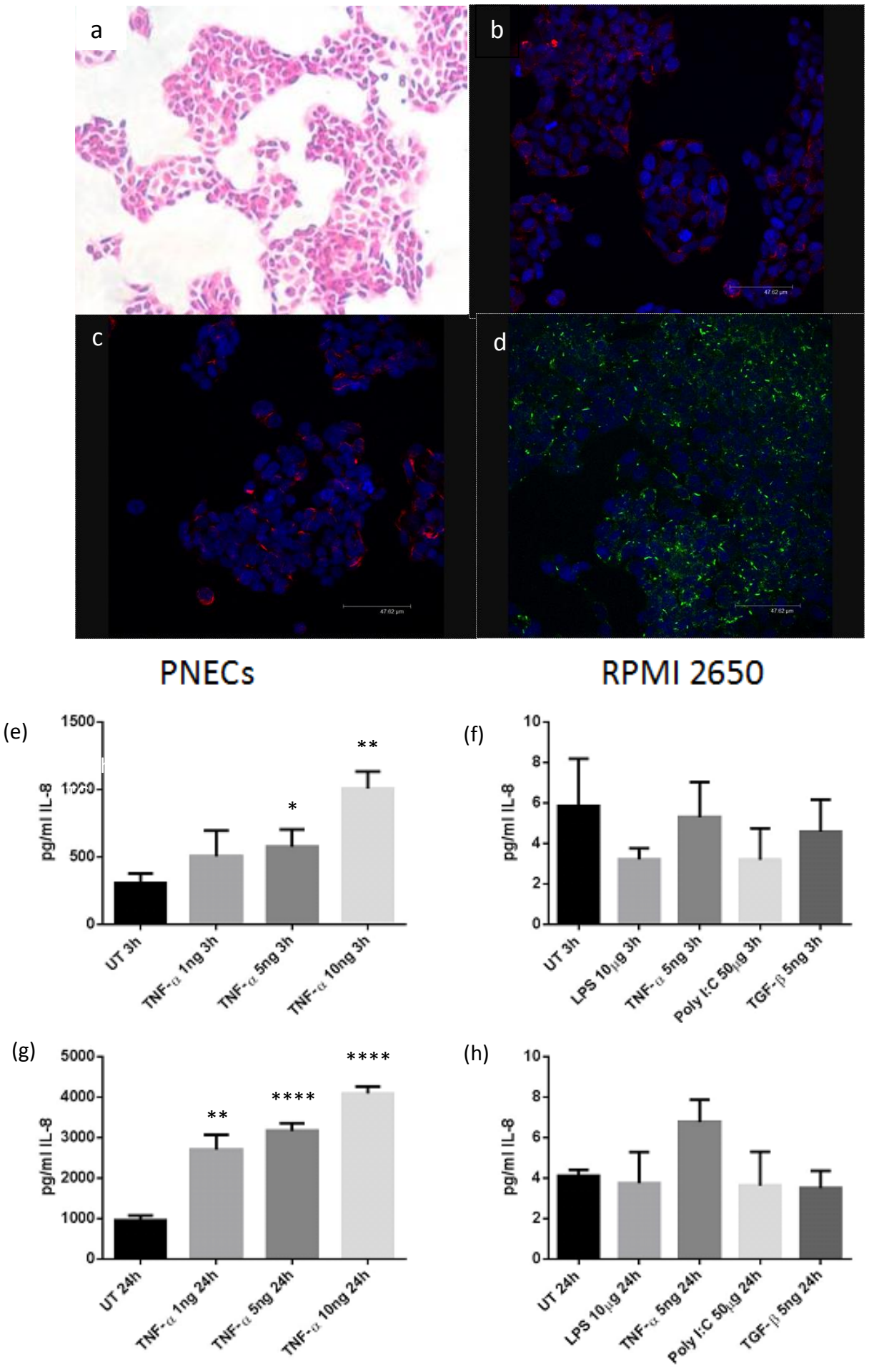

Figure 31. Cultured RPMI 2650 cells stained with (a) haematoxylin & eosin (b) pan-cytokeratin TRITC (c) vimentin TRITC (d) E-cadherin FITC. Magnification x63. Response of RPMI 2650 and PNEC cells to stimulation with inflammatory ligands (e-h). (e+f) 3 hour treatment (g+h) 24 hour treatment with inflammatory ligands (UT – untreated control cells). n=3 participants with triplicate repeats. **** = p<0.0001, *** = p<0.001, ** = p<0.01, * = p<0.05.

3.4.9 Primary fibroblast histological characterisation

Primary cultures of nasal fibroblasts were characterised using the same systematic approach as for tissue biopsy sections and primary epithelial cells. The primary nasal fibroblasts were isolated using an outgrowth technique directly from the matched parent tissue biopsies to validate their source. Figure 32 shows the haematoxylin and eosin staining appearances alongside the immunocytochemical microscopy results. Primary nasal fibroblasts in culture demonstrated their typical spindle like appearance in confluent monolayers. They showed strong staining for the mesenchymal markers TRITC conjugated vimentin and TRITC conjugated fibronectin together with positive staining for FITC conjugated collagen 1. Negative staining for the epithelial markers was also observed in staining for TRITC conjugated cytokeratin 17 and FITC conjugated E-cadherin.

Primary nasal fibroblast cells were also investigated with scanning and transmission electron microscopy (Figure 33). Scanning electron microscopy showed the typical fibroblast appearances of elongated spindle like cells in contrast to the isolated primary nasal epithelial cells. Transmission electron microscopy showed a single confluent monolayer of adherent cells. There were no gross morphological differences between the primary nasal fibroblasts from healthy controls compared with CRSsNP participants.

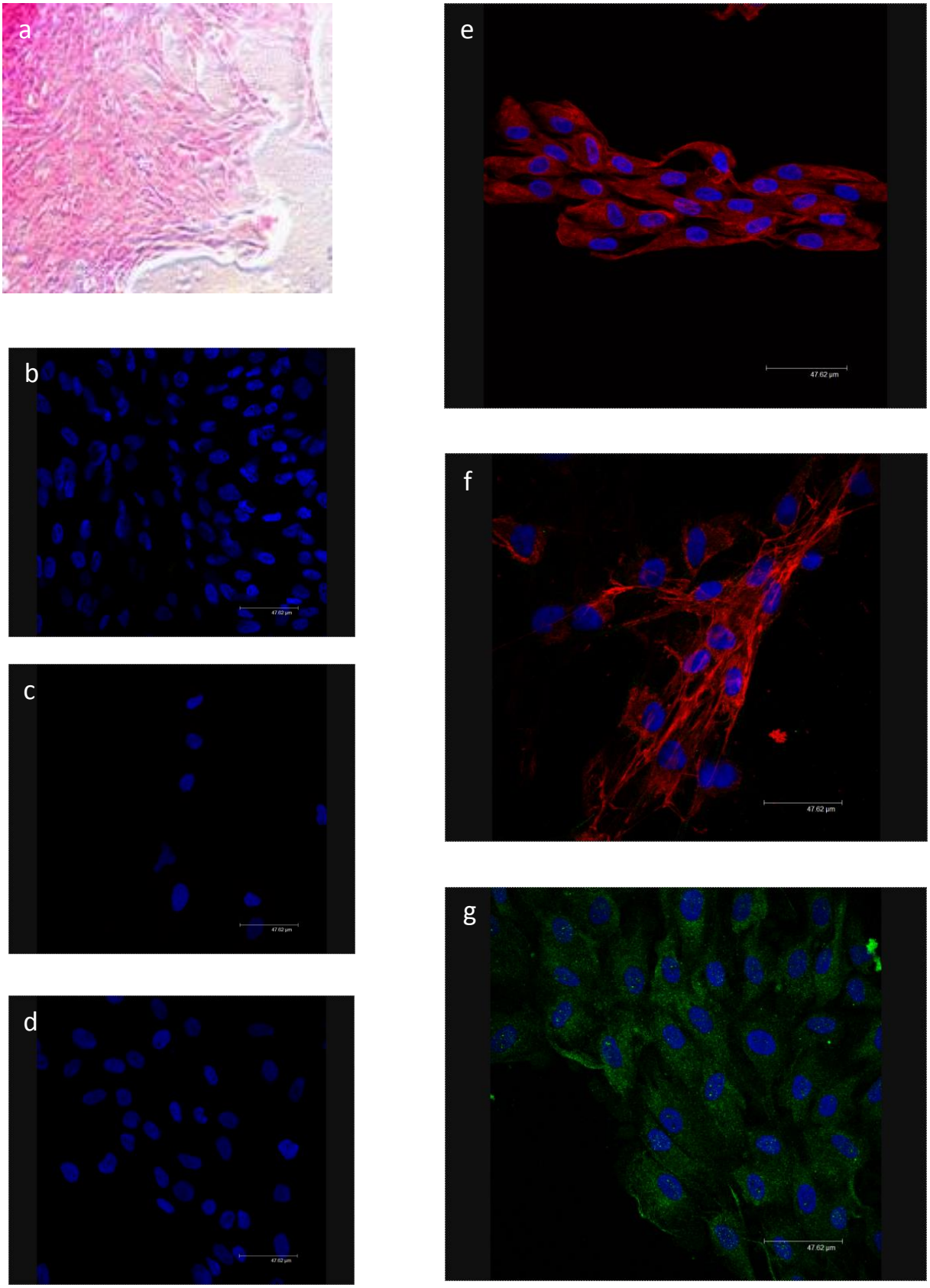

Figure 32. Cultured primary nasal fibroblasts (PNFs) stained with (a) haematoxylin and eosin, magnification x40. (b) secondary antibody only negative control (c) FITC conjugated E-cadherin (d) TRITC conjugated cytokeratin 17 red, (e) TRITC conjugated vimentin red (f) TRITC conjugated Fibronectin red (g) TRITC conjugated collagen 1 (b-g) magnification x63 with blue DAPI nuclear stain (n=12).

(a)

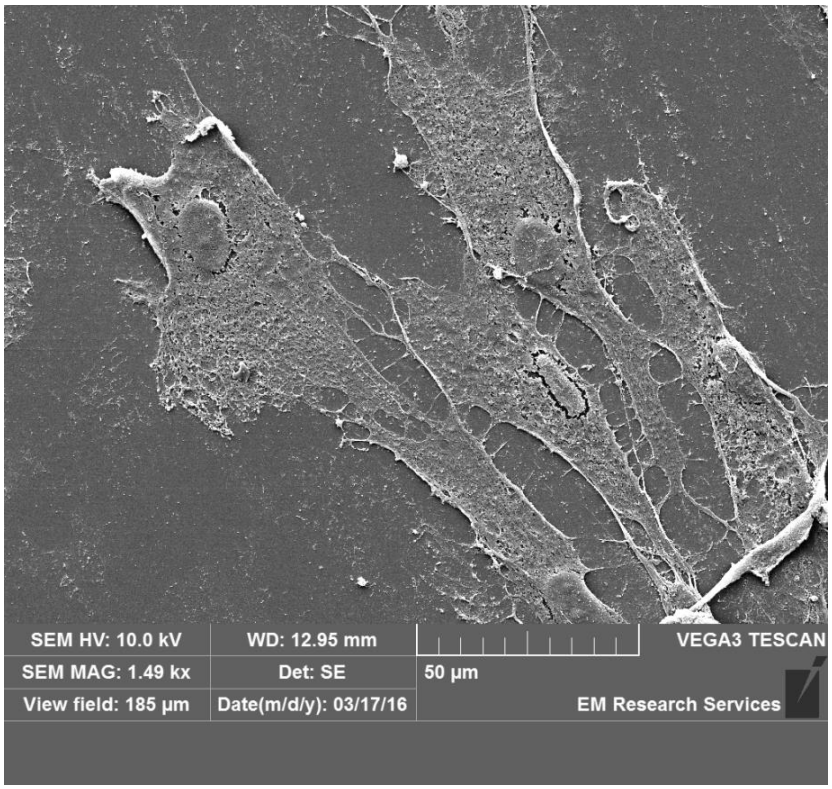

(b)

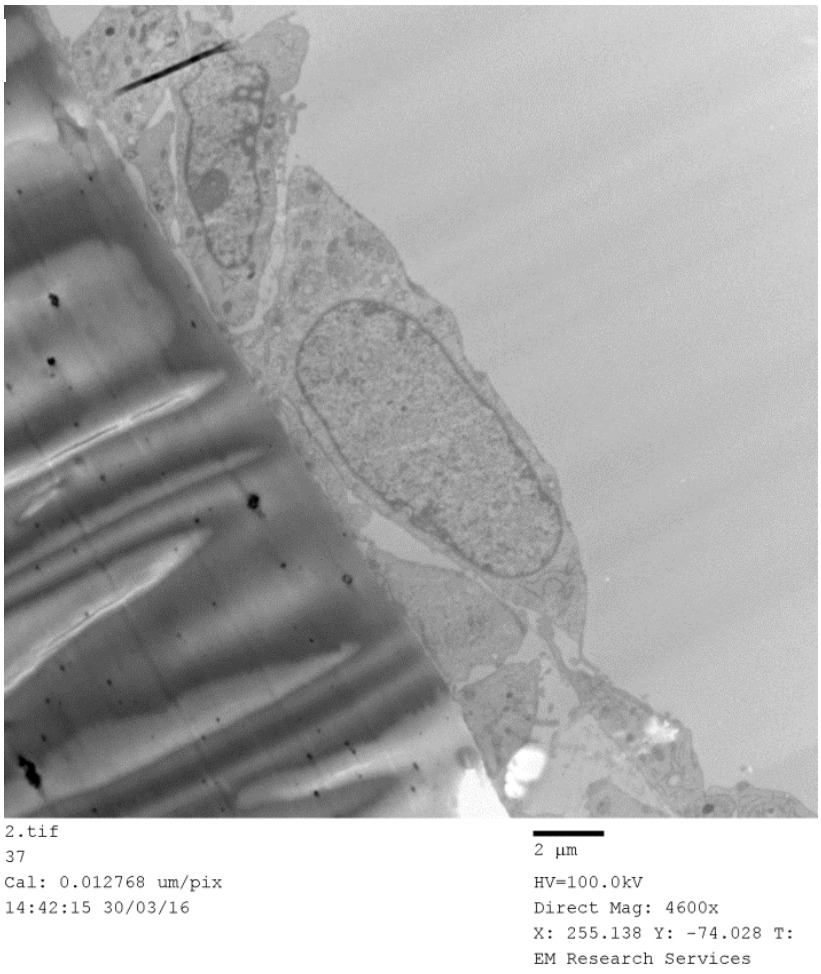

Figure 33. (a) Scanning electron microscopy image of primary nasal fibroblasts (PNFs). Magnification x1490. (b) Transmission electron microscopy of PNFs grown on a Transwell filter insert. Magnification x4600 (n=6).

3.4.10 Characterisation of primary nasal epithelial and fibroblast cell responses

3.4.10.1 Primary nasal epithelial cell viability following disease specific stimuli

Confluent primary cultures of nasal epithelial (PNEC) and fibroblast (PNF) cells were investigated in tissue culture conditions. Initially the cellular viability of PNECs in response to culture with a range of disease specific stimuli was assessed by flow cytometry with propidium iodide staining as shown in Figure 34. The baseline viability of unstimulated cells was consistent across all treatment groups and confirms that the cells characterised in the previous sections are both the correct cell type and viable. Interestingly, co-culture for 24 hours with either increasing doses of whole cell lysates of laboratory reference strains of *Pseudomonas aeruginosa, Haemophilus influenzae* or diesel exhaust particles did not have any effect on PNEC viability. Co-culture with increasing doses of cigarette smoke extract (CSE) and hydrogen peroxide (H_2O_2) did, however, produce a statistically significant ($p<0.01$) dose dependent effect on PNEC viability. Co-culture with the endoplasmic reticulum (ER) stress inducing agent thapsigargin appears to have a statistically significant ($p<0.001$) threshold effect from concentrations of 10μM or greater.

3.4.10.2 Epithelial alarmin release following disease specific stimuli

Using identical co-culture conditions the release of the alarmin IL-1α was measured by ELISA (Figure 35). Interestingly the greatest IL-1α release was triggered by co-culture with agents that promote either oxidative or endoplasmic reticulum stress rather than whole cell lysates of respiratory bacteria. Co-culture with increasing concentrations of standardised diesel exhaust particles did not affect alarmin release.

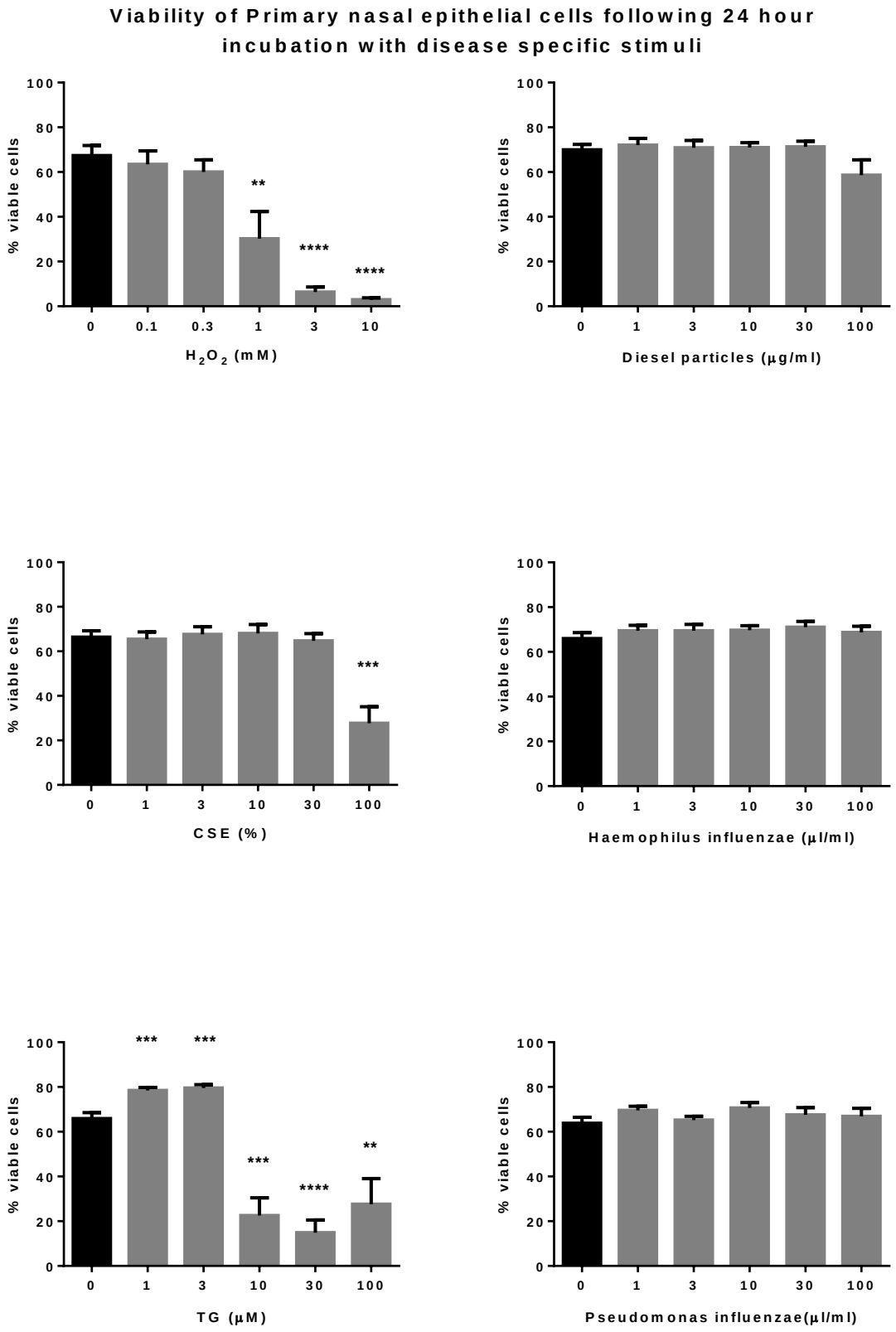

Figure 34. Primary nasal epithelial cell (PNEC) viability following 24 hour stimulation with relevant disease specific stimuli. (H_2O_2- hydrogen peroxide, CSE – cigarette smoke extract, TG – thapsigargin). Viability assessed by propidium iodide flow cytometry. n=3 participants with triplicate repeat. **** = p<0.0001, *** = p<0.001, ** = p<0.01, * = p<0.05.

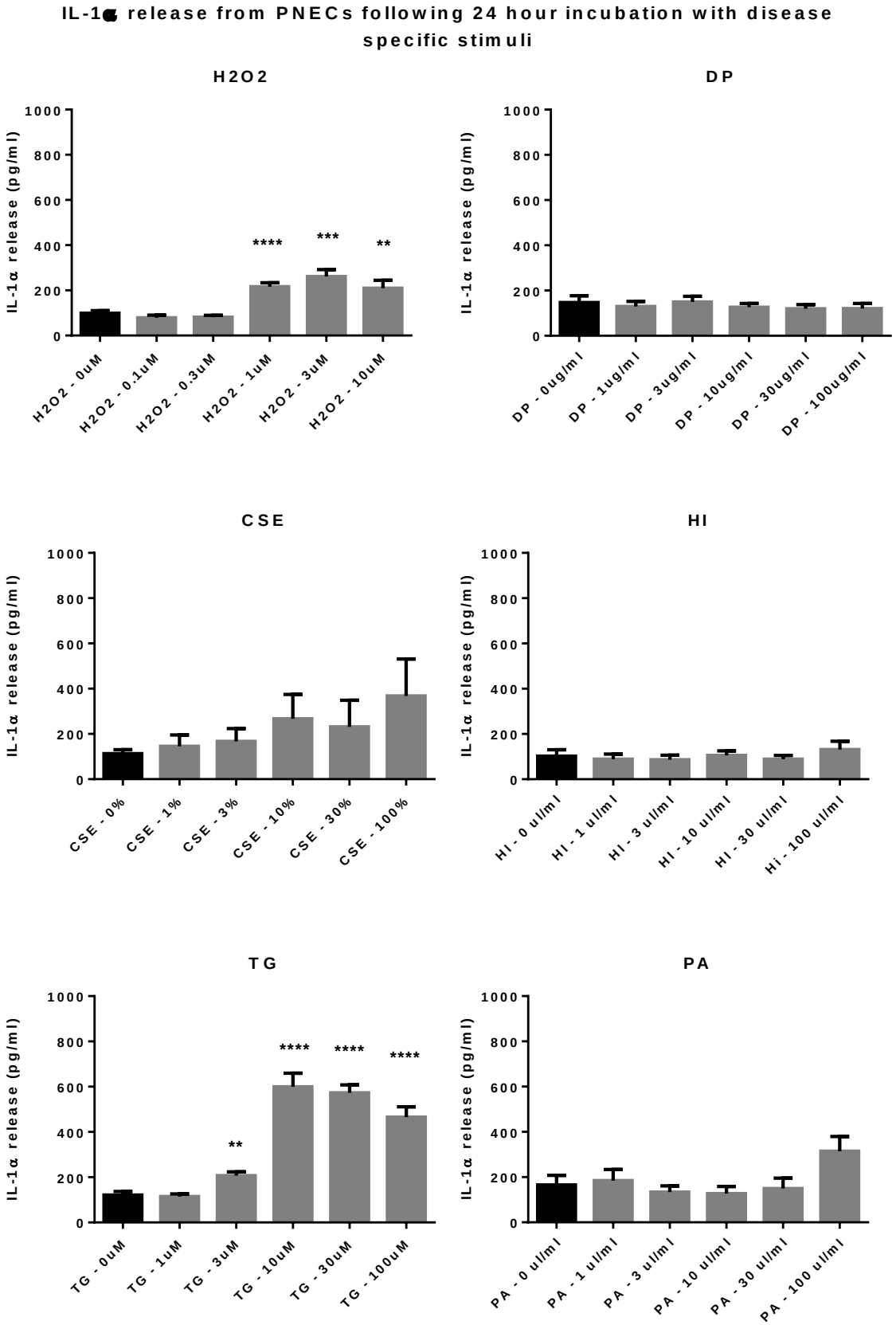

Figure 35. Primary nasal epithelial cell (PNEC) IL-1α alarmin release following 24 hour stimulation with relevant disease specific stimuli. (H_2O_2- hydrogen peroxide, CSE – cigarette smoke extract, TG – thapsigargin, DP – diesel particles, HI – *Haemophilus influenzae*, PA – *Pseudomonas aeruginosa*). IL-1α release quantified by ELISA. n=3 participants, triplicate repeats for each participant. **** = p<0.0001, *** = p<0.001, ** = p<0.01, * = p<0.05.

3.4.10.3 Fibroblast responses to human recombinant alarmin proteins

Cultures of primary nasal fibroblast cells were stimulated with a range of recombinant human alarmin proteins to stimulate an inflammatory response. The most significant responses to the panel of alarmins tested were seen with IL-1α ($p<0.05$, Figure 36).

Importantly, the physiological response to challenge with an alarmin confirms that the fibroblasts characterised from the last section are also able to produce appropriate inflammatory responses. The next most marked response was seen to co-culture with IL-1β, though the responses were not always statistically significant which is interesting given the two ligands share a common receptor. The viral analogue poly I:C produced the next most potent response. The variation on the magnitude of response precluded statistical significance. The bacterial ligand LPS generated a similar inflammatory response from cultured fibroblasts ($p<0.01$ - $p<0.05$) with very minimal response from HMGB-1. In response to co-culture with the alarmin proteins detailed, a similar reproducible amount of the pro-inflammatory cytokines IL-6 and IL-8 were produced, approximately 3-400ng/ml. The amount of TNF-α released was very minimal, essentially on the limit of detection of the ELISA kit.

I selected 500pg/ml IL-1α as a reference ligand to screen for a range of cytokine responses from stimulated PNFs on the basis of maximal primary nasal fibroblast stimulation with the alarmins IL-1α and IL-1β. The strongest and only statistically significant response ($p<0.01$, Figure 37) in cytokine production from stimulated PNFs was seen in the amounts of IL-6 and IL-8, with small but measurable amounts of monocyte chemotactic protein 1 (MCP-1) and Granulocyte-macrophage colony-stimulating factor (GM-CSF).

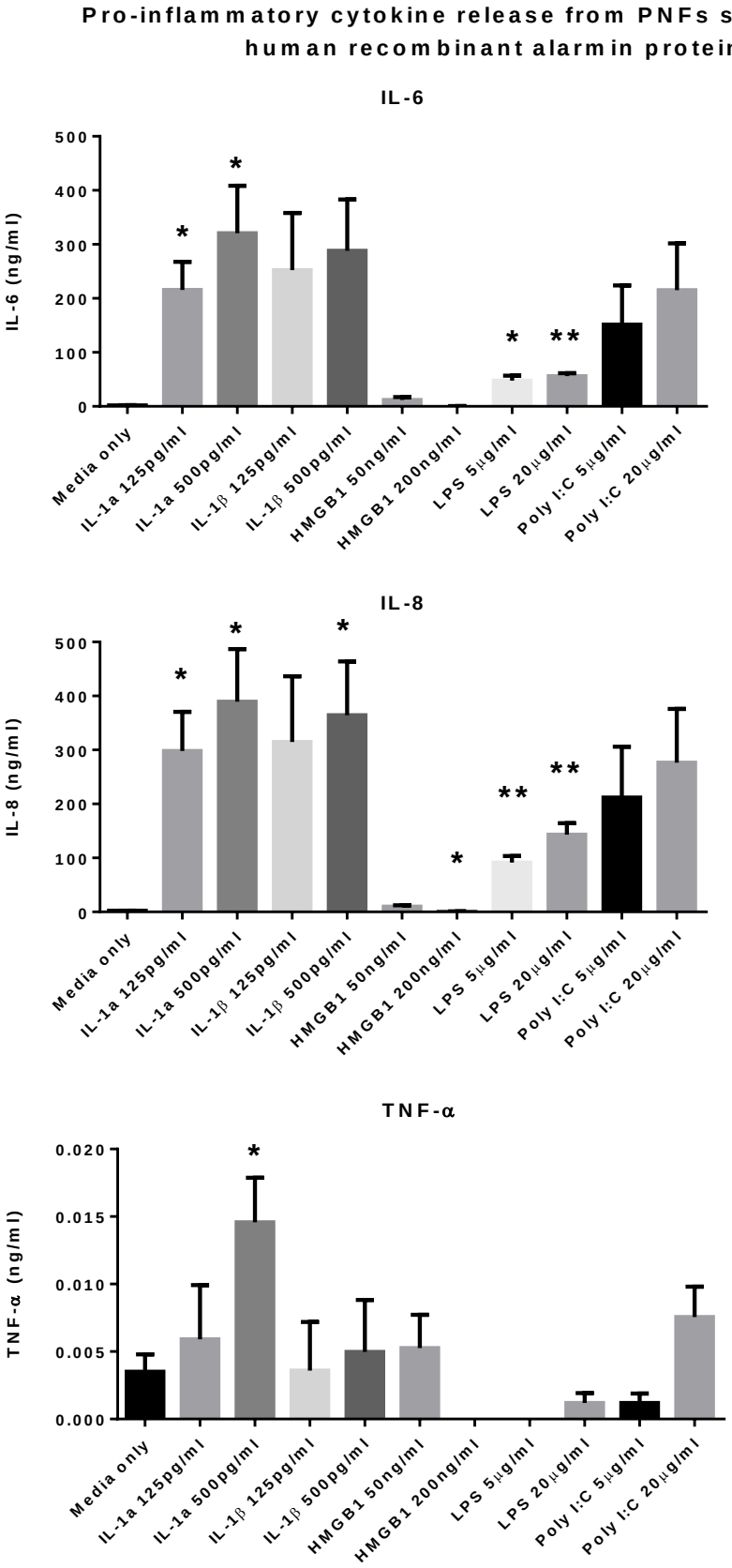

Figure 36. Primary nasal fibroblast (PNF) IL-6, IL-8 and TNF-α inflammatory cytokine release following stimulation with human recombinant alarmin proteins as detailed along the x-axis. Protein levels determined by ELISA. n=3 participants per group, triplicate repeats for each participant. ** = $p<0.01$, * = $p<0.05$.

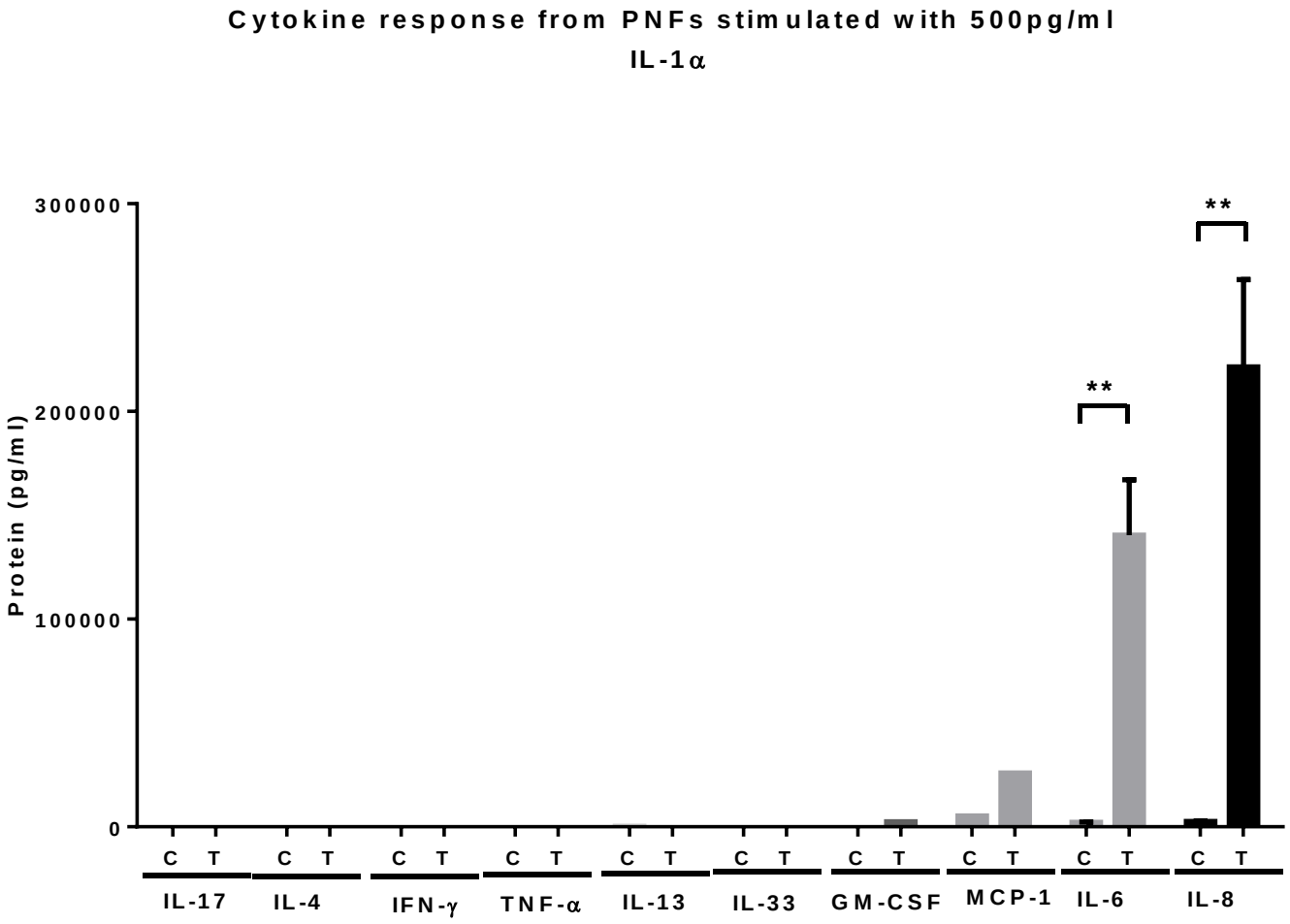

Figure 37. Primary nasal fibroblast (PNF) cytokine release following stimulation with the human recombinant alarmin protein IL-1α. (C = media only control, T = 500pg/ml IL-1α treatment). Protein levels determined by ELISA. n=3 participants per group, with triplicate repeats for each participant. ** = $p<0.01$, * = $p<0.05$.

3.4.10.4 Fibroblast responses to stimulation with synergistic human recombinant alarmin proteins

To determine if there was any synergy in alarmin mediated PNF inflammatory responses, combinations of recombinant alarmin proteins were co-cultured with primary nasal fibroblasts. Of the panel of alarmin proteins used, the greatest response by far was found in response to stimulation of the IL-1 receptor by either IL-1α or IL-1β proteins. The combination of additional alarmin proteins produced no additional effect greater than either IL-1α or IL-1β proteins alone.

3.4.10.5 Comparison of upper and lower airway fibroblast alarmin responses

Primary lung fibroblasts (PLFs) were co-cultured with identical conditions to the primary nasal fibroblast challenge experiments, to determine if airway fibroblasts from different positions of the respiratory tract have differing responses to alarmins.

When PLF co-cultures with the same panel of alarmin proteins were compared to PNF responses, there are a number of similarities but the responses are by no means identical (Figure 39). PLFs also show the greatest response to the IL-1R ligands IL-1α and IL-1β, though the overall response is less marked. Also similar to PNFs was the negligible response to HMGB-1 co-culture. The pattern of relative amounts of IL-6, IL-8 and negligible TNF-α release is also similar. Of note however, the PLFs do show statistically significant responses to the viral ligand Poly I:C ($p<0.01$ - $p<0.05$) , although the potency is much less. Similarly the response to LPS as a bacterial ligand is much less potent and also not statistically significant.

A similar pattern is observed when comparing PLFs with PNFs looking to see if any synergy between alarmins is affected, with the major effect solely in response to either IL-1α or IL-1β.

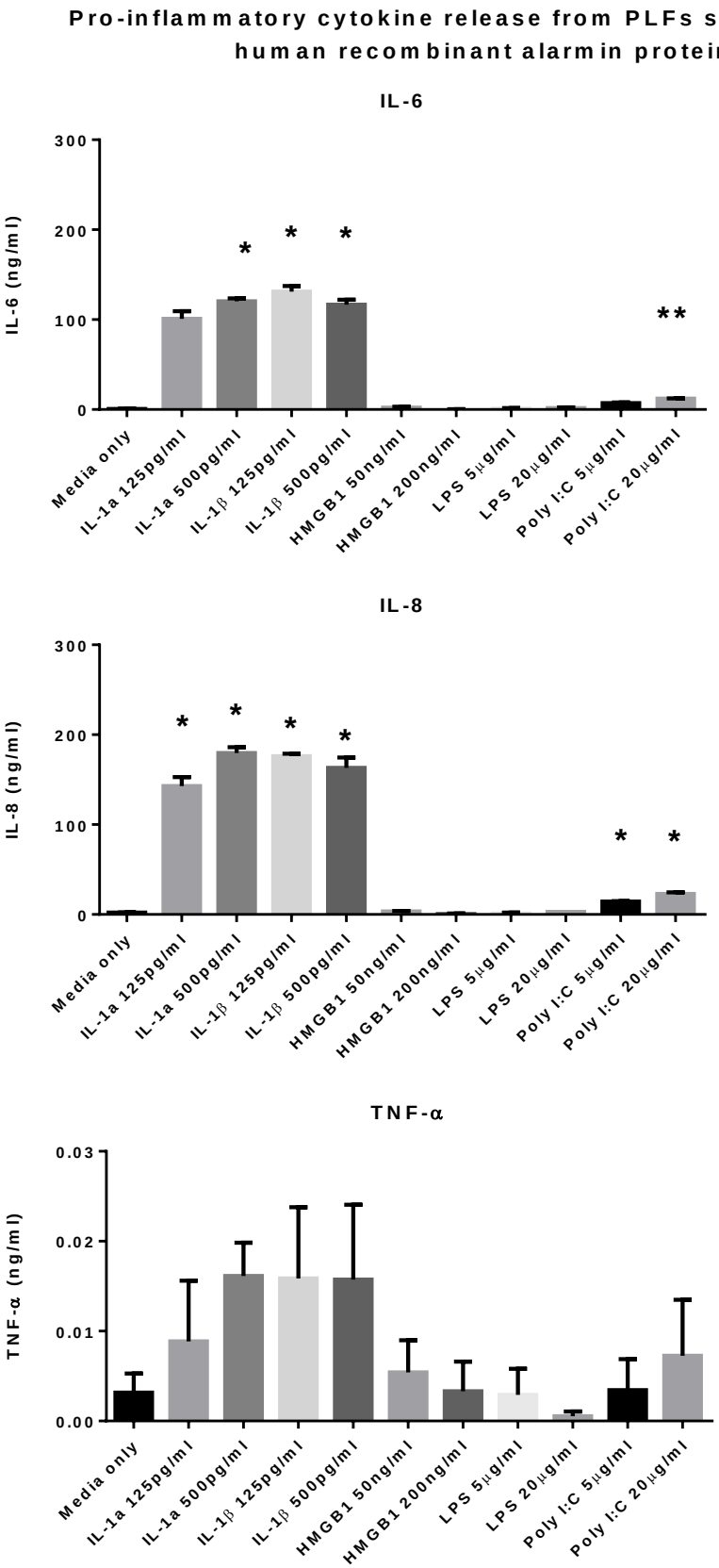

Figure 39. Primary lung fibroblast (PLF) IL-6, IL-8 and TNF-α inflammatory cytokine release following stimulation with human recombinant alarmin proteins as detailed along the x-axis. Protein levels determined by ELISA. n=3 participants per group, with triplicate repeats for each participant. ** = $p<0.01$, * = $p<0.05$.

3.4.10.6 Fibroblast response to alarmins

Primary cultures of fibroblasts isolated from healthy control and chronic rhinosinusitis participants were compared in their responses to the same range of human recombinant alarmin proteins as shown in Figure 40. While all fibroblasts were able to mount an inflammatory response there was no significantly different response between healthy control and chronic rhinosinusitis without nasal polyp fibroblasts

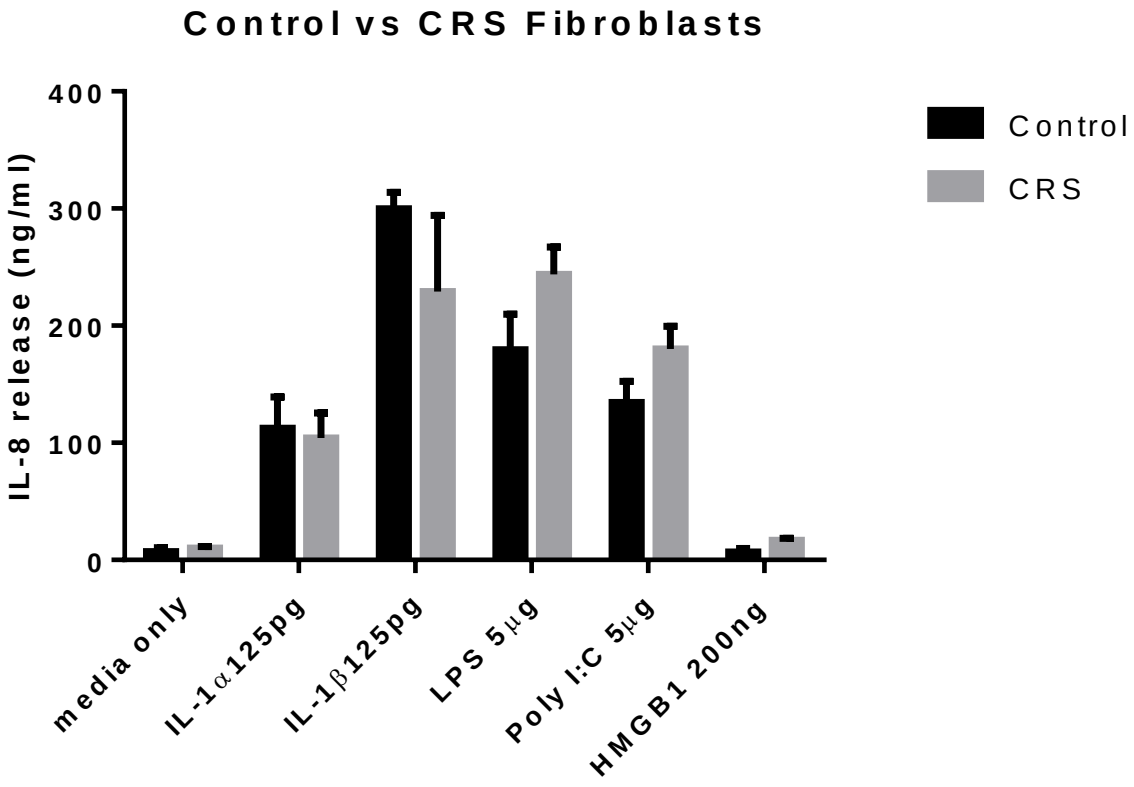

Figure 40. IL-8 response in stimulated fibroblasts isolated from CRSsNP and control participants. Fibroblasts stimulated with human recombinant alarmin proteins as detailed along the x-axis. Protein levels determined by ELISA. n=3 participants per group, with triplicate repeats for each participant.

3.4.10.7 Primary nasal fibroblast responses to co-culture with conditioned macrophage media

The inflammatory IL-6 and IL-8 cytokine responses from primary nasal fibroblasts were also measured in response to co-culture with conditioned media from macrophages (Figure 41). Primary nasal fibroblasts, n=4 plus triplicate technical repeats, were co-cultured with conditioned media from macrophages that were either quiescent (M0), classically activated (M1) or alternatively activated (M2). The experiments were performed with macrophages derived from the THP-1 cell line, n=3 plus triplicate technical repeats and also peripheral blood mononuclear cells (PBMCs) from n=3 healthy human volunteers in triplicate technical repeats. THP-1 cells showed a small but significantly greater IL-6 and IL-8 response (p $p<0.001$ - $p<0.01$) when primary nasal fibroblasts were cultured with conditioned media from M0 and M2 macrophages than with only culture media. In comparison primary nasal fibroblasts co-cultured with conditioned media from classically activated M1 macrophages produced a potent response of both IL-6 and IL-8. Both the IL-6 and IL-8 responses were statistically significant ($p<0.01$ – $p<0.0001$ respectively), though the IL-8 released was one order of magnitude greater at approximately 150ng/ml detected in the cell culture supernatants.

Attempts at modulating the inflammatory response were made using IL-1α and IL-1β blocking antibodies and an IL-1α receptor antagonist. Used separately IL-1α and IL-1β blocking antibodies significantly reduced the IL-6 and IL-8 responses ($p<0.05$ – $p<0.001$), though their effect size was much greater in combination ($p<0.01$ – $p<0.0001$ respectively). The downregulation of the IL-6 and IL-8 response seen when the IL-1α receptor antagonist was used was of similar magnitude to the combination of IL-1α and IL-1β blocking antibodies.

Following the initial success with the immortalised THP-1 cell line similar experiments were repeated using macrophages derived from peripheral blood mononuclear cells (PBMCs) isolated from healthy volunteers. Neither M0 nor M2 macrophages showed a significant release of IL-6 or IL-8 from nasal fibroblasts in co-culture experiments with conditioned media. Similar to the THP-1 cell line experiments a potent IL-6 and IL-8 release was seen in response to co-culture with classically activated M1 macrophages. Both IL-6 and IL-8 release from conditioned M1 macrophage media co-culture demonstrated a highly significant response ($p<0.0001$), with approximately 40ng/ml IL-6 and 200ng/ml IL-8 measured. The

effect of the conditioned M1 macrophage media could also be significantly ($p<0.05 – 0.001$) reduced by blockage of the IL-1 receptor. Due to the limited supply of patient derived macrophages compared to THP-1 cell line derived macrophages, there were not enough cells to repeat the IL-1α blockage using IL-1α and IL-1β neutralising antibodies either independently or in combination. Instead the IL-1α receptor was blocked directly, with a similar effect size.

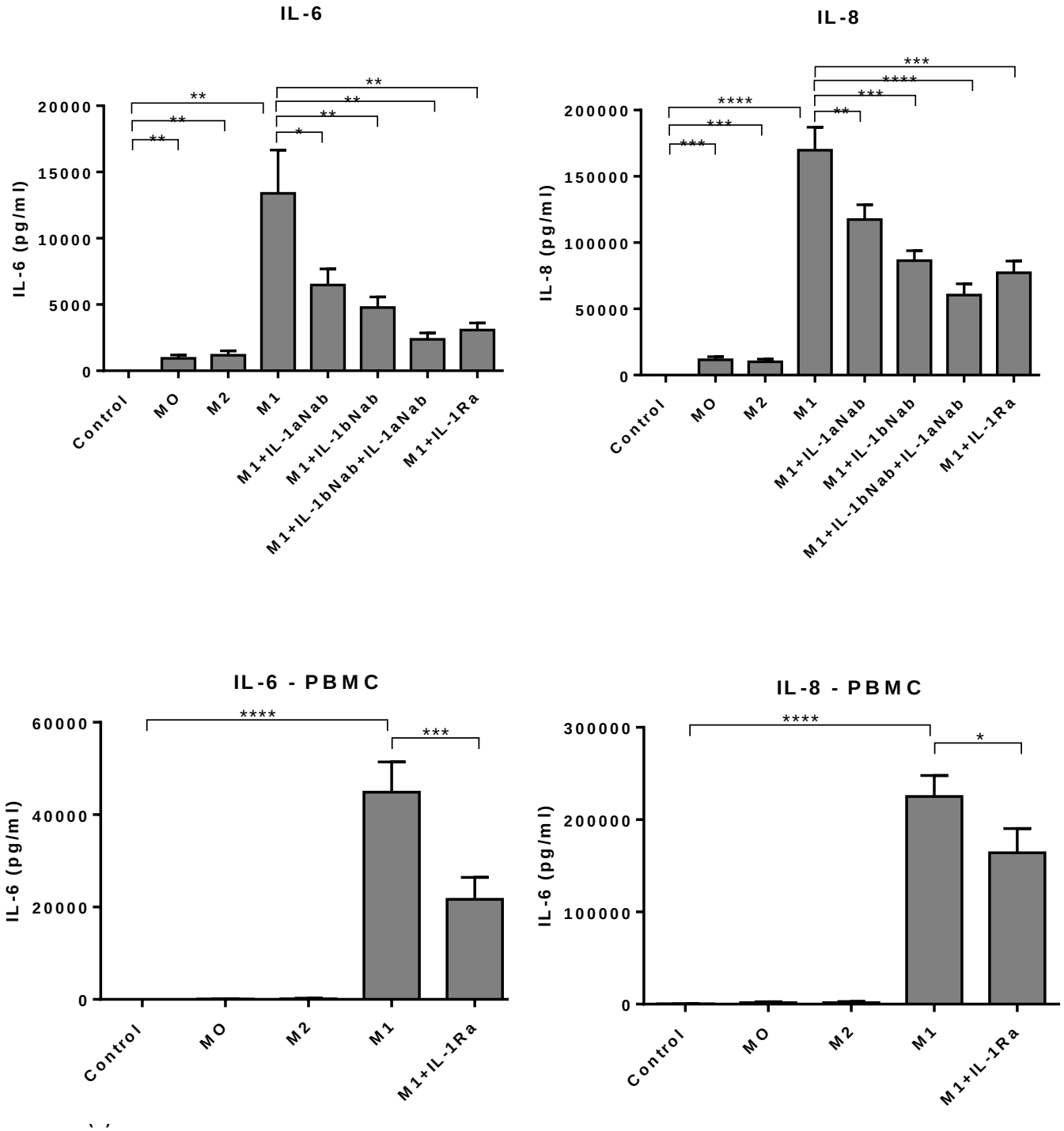

Figure 41. Histograms of IL-6 and IL-8 cytokine released following primary nasal fibroblast co-culture with conditioned media from resting macrophages (M0), classically activated macrophages (M1) and alternatively activated macrophages (M2). Panels (a+b) macrophages derived from THP-1 cell line, (c+d) macrophages obtained from peripheral blood mononuclear cells (PBMCs) from healthy human volunteers. PNFs n=4, THP-1 n=3, PBMCs n=3 plus triplicate repeat. Nab – neutralising antibody, Ra –receptor antagonist. **** = $p<0.0001$, *** = $p<0.001$, ** = $p<0.01$, * = $p<0.05$.

3.5 Discussion

Chronic rhinosinusitis is a very common condition yet our understanding of its pathophysiology of is incomplete. The disease causes a large personal (Hastan et al., 2011, Meltzer et al., 2004) and societal (Ray et al., 1999, Smith et al., 2015) burden. A better understanding of the disease mechanisms involved in producing the persistent, exaggerated upper airway responses will no doubt translate into more modern anti-inflammatory medications. Chronic rhinosinusitis represents a heterogeneous group of conditions with similar nasal symptoms. It is characterised principally by the presence or absence of nasal polyps, though a number of emerging endotypes or sub-phenotypes have been hypothesised that may well demonstrate differing disease mechanisms (Akdis et al., 2013, Tomassen et al., 2016). To further study the condition requires careful phenotyping of recruited participants to draw meaningful conclusions. Within this chapter the results of a carefully phenotyped cohort of age and sex matched participants has been detailed. Patient participants have been selected based on a combination of their validated patient reported outcome measure symptom scores (Hopkins et al., 2009a), endoscopic appearance and radiological imaging scores (Lund and Mackay, 1993) for both CRSsNP and healthy control volunteers. All participants followed the pan-European consensus document for surgical treatment of their chronic sinusitis having failed maximal medical therapy (Fokkens et al., 2012). Once recruited into the study participants were characterised histologically with a biopsy to look for evidence of normal healthy mucosa or features consistent with chronic rhinosinusitis. The histological appearances of tissue biopsies from healthy control and chronic rhinosinusitis without nasal polyp participants included in the study are comparable with histological appearances in the published literature (Kou et al., 2012) and hence appropriate for further detailed CRSsNP studies.

The microbiological environment of the recruited participants was studied using conventional culture and sensitivity techniques as well as a molecular based approach with multiplex quantitative RT-PCR. With the exception of one study participant healthy control volunteers did not grow any pathogens typical of sinusitis or respiratory tract infection. Only three of the CRSsNP patient participants grew clinically significant cultures with a conventional technique and there were no polymicrobial infections demonstrated. This perhaps under represents the bacterial load in the sinonasal cavities of such participants and may be a reflection of the sensitivity of conventional culture to detect relevant microbes,

especially if they are encompassed in a biofilm. A serious challenge of treating patients with chronic infective and inflammatory conditions is that a significant proportion of patients with clinical and laboratory signs of infection do not have organisms detected by traditional culture methods (Ramakrishnan et al., 2016, Tande and Patel, 2014). This can be due to the recalcitrance of biofilm-encased bacteria, which are often present as dormant forms within the biofilms. As a result increasingly molecular techniques are being used to identify the microbiome of the sinonasal cavities more accurately (Boase et al., 2013a, Aurora et al., 2013). To study the whole microbiome of the sinonasal cavity samples is a large and ultimately expensive study beyond the scope of this thesis, however, here I have employed molecular techniques to look for the common upper respiratory tract viruses and bacteria present in a cohort of the recruited patient participants. Initially a screen was performed for viral nucleic acids for molecular detection of ten common respiratory viruses; *Influenza A, Influenza B, Rhinovirus, Respiratory Syncytial Virus, Parainfluenza 1-4, Adenovirus* and *Human metapneumovirus*. Surprisingly the swab results from all participants came back negative for viral nucleic acids. This is especially surprising in the chronic rhinosinusitis participants as chronic rhinosinusitis patients have previously been shown to have high rates of detection of respiratory viruses in nasal lavage and mucosa (Cho et al., 2013), being implicated as triggers of disease flare up. Samples of microbial nucleic acids were collected using the Public Health Laboratory England standardised nucleic acid swab technique, plus samples were taken from both sides of the sinonasal passages to increase the chance of detection. On reviewing the literature it would appear that viral nucleic acids are potentially best detected with tissue biopsies or scraping of the mucosa (Jang et al., 2006), although this does not always yield positive results for viral infection of the sinuses and one study from New Zealand, like the results presented here also could not identify any similar respiratory viruses (Wood et al., 2011). The same mucosal swabs were analysed using RT-PCR to detect nucleic acid from common respiratory pathogens. Unlike the negative results for viral nucleic acids, bacterial pathogens showed seven positive results, six of which were from CRSsNP. Positive molecular detection of *Streptococcus pneumoniae* and *Haemophilus influenza* were shown and in two chronic rhinosinusitis participants both were detected. Despite only using a limited panel of five respiratory bacterial pathogens, the fact that two were detected and polymicrobial pathogens were identified suggests that conventional microbial culture is not as sensitive in analysing the microbial environment of the sinonasal cavities. Such a finding would justify the use of molecular microbiome analysis in future

work once the cost is more reasonable with its increased adoption. It is likely that increased use of microbiome analysis in standard clinical microbiological diagnostic work up is not far from adoption on discussing with colleagues in the local Public Health England Laboratory.

Since I am especially interested in the role of structural epithelial and fibroblast sinonasal cells in CRSsNP, biopsies were characterised to detail the presence and distribution of these particular cells within the tissue samples. Knowledge of the composition of the tissue biopsy facilitated the generation of isolated matched primary cells for culture. Once matched primary cells were isolated they were themselves characterised to ensure the appropriate cells had been isolated and cultured. Epithelial cells were harvested under direct vision from the middle meatus, an anatomically consistent landmark and key sinus drainage point within the paranasal sinus complex. Cytological brushing allowed targeting of a precise location and the process of brushing cells removes only the mucosal layer, therefore all epithelial cells were reproducibly isolated from the same location between patient participants.

Epithelial cells were grown in standardised submerged culture conditions. Upon initial harvesting epithelial cells demonstrated motile cilia visible with live phase contrast microscopy. Motile cilia were present for typically four days of standard submerged tissue culture upon which there mobility were lost. In an effort to maintain motile cilia numerous attempts were made to culture the primary epithelial cells at a more physiological air liquid interface (Muller et al., 2013, Ong et al., 2016). Unfortunately despite these attempts using a variety of protocols I was not able to successfully culture primary nasal epithelial cells reliably to form a differentiated epithelium with motile cilia. From the literature it typically takes up to thirty days to form a differentiated epithelium, though within that time I found that cells would become non-viable detach, float in the media and promote infection of the cultures. Bearing this in mind, I was concerned that further study using this system would more likely be characterising the inflammation from dead and dying cells undergoing physiological inflammatory processes such as necrosis rather than any inflammatory processes from the inflamed CRSsNP tissues and cells of origin.

The primary epithelial cells grown in culture were compared between those from healthy control participants and those from CRSsNP. Comparison with electron microscopy showed the greatest difference, with healthy control epithelial cells showing cilial like structures on

their apical surface in both scanning and transmission electron microscopy in addition to the formation of a pseudostratified epithelium. It is perhaps not surprising that primary epithelial cells from sinusitis participants did not demonstrate features consistent with a healthy epithelium when the histological analysis of the parent tissue biopsies also do not show a healthy ciliated pseudostratified epithelium.

The RPMI 2650 commercially available cell line was investigated to see if in selected circumstances it could be used as a substitute for primary epithelial cells when large numbers of cells were needed, to rapidly expand a cell line or if participants were in short supply. Unlike in many other human conditions, there is a lack of well-validated reliable cellular models to study CRS. The only readily available commercial sinonasal cell line RPMI 2650 is often used in sinonasal studies (Bruno et al., 2014, Pace et al., 2014, Kim et al., 2014, Prevete et al., 2011) yet there is little published data about its relationship to sinonasal cells and its validity as a cellular model. There are no commercially available sinonasal fibroblast cell lines in either the European Collection of Authenticated Cell Cultures (ECACC) or the American Type Culture Collection (ATCC). There are of course some shortcomings from the experimental approach used to compare patient derived primary nasal epithelial cells (PNECs) with the sinonasal cell line RPMI 2650. Firstly both cell types have been grown in submerged culture rather than at a more physiological air-liquid interface to force differentiation. This approach was chosen as earlier air-liquid interface culture experiments were not successful to create a differentiated ciliated epithelium with RPMI 2650 cells in agreement with previous work investigating the cell line in nasal drug delivery studies (Wengst and Reichl, 2010, Merkle et al., 1998). Secondly, a major function of cells of the sinonasal cavity is in mucociliary clearance, which due to the nature of submerged culture could not be assessed here.

From these discrete investigations the sinonasal cell line RPMI 2650 has been shown to be significantly different from patient derived PNECs in terms of its cellular morphology, surface marker expression and biological response to CRS disease relevant inflammatory ligands such as TNF-α (Karosi et al., 2012, Nonaka et al., 2010a, Mfuna-Endam et al., 2011, Cormier et al., 2009). Whilst this is initially disappointing it is perhaps not surprising on further investigation of the cell-line. It was derived from an anaplastic squamous cell carcinoma of the nasal septum in a 52 year old male patient (Moore and Sandberg, 1964). Tumour cells were isolated from the patient's metastatic pleural effusion and grown as adherent nasal

epithelial cells. The cell line demonstrates a similar diploid karyotype to healthy nasal epithelial cells (Moorhead, 1965). It has also been shown to have similarity in terms of the expressed surface cytokeratins (Moll et al., 1983) and produces a typical functional mucoid material visible on the cells apical surface (Moore and Sandberg, 1964). To date the cell line has only been validated as a model to study the regulation of TGF-β biology in house dust mite related allergic rhinitis (Salib et al., 2005). The metastatic, neoplastic source of these cells perhaps explains the mixed epithelial and mesenchymal phenotype and growth pattern in cell culture. The combination of the marked morphological differences, growth pattern and response to inflammatory stimulus demonstrated by RPMI 2650 cells are significantly different to primary nasal epithelial cells. In conclusion no further work was pursued with this cell line and all remaining work was done with patient derived primary human cells.

Fibroblast cells were generated by an outgrowth technique in selective cell culture media from characterised tissue biopsy samples. All samples collected from CRSsNP participants were of the uncinate process, an anatomically consistent landmark in the ostiomeatal complex of the middle meatus allowing reproducibility between patient participants. Healthy control participants were recruited undergoing operations that used the nose as an access route for other structures, such as non-functioning pituitary gland lesions or for the repair of a leak of cerebrospinal fluid from the skull base. All healthy control participants were confirmed to have no sinusitis symptoms, endoscopic or radiological findings therefore it is not ethically appropriate to operate surgically on their healthy sinuses. For this reason, healthy control participants' tissue biopsies were all taken from the sphenoid sinus or skull base as part of their operative procedure. This allowed consistency in the tissue biopsy sample and hence fibroblast cells from healthy controls. However, the healthy control tissue biopsies are from an anatomically different sinus location to the CRSsNP participants. This is the current standard in the literature for healthy control tissue samples (Miljkovic et al., 2014, Jardeleza et al., 2013, Tomassen et al., 2016, Wang et al., 2015).

By isolating and characterising the cultured epithelial and fibroblast structural cells I have removed the recruited immune cells typical of the resulting chronic inflammatory processes as shown in Figure 13. Exactly why the immune cell chemotaxis takes place is not clear and by removing them from the main structural cells it may be that there are differences between the epithelial and fibroblast cells from healthy control and CRSsNP participants that

initiate or maintain the state of persistent inflammation similar to that seen in other chronic inflammatory conditions (Naylor et al., 2013).

The differences in the microscopic appearance between healthy control and chronic rhinosinusitis patient participants are quite dramatic. In health the mucosal layer is best demonstrated in the scanning and transmission electron microscopic appearances with the abundant cilia upon a pseudostratified epithelial layer. In CRSsNP the epithelial loss is marked and the epithelium is replaced by fibrotic matrix as seen in the electron microscopic appearances, tinctorial and immunohistochemically stained images (Figure 13 - Figure 16). This is in keeping with the published literature regarding the pathophysiology of CRSsNP (Van Crombruggen et al., 2011) (Van Bruaene et al., 2012, Kou et al., 2012). The transmission electron microscopy images of tissue biopsies from CRSsNP interestingly show a marked difference in terms of the mitochondria visible. Healthy control participant's images show abundant, healthy mitochondria which supply the energy to the cilial axonemes for mucociliary clearance function of the mucosa. The presence of abnormal, swollen unhealthy looking mitochondria, or even loss of mitochondria in CRSsNP participant biopsies may well be a source of sterile inflammation from necrotic and related cell death pathways as the organelles release their alarmins (Conrad et al., 2016). The increased fibrosis seen in CRSsNP may also be a key factor in the pathophysiology in the disease process. As a result study of the fibroblast in sinonasal disease may offer important insights into the CRSsNP disease process. Additionally analysis of fibroblasts in upper airway diseases may offer insights into conditions with related fibrotic and mucosal inflammatory processes. If the core mechanisms of fibrosis and inflammation were understood and applicable in anatomically different tissue sites it would allow aspects of fibrosis research to be carried out where access to disease tissue is simplest. With the exception of the skin, the sinonasal mucosa is amongst the most accessible epithelial surfaces in the body. Access to material to harvest for cell, tissue and microbiological research can be provided by a variety of brushings, small biopsies, mucosal scrapes or swabs from the clinic. The nose thus offers a convenient portal for the study of generic inflammatory mechanisms and the introduction of novel therapies. Sinonasal disease surveillance is likewise very straightforward, as office based endoscopic nasal assessment readily supplements well-validated disease symptom scores. Sinonasal medications are also often topically applied via a nasal aerosol, with minimal systemic exposure.

Within the respiratory system Idiopathic pulmonary fibrosis (IPF) represents the most common progressive interstitial lung disease, characterised by proliferation of fibroblasts and deposition of extracellular matrix. Once established, the disease typically progresses to respiratory failure. The postulated pathogenesis is of repetitive respiratory epithelial injury, followed by airway remodelling and an increase in mesenchymal cells including fibroblasts and activated myofibroblasts, either by proliferation of pre-existing resident cells or via epithelial to mesenchymal transition (EMT) (Loomis-King et al., 2013). Accumulation of fibroblasts is associated with an increase in chronic inflammation. Similar epithelial cell loss, fibroblast accumulation and chronic inflammation are seen in upper airway inflammatory diseases. There are no *in vivo* IPF models that mirror human disease progression, and animal models of upper airway inflammation are similarly limited. Human studies targeting the fibro-proliferation in IPF have shown initial promise, though no superiority to placebo in randomised controlled trials of prednisolone, azathioprine, Interferon-γ, anti-TNF-α and endothelin receptor antagonists has been shown. Focus is now shifting towards specific fibroblast targeted therapies. Lower airway tissue samples can be isolated using variety of methods such as bronchoscopic guided biopsy or cellular brushings, though in patients with declining respiratory function these are not without risk. However, since the upper airways are lined by similar respiratory epithelium, it would be possible to use the more accessible sinonasal epithelium as a window into the mechanisms of disease further down the airway.

The literature detailing the potential mechanisms of lower airway inflammatory disease is much more extensive than the published work on the upper airway and sinusitis. As a result the cellular investigations described here are guided by advances in the lower airway disease literature. A similar approach in an unrelated field within otolaryngology, Human Papilloma Virus (HPV) mediated head and neck cancer research, following progress in the gynaecological cancer literature has yielded significant translational benefits for patients with oropharyngeal cancer (D'Souza et al., 2007, Guo et al., 2016). Within our airways research group colleagues have identified that the epithelial alarmin IL-1α is sufficient and essential to generate inflammatory responses in human lung fibroblasts (Suwara et al., 2014). Further, the inflammation can be pharmacologically blocked by commercially available monoclonal blocking antibodies and receptor antagonists that have been shown to be safe in clinical trials (Singh et al., 2016). Due to the ready availability for potential topical delivery of IL-1α medications and the extensive epithelial damage seen in CRSsNP the epithelial IL-1α alarmin mechanism was investigated with the primary sinonasal cells.

Epithelial cells were stimulated with a range of disease specific stimuli together with thapsigargin (Figure 34), a known potent inducer of epithelial stress as a positive control (Suwara et al., 2014). The viability of primary epithelial cells was maintained across a range of concentrations of respiratory tract bacteria and cigarette smoke extract. Significant cell death was only seen with supra physiological concentrations of 100% cigarette smoke extract, mM concentrations of the oxidative stress inducing hydrogen peroxide and high doses of the endoplasmic reticulum stressor thapsigargin. When the culture supernatants of these matched cultures were measured for release of the epithelial alarmin IL-1α only very small amounts were measurable (Figure 35). The only measurably significant IL-1α release was demonstrated with supra physiological hydrogen peroxide or thapsigargin. The epithelial cells however, are not the only possible mucosal source of alarmins such as IL-1α. Since lower airway fibroblasts have previously been shown to be particularly inflammatory in response to IL-1α, the response of sinonasal fibroblasts to alarmins as a driver of inflammation was investigated. Primary cultures of nasal fibroblasts were shown to be responsive to a range of alarmins, mounting appropriate pro-inflammatory cytokine responses. Across the panel of alarmins investigated, IL-1α produced the most potent and significant response in primary nasal fibroblasts. When directly compared to primary lung fibroblasts in the same experimental conditions nasal fibroblasts were approximately twice as responsive to co-culture with IL-1α. However, direct comparisons between healthy control and CRSsNP participant primary nasal fibroblasts' response to alarmins did not show any statistically significant differences, suggesting there are potentially more factors involved, most likely the local inflammatory environment of the sinonasal mucosa. Since nasal fibroblasts demonstrated such a potent response to the alarmin IL-1α alternate sources of IL-1α were investigated within the inflammatory milieu of the nasal mucosa.

Resident tissue macrophages are a prominent source of IL-1α and on reviewing the histology of CRSsNP and healthy control tissue in Figure 13 there is an increase in the number of macrophages in CRSsNP tissue biopsies. Tissue resident macrophages are also able to recognize the danger signals released from necrotic cells via pattern recognition receptors and secrete IL-1 resulting in acute neutrophilic inflammation (Kono et al., 2014). Neutrophilic infiltration is also seen as feature in the presented CRSsNP histology. It is therefore plausible that the epithelial cell damage, a hallmark of CRSsNP (Kou et al., 2012) is sensed either directly by the underling stromal fibroblasts or in combination by the resident macrophages, which in turn amplify the immune response by secretion of pre-formed IL-1 with neutrophil

chemotaxis. Within the histology of Figure 13 there is also an increase in the number of CD3 positive T-cells which is also not surprising; the cell death visible in the epithelial layer will also stimulate the acquired immune response by activating T cells.

The possible mechanism of macrophage mediated IL-1α was investigated by co-culture experiments together with independent pharmaceutical blockage of IL-1α and IL-1β using neutralising antibodies and blockage of the IL-1 receptor with IL-1α receptor antagonist. Primary fibroblasts cultured with conditioned media from resting M0 macrophages, classically activated M1 macrophages or alternatively activated M2 macrophages were measured for the most prominent inflammatory cytokines, IL-6 and IL-8, shown to be released in earlier stimulus experiments (Figure 41). Neither conditioned media from patient derived M0 or M2 macrophages produced significant IL-6 or IL-8 responses in primary nasal fibroblasts. In contrast, however conditioned media from classically activated M1 macrophages produced a dramatic release of nanogram concentrations of IL-6 and IL-8 which could be significantly blocked with a combination of blocking the IL-1α and IL-1β components of the IL-1 receptor pathway. When the effects of conditioned media from activated M1 macrophages were blocked by either IL-1α or IL-1β alone it resulted in less IL-6 and IL-8 release, though the reduction was not as marked as in combination with blockage of IL-1α demonstrating greater inhibition than IL-1β. When used in combination the IL-1α and IL-1β neutralising antibodies had the greatest effect. This result is not surprising as either IL-1α or IL-1β ligands can stimulate the IL-1 receptor. The combined effect of IL-1α and IL-1β neutralising antibodies was as expected and similar to the effect size when the IL-1 receptor antagonist was used as both strategies should block stimulus of the IL-1 signalling pathway. The high IL-8 release from nasal fibroblasts cultured with conditioned media from classically activated M1 macrophages was in the order of 150-200ng/ml. When reviewing the CRSsNP immunohistochemical immune cell staining the high levels of nasal fibroblast derived IL-8 would correlate well with the neutrophilic infiltrate seen as IL-8 is a known potent C-X-C motif neutrophil chemokine (de Oliveira et al., 2016). IL-8 primarily induces chemotaxis in neutrophils (Kay et al., 2008), was historically called neutrophil chemotactic factor (Yoshimura et al., 1987) and is also chemotactic for other granulocytes (Proudfoot, 2002). When the immunohistochemical staining for immune cells in chronic sinusitis tissues are compared to the fluorescent immunohistochemical staining of tissue sections for epithelial and fibroblast markers there is co-localisation of recruited immune cells and nasal fibroblasts within the lamina propria.

Taken together the histological images presented in this chapter of CRSsNP with the isolated primary sinonasal cells and their co-culture experiment responses may help to explain some of the characteristic appearances of epithelial cell loss, immune cell recruitment and fibrotic basement membrane thickening seen when compared to healthy sinonasal mucosa.

3.6 Conclusion

A well phenotyped cohort of healthy control and chronic rhinosinusitis patient participants has been recruited. From this cohort the participants have been characterised based on their clinical, endoscopic, radiological, microbiological and histological appearances consistent with the published literature. An initial analysis of possible inflammatory mechanisms has been considered and a HTA approved biobank of recruited tissue biopsy, microbiological and primary cellular samples established for further study as described in the following chapters 4 and 5.

4 Results – Sinonasal environment analysis

4.1 Specific aims & objectives

The specific aims and objectives for this phase of research were to measure the sinonasal micro environment of participants and their subsequent study samples with non-polypoid chronic rhinosinusitis (CRSsNP) and a cohort of healthy control volunteers. I aimed to measure the environmental milieu of the sinonasal mucosal lining fluid - i.e. the mucus- in continuity with the mucosal surface to characterise its constituent inflammatory mediators in health and CRSsNP. The same panel of inflammatory mediators were investigated in whole lysates of matched tissue biopsies, isolated primary epithelial and fibroblast samples and venous blood serum samples to determine if the inflammatory micro environment was preserved between different types of study samples.

4.2 Scientific rationale for experimental approach

To ensure the laboratory study of my CRSsNP and control samples are as representative of the situation in vivo I assayed the mucosal microenvironment in health and CRSsNP. In chapter 3, I have demonstrated well phenotyped cohorts of CRSsNP participants and controls and their associated study samples. So far I have presented information on the morphological appearance of histological and cellular samples together with clinical symptom scores, surface protein expression and microbiological data. However, I do not have any information on the inflammatory micro environment of the mucosal surfaces in CRSsNP and health. It is important to identify the mediators present in the inflammatory environment in the sinonasal cavities (a) so that this information can be used to help replicate these physiological conditions in any in vitro cellular based experiments and (b) can be used to help develop CRS biomarkers.

4.3 Methods

4.3.1 Mucosal lining fluid samples

Once enrolled in the study, patients proceeded to surgery as normal. Following induction of general anaesthesia prior to their operation a mucosal lining fluid analysis sample was taken. A 7x30mm piece of leukosorb filter paper (BSP0669 Pall life sciences, US) was applied to the anterior portion of the inferior nasal turbinate for two minutes (Figure 42) to absorb nasal secretions as has been utilised in studies of allergic rhinitis (Nicholson et al., 2011). It was transported back to the lab and stored at -80˚C.

Once ready for analysis the mucosal lining fluid was eluted out of the filter paper. The filter paper was placed into filter cups within Eppendorf tubes (Costar spin-X, cellulose acetate) and 500µl of assay buffer added (PBS, 1% BSA, 0.05% Tween-20, Sigma UK). Spin filtration was performed by centrifugation at 16 000g for 5 minutes. The eluted fluid was collected and either used immediately for analysis by ELISA or stored as aliquots at -80˚C.

(a) (b)

Figure 42. Mucosal lining fluid analysis technique. (a) The leukosorb filter paper strips are placed along the inferior turbinate, just inside the nose. (b) Photograph of a healthy volunteer for mucosal lining fluid analysis, once inserted in the nose a spirometry nasal clip is placed to apply even pressure for absorption for two minutes. (a) Image adapted from (Chawes et al., 2010).

4.3.2 Serum sample processing

A blood sample was taken from each participant to determine if chronic sinusitis is associated with any systemic signal of inflammation in the peripheral blood. A 5ml sample was collected, stored in a serum separating vacutainer tube and transported back to the laboratory. The serum was separated out by centrifugation at 3500 rpm for 10 minutes in a Thermo IEC Centra CL2 centrifuge, with 500µl aliquots stored at -80˚C.

4.3.3 Protein isolation

Protein was isolated from tissue biopsies by homogenisation with a lysis buffer and protease inhibitor. Two tablets of protease inhibitor (Roche Complete Mini 11836153001, Switzerland) were dissolved in 10ml of RIPA lysis buffer (Sigma R0278, UK). 500µl aliquots of RIPA buffer/protease inhibitor were prepared and 100mg of tissue was added. Samples were homogenised with a bead homogeniser (Qiagen TissueLyser II, Netherlands) for two cycles of 2 minutes at 30Hz. Homogenised samples were then centrifuged at 13 000 RPM for 10 minutes at 4˚C to pellet any debris. Samples were then transferred to a new Eppendorf tube to determine the protein extraction yield.

4.3.4 Protein extraction quantification

Determination of the yield of protein extracted was performed by the copper ion based colorimetric BCA (bicinchoninic acid assay) technique (Pierce 23225, USA). The technique was run as per manufacturer's instructions using the 96 well microplate method. 25µl of standards and samples were pipetted onto a 96 well plate and the absorbance was measured at 562nm on a Multiskan FC spectrophotometer (Thermoscientific, USA).

4.3.5 Enzyme linked Immunosorbent assay (ELISA)

Sandwich ELISA kits were used in a pilot study to quantify the amount of mediators present in mucosal lining fluid swabs. A 96 well format ELISA kit was used to measure the amount of cytokines including IL-8 and IL-1α present as per manufacturer's instructions (DY208, R&D systems USA). The amount of cytokine present was read by the optical densities at 450nm compared to the standard curve on a Multiskan FC spectrophotometer (Thermoscientific, USA).

4.3.6 MSD Electrochemiluminescence multiplex analysis

Multiplex MSD electrochemiluminesce is a similar technique to ELISA, using a 96 well microplate format to quantify the total protein concentration of a given sample (Figure 43). The main advantage it offers over conventional ELISA is the ability to analyse individual samples for multiple mediators from small sample volumes that would not otherwise be possible to achieve from individual ELISAs. MSD assays are also sandwich immunoassays, though they utilise electrochemiluminescence to generate a light signal rather than a colour change. Sample analytes bind to capture antibodies that are immobilised on a working electrode; detection antibodies complete the sandwich technique. Appropriate buffers are added to provide the chemical environment for electrochemiluminescence, a voltage is then applied to the working electrode which causes captured analytes to emit light which is then measured in the MSD QuickPlex SQ 120 plate reader (Mesoscale discovery, US).

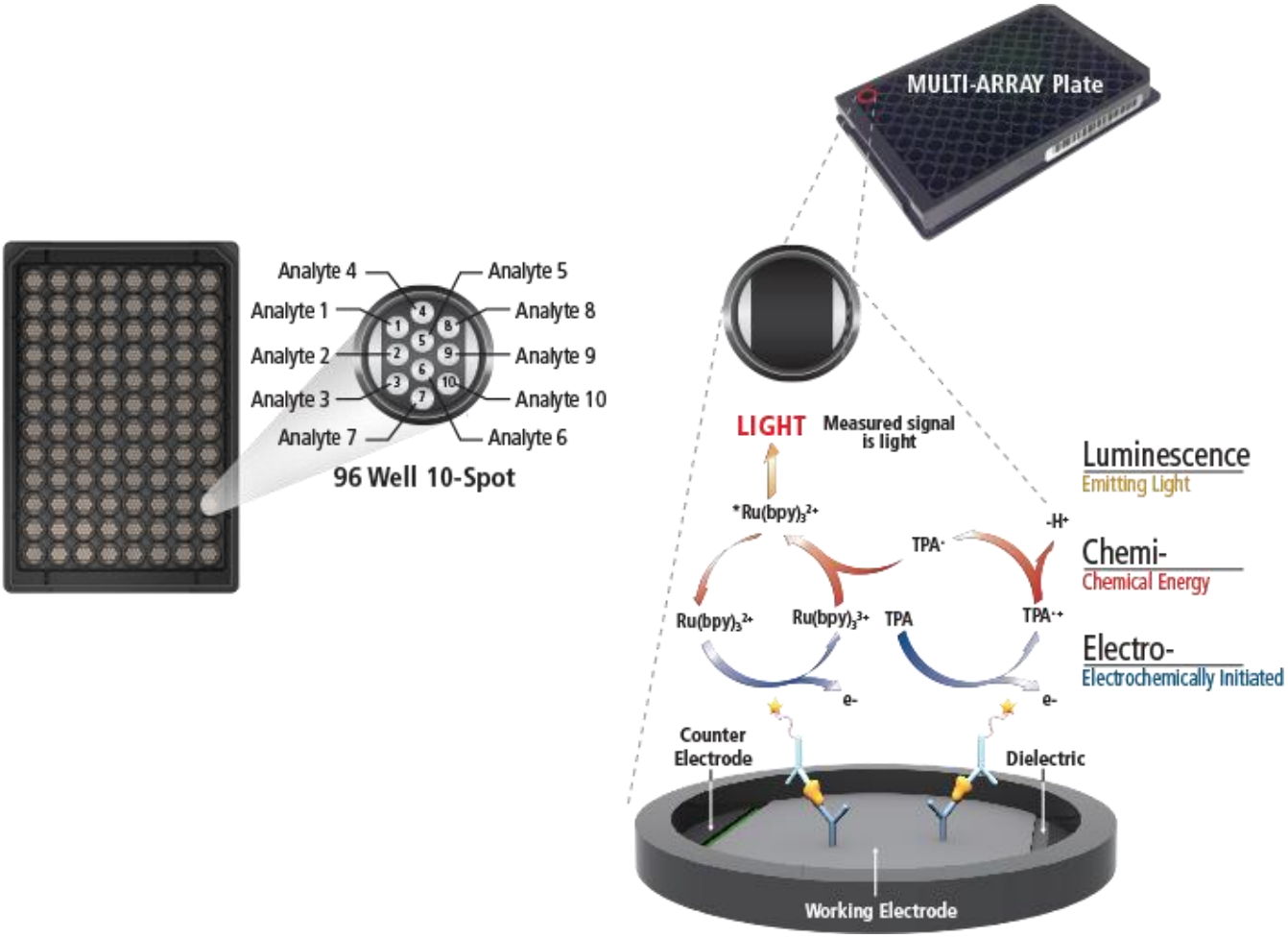

Figure 43. Principle of MSD electrochemiluminescence. Capture of a mediator within a sandwich immunoassay which generates light on the application of an electric current. Image adapted from (Discovery, 2016).

4.3.6.1 Bioinformatics analysis of inflammatory mediators

Results from the multiplex analysis of sample analytes were interrogated using bioinformatics techniques to identify how the various mediators may interact in CRSsNP. Differentially expressed mediators were entered into the open access bioinformatics tools NetworkAnalyst (http://www.networkanalyst.ca) as per Xia et al in Nature Protocols (2015), WEB-based GEne SeT AnaLysis Toolkit (WebGestalt) (http://www.webgestalt.org/) as per Wang et al (2013), GOstats Bioconductor Gene ontology and gplots Heatmap2 open source R package (https://www.bioconductor.org/packages/devel/bioc/html/GOstats.html/) as per Falcon and Gentleman (2007) and (Gregory R. Warnes et al., 2016).

4.4 Results

4.4.1 Sinonasal micro environment analysis

A pilot group for mucosal lining fluid analysis was used to see if I could utilise the technique to assay the sinonasal micro environment. Five volunteers participated in this test group with a range of nasal symptoms. Their sinonasal outcome test 22 (SNOT-22) scores varied from 3 to 22. From each participant the fluid eluted from the mucosal lining fluid analysis was analysed to determine firstly if any alarmins or cytokines could be detected by ELISA and if so, their respective concentrations.

Analysis of the eluted mucosal lining fluid demonstrated measurable amounts of the alarmin IL-1α and the cytokine IL-8. IL-1α was measured in the range 130 – 320pg/ml and IL-8, 40-140ng/ml, demonstrating mucosal lining fluid concentrations well within the working tolerances of the ELISA kits (Figure 44). Whilst the sample number is much too small to draw statistically significant inferences, the possibility of a positive correlation between SNOT-22 score and IL-1α mucosal lining fluid concentrations appears to warrant further exploration.

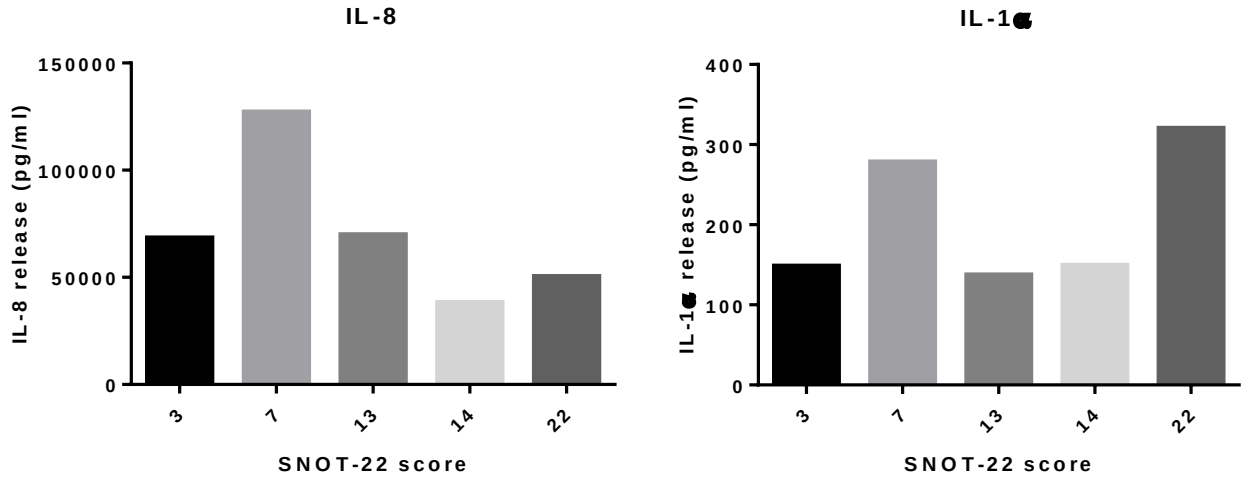

Figure 44. Histograms to show the pilot amounts of IL-8 and IL-1α detected from eluted mucosal lining fluid of anonymised volunteers by ELISA. The volunteers are identified by their Sino Nasal Outcome Test-22 (SNOT-22) score along the x axis (n=5).

Following pilot proof of principle, 40 participants consisting of 18 healthy controls and 22 CRSsNP patients were selected for further analysis. The technique established in section 4.3.1 was used to generate mucosal lining fluid samples for multiplex MSD electrochemiluminesce using the V-PLEX Human Biomarker 40-Plex Kit (Mesoscale discovery, US). The measurements for the 40 different human biomarker mediators were compared between the CRSsNP and control groups and are displayed in Figure 45 and Table 6. The expression of 13 of the 40 human biomarker panel mediators was significantly different in CRSsNP and healthy control samples using a Mann Whitney U test ($p<0.05$ – $p<0.005$). The raw data was Log 10 transformed to make the data spread more uniform and the same pattern of difference was obtained with an un-paired t-test. The 13 mediators comprised a group of 5 chemokines, 3 cytokines, 3 angiogenesis mediators and 2 vascular injury mediators (Table 5).

	Mediator
5 chemokines	Macrophage inflammatory protein 1-alpha (MIP-1alpha/CCL3)
	Macrophage inflammatory protein 1-beta (MIP-1beta/CCL4)
	Monocyte chemoattractant protein 4 (MCP-4/CCL13)
	Thymus and activation regulated chemokine (TARC/CCL17)
	Eotaxin 3 (CCL26)
3 cytokines	Interleukin 10 (IL-10)
	Interleukin 6 (IL-6)
	Interleukin 17 (IL-17)
3 angiogenesis mediators	Basic fibroblast growth factor (bFGF)
	Placental growth factor (PlGF)
	Soluble Fms-like tyrosine kinase 1 (sFlt-1) / vascular endothelial growth factor receptor 1 (VEGFR1)
2 vascular injury mediators	Serum amyloid A (SAA)
	Vascular cell adhesion molecule 1 (VCAM-1/CD106)

Table 5. List of significantly different CRSsNP mucosal lining fluid mediators.

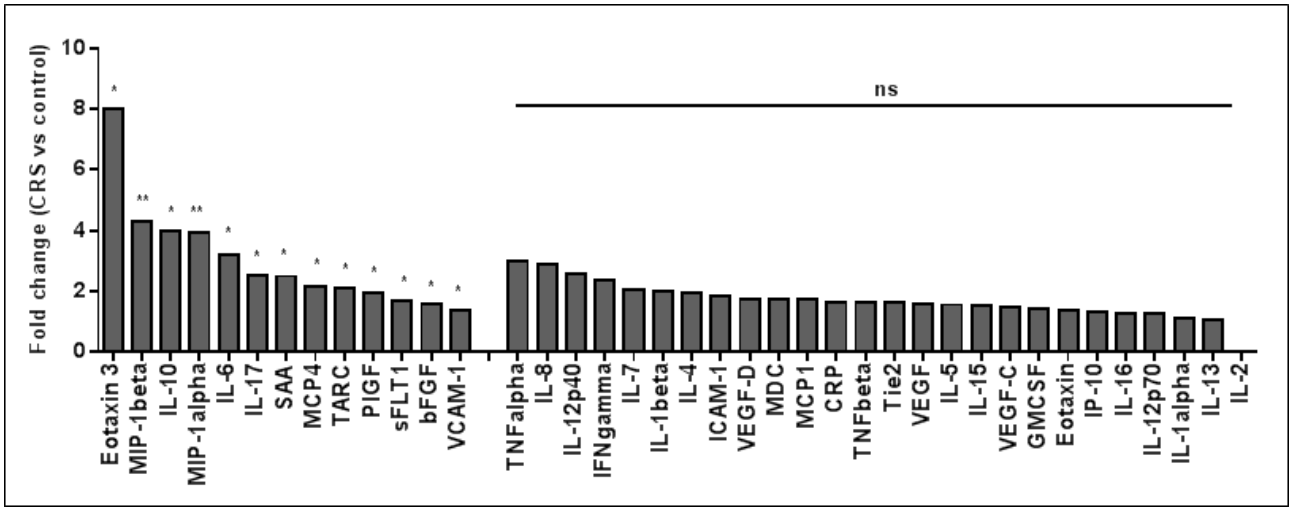

Figure 45. Histograms to show the relative fold change of mucosal lining fluid markers in CRSsNP participants compared to controls. * = p<0.05, ** =p<0.005, n=40 participants.

	Control		CRS				
Marker	Median (pg/ml)	Range (pg/ml)	Median (pg/ml)	Range (pg/ml)	fold change	p-value	p-value
Eotaxin 3	11.68	0-708.57	93.42	0-2799.62	8.00	0.0207	*
MIP-1beta	46.58	9.19-244.86	200.4	7.93-1740	4.30	0.0018	**
IL-10	0.09104	0-1.22	0.3635	0-2.66	3.99	0.0344	*
MIP-1alpha	22.41	7.34-133.77	88.77	8.89-809.32	3.96	0.0037	**
IL-6	3.353	0.79-46.22	10.82	0.30-815.95	3.23	0.0416	*
IL-17	1.445	0-17.73	3.637	0.07-21.72	2.52	0.0475	*
SAA	1257	216.77-13953.01	3152	321.80-134678.30	2.51	0.0174	*
MCP4	11.07	5.41-78.96	23.96	3.02-87.33	2.16	0.0148	*
TARC	18.1	3.70-159.38	37.9	2.03-133.31	2.09	0.0388	*
PIGF	25.55	13.30-95.21	49.86	11.17-206.01	1.95	0.0188	*
sFLT1	256.2	96.83-1067.99	429.8	28.90-3057.15	1.68	0.0218	*
bFGF	15.88	1.02-79.85	25.33	2.21-69.24	1.60	0.0218	*
VCAM-1	1506	88.03-8366.40	2071	98.16-27388	1.38	0.0416	*
TNFalpha	0.207	0-2.48	0.626	0-5.91	3.02	0.1422	ns
IL-8	4158	79.36-186497.7	12028	309.26-183320	2.89	0.3769	ns
IL-12p40	1.399	0.27-9.51	3.62	0.37-18.77	2.59	0.0741	ns
IFNgamma	0.7294	0-2992.93	1.723	0-145.68	2.36	0.1253	ns
IL-7	13.8	3.91-48.95	28.59	4.79-60.31	2.07	0.0787	ns
IL-1beta	17.21	0.86-637.23	34.45	0.97-1047.46	2.00	0.3347	ns
IL-4	0.05214	0-0.30	0.102	0-1.17	1.96	0.1778	ns
ICAM-1	2689	385.24-9382.23	5038	264.52-16112.08	1.87	0.0577	ns
VEGF-D	66.29	0-489.13	117.3	23.34-366.22	1.77	0.3769	ns
MDC	56.77	12.11-360.09	100.1	14.26-323.23	1.76	0.2713	ns
MCP1	164.9	25.74-461.99	288.1	13.31-784.12	1.75	0.1311	ns
CRP	7249	540.09-60334.98	12059	723.38-398357.1	1.66	0.1616	ns
TNFbeta	0.136	0-0.67	0.2249	0.08-1.44	1.65	0.062	ns
Tie2	185.9	0-556.27	301.2	20.70-967.78	1.62	0.1383	ns
VEGF	865.5	228.78-5047.48	1362	202.17-4593.71	1.57	0.2065	ns
IL-5	1.36	0.37-3.26	2.12	0.15-5.94	1.56	0.0615	ns
IL-15	1.363	0.37-3.25	2.117	0.15-5.94	1.55	0.0615	ns
VEGF-C	176.7	87.22-1629.34	258.1	34.51-3333.66	1.46	0.1535	ns
GMCSF	0.4908	0.09-2.52	0.7013	0.08-9.39	1.43	0.2956	ns
Eotaxin	47.45	8.46-244.39	66.1	4.43-268.09	1.39	0.2065	ns
IP-10	471.1	19.70-6424	628.2	60.96-8749.44	1.33	0.1985	ns
IL-16	527.7	4.35-2058.67	661	9.22-6919.09	1.25	0.2268	ns
IL-12p70	0.1194	0-0.65	0.1494	0-1.88	1.25	0.5836	ns
IL-1alpha	89	13.95-424.83	100.4	12.89-393.17	1.13	0.6311	ns
IL-13	0.7633	0-1.81	0.7959	0-4.83	1.04	0.3148	ns
IL-2	0	0-1.23	0	0-3.67	0.00	0.6818	ns

Table 6. Table to summarize mucosal lining fluid marker data. ns = non-significant p value.

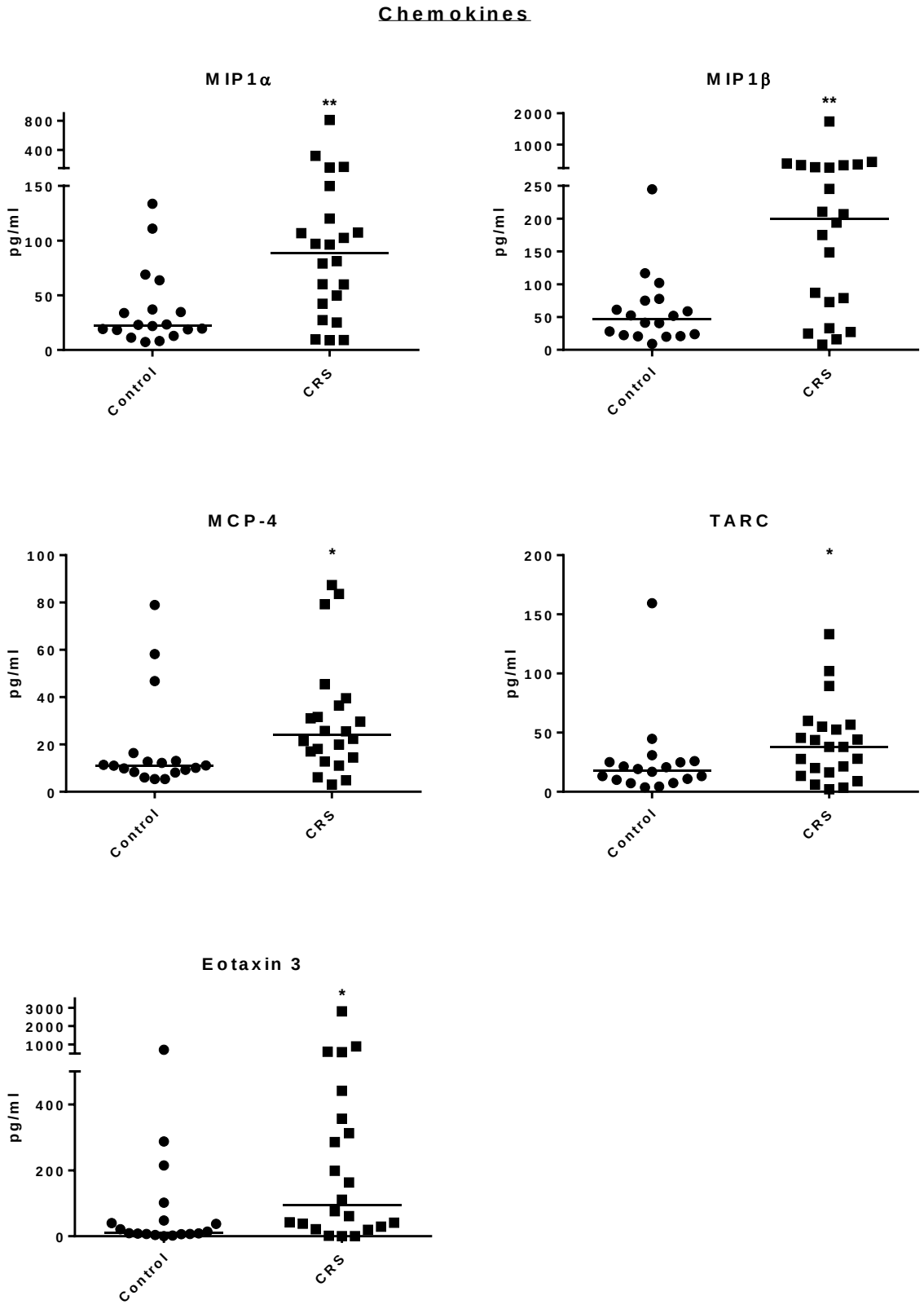

Figure 46. Column scatter plots of discriminant chemokine mediators between CRSsNP and healthy control participants. * = p<0.05, ** =p<0.005, n=40.

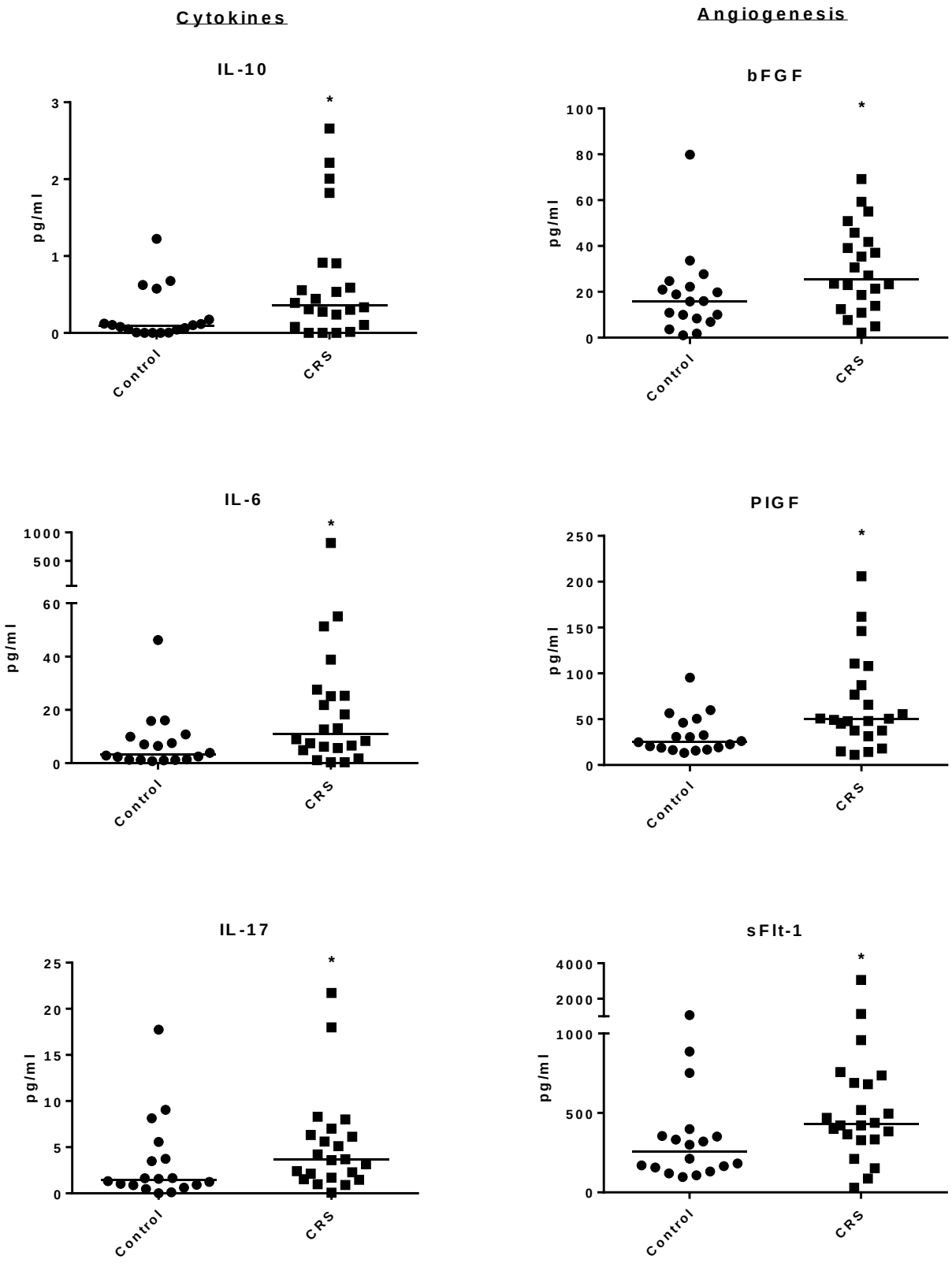

Figure 47 Column scatter plots of the discriminant cytokine and angiogenesis mediators between CRSsNP and healthy control participants. * = p<0.05, ** =p<0.005, n=40.

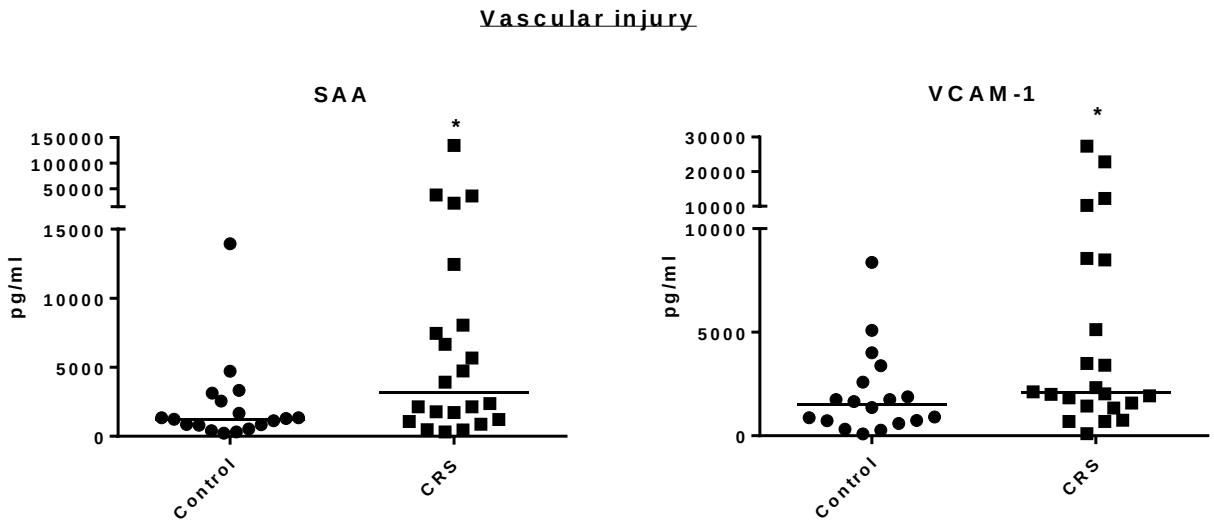

Figure 48. Column scatter plots of the discriminant vascular injury mediators between CRSsNP and healthy control participants. * = p<0.05, ** =p<0.005, n=40.

4.4.1.1 Relationship between mediators and symptom scores

The 13 discriminant mucosal lining fluid mediators (Table 5) were compared to the rhinological subscale of the sinonasal outcome test 22 (RSNOT-22) patient reported outcome measure scores. All 13 were associated with the SNOT-22 rhinological sub-scale symptom scores (p<0.05 – p<0.01) by Spearman's rank-order correlation (Appendix and Figure 49-Figure 51). A Spearman's rank-order correlation was also run to assess the relationship between RSNOT-22 and mucosal lining fluid mediators in CRSsNP participant samples alone. Preliminary analysis showed the relationship to be monotonic, as assessed by visual inspection of a scatterplot. Within this CRSsNP sub group analysis there was a positive correlation between RSNOT-22 and MIP1a, MIP1b, sFLT1 and VCAM (rs = .424,.455,.453,.498 respectively, all p < 0.05).

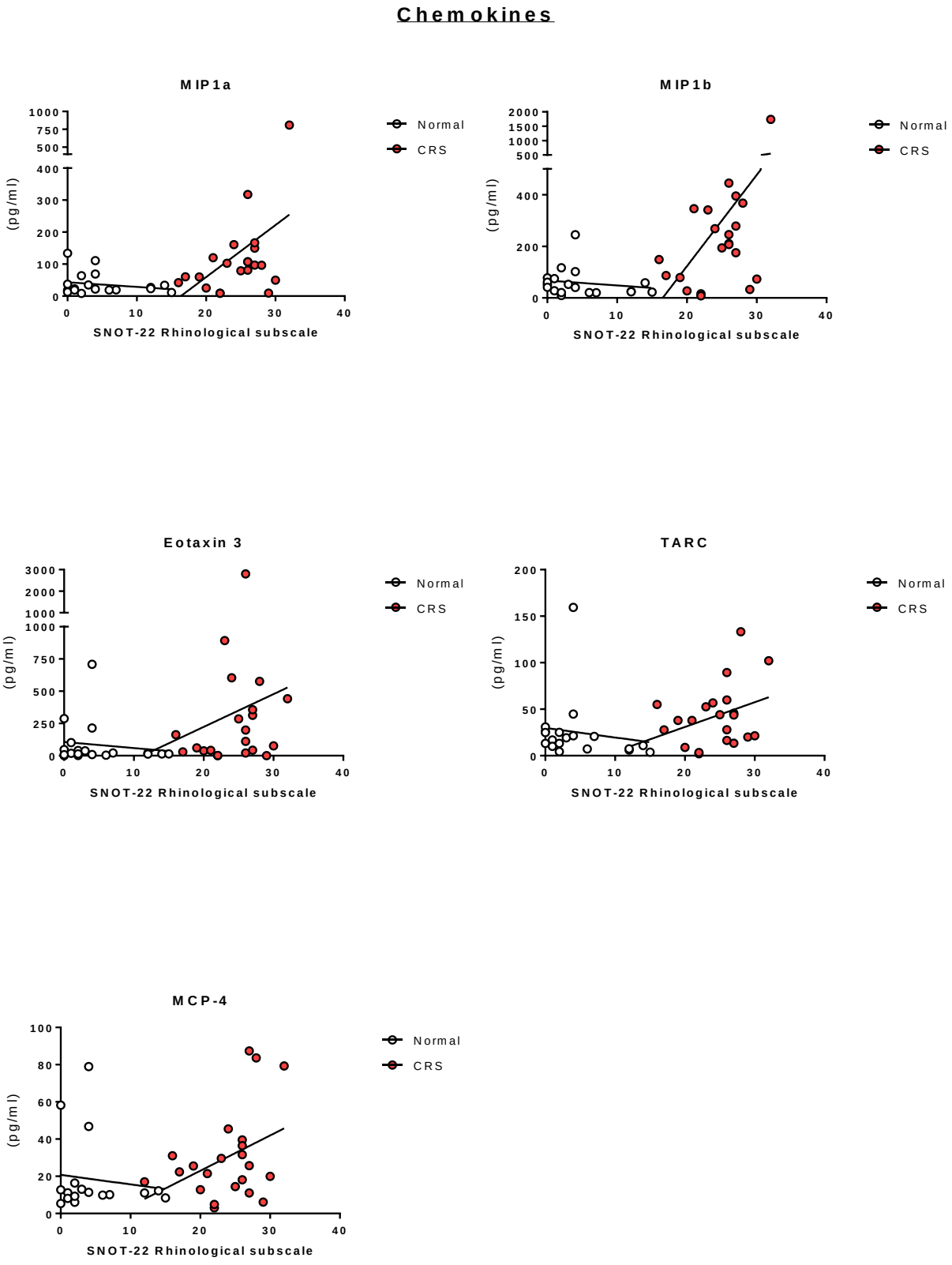

Figure 49. XY plots to show relationship between SNOT-22 rhinological subscale symptom scores and significantly differentially expressed mucosal lining fluid chemokine markers, n=40.

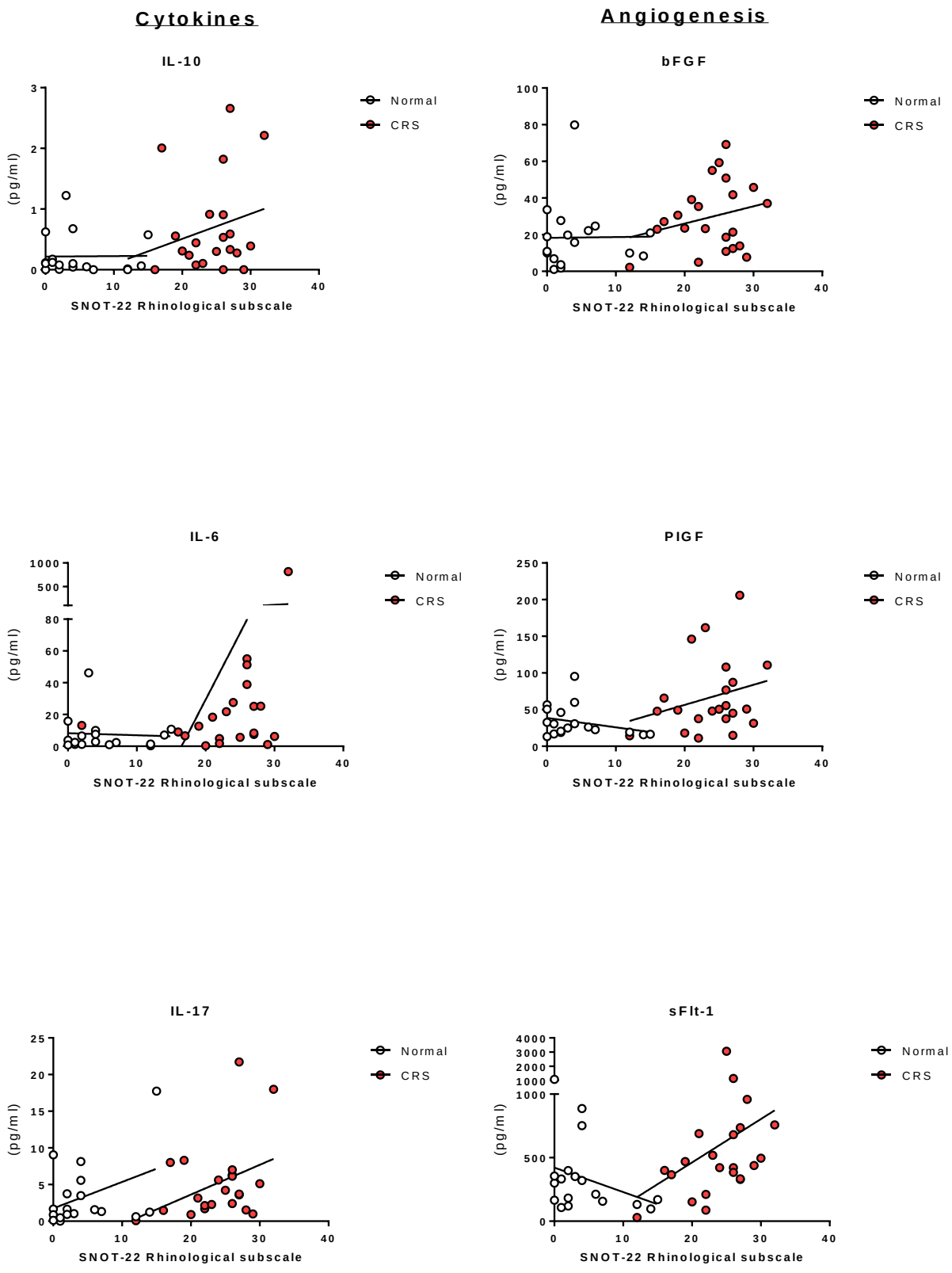

Figure 50. XY plots to show relationship between SNOT-22 rhinological subscale symptom scores and significantly differentially expressed mucosal lining fluid cytokine and angiogenesis markers, n=40.

Vascular injury

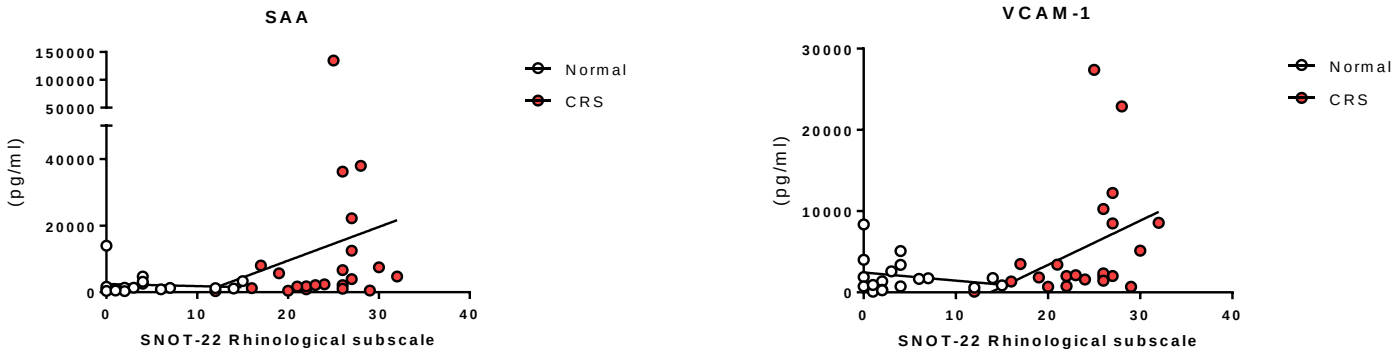

Figure 51. XY plots to show relationship between SNOT-22 rhinological subscale symptom scores and significantly differentially expressed mucosal lining fluid vascular injury markers, n=40.

4.4.2 Factor analysis

A factor analysis was used to try to make sense of the multiple correlations among the markers which discriminate controls and patients. Measurement of the nasal microenvironment in such a way has the potential to revolutionise CRS phenotyping which is currently quite crude – allergy or no allergy; polyps or no polyps. Exploratory factor analysis was run on the 13 discriminant biomarker levels in my 40 CRSsNP and control participants. The suitability of factor analysis was measured as a part of the analysis. Firstly, inspection of the correlation matrix shows that all protein markers had multiple correlation co-efficients greater than 0.4 (Table 8). Secondly, the cumulative Kaiser-Meyer-Olkin (KMO) measure of sampling adequacy was satisfactory at 0.700, classified as 'middling' by Kaiser (Kaiser, 1974). Finally, Bartlett's test of sphericity was statistically significant ($p<0.0005$), again suggesting that the data was likely to be suitable for factor analysis.

On performing a factor analysis five factors explained more than 89.5% of the total variance of the mediators: 44.1%, 19.8%, 11.9%, 7.6% and 6.3% respectively (Figure 52). Analysis of the scree plot shows an inflection point at four factors where the graph flattens (Figure 52) and addition of further factors adds very little to the total variance explained (Cattell, 1966). Inspection of the rotated component matrix confirmed the selection of a four factor solution as it met the interpretability criterion.

Use of a four factor solution explained 83.3% of the total variance. Varimax orthogonal rotation was used to aid interpretation (Table 7). Analysis of the rotated solution confirmed a simple structure (Thurstone, 1948) with strong loadings of pro-inflammatory items on factor 1, vascular inflammatory items on factor 2, chemokine and growth factor items on factor 3 and regulatory items on factor 4. The model thus has convincing face validity, though being critical of these groupings factor 3 does not demonstrate as clean loading of items into the factor. Placental growth factor (PlGF) and basic fibroblast growth factor (bFGF) do not show as clean loading between the factors compared to the remaining 11 mediators in the rotated component matrix (Table 8) and have therefore been italicised in Table 9.

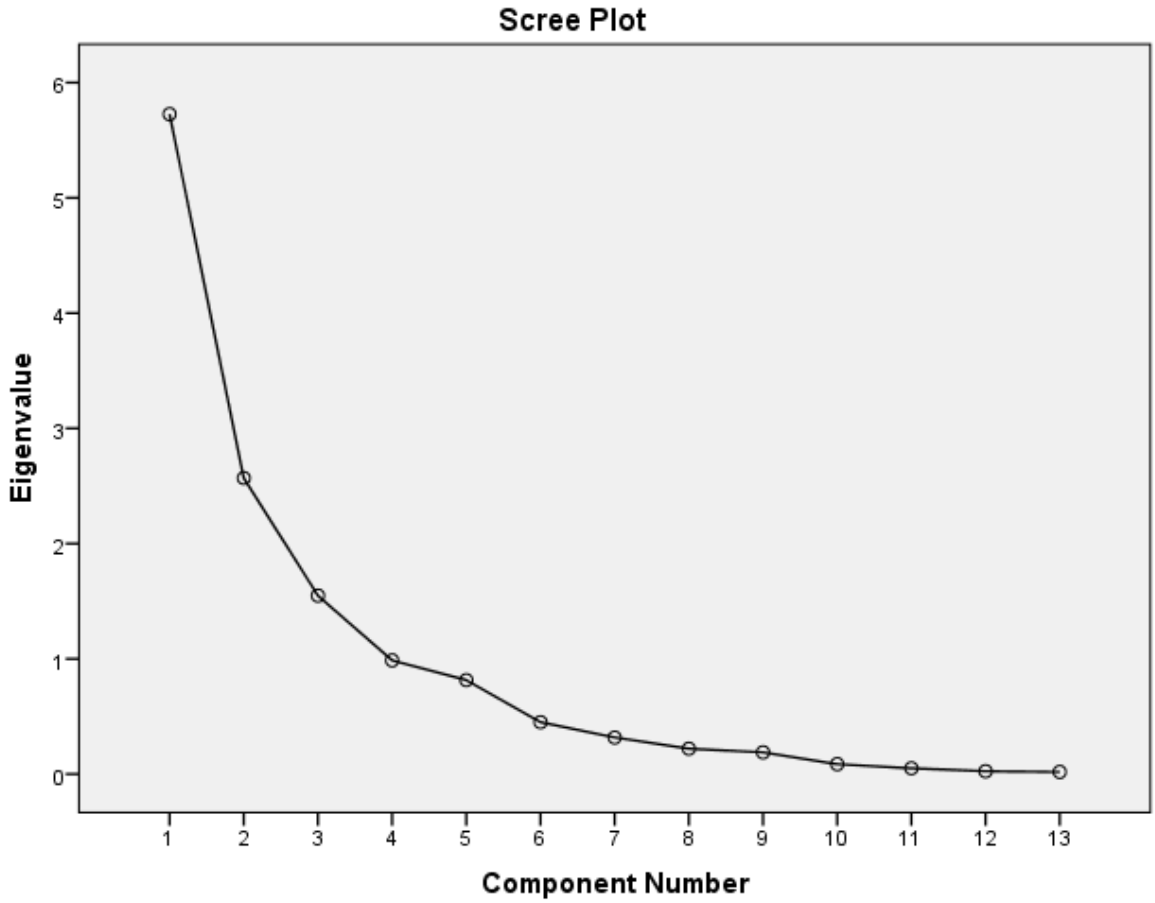

Figure 52. Scree plot demonstrating Eigen values for the 13 CRSsNP discriminatory mucosal lining fluid mediator factor analysis.

Total Variance Explained

Component	Initial Eigenvalues			Extraction Sums of Squared Loadings			Rotation Sums of Squared Loadings		
	Total	% of Variance	Cumulative %	Total	% of Variance	Cumulative %	Total	% of Variance	Cumulative %
1	5.727	44.050	44.050	5.727	44.050	44.050	3.020	23.234	23.234
2	2.568	19.757	63.808	2.568	19.757	63.808	2.898	22.289	45.523
3	1.548	11.909	75.716	1.548	11.909	75.716	2.854	21.954	67.476
4	.987	7.590	83.307	.987	7.590	83.307	2.058	15.830	83.307
5	.815	6.269	89.576						
6	.450	3.463	93.039						
7	.317	2.442	95.481						
8	.220	1.693	97.174						
9	.189	1.452	98.626						
10	.086	.661	99.287						
11	.050	.385	99.671						
12	.024	.187	99.858						
13	.018	.142	100.000						

Extraction Method: Principal Component Analysis.

Table 7. Table demonstrating the percentage total variance of the 13 discriminant mucosal lining fluid markers.

Rotated Component Matrix[a]

	Factor			
	1	2	3	4
IL6	**.941**	.003	.058	.219
MIP1a	**.894**	.052	.182	.317
MIP1b	**.884**	.099	.349	.229
SAA	-.045	**.970**	.051	-.008
sFlt1	.075	**.902**	.170	.144
VCAM1	.139	**.894**	.262	.090
TARC	.296	.233	**.863**	.037
Eotaxin3	.067	-.032	**.807**	-.117
MCP4	.330	.171	**.702**	.455
bFGF	-.079	.359	**.646**	.330
PIGF	.340	.324	**.518**	.091
IL17	.279	.085	.141	**.882**
IL10	.353	.086	-.009	**.843**

Extraction Method: Principal Component Analysis.

Rotation Method: Varimax with Kaiser Normalization.

a. Rotation converged in 6 iterations.

Table 8. Discriminant CRSsNP mucosal lining fluid factor analysis rotated loadings matrix.

Factor	Name	Mucosal lining fluid marker
Factor 1	Pro-inflammatory	Macrophage inflammatory protein 1α (MIP-1α)
		Macrophage inflammatory protein 1β (MIP-1β)
		Interleukin 6 (IL-6)
Factor 2	Vascular inflammatory	Serum amyloid A (SAA)
		Fms-like tyrosine kinase 1 (sFlt1)
		Vascular cell adhesion molecule 1 (VCAM-1)
Factor 3	Chemokine & growth	Eotaxin 3
	factor	Thymus and activation regulated chemokine (TARC)
		Monocyte chemo attractant protein 4 (MCP-4)
		Placental growth factor (PlGF)
		Basic fibroblast growth factor (bFGF)
Factor 4	Regulatory	Interleukin 10 (IL-10)
		Interleukin 17 (IL-17)

Table 9. The four key components characterising CRSsNP inflammation and their 13 key constituent mediators.

4.4.3 Bioinformatics analysis of inflammatory gene pathways

WEB-based Gene SeT AnaLysis Toolkit (WebGestalt) was used to identify other disease associations of the 13 key mucosal lining fluid mediators (Table 6) and multiple hypothesis testing correction has been applied, the results are shown in (Table 10). The top 15 disease associations included respiratory tract infections, inflammation, common cold, nasal polyps and sinusitis further confirming the specificity of the mucosal lining fluid analysis results. WebGestalt also provides details of drug associations (Table 11). Dexamethasone, dinoprostone - a prostaglandin E2, anakinra - an IL-1 receptor antagonist, and immune globulin were found to be significantly associated with the CRSsNP differentially expressed mucosal lining fluid mediators.

The 13 key CRSsNP mediators were inputted into Network Analyst. The protein-protein interaction network generated is shown in Figure 53. Using Heatmap2 in gplots a heat map displaying log(protein concentration) of the 13 key CRSsNP mediators was created (Figure 54). GOstats was used to further analyse the differentially expressed mediators. A flow diagram highlighting key gene ontology biological processes (GO BP) categories significantly overrepresented in red was created (Figure 55 & Figure 56).

WebGestalt top 15 disease associations	Corrected p value
Respiratory Tract Infections	p=1.17x10-11
Inflammation	p=1.17x10-11
Common Cold	p=1.17x10-11
Bronchiolitis	p=5.59x10-10
Bronchitis	p=7.40x10-10
Necrosis	p=5.89x10-9
Immune System Diseases	p=1.01x0-8
Infection	p=9.33x10-8
Respiratory Tract Diseases	p=3.74x10-7
Lymphoproliferative Disorders	p=3.74x10-7
Nasal Polyps	p=3.74x10-7
Chorioamnionitis	p=4.69x10-7
Sinusitis	p= 7.49x10-7
Encephalitis	p= 7.88x10-7
Disease Progression	p= 1.09x10-6

Table 10. The top 15 disease associations calculated by WEB-based Gene SeT AnaLysis Toolkit (WebGestalt) of the 13 key CRSsNP mediators. p values corrected for multiple hypothesis testing.

WebGestalt drug associations	Corrected p value
Dexamethasone	p=0.0012
Dinoprostone	p=0.0008
Anakinra	p=0.0004
Immune globulin	p=0.0003

Table 11. Four identified drug associations calculated by WEB-based Gene SeT AnaLysis Toolkit (WebGestalt) of the 13 key CRSsNP mediators. p values corrected for multiple hypothesis testing.

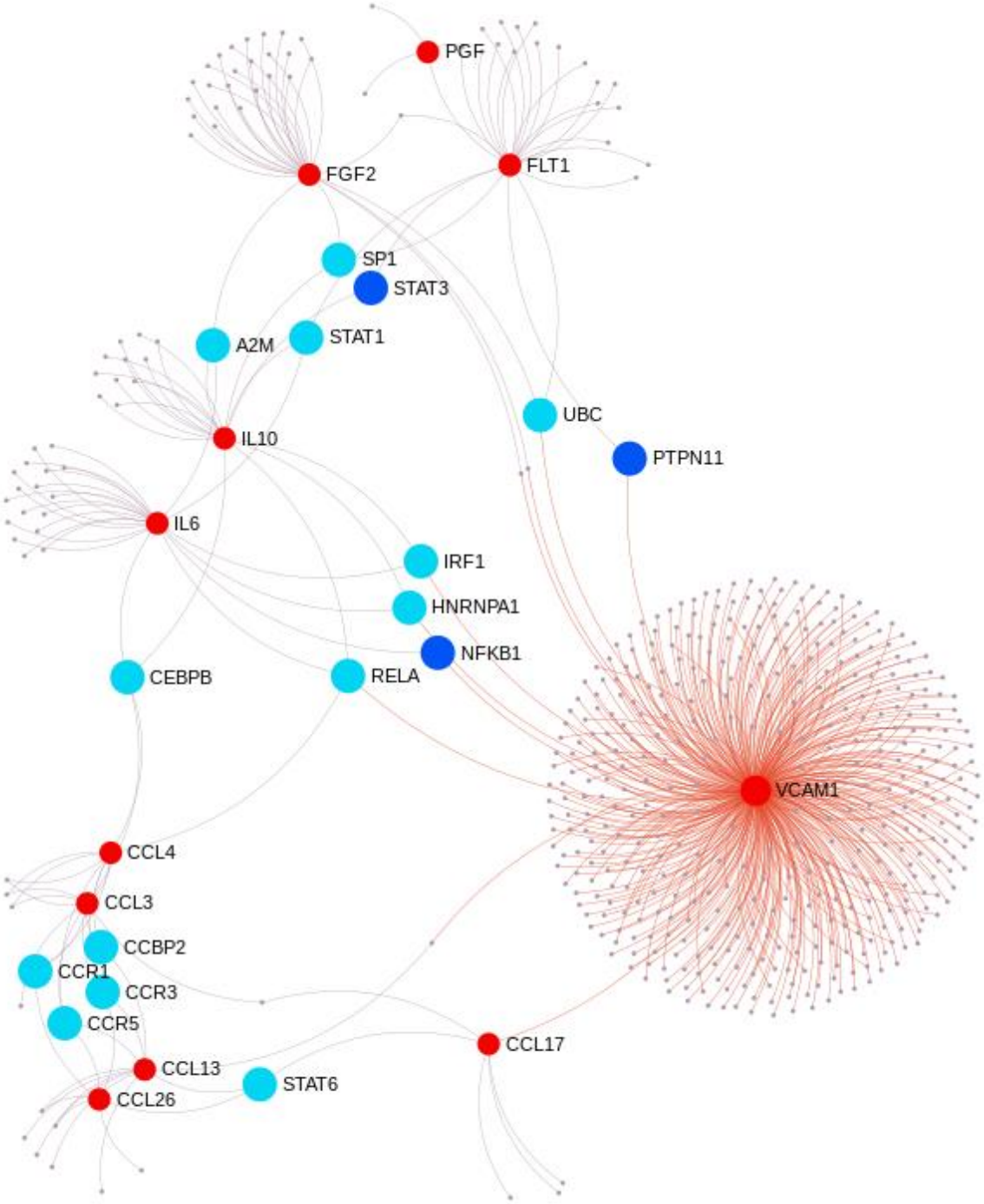

Figure 53. NetworkAnalyst protein-protein interaction network of the 13 key CRSsNP mediators shown in red, with their associated receptors and interactions in blue.

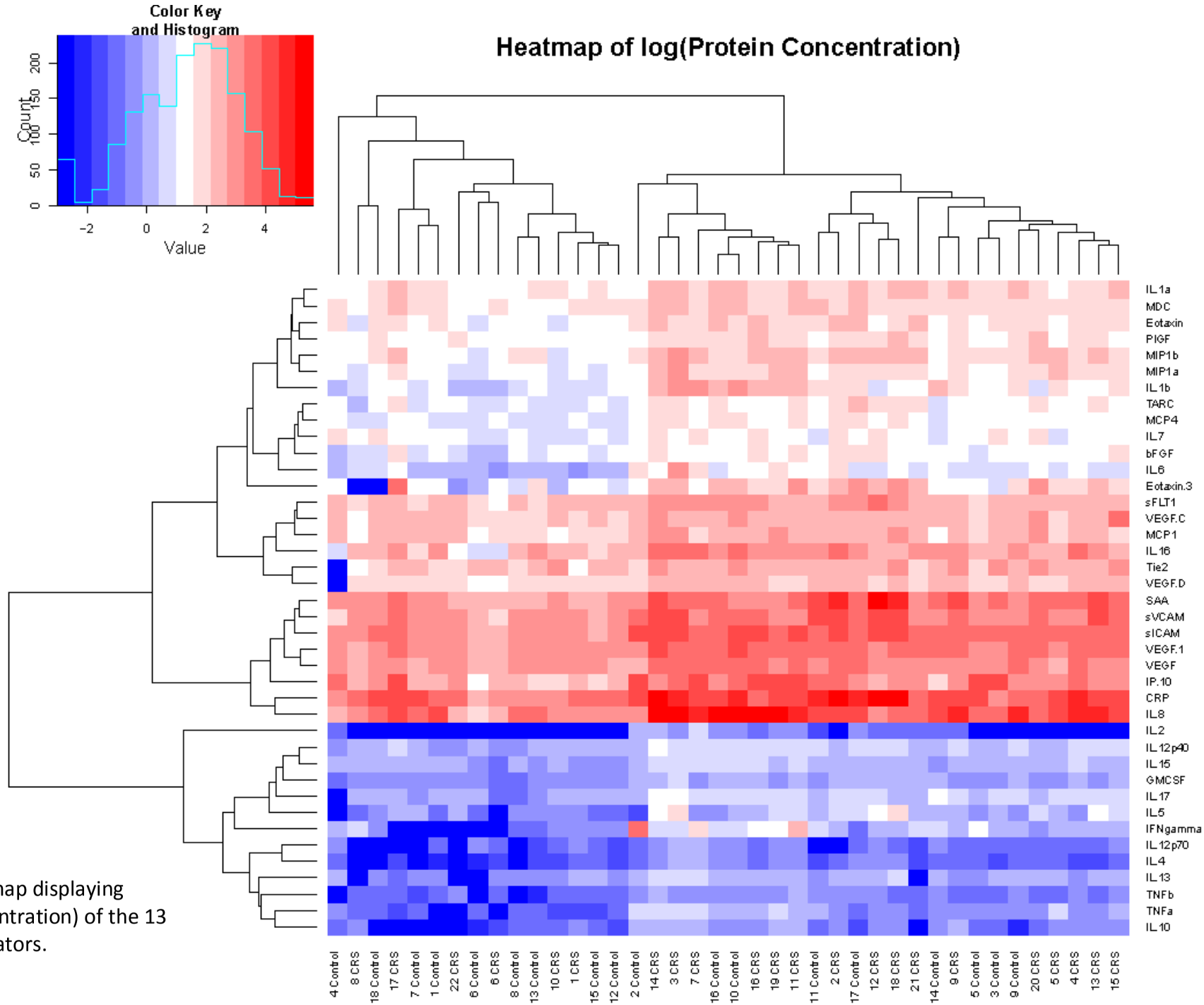

Figure 54. Heat map displaying log(protein concentration) of the 13 key CRSsNP mediators.

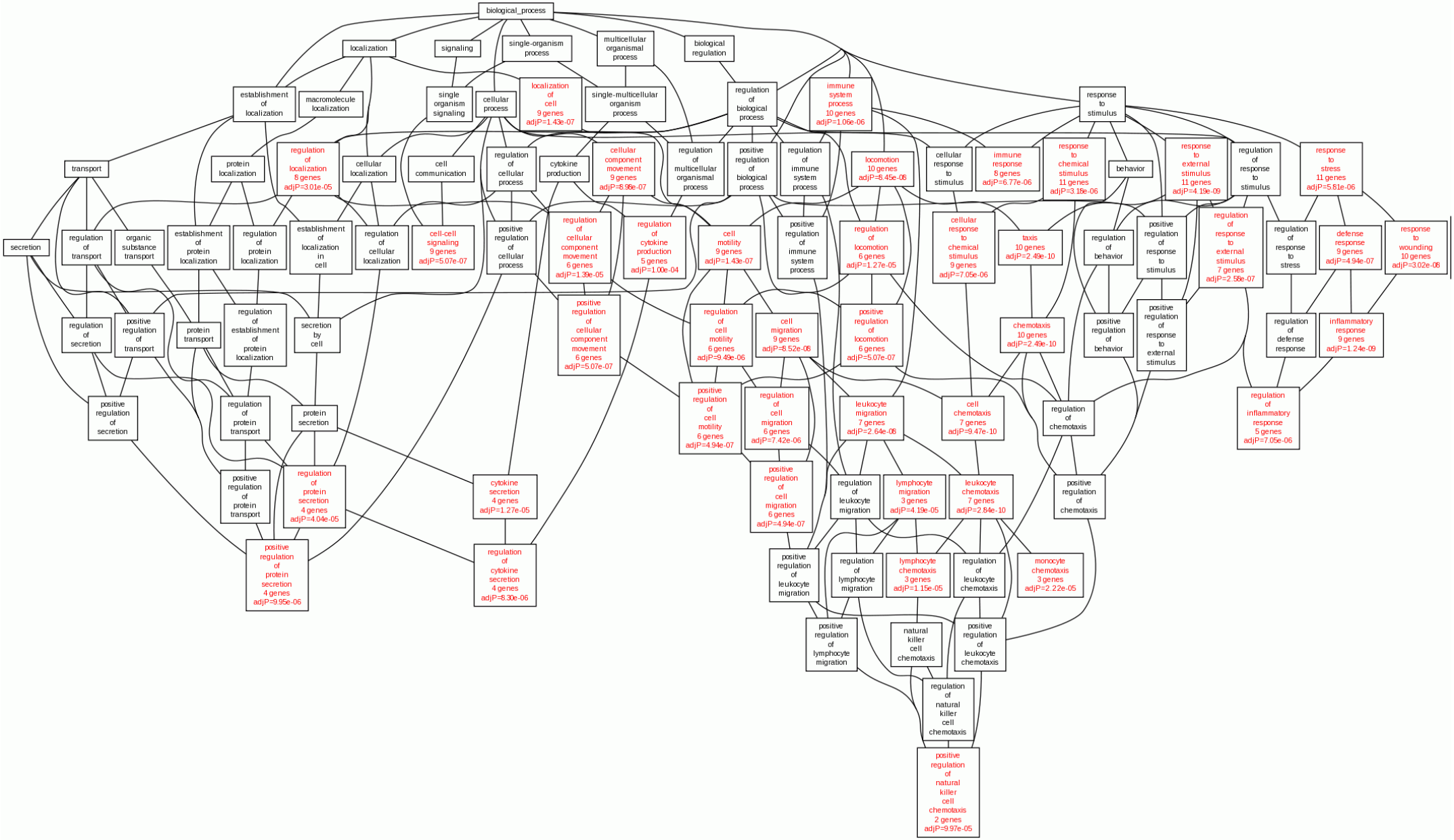

Figure 55. Flow diagram highlighting key gene ontology biological processes (GO BP) categories significantly overrepresented in red.

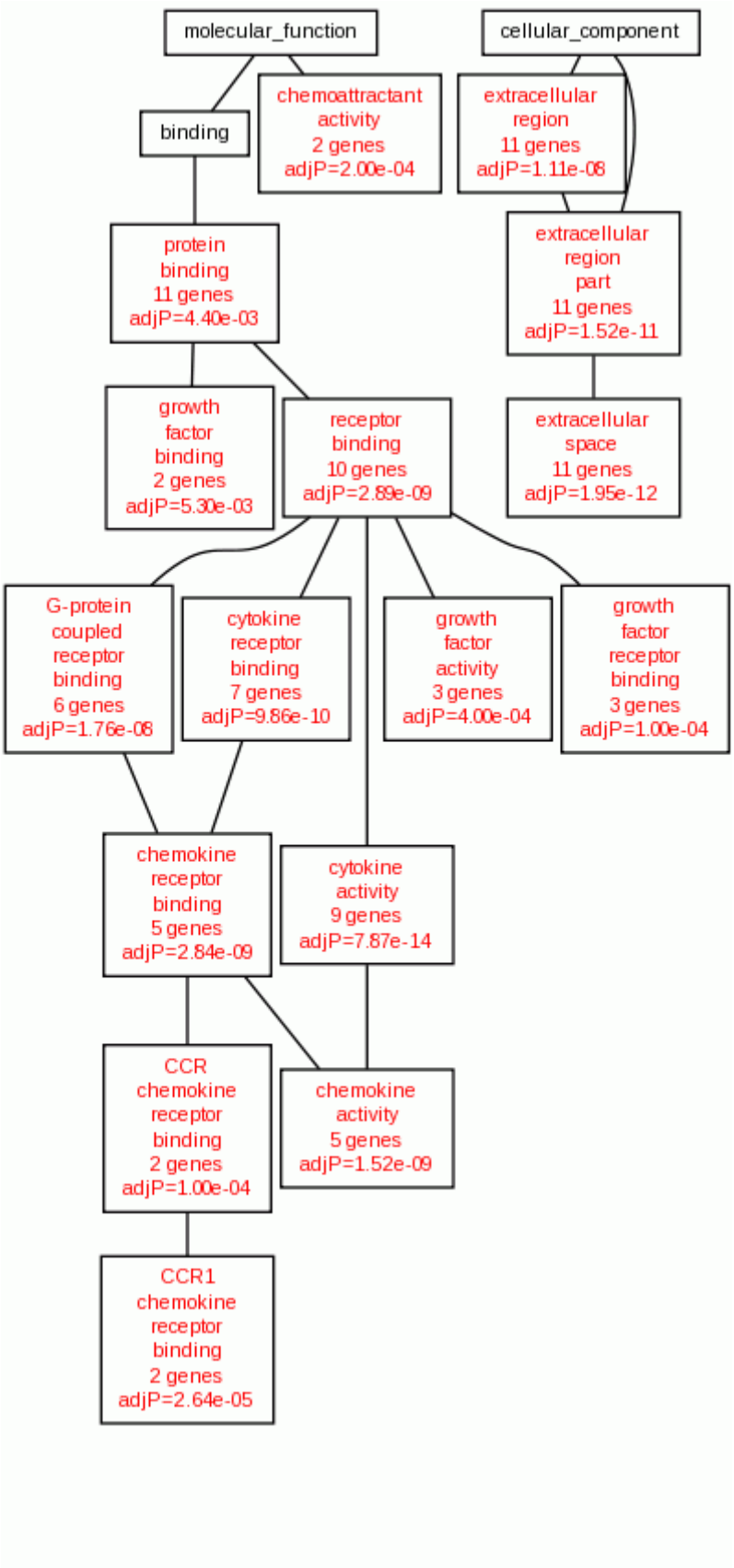

Figure 56. Flow diagram highlighting key gene ontology (GO) molecular and cellular categories significantly overrepresented in red.

4.4.4 qRT-PCR tissue biopsy replications of differentially expressed mucosal lining fluid mediators

Quantitative real time PCR was used to investigate tissue biopsy mRNA for the 13 key CRSsNP mediators. The five chemokine mediators (Factor 3, Table 9) were also replicated at the mRNA level in their tissue biopsies ($p<0.001$-$p<0.05$, Figure 58). Two of the three cytokine mediators seen in mucosal lining fluid could also be replicated at the mRNA level in tissue biopsies (Figure 59); interleukin 10 and interleukin 17 ($p<0.001$). However, differential expression of interleukin 6 mRNA in tissue biopsies was not replicated despite multiple attempts. Only one of the three angiogenesis biomarkers, basic fibroblast growth factor showed a statistically significant ($p<0.05$) upregulation in mRNA from CRSsNP tissue biopsies compared to controls (Figure 58). Whilst both vascular injury mediators, Serum amyloid A (SAA) and Vascular cell adhesion molecule 1 (VCAM-1/CD106) showed increased mRNA levels in CRSsNP participants consistent with the mucosal lining fluid protein samples, neither reached statistical significance (Figure 57).

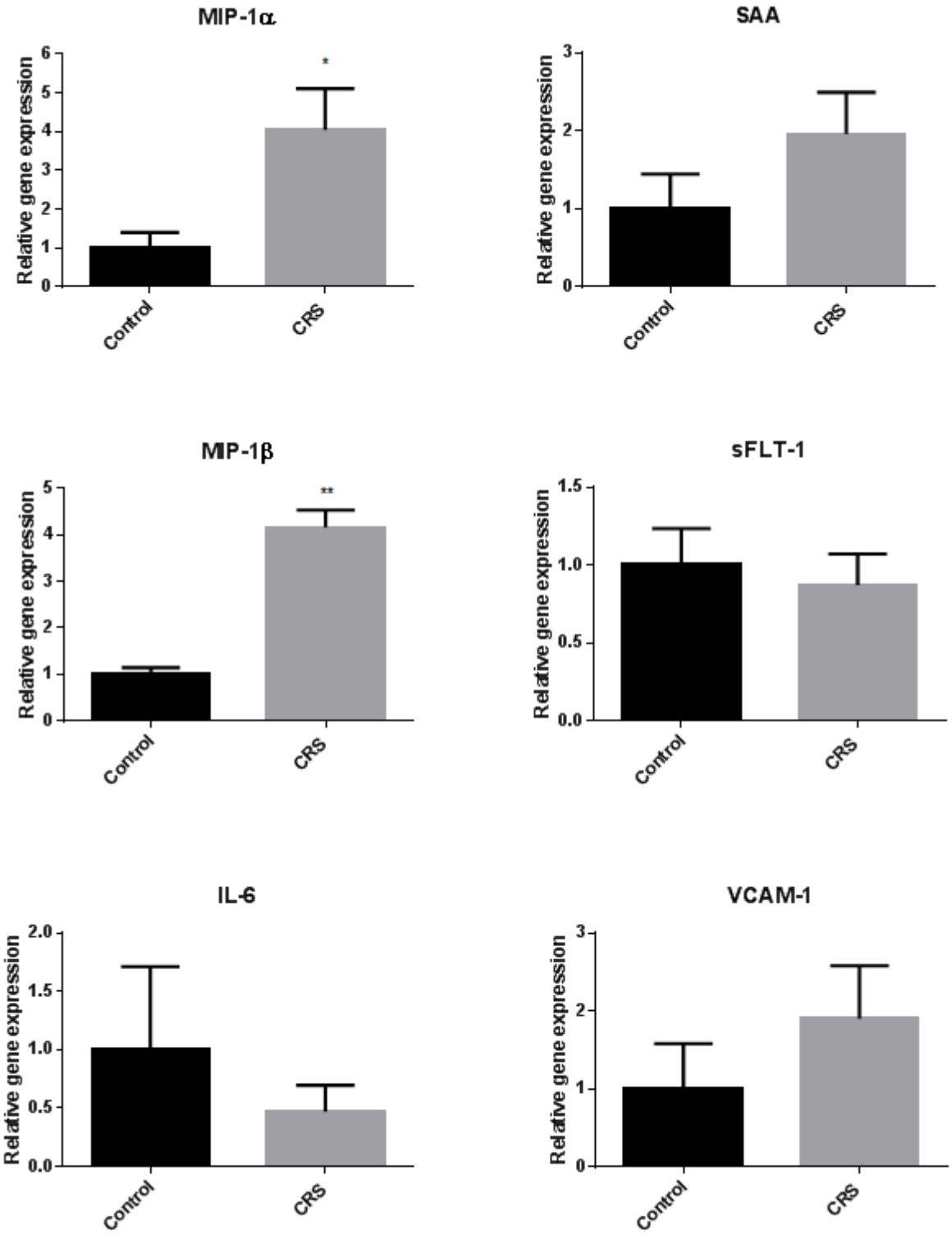

Figure 57. qRT-PCR tissue biopsy sample replications of key CRSsNP Factor 1 pro-inflammatory mediators (left column) and Factor 2 vascular inflammatory mediators (right column), n=6 with triplicate repeat. *** = p<0.001, ** = p<0.01, * = p<0.05.

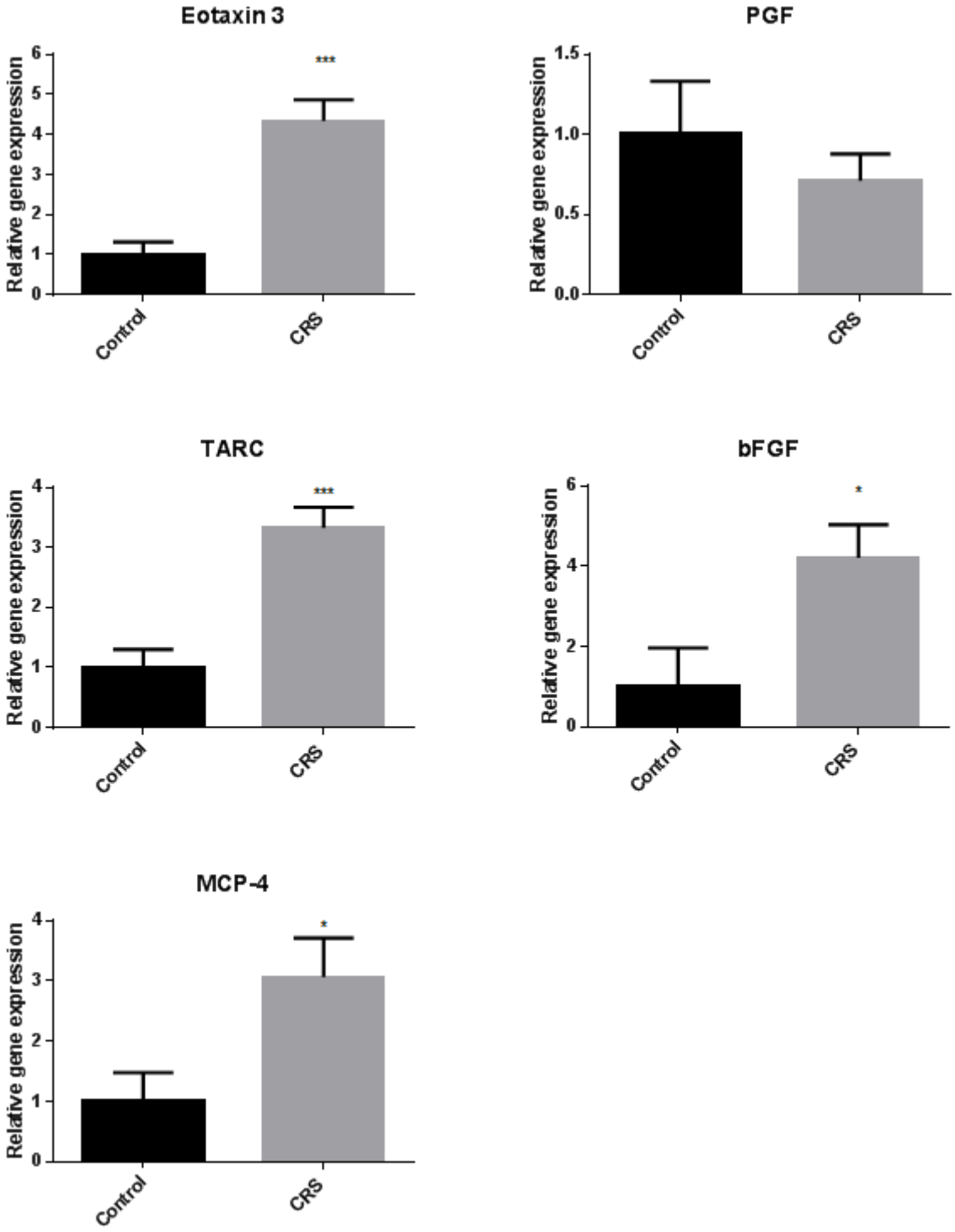

Figure 58. qRT-PCR tissue biopsy sample replications of key CRSsNP Factor 3 chemokine & growth factor mediators, n=6 with triplicate repeat. . *** = p<0.001, ** = p<0.01, * = p<0.05.

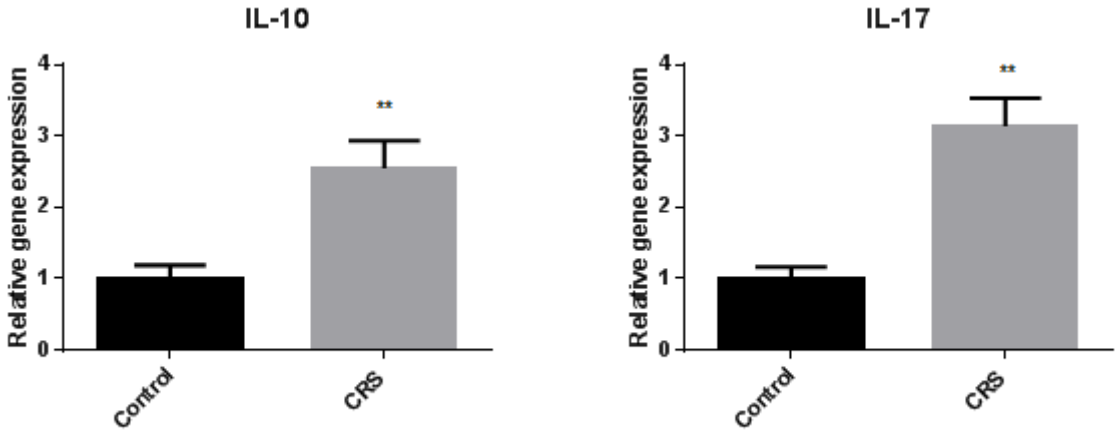

Figure 59. qRT-PCR tissue biopsy sample replications of key CRSsNP Factor 4 regulatory mediators, n=6 with triplicate repeat.

4.4.5 qRT-PCR cellular analysis of differentially expressed mucosal lining fluid markers

Quantitative real time RT-PCR was also used to investigate if the 13 key CRSsNP mediators were preserved in primary cultures of CRSsNP and control epithelial and fibroblast cells.

Only one of the mediators, macrophage inflammatory protein 1-alpha (MIP-1alpha/CCL3) demonstrated statistically significant ($p<0.01$) expression between primary cell cultures from CRSsNP participants and healthy controls. Fibroblasts from CRSsNP participants demonstrated an approximately three fold upregulation in their MIP-1alpha mRNA when compared to healthy control fibroblasts (Figure 60). MIP-1beta and MCP-4 appear to show a similar trend to MIP-1alpha, though do not reach statistical significance. The relative gene expression levels detectable in the cells, however were markedly less than those seen in tissue biopsy samples as highlighted by the split in the y axis. In general the levels of the 13 key CRSsNP mediator genes were notably lower in primary cultures of both epithelial and fibroblast cells than in tissue biopsy samples. The sole exception was basic fibroblast growth factor (bFGF) which showed the highest expression in primary cultures of fibroblast cells (Figure 61), with an approximate 10 fold increase in fibroblast mRNA levels compared to tissue samples. This is perhaps not surprising as it is a fibroblast derived product. Vascular cell adhesion molecule 1 (VCAM-1/CD106) and interleukin 6 (IL-6) both also showed higher relative gene expression in primary cultures of nasal fibroblasts than in their respective tissue biopsy samples (Figure 61 and Figure 62).

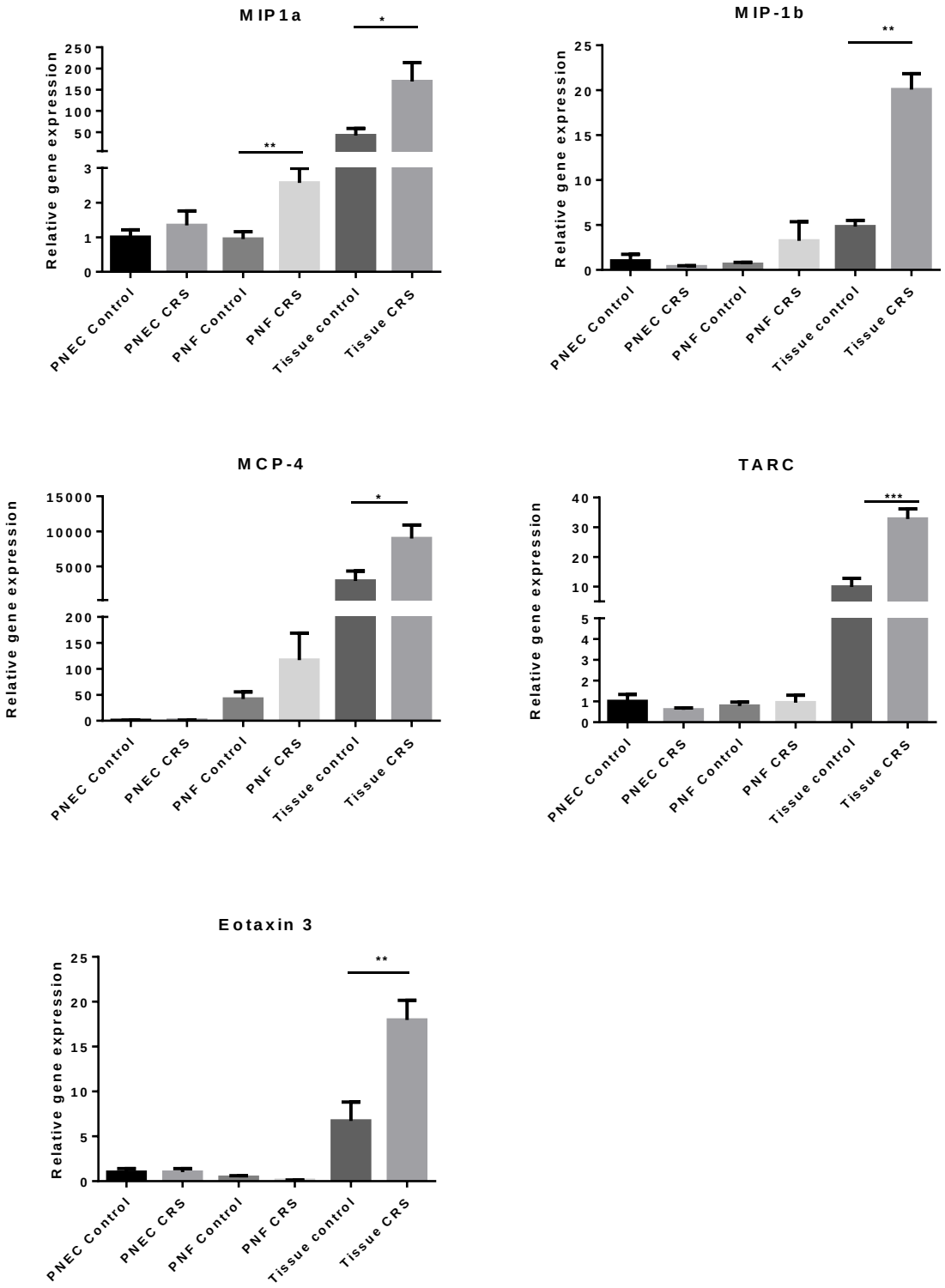

Figure 60. qRT-PCR PNEC, PNF and tissue biopsy sample replications of differentially expressed mucosal lining fluid chemokine mediators, n=6 with triplicate repeat.

*** = $p<0.001$, ** = $p<0.01$, * = $p<0.05$.

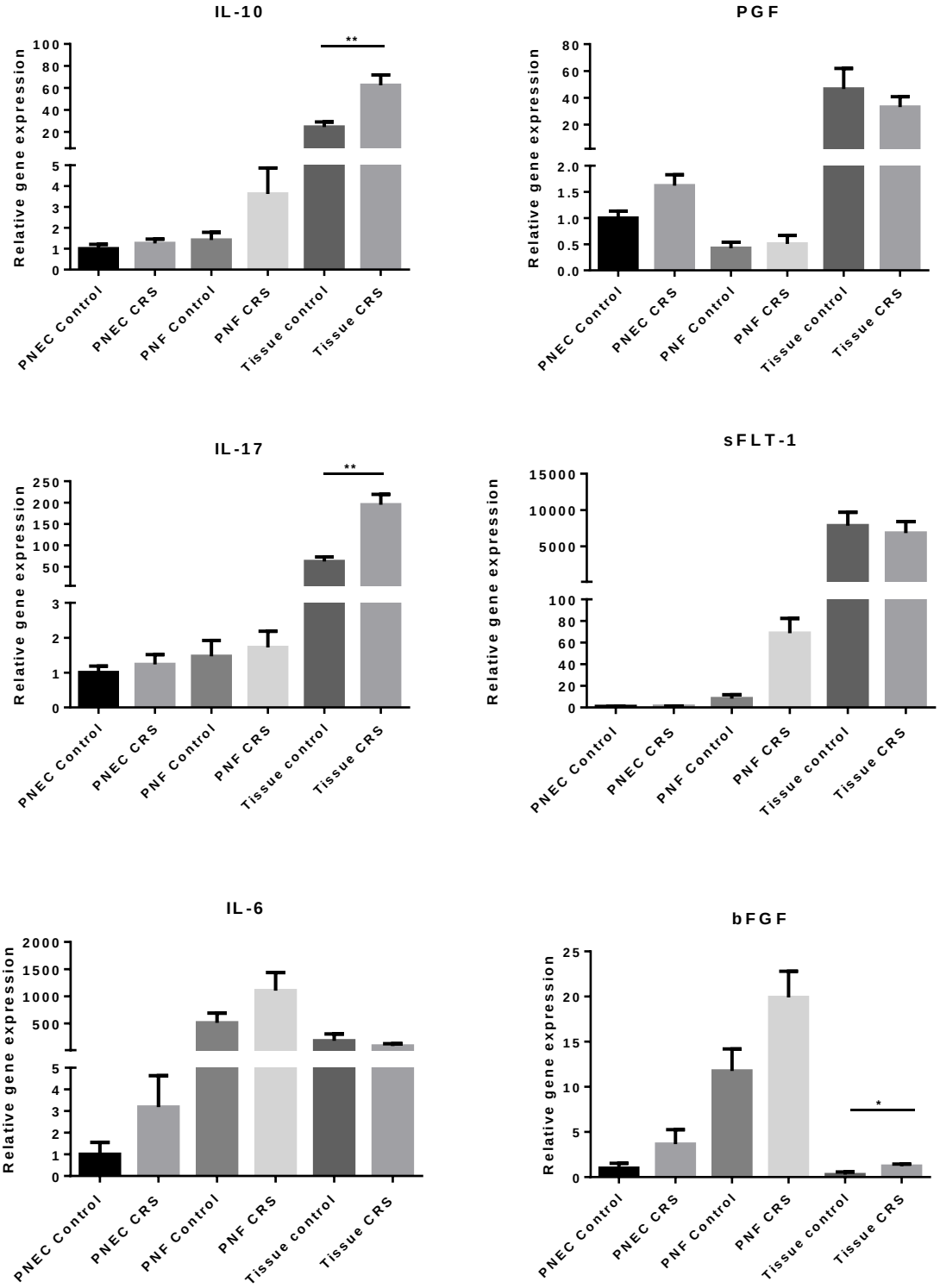

Figure 61. qRT-PCR PNEC, PNF and tissue biopsy sample replications of differentially expressed mucosal lining fluid cytokine and angiogenesis mediators, n=6 with triplicate repeat. *** = $p<0.001$, ** = $p<0.01$, * = $p<0.05$.

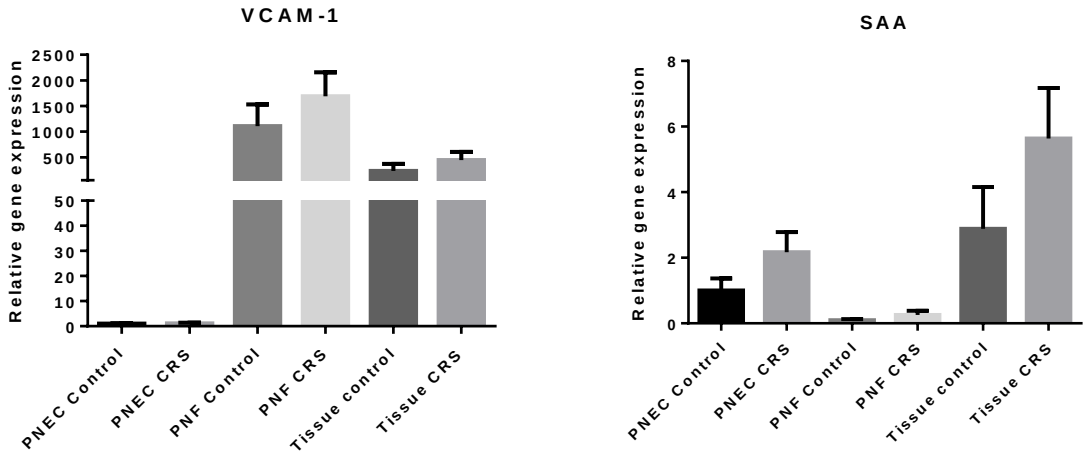

Figure 62. qRT-PCR PNEC, PNF and tissue biopsy sample replications of differentially expressed mucosal lining fluid vascular injury mediators, n=6 with triplicate repeat. *** $p<0.001$, ** $p<0.01$, * $p<0.05$.

4.4.6 Tissue biopsy samples multiplex protein analysis

Total protein was isolated from tissue biopsies of CRSsNP and healthy control participants and compared with the MSD multiplex analysis findings from mucosal lining fluid swabs (Section 4.3.1). Protein was isolated, quantified and standardised at 2mg/ml (see 4.3.3 and 4.3.4) prior to analysing with an identical multiplex MSD electrochemiluminesce using the V-PLEX Human Biomarker 40-Plex Kit (Mesoscale discovery, US).

Analysis of isolated protein from the tissue biopsy samples showed 15 ($p<0.05$ – $p<0.001$) differentially expressed mediators between CRSsNP and healthy control samples (Figure 63Table 13). The proteins identified from the tissue biopsy samples consisted of a group of 7 chemokines, 6 cytokines, and 2 vascular injury mediators (Table 12).

	Mediator
7 chemokines	Monocyte chemoattractant protein 1 (MCP-1/CCL2)
	Macrophage inflammatory protein 1-beta (MIP-1beta/CCL4)
	Eotaxin (CCL11)
	Monocyte chemoattractant protein 4 (MCP-4/CCL13)
	Thymus and activation regulated chemokine (TARC/CCL17)
	Macrophage-derived chemokine (MDC/CCL22)
	Eotaxin 3 (CCL26)
6 cytokines	Interleukin 4 (IL-4)
	Interleukin 5 (IL-5)
	Interleukin 8 (IL-8)
	tissue necrosis factor alpha (TNF-alpha)
	tissue necrosis factor beta (TNF-beta)
	granulocyte monocyte colony stimulating factor (GM-CSF)
2 vascular injury mediators	Serum amyloid A (SAA)
	C reactive protein

Table 12. List of significantly different CRSsNP tissue biopsy mediators.

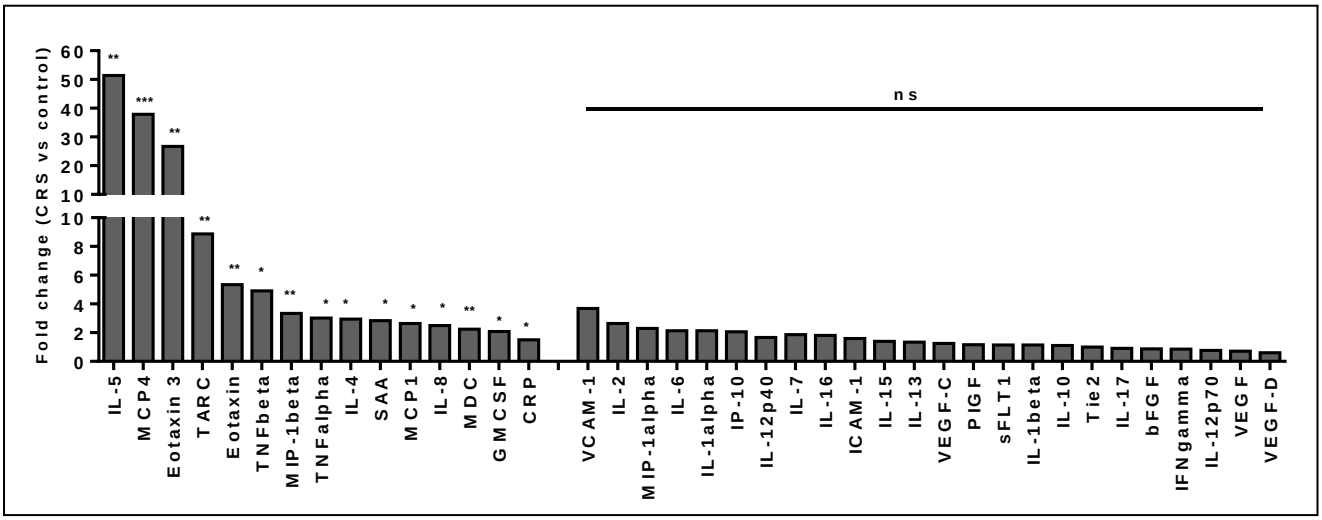

Figure 63. Histograms to show the relative fold change of tissue biopsy lysates in CRSsNP participants compared to controls. *** p<0.001, ** p<0.01, * p<0.05., n=19 participants

	Control		CRS				
Marker	Median (pg/ml)	Range (pg/ml)	Median (pg/ml)	Range (pg/ml)	fold change	p-value	p-value
IL-5	0.22	0.05-0.86	11.31	0.53-24.35	51.41	0.0029	**
MCP4	29.49	14.9-55.35	1118	28.20-3444	37.91	0.0005	***
Eotaxin 3	963.2	322.4-2186.8	25771	793.9-85203	26.76	0.0026	**
TARC	11.47	6.74-29.47	101.8	11.47-146.5	8.88	0.0012	**
Eotaxin	20.94	9.97-60.49	112	23.50-824.9	5.35	0.0012	**
TNFbeta	0.126	0.072-0.196	0.619	0.08-2.57	4.91	0.0245	*
MIP-1beta	102.2	35.23-282.62	342	98.88-5219.17	3.35	0.0098	**
TNFalpha	0.424	0.296-0.839	1.281	0.267-9.153	3.02	0.0283	*
IL-4	0.1066	0.07-0.22	0.3144	0.06-0.591	2.95	0.0221	*
SAA	29673	12518-61053	84103	26663-1187515	2.83	0.0130	*
MCP1	189	90.64-392.62	498	33.28-4901.6	2.63	0.0283	*
IL-8	174.9	758.49-2034	438	93.36	2.50	0.0358	*
MDC	162.7	142.3-402.9	363.9	211.26-2419	2.24	0.0026	**
GMCSF	0.2113	0.054-.218	0.4391	0.09-1.398	2.08	0.0220	*
CRP	49836	33844-60927	75419	9499-174336	1.51	0.0283	*
VCAM-1	740.8	476-3149	2736	543.1-13649	3.69	0.0831	ns
IL-2	0.3542	0.126-2.28	0.9326	0.20-2.27	2.63	0.1490	ns
MIP-1alpha	58.19	33.33-157.41	134	41.03-9291.34	2.30	0.0831	ns
IL-6	11.55	0.29-51.6	24.66	0.12-796.7	2.14	0.3402	ns
IL-1alpha	0.3883	0.09-0.48	0.829	0.27-5.45	2.13	0.2667	ns
IP-10	202.8	134.6-2526	420.1	72-107981	2.07	0.4789	ns
IL-12p40	4.06	1.22-5.59	6.787	2.64-25.20	1.67	0.0556	ns
IL-7	1.016	0.52-4.88	1.902	0.42-5.04	1.87	0.7732	ns
IL-16	1969	958.3-3504.4	3569	639.7-6220.4	1.81	0.1198	ns
ICAM-1	35507	21857-47052	56903	3915-288877	1.60	0.2268	ns
IL-15	3.078	2.17-5.21	4.289	0.89-14.30	1.39	0.5918	ns
IL-13	2.295	1.748-3.873	3.062	1.77-8.71	1.33	0.2268	ns
VEGF-C	146.3	103.6-222.9	182.8	67.8-600.4	1.25	0.4824	ns
PIGF	104.2	93.73-171.40	121.6	21.76-357.43	1.17	0.4824	ns
sFLT1	4220	3614-8368	4805	318.2-8392	1.14	0.7108	ns
IL-1beta	0.967	0.31-1.33	1.101	0.10-52.42	1.14	0.5962	ns
IL-10	0.1138	0.089-0.127	0.1263	0.067-0.597	1.11	0.9636	ns
Tie2	12272	0-556.27	12218	20.70-967.78	1.00	0.9999	ns
IL-17	0.7785	0.09-9.27	0.7097	0.528-62.94	0.91	0.3355	ns
bFGF	43892	21337-77393	38646	318.95-57866	0.88	0.3845	ns
IFNgamma	1.034	0.39-1.68	0.878	0.31-20.83	0.85	0.9999	ns
IL-12p70	0.0346	0.02-0.04	0.0268	0.02-0.09	0.77	0.8000	ns
VEGF	270.6	135.9-533.9	194.9	202.17-4593.71	0.72	0.1956	ns
VEGF-D	130.5	54.81-216.1	78.05	34.1-162.84	0.60	0.2991	ns

Table 13. Table to summarize tissue biopsy lysate data. ns = non-significant p value.

4.4.7 Isolated epithelial and fibroblast cells multiplex protein analysis

Protein was also isolated from cultures of primary nasal epithelial cells and primary nasal fibroblasts using the same methods detailed in sections 4.3.3 and 4.3.4. Samples of protein were standardised at 2mg/ml and healthy control samples were compared to CRSsNP using the V-PLEX Human Biomarker 40-Plex Kit (Mesoscale discovery, US). When compared to healthy control samples epithelial cells from CRSsNP participants showed one statistically significant mediator (p=0.0274), interleukin 5 (IL-5) to be upregulated by a factor of 1.34x compared to healthy control cells.

When primary nasal fibroblasts were analysed using the same technique, one mediator – interleukin 1β (IL-1β) - was also shown to be statistically significantly upregulated by a factor of 3.3x (p= 0.0469) in CRSsNP participants compared to healthy control fibroblasts.

The comparison of mediators differentially expressed in tissue biopsies, mucosal lining fluid and cellular samples is tabulated (Table 14), presented in a Venn diagram (Figure 64) and in histograms detailing the relative concentrations of a representative selection of matched participant samples (Figure 65). Figure 65 shows the most marked differences are seen between CRSsNP participants and controls in tissue biopsy samples.

4.4.8 Serum samples multiplex protein analysis

Serum samples from CRSsNP and healthy control participants were compared using the same V-PLEX Human Biomarker 40-Plex Kit (Mesoscale discovery, US) to determine if any systemic signals from CRSsNP can be detected in participants' blood. No significant differences were identified.

Mucosal lining fluid		
Marker	**fold change**	**p-value**
Eotaxin 3	8.00	0.0207
MIP-1beta	4.30	0.0018
IL-10	3.99	0.0344
MIP-1alpha	3.96	0.0037
IL-6	3.23	0.0416
IL-17	2.52	0.0475
SAA	2.51	0.0174
MCP4	2.16	0.0148
TARC	2.09	0.0388
PIGF	1.95	0.0188
sFLT1	1.68	0.0218
bFGF	1.60	0.0218
VCAM-1	1.38	0.0416

Tissue		
Marker	**fold change**	**p-value**
IL-5	51.41	0.0029
MCP4	37.91	0.0005
Eotaxin 3	26.76	0.0026
TARC	8.88	0.0012
Eotaxin	5.35	0.0012
TNF beta	4.91	0.0245
MIP-1beta	3.35	0.0098
TNF alpha	3.02	0.0283
IL-4	2.95	0.0221
SAA	2.83	0.0130
MCP1	2.63	0.0283
IL-8	2.50	0.0358
MDC	2.24	0.0026
GMCSF	2.08	0.0220
CRP	1.51	0.0283

Table 14. Comparison of the discriminant CRSsNP mediators in mucosal lining fluid swabs and tissue biopsy lysates.

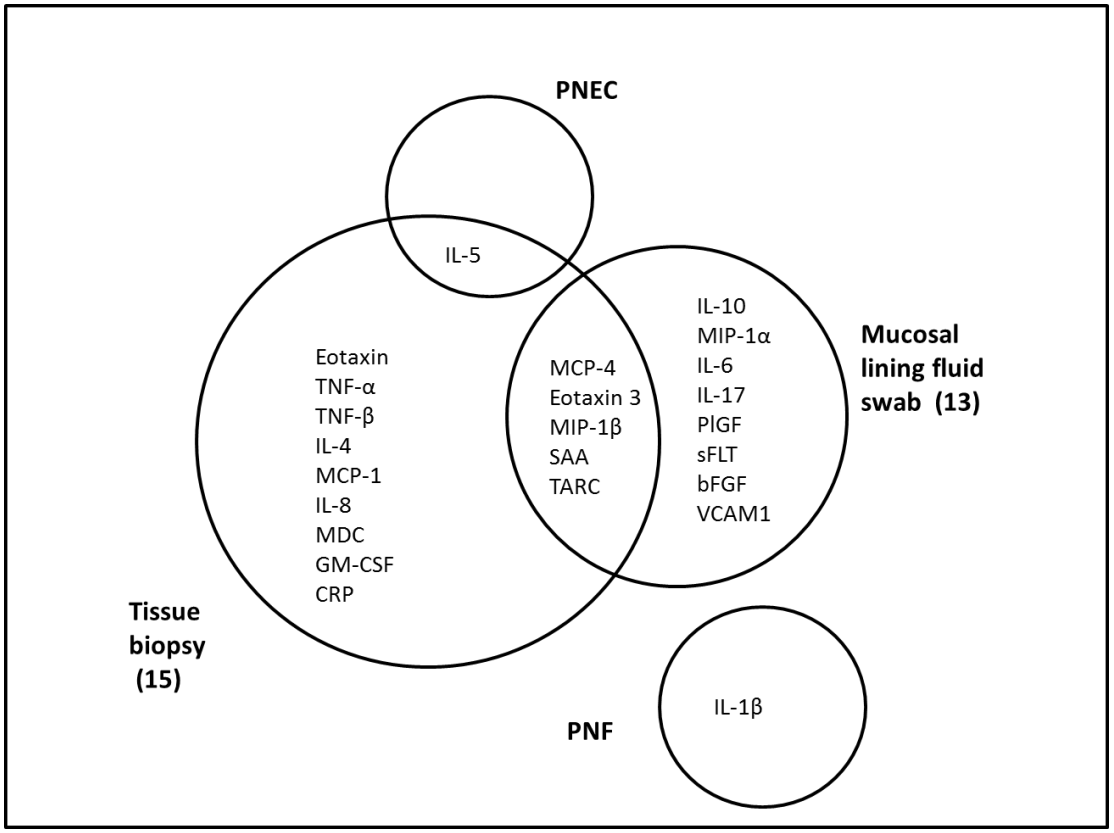

Figure 64. Venn diagram demonstrating the statistically significant protein mediators compared between the different CRSsNP and healthy control samples.

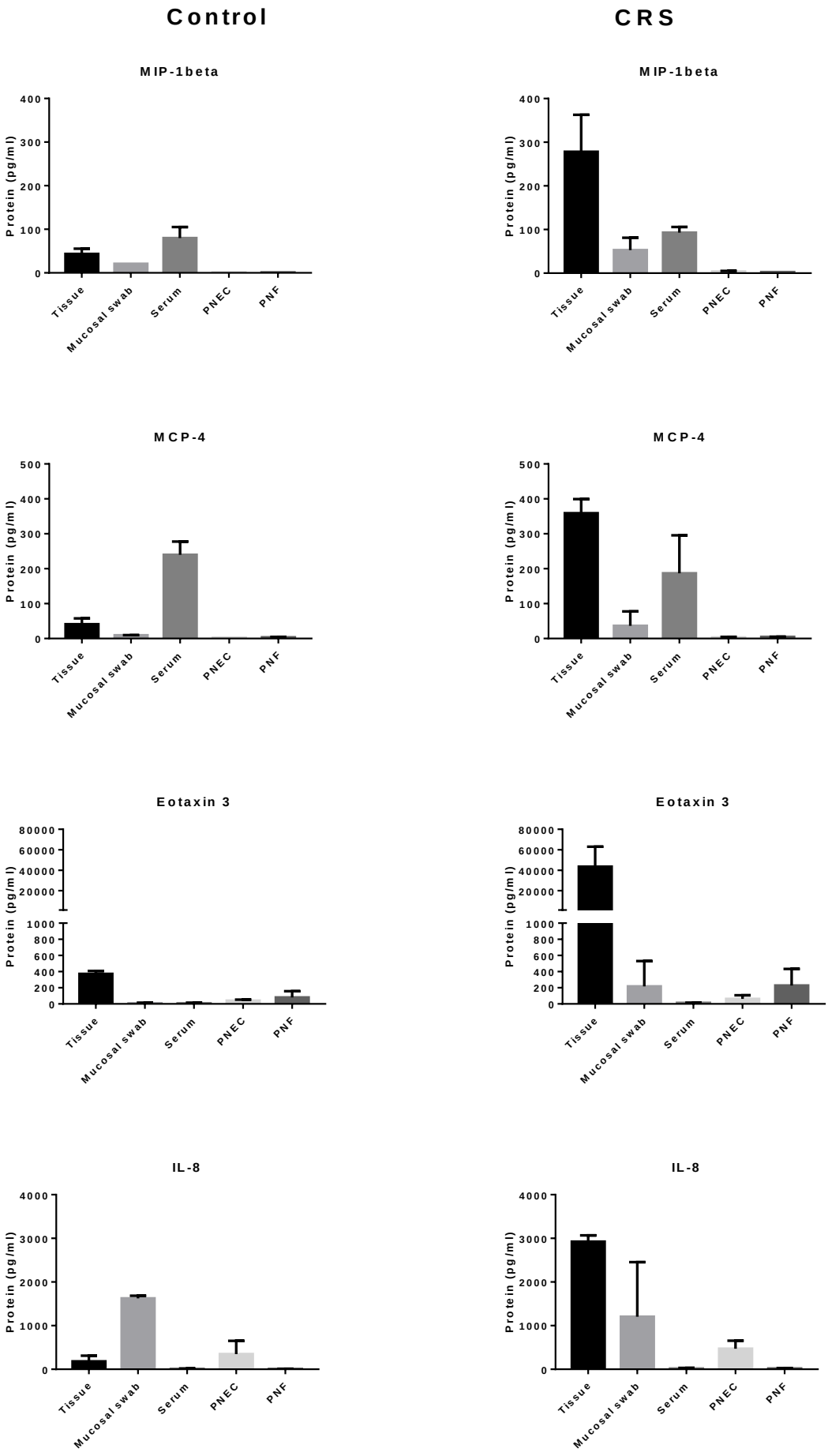

Figure 65. Representative histograms to compare the amounts of mediators present in matched participants tissue, mucosal swab, serum and cellular samples. Control samples are shown on the left column and CRSsNP the right column.

4.5 Discussion

4.5.1 Potential value of CRS biomarker profiling

The current gold standard criteria for the diagnosis and management of chronic rhinosinusitis are presented in the EPOS 2012 international consensus document (Fokkens et al., 2012). The principal factors that determine diagnosis and management algorithms are the presence of sinonasal symptoms supported by endoscopic and radiological appearances. Within current clinical practice no biomarkers have been defined to support the diagnosis or guide medical or surgical treatment selection in CRS patients. In contrast, there are well recognised biomarkers of systemic inflammatory conditions with CRS components - e.g. serum cANCA in granulomatosis with polyangiitis (GPA) (Thai et al., 2014) (Kallenberg et al., 2006) serum angiotensin converting enzyme (ACE) in sarcoidosis (Costabel and Teschler, 1997) and rheumatoid factor in rheumatoid arthritis (Onuora, 2012). Such biomarkers are valuable adjuncts in confirmation of diagnosis and monitoring response to treatment. The ability to assay the sinonasal environment with a biomarker or panel of markers may offer an objective 'inflammatory score' measure in addition to the subjective self and observer rated symptom, endoscopic and radiological scores. In particular, there is currently lack of clarity and guidance as to the optimum point at which to progress from medical management to surgical intervention (Bassiouni et al., 2013) (Benninger et al., 2015). CRS biomarkers have the potential therefore both to rationalise and personalise management (Deroee et al., 2009, Divekar et al., 2015, Riechelmann et al., 2005). Measurement of the local micro environment in health and CRSsNP also usefully informs replication of the CRS inflammatory milieu in future in vitro studies.

4.5.2 Sampling Methods

A variety of sampling techniques are available to collect nasal specimens.

1. The commonest is the conventional microbial culture swab on a stick, which can also be used for molecular analysis (Chalermwatanachai et al., 2015). The main drawback is its small surface area for absorption of nasal cavity mucus. Further, the convex shape of the tip restricts the portion of the absorbent swab tip which achieves tissue contact and sampling.
2. Nasal lavage to collect samples of mucus and nasal fluid has the drawback of a substantial dilutional effect from the 5-10 ml of irrigation fluid, precluding detection of certain low concentration mediators. (Bisgaard et al., 1988). Some lavage fluid may escape posteriorly

into the nasopharynx, which limits reproducibility. Nasal lavage is also variably tolerated by the subject.

3. A suction trap to aspirate nasal secretions can be used, though often yields pooled secretions rather than those in continuity with the sinonasal mucosa.
4. Nasal sampling can also be performed with brushings or a rhinoprobe curette, both of which provide cellular specimens for analysis and are relatively atraumatic although they will collect more than the mucosal layer. Lin and colleagues found that the rhinoprobe curette was especially helpful if measures of mucosal leukocytes were required in addition to epithelial cells (Lin et al., 2001).
5. Larger mucosal and tissue samples can be collected with an endoscopic guided biopsy performed under local or general anaesthesia. This however provides only a small amount of covering nasal secretions or mucus along with the tissue biopsy.

The use of a mucosal lining fluid swab as presented in this chapter has a number of distinct advantages for sampling the mucosa. Firstly it is atraumatic and well tolerated as confirmed from the pilot group of healthy laboratory colleagues, the larger patient participant cohort and from personal experience. It has a large flat standardised area of 210 mm^2 (7x30mm) that can be placed in continuity along the inferior turbinate with the aid of a simple headlight to maximise mucosal contact along its length. The strip is made of Leukosorb, a hydrophilic, synthetic absorptive matrix and measures the mucosal lining fluid directly without further dilution, enabling low concentration mediators to be detected that would not be possible with other mucus sampling techniques. The mucosal lining fluid swab technique is also relatively quick, being completed in just over two minutes confirming its suitability for use in routine clinical outpatient assessments. The ability to complete a mucosal lining fluid analysis swab with each patient would enable personalised, longitudinal monitoring of the natural history of the CRS mucosal micro environment and its response to different treatments.

4.5.3 Mucosal lining fluid characterisation

The mucosal lining fluid assay demonstrated that within this sample the expression of 13 mediators differed between CRSsNP patients and healthy control participants (Figure 45).

4.5.3.1 Chemokines

The largest group of mediators identified comprised five chemokines; macrophage inflammatory protein 1-alpha (MIP-1alpha/CCL3), macrophage inflammatory protein 1-beta (MIP-1beta/CCL4), Monocyte chemoattractant protein 4 (MCP-4/CCL13), thymus and activation regulated chemokine (TARC/CCL17) and eotaxin 3 (CCL26).

The identification of chemokine upregulation in the micro environment of the sinonasal cavities is consistent with the histological data presented in chapter 3. These results showed increased macrophages, monocytes, T-cells, eosinophils and neutrophils in CRSsNP participants compared to healthy controls appropriate for the group of C-C motif chemokines identified. MIP-1alpha/CCL3 and MIP-1beta/CCL4 are C-C motif chemokines which recruit and activate polymorphonuclear leukocytes via CCR chemokine receptors. They were first identified from lipopolysaccharide (LPS) stimulated murine macrophages in 1988 (Wolpe et al., 1988), with their human equivalents reported over the next few years (Zipfel et al., 1989) followed by a new systematic nomenclature for the emerging chemokine superfamily (Zlotnik and Yoshie, 2000) based on the position of the first two cysteine residues. MIP-1alpha and MIP-1 beta share more than 50% homology and both chemokines are inducible in most mature haematopoietic cells. Functionally both MIP-1alpha and MIP-1beta are chemoattractant for monocytes, T-cells, neutrophils and natural killer cells (Menten et al., 2002), however MIP-1alpha is preferentially chemoattractant for CD8 cytotoxic T-cells and MIP-1beta attractant for CD4 T helper cells (Taub et al., 1993).

Monocyte chemoattractant protein 4 (MCP-4/CCL13) is another member of the C-C motif chemokine family that signals via the CCR 2 and CCR 3 chemokine receptors. MCP-4 is highly chemoattractant for monocytes, lymphocytes, eosinophils and basophils in chronic inflammatory diseases (Romagnani, 2002) and it would therefore seem appropriate that it has been shown to be upregulated in mucosal lining fluid samples from CRSsNP participants together with the corresponding histological appearances shown in chapter 3.

Thymus and activation regulated chemokine (TARC/CCL17) is also a member of the C-C motif chemokine family and signals by the CCR4 chemokine receptor to induce chemotaxis in T-cells (Imai et al., 1997). Immunohistochemical staining of CRSsNP tissues in the previous chapter has demonstrated an increase in T-cell recruitment compared to healthy control tissues which would corroborate the upregulation of TARC identified in CRSsNP mucosal lining fluid swabs.

The final upregulated mucosal lining fluid chemokine to be identified was Eotaxin 3 (CCL26), also belonging to the C-C motif chemokine family. Eotaxin 3 is chemotactic for eosinophils and basophils via the CCR 3 chemokine receptor and typically results in a Th2-polarised environment including interleukins IL-4 and IL-13. A Th-2 polarised cytokine environment has been suggested to be more typical of chronic rhinosinusitis with nasal polyps (CRSwNP) (Van Crombruggen et al., 2011), although there still remains overlap between the distinct phenotypes reflecting the degree of heterogeneity in chronic rhinosinusitis (Sanchez-Segura et al., 1998, Tomassen et al., 2016) (Lee and Lane, 2011) (Derycke et al., 2014). The identification of Eotaxin 3 is also supported by an increase in CRSsNP eosinophils histologically in the previous chapter.

The identification of a group of increased chemokines in CRSsNP samples is interesting when viewed in combination with the histological data of CRSsNP in chapter 3. Histological images show damage to epithelial membranes and cilial loss suggestive of cell death pathways such as necrosis, apoptosis and also senescence –there is also airway remodelling present with increased fibrosis. The combination of these processes may suggest a role for the senescence associated secretory phenotype in CRSsNP, where senescent cells trigger production of chemokines, cytokines and proteases which can create a vicious cycle of worsening tissue damage (Munoz-Espin and Serrano, 2014). The senescence associated secretory phenotype has thus far not been investigated in CRS – and certainly merits further study - though is better characterised in respiratory diseases such as COPD (Kumar et al., 2014) and organ transplantation (Tchkonia et al., 2013)

4.5.3.2 Cytokines

Three cytokines upregulated in CRSsNP participants compared to healthy controls were found to be interleukin 6 (IL-6), interleukin 10 (IL-10) and interleukin 17 (IL-17).

IL-6 is a pleiotropic cytokine produced by almost all stromal and immune cells with a number of differing functions; it can promote granulopoiesis and neutrophil accumulation, clonal T-cell expansion, B-cell differentiation and control the acute phase response (Hirano, 2014) (Hunter and Jones, 2015), in line with the upregulation demonstrated here in my CRSsNP participants. IL-6 is regarded as a major cytokine in inflammation and host defence. It is regulated by basal physiological homeostatic mechanisms and can be significantly elevated in infective, inflammatory or neoplastic conditions. In acute infections IL-6 has protective inflammatory, anti-infective actions, however, the same anti-infective

inflammatory properties can persist and be key to the generation of chronic inflammation. Due to its pleiotropic nature the local environmental context in which IL-6 is investigated is key to its functional significance. With diseases such as CRSsNP, the sinonasal cavity is a peripheral site of inflammation therefore elevated IL-6 functions are most likely important in the recruitment of leukocytes, inflammatory activation of stromal cells and promotion of T-cell function (Jones, 2005).

Interleukin 17 is a pro-inflammatory cytokine produced from a subset of T helper (Th) cells - hence 'Th17' cells. IL-17 contributes to the pathogenesis of a number of chronic inflammatory conditions including psoriasis (Krueger, 2012), rheumatoid arthritis and ankylosing spondylitis (Komatsu et al., 2014). IL-17 was first cloned in 1993 and can to increase the pro-inflammatory IL-6 and IL-8 production in skin fibroblasts and synovial cells. IL-8 is a potent neutrophil chemokine which signals via the CXC chemokine receptor CXCR2, and so IL-17 is chemotactic for neutrophils and also monocytes. It would therefore seem appropriate that increased levels of IL-17 have been identified in mucosal lining fluid samples of CRSsNP participants. The elevated cytokine levels detected are also supported by the histology of CRSsNP participants presented with increased neutrophil and monocyte populations seen on immunohistochemistry. The common signalling between IL-17 and IL-6 is also reflected in the mucosal lining fluid samples of CRSsNP participants with upregulation of both cytokines (Figure 45 & Table 6). IL-17 is synergistic with tumour necrosis factor alpha (TNF-α) (Chabaud et al., 1999), a Th1 cytokine previously thought to be important in CRSsNP pathophysiology (Tomassen et al., 2016, Van Crombruggen et al., 2011). However in the mucosal lining fluid samples of my CRSsNP participants I was unable to measure a statistically significant increase in TNF-α levels compared to controls, although there was a trend suggesting a potential increase in CRSsNP TNF-α levels (Figure 45 and Table 6), though these did not reach significance perhaps due to the sample size.

IL 10, unlike IL-6 and IL-17 which are both predominantly pro-inflammatory is an anti-inflammatory cytokine. Why might it be upregulated in a pro-inflammatory condition? IL-10 is predominantly produced by monocytes, macrophages, neutrophils, T lymphocytes and regulatory T-cells (Moore et al., 2001) following programmed death 1 protein (PD1) signalling (Said et al., 2010). However, the detection of increased IL-10 is probably a measure of the immune systems attempt to apply a brake on the pro-inflammatory actions of the immune cells and their associated cytokines to control the levels of inflammation,

prevent host damage from an unchecked immune response and the development of autoimmune disease (Hawrylowicz and O'Garra, 2005). The increased immune cells demonstrated in CRSsNP by immunohistochemistry are all capable of producing IL-10. The increased amounts detected in the mucosal lining fluid thus most likely reflect the normal negative feedback mechanisms of the local sinonasal environment attempting to curtail inflammation. Without IL-10 production, the levels of inflammation in the sinonasal cavities could be far greater. Therefore augmenting IL-10 action emerges as a potential therapeutic target in CRS. Unfortunately, clinical trials in other inflammatory conditions to date have not translated into efficacy for IL-10 therapy in Crohn's disease (Buruiana et al., 2010), rheumatoid arthritis (van Roon et al., 2003) or psoriasis (Kimball et al., 2002).

4.5.3.3 Angiogenesis Mediators

Basic fibroblast growth factor (bFGF), Placental growth factor (PlGF) and soluble Fms-like tyrosine kinase 1 (sFlt-1), also known as vascular endothelial growth factor receptor 1 (VEGFR1) were elevated in my CRS cohort. Basic fibroblast growth factor has numerous effects on tissue repair and regeneration. It is found in the basement membrane of healthy tissue and extracellular matrix in blood vessels and can be released from damaged cells directly or by exocytosis (Ornitz and Itoh, 2001). In the previous chapter the histology of CRSsNP and healthy control participants have been evaluated and shown epithelial cell loss, infiltration of immune cells in the fibroblast rich lamina propria and basement membrane thickening. Within the CRSsNP tissues presented there is marked cellular damage and loss of epithelia with exposed basement membranes as a source for increased bFGF release from damaged cells. The increased bFGF measured in mucosal lining fluid may be increased as the by-product of attempted mucosal repair.

Placental growth factor (PlGF) was also measured at increased levels in CRSsNP participants. PlGF is a member of the vascular endothelial growth factors (VEGF), important mediators in angiogenesis and tissue repair, cloned from a cDNA library obtained from a human placenta (Maglione et al., 1991). In fact, it can stimulate angiogenesis by activation with VEGF receptor 1 which is expressed on many tissues. PlGF has been demonstrated to have a central role in pathological angiogenesis in bronchial (Mohammed et al., 2007), skin (Odorisio et al., 2006), cardiac (Luttun et al., 2002) and retinal cells (Hollborn et al., 2006) as a direct result of hypoxia and inflammatory cytokines such as interleukin 1 and the proposed CRSsNP cytokine TNF-α together with the pro-fibrotic growth factor transforming growth

factor β-1 (TGF-β). Within the sinonasal cavity hypoxia (Ball et al., 2016) has been demonstrated along with increased TNF-α (Tomassen et al., 2016, Van Crombruggen et al., 2011) and TGF-β upregulation (Van Bruaene et al., 2009, Van Bruaene et al., 2012) which may be due to altered PlGF levels. As a result the detection of increased PlGF in CRSsNP mucosal lining fluid most likely reflects the attempted tissue reparatory process occurring in the damaged sinonasal mucosa. In addition to upregulation of bFGF and PlGF soluble Fms-like tyrosine kinase 1 (sFlt-1), also known as vascular endothelial growth factor receptor 1 (VEGFR1) was measured with a statistically significant increase in CRSsNP mucosal lining fluid. Soluble Fms-like tyrosine kinase 1 is the receptor for circulating proangiogenic VEGF growth factors and binds free VEGF or PlGF, thus reducing their effect. As with the relationship of IL-10 to IL-6 and IL-17, sFlt-1 is a natural brake on unchecked angiogenesis and dysregulated tissue repair. The pro-angiogenic placental growth factor was found to have a fold change increase of 1.95 ($p=0.0188$), whereas the antiangiogenic sFlt-1 had a slightly lower fold change of 1.67 ($p=0.0218$), which although represents a crude assumption independent of stoichiometry of the ligand and receptor interactions, may suggest a net increase in the pro-angiogenic effect of PlGF.

4.5.3.4 Vascular Injury Mediators

The final mucosal mediators to be upregulated in CRSsNP mucosal lining fluid were the two vascular injury mediators; Serum amyloid A (SAA) and Vascular cell adhesion molecule 1 (VCAM-1/CD106). Serum amyloid A proteins are acute phase proteins produced in response to pro-inflammatory cytokines and have been implicated in a number of pathologies including atherosclerosis (King et al., 2011), Alzheimer's disease (Chung et al., 2000) and rheumatoid arthritis (O'Hara et al., 2000). Serum amyloid A proteins are produced in response to IL-1, IL-6 and TNF-α pro-inflammatory cytokines which have been previously measured at increased levels in CRS (Castano et al., 2009, Mfuna Endam et al., 2010), consistent with the present findings. Vascular cell adhesion molecule 1 is a cell adhesion molecule that promotes the adhesion of monocytes, lymphocytes and eosinophils to vascular endothelium hence aiding their migration to sites of inflammation (Vestweber, 2015). The expression of vascular adhesion molecules on endothelial surfaces is induced by pro-inflammatory cytokines (van Buul et al., 2007) so the chemotaxis of circulating immune cells to the sinonasal mucosa is a co-ordinated response dependent on a combination of chemokines, pro-inflammatory cytokines and adhesion molecules. These individual factors represent the mediators that have been identified within the mucosal lining fluid of CRSsNP

participants and the combination of their actions is demonstrated in the immune cell histological images in chapter 3.

4.5.4 Mucosal lining fluid mediator summary

This work represents a larger panel of biomarkers than has been previously published in this disease. Riechelmann and colleagues (2005) investigated fifteen cytokines, three cellular activation markers and total IgE in nasal secretions collected with nasal packing sponges in a cohort of 12 patients with CRSsNP. The nasal secretions were extracted by centrifugation and then diluted by a factor of 10 prior to performing a multiplex ELISA (IL-1β, IL-2, IL-4, IL-5, IL-6, IL-7, IL-8, IL-10, IL-12 (p70), IL-13, IL-17, TNF-α, IFN-γ, granulocyte-macrophage colony-stimulating factor (GM-CSF), granulocyte colony-stimulating factor (GCS), monocyte chemoattractant protein-1 (MCP-1), and macrophage inflammatory protein-1β (MIP-1β)). From their panel of cytokines the pro-inflammatory cytokine IL-17 was below the level of detection and GM-CSF did not vary between patient groups. No statistical analysis of the individual mediators present in the healthy control and CRSsNP patient groups was performed, although they reported the remainder of nasal secretion biomarker concentrations 1-2 log fold higher in CRS participants compared to controls. The results presented in this chapter show similar results to Riechelmann et al. with increased inflammatory cytokines in the nasal mucus, however they are not in complete agreement. There may be a few reasons for this, firstly Riechelmann et al have a relatively small size of n=6 healthy controls – although there is no mention of what their criteria for healthy controls are – and n=12 CRSsNP patients. The authors acknowledge the number of study participants is too low and that the findings are exploratory. Their sampling methods are slightly different using a larger nasal packing sponge which may be significant. Nasal packing can be traumatic to the mucosa of the nasal cavities and cause small mucosal tears releasing blood onto the packing device in addition to the nasal mucus. The possibility of mucosal damage would be increased in an inflamed CRS environment with swollen, more friable mucosa and an increased blood supply related to the inflammatory process. Contamination of blood on the nasal packing sponges will mean the ELISA will not simply be measuring the mucus. In contrast to this within my study the mucus was collected atraumatically by a flat piece of 7x30mm filter paper applied to the mucosa of the inferior turbinate with no bleeding incurred.

Kuehnemund and colleagues (2004) measured the levels of inflammatory mediators in the nasal mucosa of untreated chronic rhinosinusitis patients over a period of 4 weeks. From nasal secretions using foam rubber sampling devices analogous to nasal packing they measured peptido-leukotriene (PLT) and prostaglandin E2 (PGE2) using ELISA. Additionally they measured a panel of cytokines and chemokines mRNA from an initial approximately 5mg tissue biopsy of the lateral portion of the middle turbinate of the nasal cavity and a second one after four weeks. Messenger RNA for interleukin-1α (IL-1α), interleukins 3, 5, 6, and 8, interferon gamma; tumour necrosis factor α, monocyte chemotactic proteins 1, 3, and 4 and granulocyte-macrophage colony-stimulating factor was quantified from the biopsies by quantitative real time RT-PCR. The authors were only able to measure IL-1, IL-6, IL-8, MCP-1, and TNF-α in the nasal mucosa and there was no significant difference between the initial biopsy and the one four weeks later at the end of the study. In nasal secretions very small amounts of Peptido-leukotriene ($1.4x\ 10^{-6}$ mg per milligram of protein) PGE2 ($2.99x10^{-6}$ mg per milligram of protein) were measured and there was no significant difference observed over the four week study period. Kuehnemund et al reported the first study to measure the natural course of CRS, although over a relatively short four week period. Their study shows no significant change in inflammatory mediators in the nasal cavity, however no comparator control group was included and patients were not phenotyped on the presence of nasal polyps. It is interesting that despite using a sensitive test such as qRT-PCR they were unable to measure a number of chemokines and cytokines in patients with established inflammation in their nasal cavities.

Divekar et al. (2015) published work measuring a panel of mediators in nasal mucus and serum in a cohort of 9 CRS with nasal polyp (CRSwNP) patients from baseline levels throughout the course of an acute symptomatic exacerbation compared to 10 healthy controls. They collected nasal secretions using a suction mucus trap, diluted them in NaCl and added protease inhibitors. The nasal secretions were then measured for a range of mediators IFN-γ, IL-5, IL-13, IL-17F, IL-17A, IL-17E, IL-33, IL-6, TNF-α, TNF-β and eosinophil major basic protein (MBP) using a multiplex ELISA technique. At baseline inclusion in the study CRSwNP patients had statistically significant increased levels of IL-6 in nasal secretions in agreement with the findings presented in this chapter. During an acute exacerbation their CRSwNP participants demonstrated a significant increase in IL-5, IL-6 and MBP compared to controls, with the remainder of cytokines not showing statistically significant differences.

Groger and colleagues (2013) published a study measuring nasal discharge collected from cotton wool pieces placed in the middle meatus of the sinonasal cavity for 20 minutes to allow secretion uptake. The cotton wool samples were then centrifuged to extract the nasal discharge. Unfortunately the published methodological details for the nasal secretion analysis was not complete and therefore do not allow a thorough comparison, though they report that eosinophilic cationic protein (ECP) showed statistically significant difference in nasal discharge in CRSwNP and tryptase in allergic rhinitis compared to healthy controls. The use of cotton wool pledglets in the middle meatus appears a useful atraumatic technique to measure nasal secretions, though care would have to be taken to ensure a standard volume of cotton wool is used to reproducibly compare the amounts of secretions yielded.

The 13 key CRSsNP mediators were investigated for correlations with sinonasal symptom score. The total SNOT score has been shown to measure a number of different constructs in addition to the rhinological symptoms (Browne et al., 2007). Total SNOT-22 scores are a helpful measure in the clinic, providing a holistic overview of both rhinological symptoms and quality of life. Using exploratory factor analysis Browne at al. identified that SNOT is not unidimensional and in fact contains four separate constructs within SNOT; rhinologic symptoms, ear/facial symptoms, psychological issues and sleep function. When measuring how sinonasal inflammation influences CRS, correlation of mucosal lining fluid mediators with rhinological symptoms is probably more appropriate. As a result, the mucosal lining fluid mediators were subsequently compared to the rhinological subscale of the SNOT-22 score i.e. the seven rhinological questions out of the 22 item scoring; need to blow nose, sneezing, runny nose, post nasal discharge, thick nasal discharge, facial pain/pressure and blockage/congestion of nose giving a rhinological SNOT-22 (RSNOT-22) score out of a maximum total of 35. A RSNOT-22 scoring method can help to address specific nasal symptoms rather than in combination with health related quality of life aspects such as psychological issues and sleep function which can sometimes confuse the message. All 13 key mediators showed significant non-parametric correlations with RSNOT-22. It is tempting to deduce that the greater the local mediator concentrations are in the nasal cavities, the greater the nasal symptom burden. However, such direct causal attribution is problematic, and often represents a complex mix of biological disease activity and personality together with individual perception of illness and disease reporting behaviour (Pennebaker, 1976).

Although this is the largest sample of mediators investigated in CRSsNP to date, it is still exploratory with a relatively small n=40 group and a greater sample size would provide more detailed information. Retrospective power calculations are not without problem and in general are probably best avoided as they can simply be transformations of the p value (Length, 2000). However, in this case it is interesting to look at the mucosal lining fluid mediators which fall just below significance, for example Intercellular Adhesion Molecule 1 (ICAM-1) which is used to aid leukocyte migration via endothelial cells into tissues and also by rhinovirus as a receptor – hence would seem biologically relevant to CRSsNP - has a p value of p=0.057 and a near fold doubling in CRSsNP compared to control samples. A retrospective power calculation based on its data suggests a sample size of only slightly larger n=43 would be required to reach a significance level of $p<0.05$. Such calculations only serve to highlight the need for a follow on larger study of mucosal lining fluid samples in CRS patients.

A factor analysis was performed on the mucosal lining fluid mediators to investigate if the 13 key CRSsNP mediators could be reduced into a smaller set of exploratory factors that account for most of the variance in the original variables. Exploratory factor analysis is based on correlations of mediator scores and will not necessarily reflect functional relations. The process identified four factors to account for 83.3% of the variance (Table 9). The first factor covers pro-inflammatory mediators, the second factor vascular inflammatory mediators, the third factor chemokine and growth factors and the fourth factor contains regulatory mediators. A unifying factor analysis offers an insight into the relationship of mediators under the umbrella of 'CRSsNP' and such analyses may be helpful to allow us to move beyond the over simplistic phenotyping of CRS by the presence or absence of nasal polyps and in to more definitive endotypes as per Tomassen et al. (2016)

4.5.5 Bioinformatics

Data from the CRSsNP mucosal lining fluid swabs were entered into established bioinformatics database techniques to explore their interactions Firstly the mediators were entered into WEB-based GEne SeT AnaLysis Toolkit (WebGestalt) (http://www.webgestalt.org/) as per Wang et al (2013) and Zhang et al (2005) to determine any disease and drug associations from the panel identified. The top 15 statistically significant disease associations it returned included respiratory tract infections, inflammation, common cold, infection, sinusitis, nasal polyps and a variety of other

respiratory tract infection/inflammations (Table 10). These WebGestalt disease associations provide a useful confirmation of the CRSsNP mucosal lining fluid mediators and the high return of related respiratory tract pathologies replicates the established unified airway hypothesis data (Giavina-Bianchi et al., 2016).

WebGestalt also returns a list of associated drugs for the panel of mediators. Four statistically significant associations were found: the corticosteroid dexamethasone, dinoprostone a prostaglandin E2, anakinra an IL-1 receptor antagonist, and immune globulin. Corticosteroids are widely used in CRS, though the other 3 drug associations offer interesting insights into potential pharmacological therapies. Anakinra is a recombinant IL-1 competitive receptor antagonist that blocks the pro-inflammatory actions of both IL-1α and IL-1β. It differs from the circulating IL-1 receptor antagonist (IL-1RA) by the addition of a methionine residue at its amino terminus (Schett et al., 2016). The potential anti-inflammatory effects of IL-1RA have been investigated in trials in rheumatoid arthritis and a Cochrane systematic review has shown it to be safe and modestly efficacious (Mertens and Singh, 2009), though as yet there are no trials of its efficacy in respiratory tract disorders. Dinoprostone is a PGE2 prostaglandin that has its majority of clinical use currently in obstetrics. PGE2 is generated by the metabolism of arachidonic acid via the enzyme cyclooxygenase and has been reported to have a role in modulating the inflammatory response in upper and lower airways (Machado-Carvalho et al., 2014), with reduced PGE2 levels found throughout the airways in aspirin exacerbated respiratory disease. PGE2 in the airways generates cyclic AMP via the prostanoid receptors, which results in overall negative regulation of the 5-lipoxygenase pathway and therefore less inflammatory airway leukotrienes. A down regulation of prostanoid receptors has also been found in CRS patients (Perez-Novo et al., 2005), which may be a factor in the increased upper airway inflammation seen in these tissues. The association with immune globulin is also interesting as there have been a number of cohort studies that have shown patients with refractory CRS to have a variety of immune deficiencies including common variable immune deficiency, selective IgA and IgG subclass deficiencies amongst others. An open label trial of intravenous serum globulin has shown it can be a useful therapeutic adjunct in recalcitrant CRS (Ramesh et al., 1997), although the trial was limited by a small sample size.

Differentially expressed mediators were also entered into the open access bioinformatics tools NetworkAnalyst ((http://www.networkanalyst.ca as per Xia et al in Nature Protocols (2015), GOstats Bioconductor Gene ontology and gplots Heatmap2 open source R package https://www.bioconductor.org/packages/devel/bioc/html/GOstats.html/) as per Falcon and Gentleman (2007) and (Gregory R. Warnes et al., 2016). The results of the various biological pathways provide intuitive, graphical views of the myriad of interactions underlying CRSsNP samples with established biological processes. From the illustrations in Figure 53 - Figure 56 a summary of potential interactions of the differentially expressed mediators in CRSsNP can be obtained to guide further CRSsNP investigations. Such comparative tools allow us to frame the novel, individual mediator results identified with the vast amount of bioinformatics data available on human health and disease.

4.5.6 Quantitative RT-PCR replications

Quantitative real time RT-PCR was used to investigate tissue biopsy specimens for mRNA of the thirteen differentially expressed CRSsNP sinonasal mucosal lining fluid mediators. All five chemokine mediators identified by their protein samples in mucosal lining fluid could also be replicated at the mRNA level by qRT-PCR in their tissue biopsies ($p<0.001$-$p<0.05$). Similarly two of the three cytokine mediators seen in mucosal lining fluid could also be replicated at the mRNA level in tissue biopsies (Figure 59); interleukin 10 and interleukin 17 ($p<0.001$). However, differential expression of interleukin 6 mRNA in tissue biopsies was not replicated. The lack of replication in tissue biopsies compared to mucosal fluid samples may infer that IL-6 is in fact not upregulated in tissue samples, or alternatively that due to the increased levels of IL-6 protein present in the mucosal lining fluid negative regulatory mechanisms of mRNA transcription are activated to reduce the amounts of IL-6 secreted. Only one of the three angiogenesis biomarkers, basic fibroblast growth factor, showed a statistically significant ($p<0.05$) upregulation in mRNA from CRSsNP tissue biopsies compared to controls. Whilst both vascular injury mediators, Serum amyloid A (SAA) and Vascular cell adhesion molecule 1 (VCAM-1/CD106) showed increased mRNA levels in CRSsNP participants consistent with the mucosal lining fluid protein samples, neither reached statistical significance. It would therefore appear that the mediators measured in the mucosal lining fluid are a reasonable indication, though not exact replication of the inflammatory mechanisms present in the parent tissues. The closest resemblance between the mucosal fluid protein samples and tissue biopsy mRNA levels are seen in the chemotactic and pro-inflammatory mediators.

When the protein lysates from tissue biopsies are compared to mucosal swab protein levels the greatest parity is also seen with the chemokine and cytokine mediators (Figure 64) although the amounts measured are much greater in the tissue biopsies than the mucosal swabs (Figure 65). Similarly if the amounts of mediators measured in mucosal swabs are compared to those in the epithelial cell and fibroblast samples there are minimal mediator protein levels present in the cellular samples (Figure 65). The low levels of mediator protein detected in the cellular samples are also confirmed in the mRNA expression in epithelial and fibroblast samples (Figure 60 - Figure 62). In addition to the low levels of mediators measured in the epithelial and fibroblast samples there was markedly less differentiation between control and CRSsNP samples with only MIP-1α showing statistically significant upregulation in fibroblasts at the mRNA level (Figure 60) and IL-5 in epithelial cells and IL-1β in fibroblasts at the protein level (Figure 64) which questions how closely the isolated cultured primary cells may mirror their parent tissues of origin. There was also no significant difference in any of the mediators measured in serum between healthy controls and CRSsNP participants.

4.5.7 Summary

The Multiplex MSD electrochemiluminesce approach adopted has been a very helpful investigatory tool allowing more potential targets and mediators to be analysed than with individual ELISAs in the pilot work due to constraints on sample volume. Multiplex and omic technologies yield vast quantities of data and are increasingly replacing some of the traditional techniques in health sciences research. Here, a multiplex MSD V-PLEX Human Biomarker Kit is effectively a limited 40-plex protein array. If 13 out of 40 mediators are differentially expressed in CRSsNP samples for mucosal lining fluid or 15 out of 40 tissue biopsy samples, the possibility of finding more CRS targets is optimistic. It is beyond the scope of this project, though if future funding allows a proteomics approach to compare CRS tissues to look at a much greater sample of proteins may yield some very useful insights into the potential mechanisms in CRS.

The multiplex approach utilised can potentially identify biomarkers for CRS, which would represent a very useful clinical adjunct. The mucosal lining swab technique could offer an innovative way of investigating sinonasal disease, for example in a longitudinal study; by taking a swab at diagnosis, a repeat swab in a matched patient following medical treatment, similarly prior to and following surgical treatment and any revision procedures, and also at

different times of the day. Data from such a study may be helpful in distinguishing different endotypes of CRS or predict response to medical or surgical treatment. Such a study would need to have a much larger sample size due to heterogeneity of CRS patients with similar clinical phenotypes and offer the opportunity to discriminate between different CRS endotypes.

4.6 Conclusion

Within this chapter I have identified and refined a technique to measure the inflammatory micro-environment of the sinonasal cavities in CRSsNP and health. A panel of mediators has been shown to discriminate CRSsNP participants from healthy controls based on this assay. These mucosal lining fluid sample mediators show significant overlap with analysis of tissue biopsy samples, though only a limited correlation with their matched isolated primary cells in culture. Such non-invasive measures of the mucosal lining fluid of the sinonasal environment may well provide a useful clinical adjunct to monitoring disease in the nasal cavity when combined with clinical, endoscopic and radiological findings.

The identification of mediators in the inflammatory environment in the sinonasal cavities is important when trying to replicate physiological conditions in the laboratory. In the previous chapter, experiments with the commercially available nasal cell line RPMI 2650 were discontinued as they did not appear responsive to a number of disease relevant stimuli, or representative of primary human cells (Ball et al., 2015). Work presented in this chapter has additionally questioned how reflective isolated primary epithelial and fibroblast cells are of either their parent tissue biopsies or mucosal lining fluid swab results from the sinonasal mucosa. It may be that primary cells in conventional culture do not accurately represent the CRSsNP inflammatory processes present. Therefore isolated cells will need further investigation to see if they can be effectively used to replicate and model inflammatory mechanisms in CRS tissues. In the next chapter the cells' transcriptome will be thoroughly investigated in CRSsNP and health and compared to matched tissue biopsy samples.

5 Results – Transcriptome analysis

5.1 Specific aims & objectives

The specific aims for this phase of research were to investigate the transcriptome (RNA transcripts in the cell, i.e. all of the genes that are being actively expressed) of CRSsNP and healthy control samples to identify if there are clusters of genes which are differentially expressed between the two patient groups. Both patient derived primary cells and tissue biopsies were compared to determine firstly, if there are clusters of differentially expressed genes between the patient groups and, to assess how representative the primary cells are of their parent tissues.

5.2 Scientific rationale for experimental approach

Investigating the transcriptome of CRSsNP and healthy control samples allows a comprehensive assessment of a large number of target genes between the participant cohorts. Histological assessment of tissue biopsy samples in chapter 3 demonstrated significant differences in the microscopic appearance of CRSsNP and healthy control tissues. These histological findings, combined with disease micro-environmental changes in the CRSsNP inflammatory environment established in chapter 4 predict differential gene expression in CRSsNP and control samples transcriptomes. The comparison of both the CRSsNP and control tissue biopsy samples and their matched epithelial and fibroblast cells offers an analysis of healthy and CRSsNP tissues and their isolated cell populations. Using microarrays and next generation RNA sequencing I sought to identify clusters of differential gene expression between CRSsNP and control samples and whether any differences are maintained between tissue biopsy and cellular samples as model systems.

5.3 Methods

5.3.1 RNA extraction and quality control

Total RNA was extracted from $1x10^6$ cells from each sample using a Machery Nagel NucleoSpin RNA extraction kit as per manufacturer's instructions. Determination of the RNA yield and purity was performed on a nanodrop 2000 spectrophotometer (Nanodrop, USA) and the quality checked with an Agilent 2100 Expert Bioanalyser. All RNA integrity number (RIN) scores were >8/10.

5.3.2 Microarray procedure

Microarray experiments were performed using the Illumina Bead Array HT12v4 to screen in excess of 47,231 gene probes per sample (Figure 66). The Illumina TotalPrep-96 RNA Amplification Kit was used to generate Biotin labelled (biotin-16-UTP), amplified cRNA starting from 200ng total RNA. 50 ng of the obtained biotinylated cRNA samples was hybridized onto the Illumina HumanHT-12 v4 as per manufacturer's instructions. The samples were scanned using the Illumina iScan array scanner. There were no deviations from the Illumina protocol. RNA labelling, amplification, and hybridization were performed by The Genome Centre at Barts and the London School of Medicine and Dentistry.

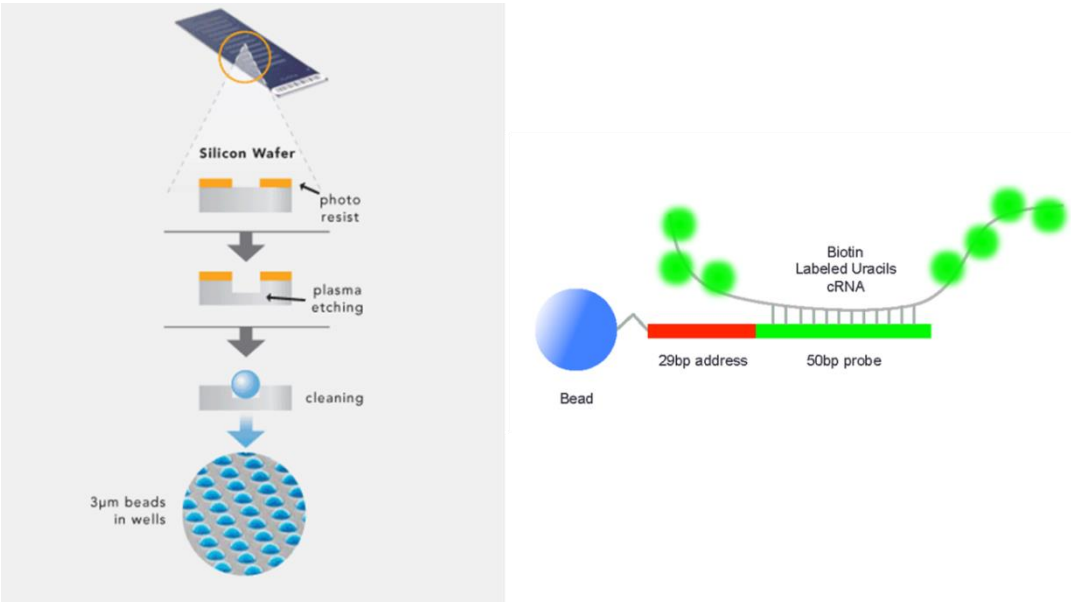

Figure 66. Schematic diagram of the Illumina Bead Array HT12v4. Oligonucleotide probes of 79 base pairs are attached to 3µm silica beads which self-assemble randomly into micro wells on the array chip using lithography on a silica slide. Hybridised probes are then scanned with a laser and fluorescence is measured which generates the raw data files for each array. Image adapted from (Illumina, 2016).

5.3.3 Microarray data analysis

Prior to analysing my microarray data, I completed Dr C Gillespie & Dr S Cockell' s R open source programming and Bioconductor course to learn how to write the command line code and perform analysis on my raw microarray data (http://bsu.ncl.ac.uk/support/courses). All the code was written by myself in R and subsequently checked for accuracy and completeness by the Newcastle Bioinformatics Support Unit. A copy of the code is included in the appendix and a summary of the methods follows here.

The Illumina Human HT12v4 Expression BeadChip data was background corrected in Illumina Beadstudio. Subsequent analysis proceeded using the lumi and limma packages in R (Bioconductor) (Du et al., 2008, Gentleman et al., 2004, Lin et al., 2008). Variant Stabilisation Transformation and Robust Spline Normalisation were applied in lumi. Only probes with a detection p-value < 0.01 in at least one sample were considered valid for downstream analysis. Differential expression was detected using linear models and empirical Bayes statistics in limma. A list of genes for each comparison was generated using a Benjamini Hochberg false discovery rate corrected p-value of 0.05 and a fold change of 1.5 as cut-offs (Benjamini and Hochberg, 1995). The raw data from the array has been deposited in the National Centre for Biotechnology Information Gene Expression Omnibus (NCBI GEO) (NCBI, 2015) public functional genomics data repository supporting Minimum Information About a Microarray Experiment (MIAME)-compliant data submissions (Brazma et al., 2001) (reference GSE69093).

5.3.4 Quantitative real time RT-PCR

Quantitative RT-PCR was used to replicate the findings of the microarray. cDNA was prepared from isolated RNA samples using the BIORAD iScript cDNA synthesis kit as per manufacturer's instructions. 10ng of cDNA template was used per qRT-PCR reaction using SYBR Green JumpStart Taq Ready Mix on an Applied Biosystems 7500 Real-Time PCR System for 35 cycles. 1µl of forward and reverse primers (NFE2L3 - as identified from the microarray analysis, forward TCCCAGCATGAGGAAAATGA, reverse TTCTGCCTCCCAGTCAGGTTT (Korecka et al., 2013)) were supplied by Eurofins per reaction. Expression levels of mRNA were normalised to those of the healthy controls for relative mRNA expression data. Products formed in the qRT-PCR reactions were verified by 2% agarose gel electrophoresis and compared to a 100 base pair ladder.

5.3.5 Immunohistochemical staining

Formalin fixed paraffin embedded tissue sections were produced from tissue biopsy samples. Sections were de-waxed and rehydrated twice in Clearene followed by 100% and 70% ethanol each for 5 minutes. Antigen retrieval was performed in 1 mM EDTA at pH8 in a microwave at 700 watts for 15 minutes. Non-specific binding was blocked using 5% bovine serum albumin in PBS with 0.2% Tween 20 (5% BSA PBST) at room temperature for 1 hour. To replicate the findings of the micro array and RT-PCR, anti NFE2L3 primary antibody (LSBio LS-B8066) at 1:200 dilution was incubated overnight at 4^{o}C in 5% BSA PBST. TRITC conjugated secondary antibody (Sigma T6778) at 1:100 dilution was incubated in 5% BSA PBST at room temperature and in darkness. Sections were counterstained and mounted with vectashield DAPI containing mounting medium (Vector laboratories H-1200). Slides were imaged on a Nikon A1 using a Nikon Eclipse NI-E upright stand with a x20 0.75Na Plan Apo lens running Nikon elements 4.30.02.

5.3.6 RNA sequencing procedure

RNA sequencing was performed using the illumina HiSeq platform. Library construction was performed using 1µg of RNA with the illumina TruSeq Stranded mRNA LT system as per manufacturer's instructions. Following library construction the libraries were assessed with an Agilent 2200 TapeStation (Agilent, US). Libraries were then standardised, pooled and the finished pools were quantified again by quantitative PCR (qPCR) using the illumina sequencing library qPCR protocol prior to loading. Libraries were loaded at 17pmol and run on the Illumina HiSeq 2500 with no deviations from the manufacturer's protocol. Sequencing was completed using 3 flow cells of Rapid Run 75bp paired end sequencing with no deviations from the protocol. RNA sequencing was completed by DBS Genomics within the School of Biological and Biomedical Sciences, Durham University.

5.3.7 RNA sequencing data analysis

RNA sequencing data was analysed using the standardised DESeq2 methodology for differential expression analysis of sequencing data (Love et al., 2014). RNA sequencing raw data in FASTQ file format was subject to quality control analysis using the Kraken toolset as per Davis et al. (2013) to remove low quality reads. Subsequently FASTQ files were aligned to the Genome Reference Consortium Human Build 38 genome (Ensembl, 2016) using the splice junction mapper Tophat (Kim et al., 2016). The outputted BAM files from Tophat were

then sorted and converted to SAM format using Samtools (Samtools, 2016). The sorted SAM files were then used by HTSeq (Anders et al., 2015) to estimate gene counts. Gene counts were then fed into the R package DESeq2 and filtered to remove genes that did not have at least 1 count across the entire dataset. Once complete, gene counts were normalised and fitted to a generalised linear model and tested for significance using a Wald test. Multiple hypothesis testing correction was carried out using the Benjamini and Hochberg methodology with a false discovery rate of 10% (Benjamini and Hochberg, 1995). RNA sequencing data analysis was performed in combination with the Computational biology facility, School of Biological and Biomedical Sciences, Durham University, UK.

5.3.7.1 RNA sequencing pathway analysis

Following differential gene expression of the RNA sequencing data (5.3.7), pathway analysis was performed using the standardised Ingenuity Pathway Analysis program (www.ingenuity.com) as per Kramer et al. (2014). Ingenuity Pathway Analysis is a software package for RNA sequencing data that uses differential expression data to generate functional outcomes and pathway analysis based on known biological pathways using a combination of public source data and a database of biological process findings extracted from the published literature.

5.4 Results

5.4.1 Microarray data

5.4.1.1 RNA quality control

Total RNA was isolated from participant samples and its concentration and quality were measured using a nanodrop 2000 and Agilent 2100 Expert Bioanalyser. High concentrations of high quality RNA without degradation suitable for subsequent microarray analysis were obtained. The RNA quality control data is presented in Table 15 and a representative electrophoretogram trace is shown in Figure 67.

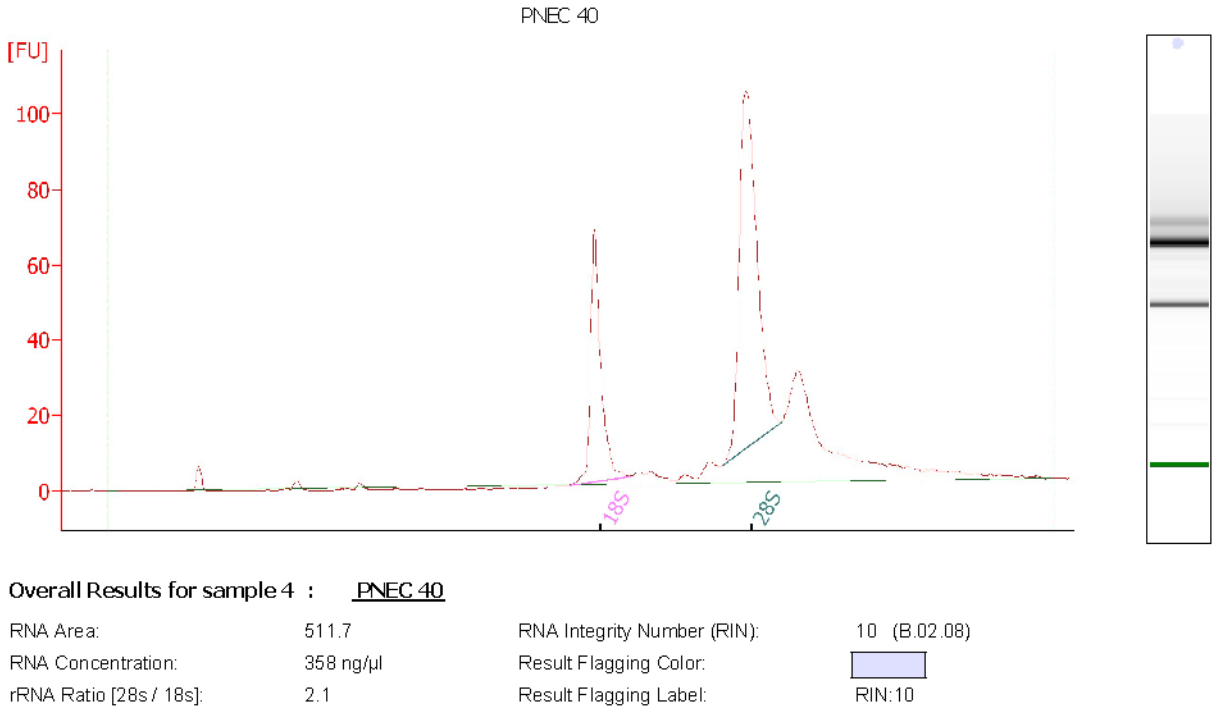

Figure 67. Example of RNA extraction quality control performed with an Agilent 2100 Expert Bioanalyser. The RNA integrity number (RIN) is calculated from the electrophoretic trace of the RNA sample, including for the presence of degradation products and a score out of 10 is assigned. In this sample a RIN score of 10 has been achieved.

Sample ID	Conc (ng/ul)	A260	A280	260/280	Bioanalyser RIN score
PNEC-1	218.2	5.454	2.539	2.15	10
PNEC-11	511.6	16.461	7.392	2.23	10
PNEC-12	380	9.5	4.474	2.12	9.7
PNEC-13	517.2	16.665	9.243	1.8	10
PNEC-14	466.5	11.662	5.561	2.1	10
PNEC-15	323	8.076	3.791	2.13	10
PNEC-16	413.5	10.338	4.886	2.12	9.5
PNEC-2	289.2	7.23	3.308	2.19	9.8
PNEC-29	345.6	8.641	4.01	2.15	10
PNEC-3	444.7	11.116	5.273	2.11	9.7
PNEC-30	379.1	9.479	4.428	2.14	9.8
PNEC-37	479.4	11.984	5.653	2.12	10
PNEC-38	271.2	6.779	3.186	2.13	10
PNEC-39	561	14.025	6.922	2.03	10
PNEC-4	427.7	10.692	5.056	2.11	9.9
PNEC-40	478.2	11.954	5.712	2.09	10
PNEC-41	500.2	12.505	6.026	2.08	10
PNEC-42	370.1	9.253	4.393	2.11	10
PNEC-43	396	9.901	4.622	2.14	10
PNEC-44	413.7	10.342	4.883	2.12	8.7
PNEC-45	374.2	9.355	4.354	2.15	9.1
PNEC-5	145.7	3.916	1.835	2.13	10
PNEC-7	273.9	6.846	3.162	2.16	9.9
PNEC-9	519.9	12.998	6.204	2.1	10
PNF-11	238.8	5.969	2.762	2.16	10
PNF-12	196.7	4.917	2.289	2.15	8.3
PNF-13	333.6	8.341	3.827	2.18	9.1
PNF-14	304.1	7.603	3.54	2.15	10
PNF-15	475.7	11.892	5.653	2.1	10
PNF-16	379.2	9.481	4.463	2.12	9.6
PNF-2	465.6	11.64	5.208	2.24	10
PNF-29	338.5	8.464	3.931	2.15	9.7
PNF-3	150.6	3.765	1.748	2.15	9.2
PNF-30	526.1	18.478	8.647	2.14	9.4
PNF-37	437.1	10.927	5.113	2.14	10
PNF-38	414.5	10.362	4.908	2.11	9
PNF-4	318.2	7.954	3.704	2.15	10
PNF-40	294.6	7.365	3.42	2.15	9.7
PNF-41	636.2	15.905	7.39	2.15	10
PNF-42	377.9	9.448	4.441	2.13	9.5
PNF-43	666.8	16.669	7.919	2.1	10
PNF-44	373.5	13.154	6.268	2.1	10
PNF-45	630	15.751	7.322	2.15	10
PNF-5	197.7	4.942	2.318	2.13	9.7
PNF-6	263.1	6.578	3.063	2.15	10
PNF-7	336.5	8.412	3.878	2.17	10
PNF-8	276.7	6.917	3.244	2.13	8.8
PNF-9	757.3	18.933	8.927	2.12	10

Table 15. Table detailing concentrations of isolated RNA, 260 and 280 absorbance and RNA integrity number (RIN) score.

5.4.1.2 Microarray data transformation and normalisation

Microarray data was obtained for 48 samples on 4 Illumina HT12v4 BeadArray chips with the raw data in IDAT files and chip layout information in SDF files. The data was entered into Illumina GenomeStudio for background modified subtraction, a function based on in built random control probes within the BeadArrays. From this process a sample probe profile of the raw data was created which contained for each of the 47,000 gene probes; the average signal, the detection p value, bead standard error and average number of beads. As a result of the background modified subtraction, only 7 sample gene probes were excluded based on the control probes and the un-normalised background corrected fluorescence data was obtained (Figure 68).

Variant stabilization transformation was performed on the background corrected data which utilises the within array technical replicates to improve differential expression reporting and reduce false positives (Lin et al., 2008, Kuhn et al., 2004). Robust spline normalisation was used for between array chip normalisation to ensure values of intensity between different bead chip arrays have similar normalisation (Du and Gang Feng, 2016). The results of transformation and normalisation of the raw fluorescence data are presented in Figure 69, and essentially ensures groups of arrays are comparable.

5.4.1.3 Microarray quality control

Quality control of microarray data was performed using the array QualityMetrics package to assess overall array quality and to diagnose batch effects. Figure 70(a) shows a false colour heat map of the distances between epithelial cell arrays. The colour scale is chosen to cover the range of distances encountered in the dataset. Patterns in this plot can indicate clustering of the arrays either due to intended biological or unintended experimental factors (batch effects). The distance between two arrays is computed as the mean absolute difference between the data of the arrays (using the data from all probes without filtering). Outlier detection was performed by looking for arrays for which the sum of the distances to all other arrays was exceptionally large. One such array was detected, and is asterisked.

A bar chart of the sum of distances to other arrays is shown in Figure 70(b), the outlier detection criterion from the previous heat map. The bars are shown in the original order of the arrays. Based on the distribution of the values across all arrays, a threshold of 3.1 was determined, which is indicated by the vertical line. The same array exceeded the threshold, was considered an outlier and therefore was excluded from the subsequent analysis.

A similar quality control analysis of the primary fibroblast arrays was performed and showed no outliers detected (Figure 78).

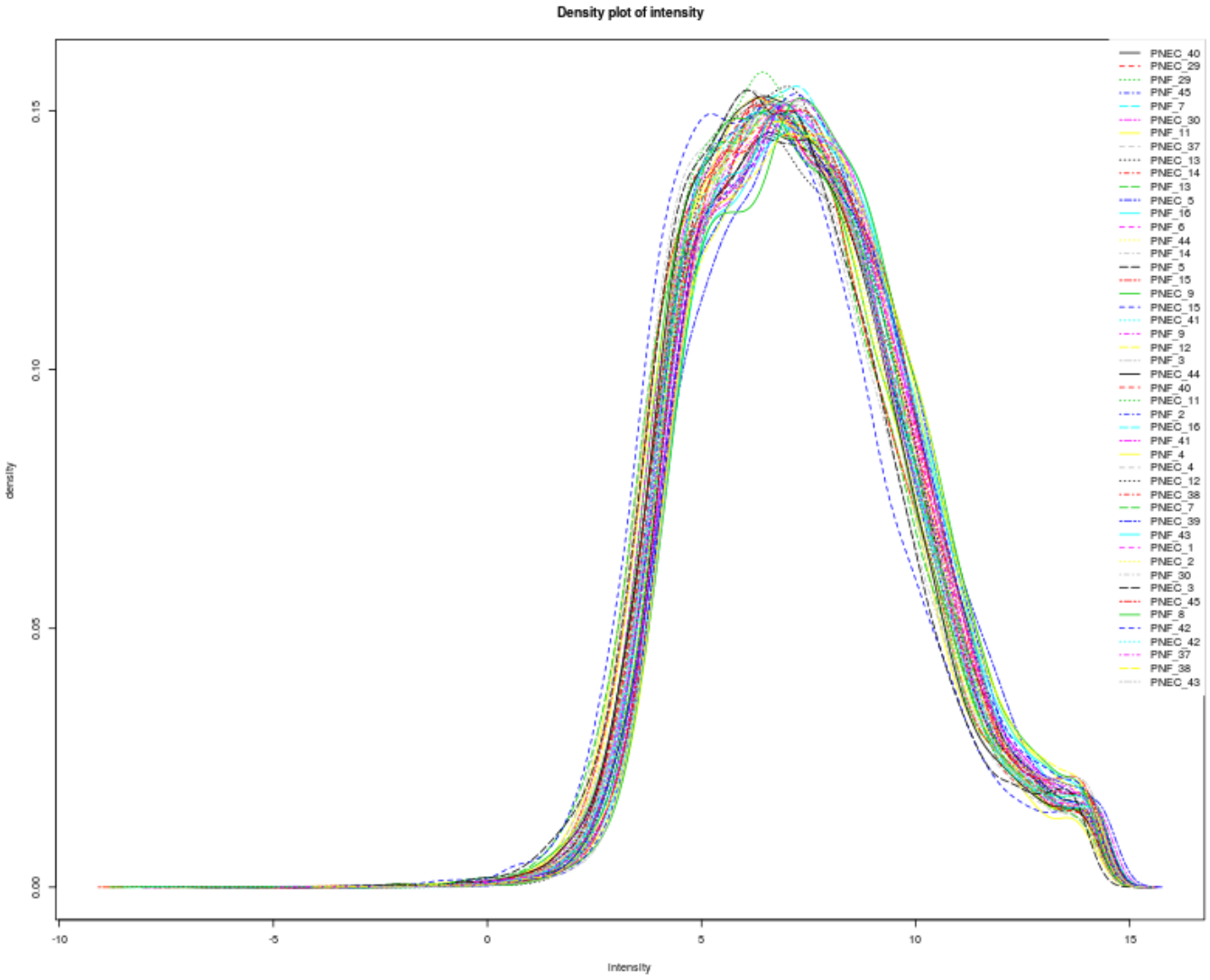

Figure 68. Raw fluorescence data from all microarrays density of intensity plot.

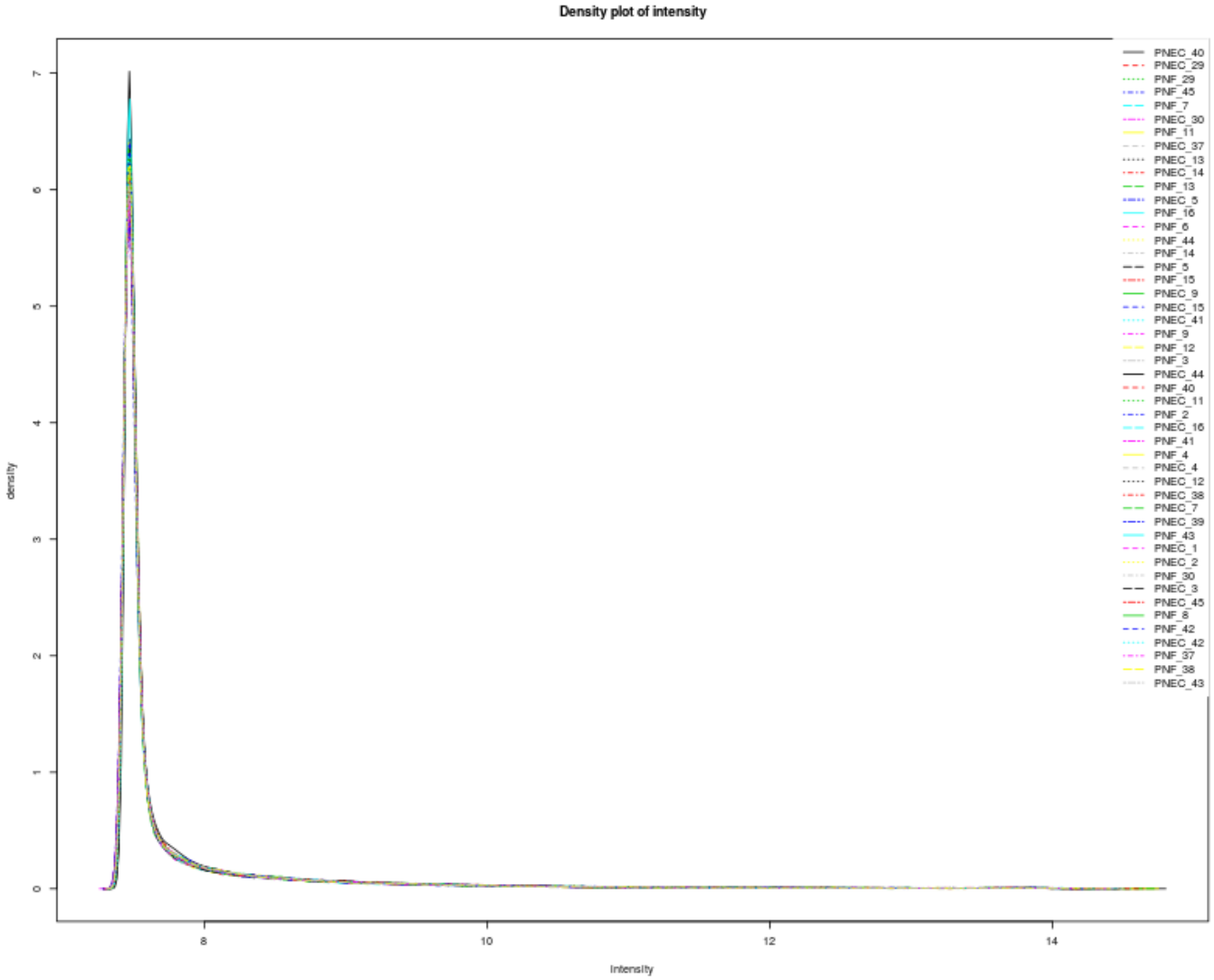

Figure 69. Background corrected microarray data following Variant Stabilisation Transformation and Robust Spline Normalisation applied in lumi to ensure the groups of arrays are comparable.

(a)

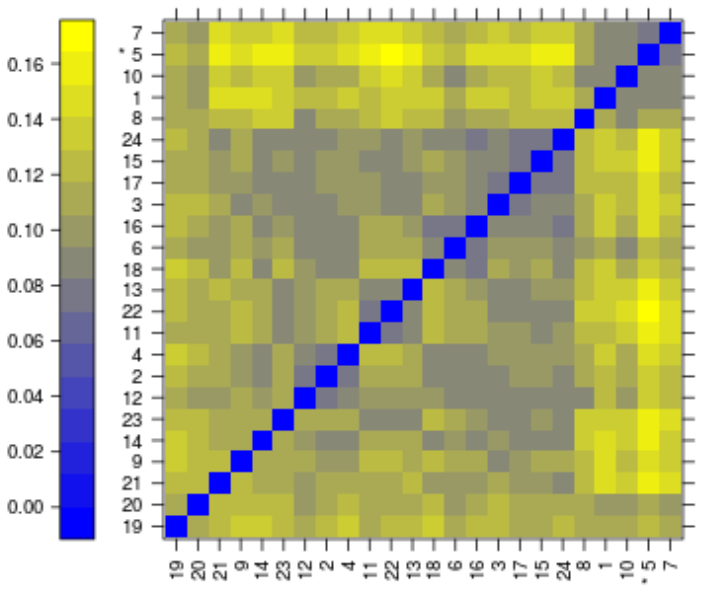

(b)

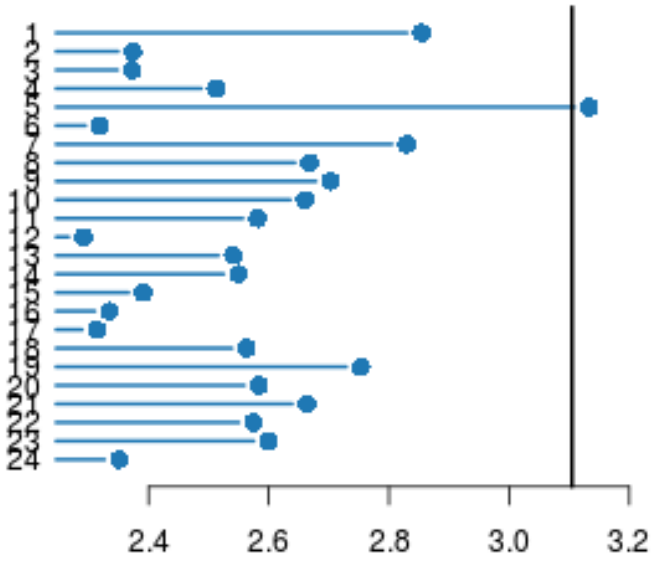

Figure 70. Array quality metrics quality control analysis of epithelial cell microarray data. (a) A false colour heat map of the distances between arrays. Patterns in the plot indicate clustering of the arrays due to either intended biological or unintended experimental factors (batch effects). The distance between two arrays is computed. Outlier detection was performed by looking for arrays for which the sum of the distances to all other arrays was exceptionally large. One such array was detected, asterisked.

(b) Outlier detection for distances between arrays, a bar chart of the sum of distances to other arrays, the outlier detection criterion from the previous figure. The bars are shown in the original order of the arrays. The same array exceeded the threshold, was considered an outlier and therefore was excluded from the subsequent analysis.

5.4.1.4 Microarray differential expression analysis

The initial comprehensive microarray analysis was a hierarchical clustering to explore for differences in gene expressions between healthy controls (n=12) and CRSsNP patients (n=12). Each gene starts in its own cluster and the most similar genes are merged according to the Euclidian distance similarity metric. The similarity metrics are recalculated between the genes and the new cluster and the process is repeated until all genes are in a single cluster. Hierarchical clustering analysis clearly separated samples based on their cell type, confirming the difference between epithelial and fibroblast samples. The cluster analyses however did not significantly discriminate between healthy controls and CRSsNP participants as illustrated in the principal components plot (Figure 71) and cluster dendrogram (Figure 72). Figure 73 presents the Euclidian distance between all the pairs of samples in the study in a heat map, so the smaller the number, the more similar two arrays are to one another. Each array has a zero distance from itself, which represents the diagonal red stripe.

Microarray analysis of isolated primary nasal epithelial cells was performed following Benjamini Hochberg correction for multiple hypothesis testing. No significantly differential (>50% up or down) gene expression was found (Figure 76 & Figure 77). Principal components analysis (Figure 74) and cluster dendrogram analysis (Figure 75) of primary nasal epithelial cells did not group cells between CRSsNP samples and healthy controls. A similar comparison of fibroblast cells from control and CRSsNP participants identified one significantly differentially expressed gene (Figure 81, Figure 82 and Table 16), nuclear factor erythroid-derived 2-like 3 (NFE2L3, p= 0.000015, p= 0.0471 following multiple hypothesis testing correction). NFE2L3 is a transcription factor with potential roles in inflammation that was 60% upregulated in CRSsNP fibroblast cells compared to healthy controls. However, principal components analysis (Figure 79) and cluster dendrogram analysis (Figure 80) of primary nasal fibroblast cells did not group cells overall between CRSsNP samples and healthy controls.

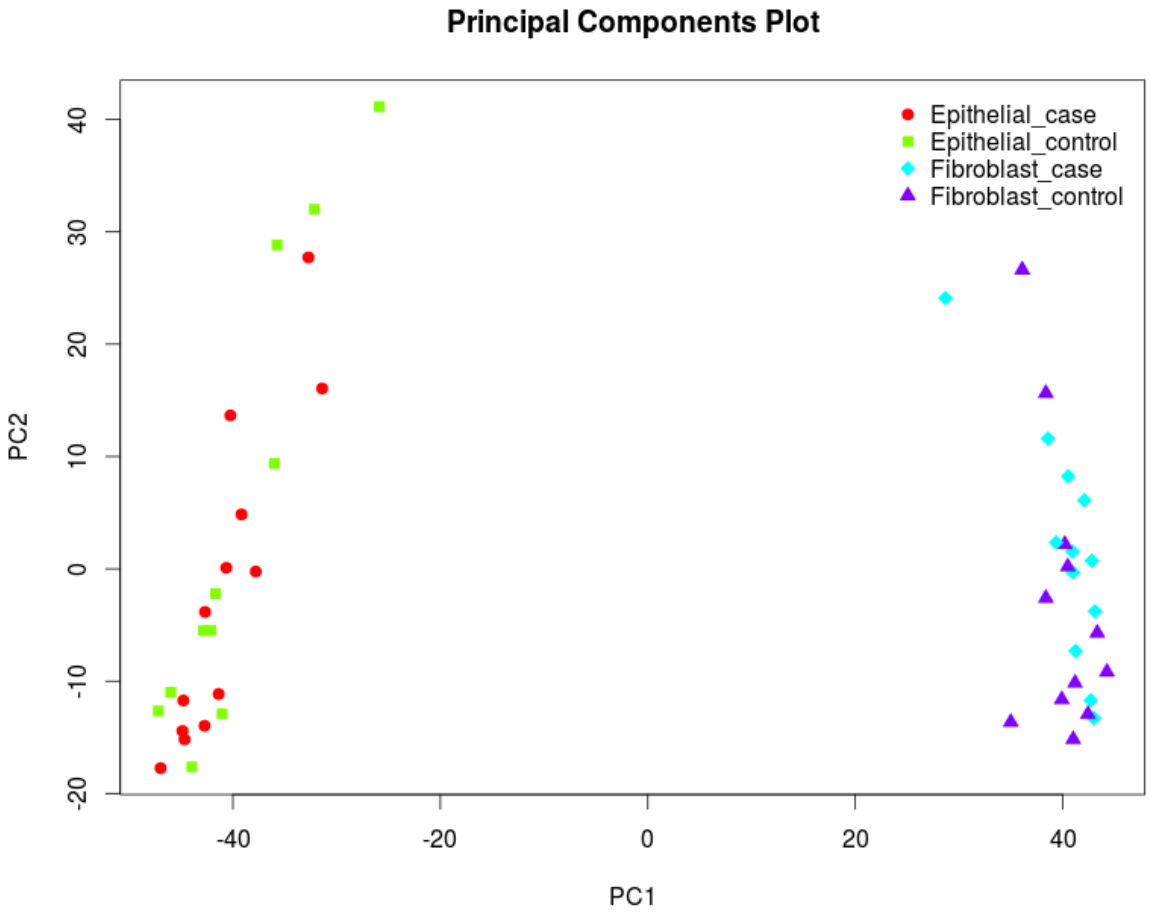

Figure 71. Principal components analysis plot of all arrays including cases (CRSsNP participants) vs controls for both primary nasal epithelial cells and primary nasal fibroblasts. The samples are principally separated on the basis of the cell type of origin, either epithelial or fibroblast rather than case (CRSsNP) or control.

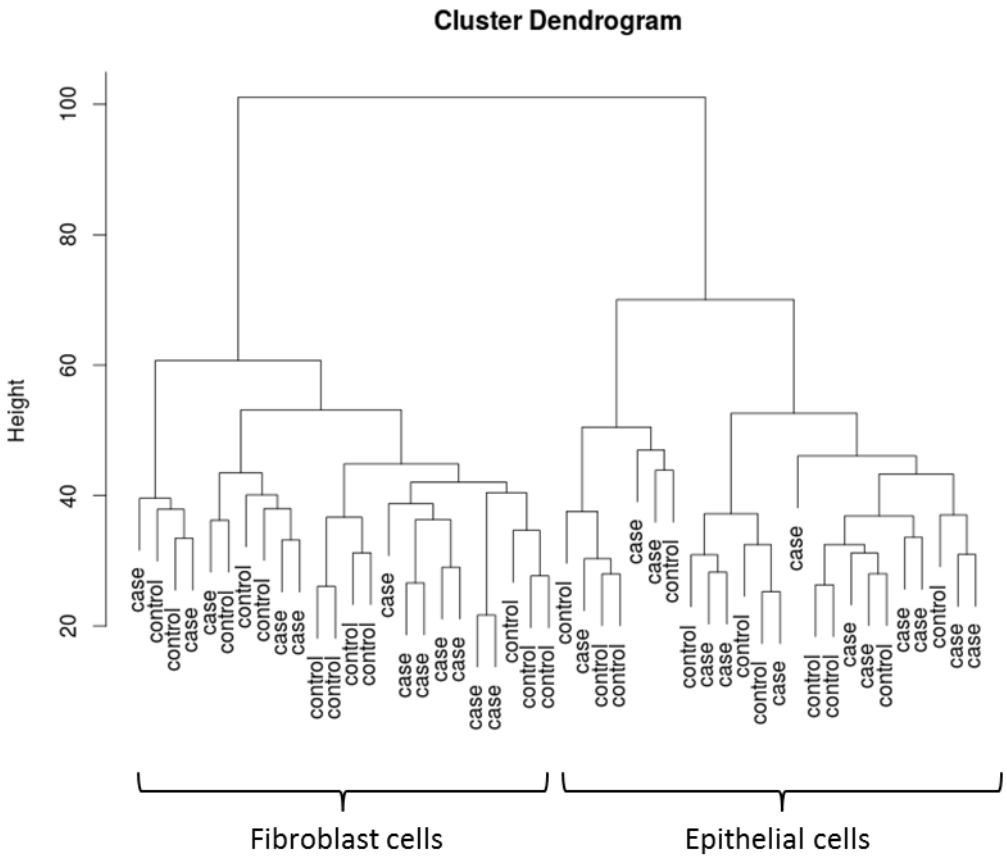

Figure 72. Dendrogram produced by hierarchical clustering of CRSsNP and healthy control gene samples. Each gene starts in its own cluster and the most similar genes according to the Euclidian distance similarity metric are merged. The similarity metrics are recalculated between the genes and the new cluster and the process is repeated until all genes are in a single cluster. The samples are principally separated on the basis of the cell type of origin, either epithelial or fibroblast rather than case (CRSsNP) or control.

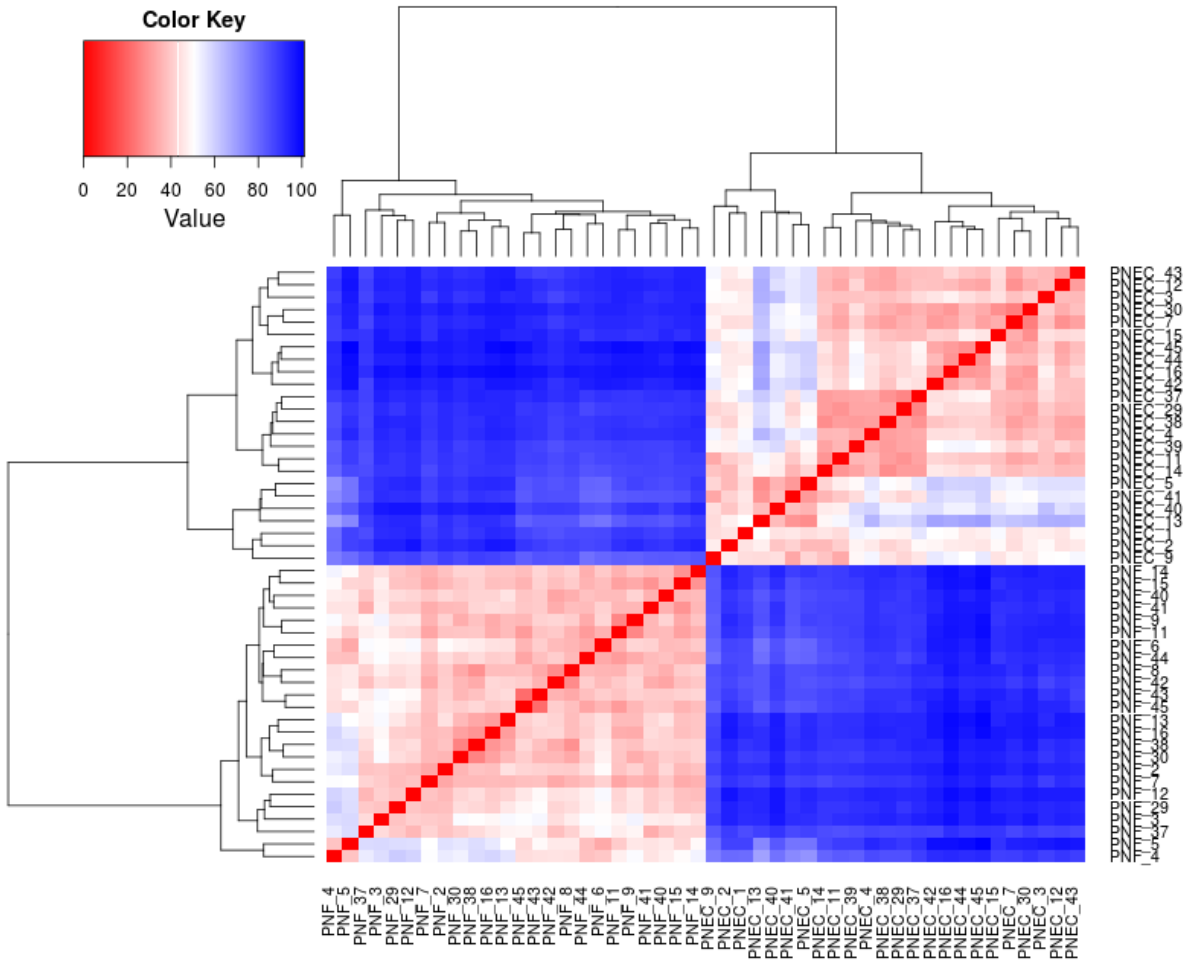

Figure 73. Heat map representation of Euclidian distance data from all the primary nasal epithelial and fibroblast arrays.

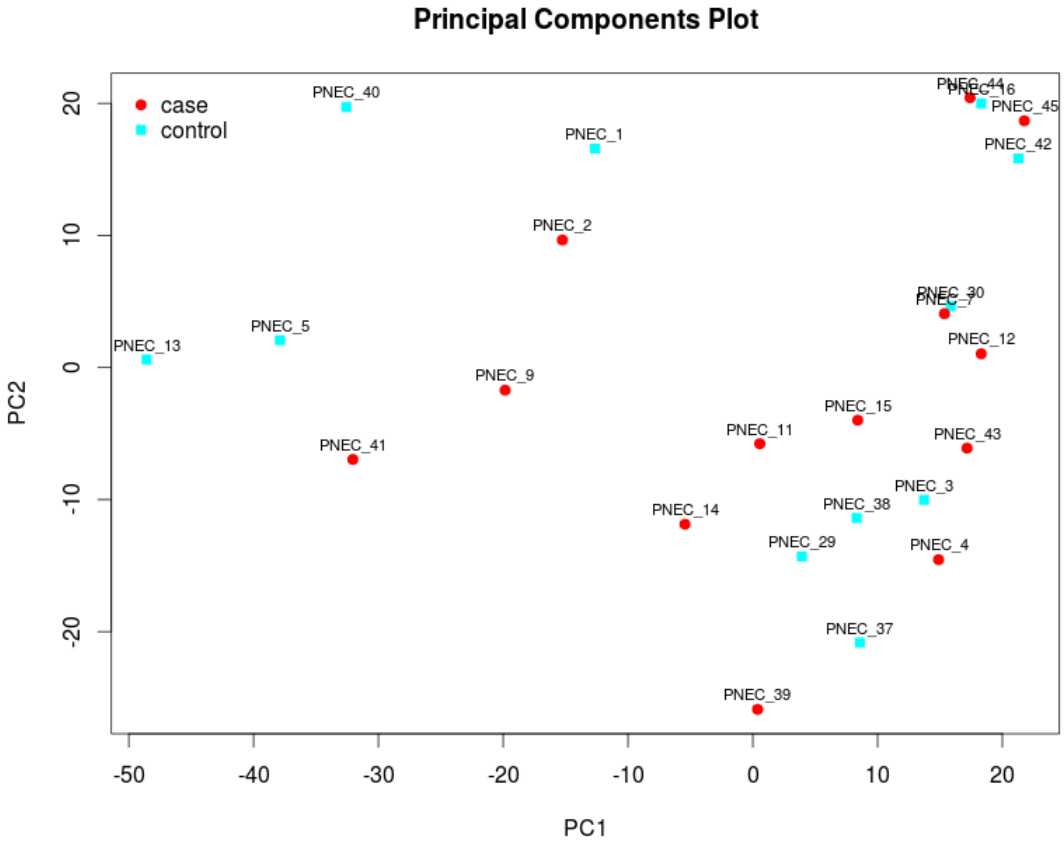

Figure 74. Principal components analysis plot of all the primary nasal epithelial cells

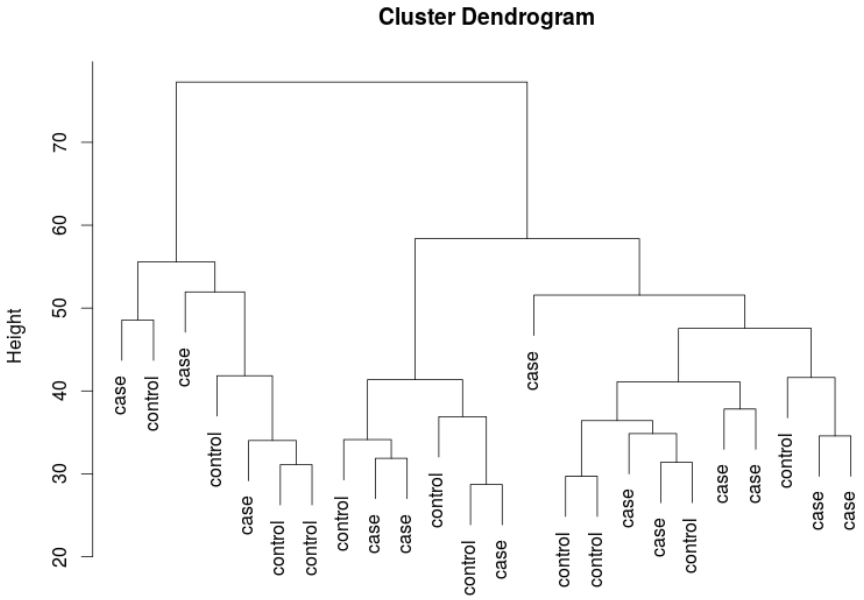

Figure 75. Cluster Dendrogram of all the primary nasal epithelial cells

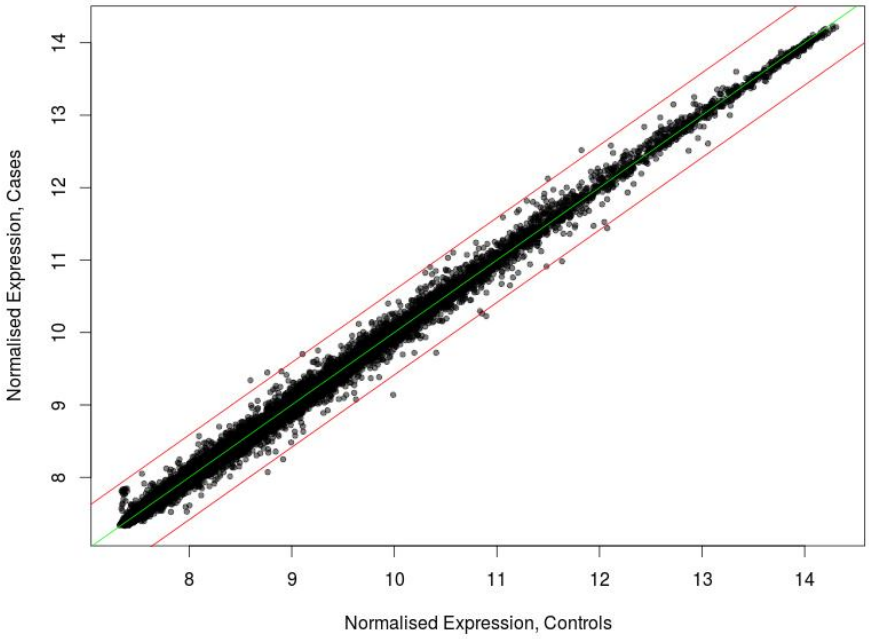

Figure 76. XY scatter plot of all primary nasal epithelial cells. Points outside of the two red lines represent genes that are more than 50% up or down regulated.

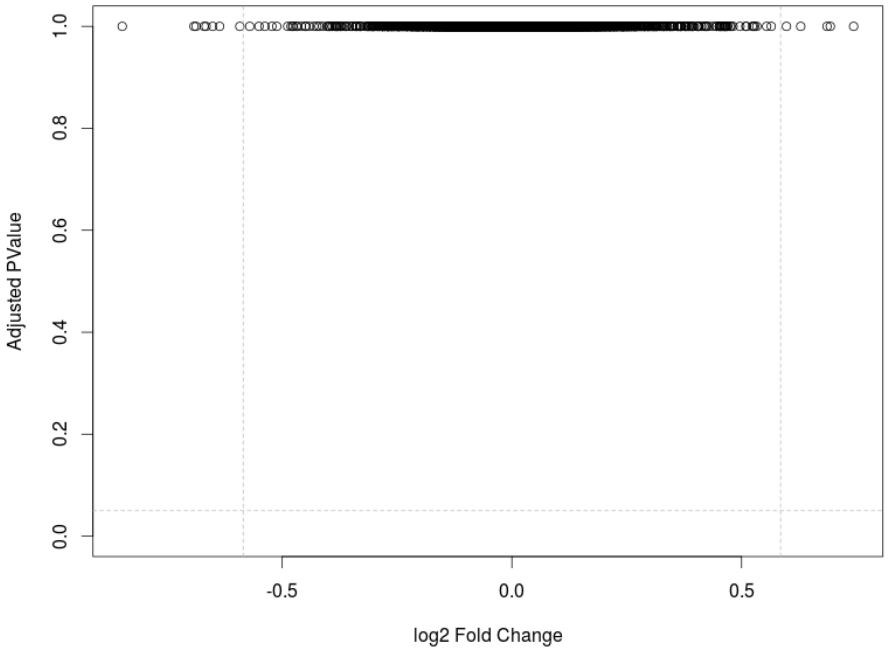

Figure 77. Volcano plot of all primary nasal epithelial cells. Points outside of the two dashed vertical lines represent genes that are more than 50% up or down regulated. No points are also below the dashed horizontal line demonstrating no statistically significant ($p<0.05$) differentially expressed genes following multiple hypothesis testing correction.

(a)

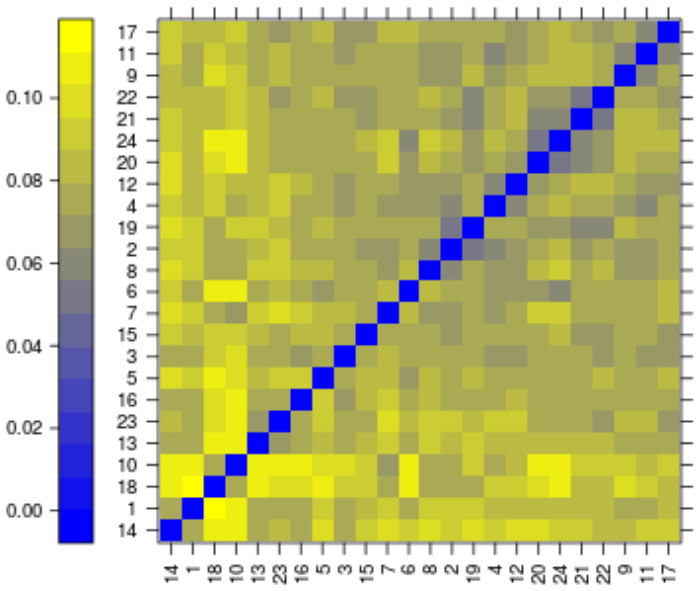

(b)

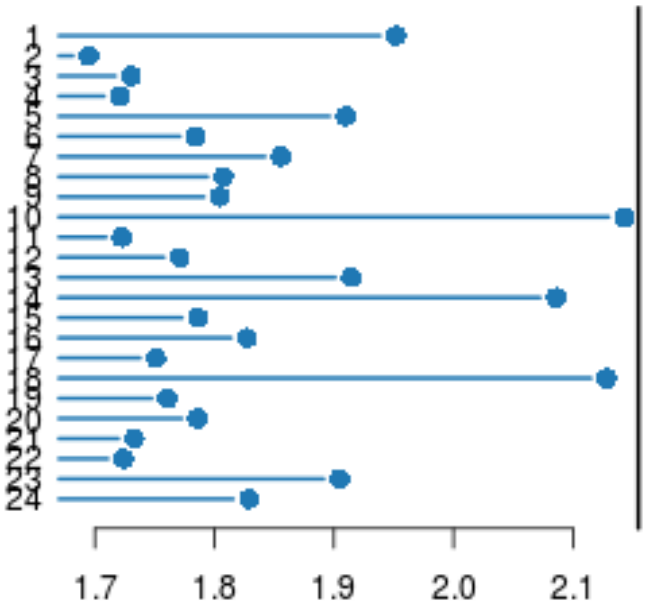

Figure 78. Array quality metrics quality control analysis of fibroblast microarray data. (a) A false colour heat map of the distances between arrays. Patterns in this plot can indicate clustering of the arrays either due to intended biological or unintended experimental factors (batch effects). The distance between two arrays is computed. Outlier detection was performed by looking for arrays for which the sum of the distances to all other arrays was exceptionally large. No outlier arrays were detected.

(b) Outlier detection for distances between arrays - a bar chart of the sum of distances to other arrays, the outlier detection criterion from the previous figure. Based on the distribution of the values across all arrays, a threshold of 2.15 was determined, which is indicated by the vertical line. None of the arrays exceeded the threshold and was considered an outlier.

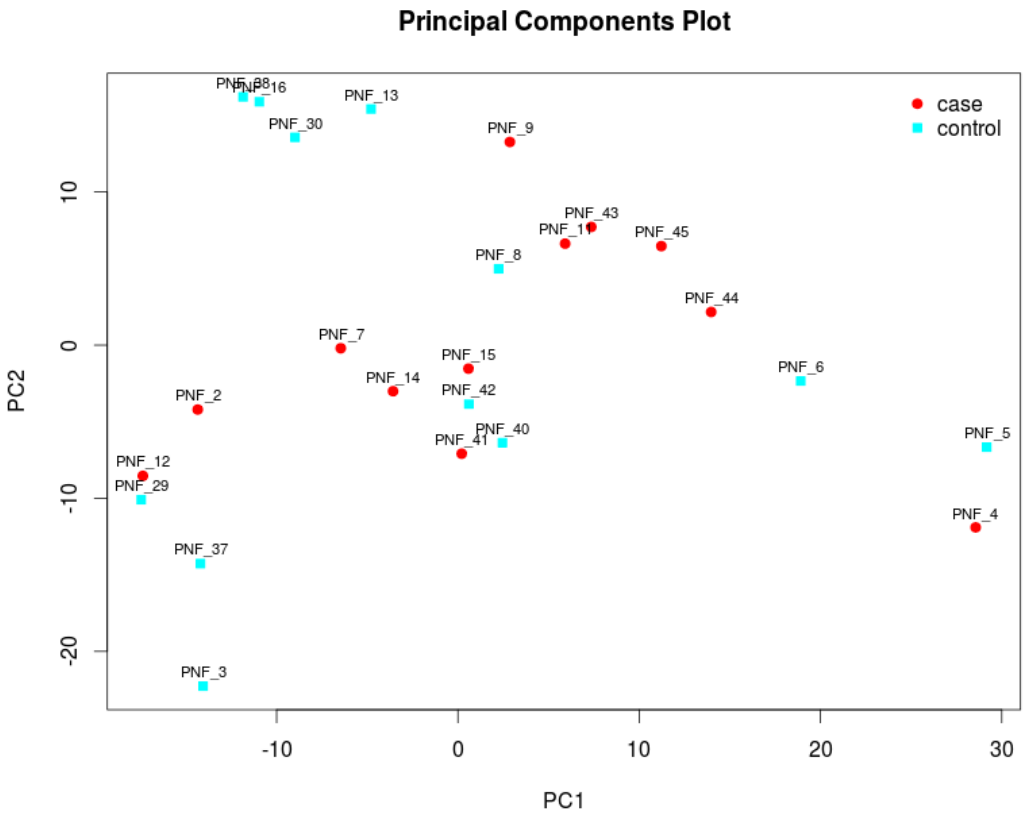

Figure 79. Principal components analysis plot of all the primary nasal fibroblasts

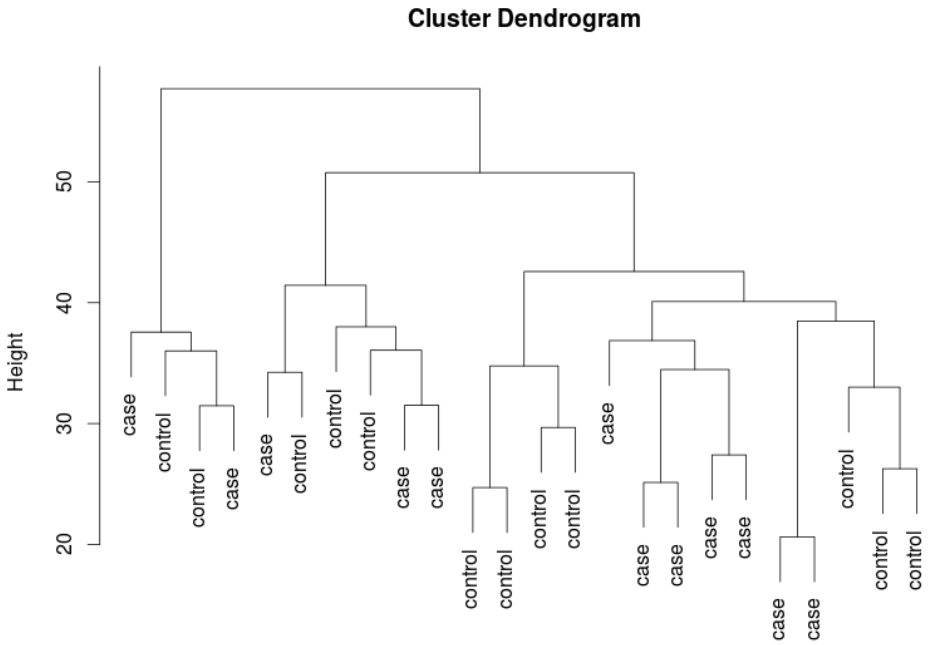

Figure 80. Cluster Dendrogram of all the primary nasal fibroblast cells

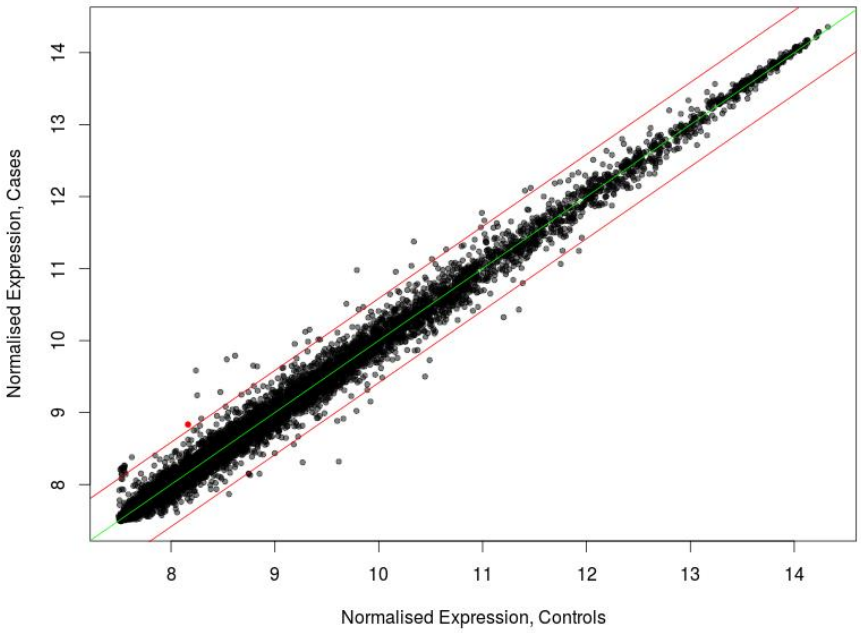

Figure 81. XY scatter plot of all primary nasal fibroblast cells. Points outside of the two red lines represent genes that are more than 50% up or down regulated.

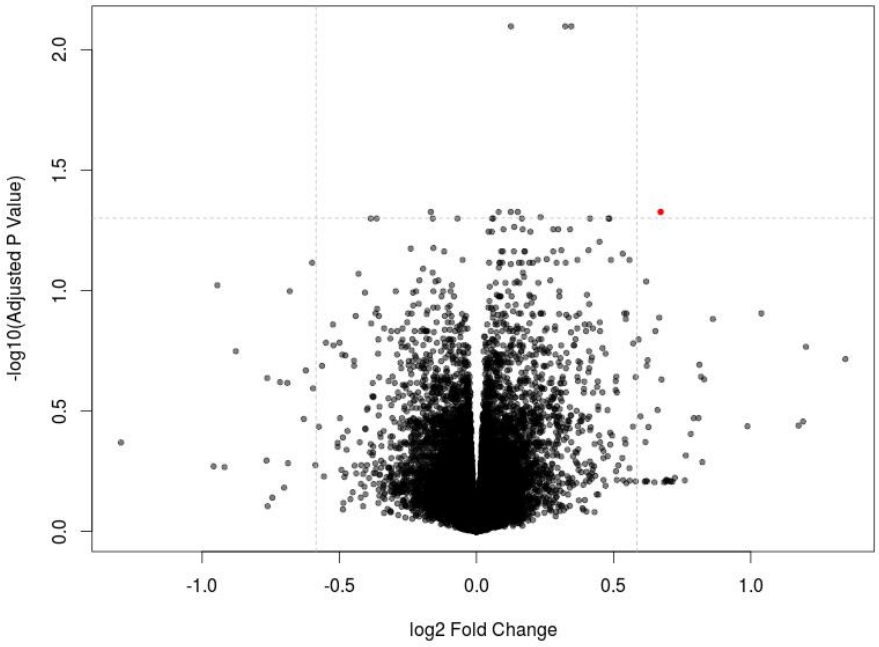

Figure 82.Isolated fibroblast cells volcano plot to identify any statistically significant differential gene expression between CRSsNP and control samples following Benjamini-Hochberg multiple hypothesis testing correction. Points outside the dashed vertical lines demonstrate either a 50% up or down regulation in gene expression. Points above the dashed horizontal line show a statistically significant difference of greater than $p<0.05$. Points that satisfy both differential expression criteria and statistical significance have been coloured red. In this instance one gene fulfils both criteria; NFE2L3.

	SYMBOL	CHROMOSOME	DEFINITION	logFC	AveExpr	t	P.Value	adj.P.Val	B	Ratio
	SFRP4	7	Homo sapiens secreted frizzled-related protein 4 (SFRP4), mRNA.	1.344908	8.912574711	3.310307	0.00302296	0.19233388	-1.771462372	2.54014
	IFI27	14	Homo sapiens interferon, alpha-inducible protein 27 (IFI27), transcript var	1.201211	9.137254506	3.461527	0.00209343	0.17111798	-1.433183989	2.299327
	KIAA1199	15	Homo sapiens KIAA1199 (KIAA1199), mRNA.	1.190909	10.38466725	2.509215	0.01950378	0.34944956	-3.459345354	2.282966
	RARRES1	3	Homo sapiens retinoic acid receptor responder (tazarotene induced) 1 (RA	1.174274	9.204023653	2.446651	0.02238635	0.36359492	-3.581344633	2.256793
	LXN	3	Homo sapiens latexin (LXN), mRNA.	1.038747	10.85723363	3.915739	0.00068236	0.12431806	-0.394735482	2.054443
	RARRES1	3	Homo sapiens retinoic acid receptor responder (tazarotene induced) 1 (RA	0.988121	8.745864341	2.435505	0.02293957	0.3657751	-3.602895292	1.9836
	NDN	15	Homo sapiens necdin homolog (mouse) (NDN), mRNA.	0.862027	9.222186102	3.812839	0.00088121	0.13125923	-0.632312334	1.81759
	OSAP	4	Homo sapiens ovary-specific acidic protein (OSAP), mRNA.	0.830036	9.708155617	3.067986	0.00540094	0.23338707	-2.302773269	1.77773
	IRX3	16	Homo sapiens iroquois homeobox 3 (IRX3), mRNA.	0.823707	10.09986785	1.90407	0.06934812	0.5151195	-4.557033941	1.769949
	C4orf49	4	Homo sapiens chromosome 4 open reading frame 49 (C4orf49), mRNA.	0.818713	9.742693213	3.105265	0.00494343	0.22776917	-2.222007707	1.763832
	C4orf49	4	Homo sapiens chromosome 4 open reading frame 49 (C4orf49), mRNA.	0.812935	9.235819644	3.218483	0.00377153	0.20327221	-1.974488512	1.756782
	PITX1	5	Homo sapiens paired-like homeodomain transcription factor 1 (PITX1), mI	0.80961	8.880326543	2.572341	0.01694832	0.33846173	-3.334529573	1.752738
	LOX	5	Homo sapiens lysyl oxidase (LOX), mRNA.	0.792341	10.55933149	2.572032	0.01696	0.33846173	-3.335143347	1.731882
	IL6	7	Homo sapiens interleukin 6 (interferon, beta 2) (IL6), mRNA.	0.781296	11.38372944	2.322748	0.02929047	0.39369831	-3.817658683	1.718674
	TNFRSF19	13	Homo sapiens tumor necrosis factor receptor superfamily, member 19 (TN	0.76311	9.572760341	2.005378	0.05669675	0.4840288	-4.387235063	1.697145
	GAGE2B	X	Homo sapiens G antigen 2B (GAGE2B), mRNA.	0.759604	8.001994624	1.541319	0.13673969	0.61370582	-5.110473371	1.693026
	OXTR	3	Homo sapiens oxytocin receptor (OXTR), mRNA.	0.723286	10.67680296	1.58618	0.12620562	0.59871248	-5.046960018	1.650938
	GAGE5	X	Homo sapiens G antigen 5 (GAGE5), mRNA.	0.71414	7.907636466	1.507615	0.14512068	0.62100365	-5.157221187	1.640505
	GAGE12G	X	Homo sapiens G antigen 12G (GAGE12G), mRNA.	0.707875	7.908267456	1.508825	0.14481267	0.62065998	-5.155557303	1.633397
	GAGE4	X	Homo sapiens G antigen 4 (GAGE4), mRNA.	0.70689	7.878341021	1.526393	0.14040101	0.61713247	-5.131279769	1.632281
	GAGE12I	X	Homo sapiens G antigen 12I (GAGE12I), mRNA.	0.697254	7.860512696	1.533818	0.13856964	0.61531777	-5.120949411	1.621415
	GAGE6	X	Homo sapiens G antigen 6 (GAGE6), mRNA.	0.692344	7.866124981	1.54135	0.13673209	0.61370582	-5.110429557	1.615907
	LOC645037	X	Homo sapiens similar to GAGE-2 protein (G antigen 2) (LOC645037), mRNA	0.692272	7.878956871	1.549544	0.13475583	0.6099736	-5.09893781	1.615827
	GAGE4	X	Homo sapiens G antigen 4 (GAGE4), mRNA.	0.68923	7.896017609	1.508407	0.14491902	0.62088743	-5.156132247	1.612423
	GAGE5	X	Homo sapiens G antigen 5 (GAGE5), mRNA.	0.683749	7.88786003	1.489726	0.14973672	0.62475782	-5.181691776	1.606308
	CCL2	17	Homo sapiens chemokine (C-C motif) ligand 2 (CCL2), mRNA.	0.674783	11.74463036	3.061589	0.00548343	0.23390387	-2.316593781	1.596356
*	NFE2L3	7	Homo sapiens nuclear factor (erythroid-derived 2)-like 3 (NFE2L3), mRNA.	0.671562	8.499141339	5.423933	1.58E-05	0.04713394	3.116888575	1.592796
		9	Homo sapiens mRNA; cDNA DKFZp686F09166 (from clone DKFZp686F0916(	0.666338	9.651848706	3.826824	0.00085115	0.12941132	-0.600089655	1.587039
	SULF1	8	Homo sapiens sulfatase 1 (SULF1), mRNA.	0.660487	11.7915015	2.678963	0.01333009	0.31324555	-3.119995164	1.580616
	LOC648210		PREDICTED: Homo sapiens similar to Heterogeneous nuclear ribonucleopr	0.652277	11.34245949	3.640314	0.00135013	0.14725138	-1.027869433	1.571647
	GAGE12C	X	Homo sapiens G antigen 12C (GAGE12C), mRNA.	0.648975	7.872974119	1.490619	0.1495036	0.62475782	-5.180476445	1.568054
	FBXO32	8	Homo sapiens F-box protein 32 (FBXO32), transcript variant 2, mRNA.	0.627055	10.12003967	2.424605	0.02349283	0.36843859	-3.62391701	1.544409
	FBXO32	8	Homo sapiens F-box protein 32 (FBXO32), transcript variant 1, mRNA.	0.62418	8.604043051	3.291938	0.00316013	0.19451766	-1.812228829	1.541335
	GAGE12F	X	Homo sapiens G antigen 12F (GAGE12F), mRNA.	0.622278	7.834965261	1.519026	0.1422373	0.61905592	-5.141487469	1.539304
	TMEM158	3	Homo sapiens transmembrane protein 158 (TMEM158), mRNA.	0.621124	10.82233595	3.198829	0.00395362	0.20524501	-2.017686651	1.538073
	ITGB1	10	Homo sapiens integrin, beta 1 (fibronectin receptor, beta polypeptide, an	0.618841	10.95824769	4.277593	0.00027628	0.09169652	0.447318474	1.535641
	GAGE5	X	Homo sapiens G antigen 5 (GAGE5), mRNA.	0.617517	7.835190829	1.522844	0.1412833	0.61732337	-5.13620288	1.534232
	SOD2	6	Homo sapiens superoxide dismutase 2, mitochondrial (SOD2), nuclear ger	0.616111	10.1600804	2.224146	0.03612442	0.42544305	-4.000368197	1.532737
	GAGE12J	X	Homo sapiens G antigen 12J (GAGE12J), mRNA.	0.613682	7.861514996	1.506496	0.14540614	0.62126141	-5.158759731	1.530159
	DHRS3	1	Homo sapiens dehydrogenase/reductase (SDR family) member 3 (DHRS3)	0.597898	9.716530087	2.605116	0.01574831	0.33246721	-3.269068429	1.51351
	GLRX	5	Homo sapiens glutaredoxin (thioltransferase) (GLRX), mRNA.	0.591237	11.27764047	3.55599	0.00166125	0.15959217	-1.219687951	1.506538

Table 16. Table displaying the most differentially upregulated primary nasal fibroblast genes. Only NFE2L3 reaches statistical significance following multiple hypothesis testing correction (highlighted with *).

5.4.2 Quantitative real time RT-PCR replication data

Quantitative real time RT-PCR was used to replicate the microarray findings. A statistically significant (p=0.0352) greater than two fold upregulation in the NFE2L3 gene in CRSsNP fibroblast cells was seen (Figure 83). Figure 83(b) demonstrates an increase in NFE2L3 in CRSsNP epithelial cells compared to control cells, however this does not reach statistical significance (p=0.1980).

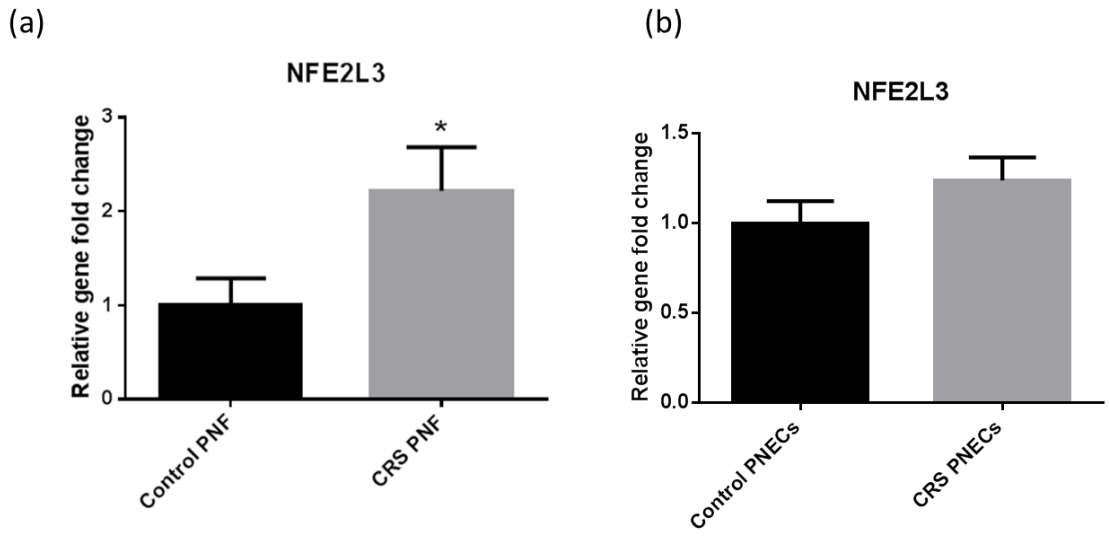

Figure 83. qRT-PCR replication of NFE2L3 gene expression between CRSsNP (n=12) and control fibroblasts (PNFs, n=12) and epithelial cells (PNECs, n=12). Relative gene expression has been normalized to healthy control cells. * = $p<0.05$.

To corroborate the mainly negative findings from the microarray, qRT-PCR replications of fifteen primer pairs from the most differentially expressed microarray probes between CRSsNP (n=12) and control fibroblasts (n=12) and epithelial cells (n=12) were analysed. Although there were trends of increased expression of IL-6, CCL2, Interferon alpha-inducible protein 27 (IFI27) and Integrin beta-1 (ITGB1/CD29) in CRSsNP PNFs, none was significantly different consistent with the microarray. Representative samples of these qRT-PCRs are shown in

Figure 84.

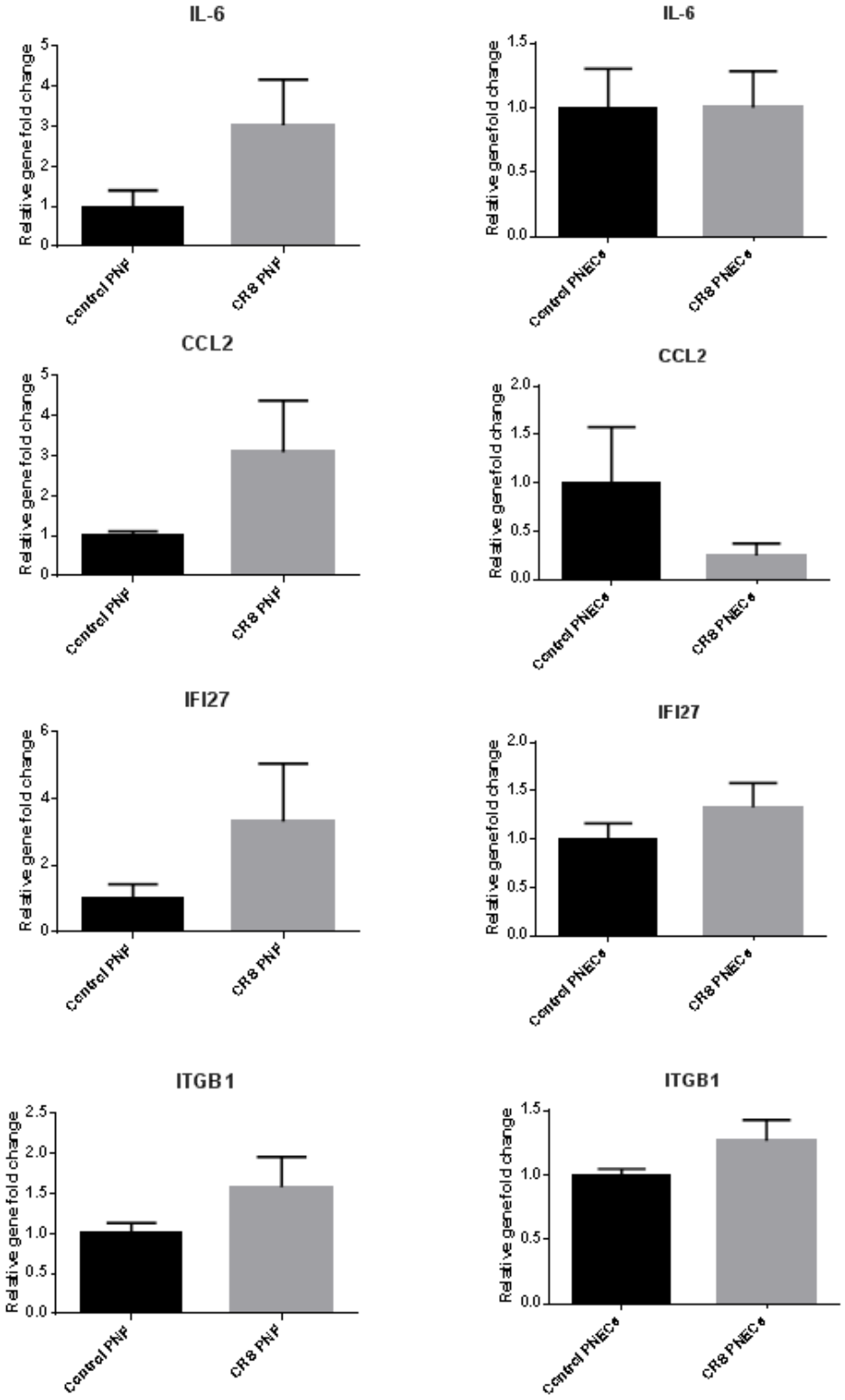

Figure 84. qRT-PCR replication of a sample of the 15 primer pairs from the most differentially expressed microarray probes between CRSsNP (n=12) and control fibroblasts (n=12) and epithelial cells (n=12). Relative gene expression has been normalized to the level of the control fibroblasts (PNFs) and epithelial cells (PNECs). In all cases no statistical

significance was identified (p>0.05). (IL-6 – interleukin 6, CCL2 - chemokine (C-C motif) ligand 2, IFI27 - Interferon alpha-inducible protein 27, ITGB1 - Integrin beta-1, also known as CD29).

5.4.3 Immunohistochemical replication data

Fluorescent immunohistochemical staining of healthy control and CRSsNP tissue sections was then used to determine if there was any difference in the amounts of the NFE2L3 transcription factor protein within the tissues. Figure 85 shows typical examples of the expression of NFE2L3 in healthy control and CRSsNP tissue sections. The greatest difference is demonstrated in the fibroblast rich lamina propria, with a smaller increase in the epithelial layer. Quantitatively, there is an increase in staining highlighted by the increased signal from CRSsNP samples in agreement with the qRT-PCR PNEC and PNF replication data (Figure 84).

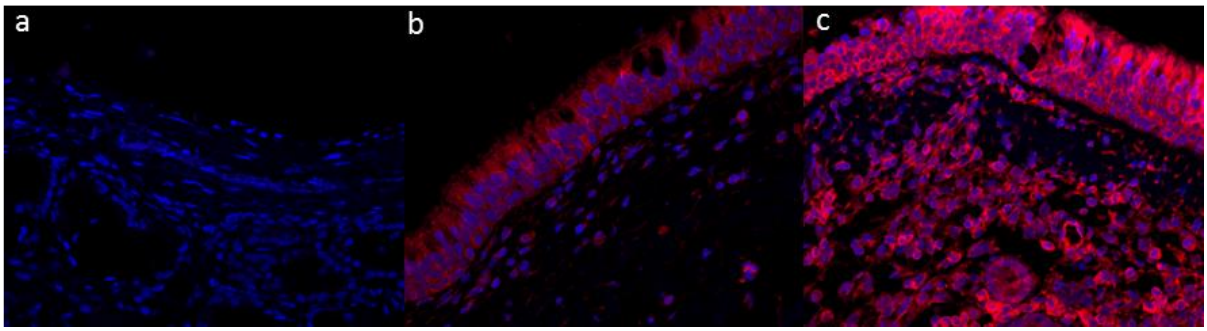

Figure 85. Fluorescent immunohistochemical staining of CRSsNP and control tissue sections. Tissues have been stained with anti NFE2L3 primary antibody and TRITC conjugated secondary antibody (red). Sections have been counterstained with DAPI nuclear staining (blue). (a) no primary control section (b) healthy control sample (c) CRS tissue sample. Magnification x40.

5.4.4 RNA sequencing data

Sequencing data was available for all of the cellular and tissue samples, however data for three of the tissue biopsy samples did not have sufficient read counts to be reliably used for differential expression testing. Two CRSsNP tissue samples and one control tissue sample therefore had to be excluded, leaving 3 CRSsNP versus 4 healthy control tissue samples and 5 CRSsNP versus 5 control epithelial and fibroblast cell samples. A principal components analysis was first performed on all the RNA sequencing data and shows samples are principally separated dependent on their tissue or cell of origin (Figure 86). The primary nasal epithelial cells are tightly clustered together and do not appear to show any segregation between CRSsNP and control samples. The most separation between CRSsNP and control samples is seen in tissue biopsies, with primary nasal fibroblast samples showing some differentiation in CRSsNP and control samples. Figure 87 presents the Euclidean

distance metrics for each of the samples in a heat map where the three distinct clusters of tissue biopsies, epithelial cells and fibroblasts can be seen. The greatest differential expression can be seen within the tissue biopsy cluster.

5.4.4.1 RNA sequencing differential gene expression analysis

Differential expression analysis was performed using the *DESeq2* package within Bioconductor as per (Love et al., 2014). When CRSsNP tissue biopsies were compared to control tissue biopsies 239 genes were found to be significantly differentially expressed following multiple hypothesis testing correction. An example of the most differentially expressed genes is presented in Table 17, with the complete list included in the appendix. Figure 88 presents the differentially expressed genes in an MA plot; where the log ratios of the gene measurements are called 'M' values represented on the vertical axis. The mean average values of the measurements are called 'A' values and are represented on the horizontal axis. Each point represents a single gene and those coloured red are significantly differentially expressed between CRSsNP and controls following multiple hypothesis testing correction.

Using the fibroblast samples, 60 genes were found to be differentially expressed between CRSsNP and control samples as shown in Figure 89. The most differentially expressed samples are listed in Table 18, with details of the complete list again presented in the appendix. Similar to the microarray data, no genes were found to be significantly differentially expressed between CRSsNP and control primary nasal epithelial cells.

5.4.4.1.1 Comparison of matched cellular and tissue samples

Differential gene expression was also used to examine how similar or representative primary epithelial and fibroblast cells were of their matched parent tissue biopsies in both CRSsNP and health. Figure 91 to Figure 94 present comparisons of CRSsNP and control tissue biopsies with matched isolated epithelial and fibroblast cells and show substantial differences in terms of differentially expressed genes (n=15,685-20,350).

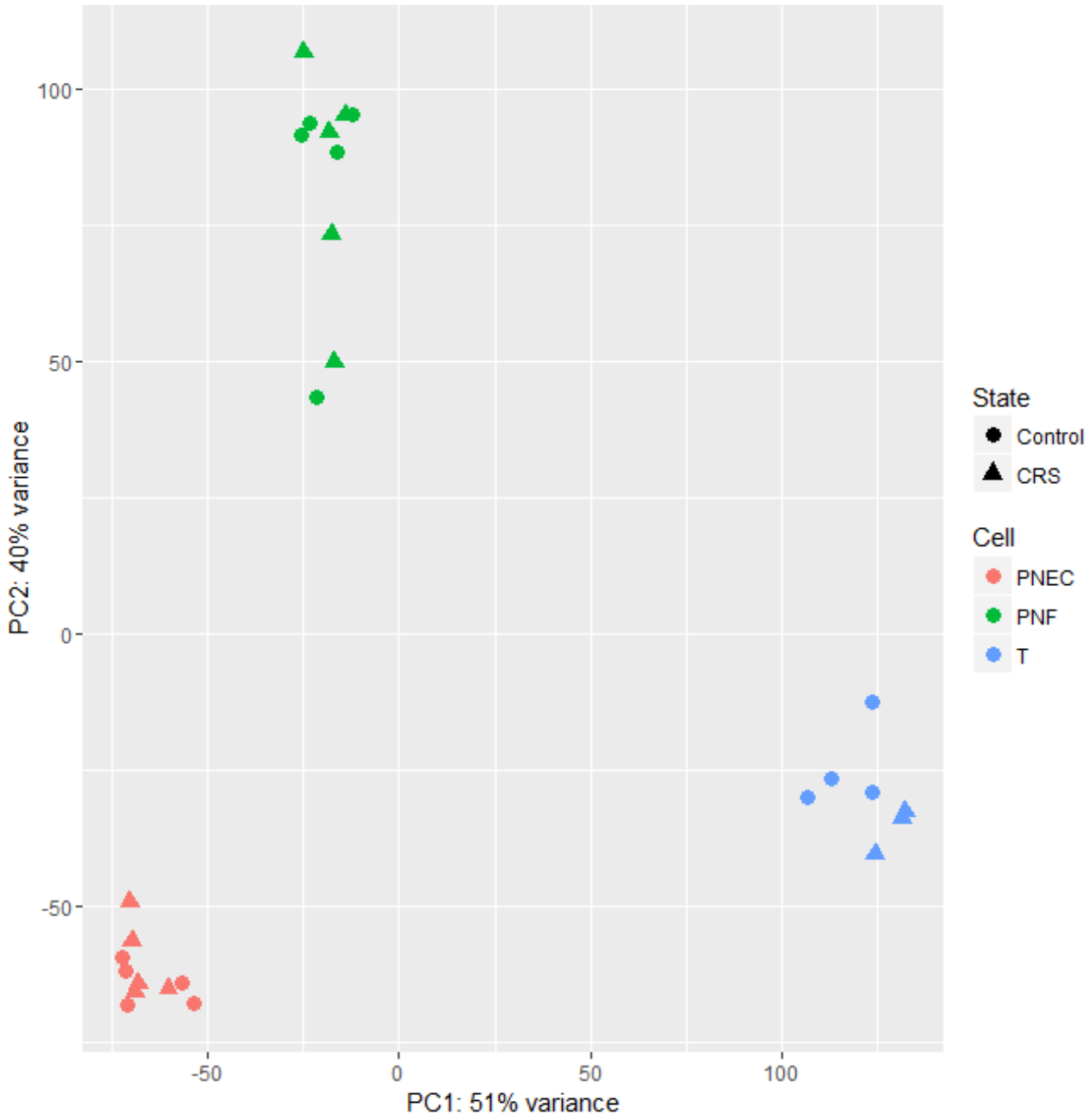

Figure 86. Principal components analysis of primary nasal epithelial cell (PNEC), primary nasal fibroblast (PNF) and tissue biopsy (T) samples from both CRSsNP and healthy control cohorts. The samples are principally separated dependent on their tissue or cell of origin, with some separation between CRSsNP and control tissue and PNF samples.

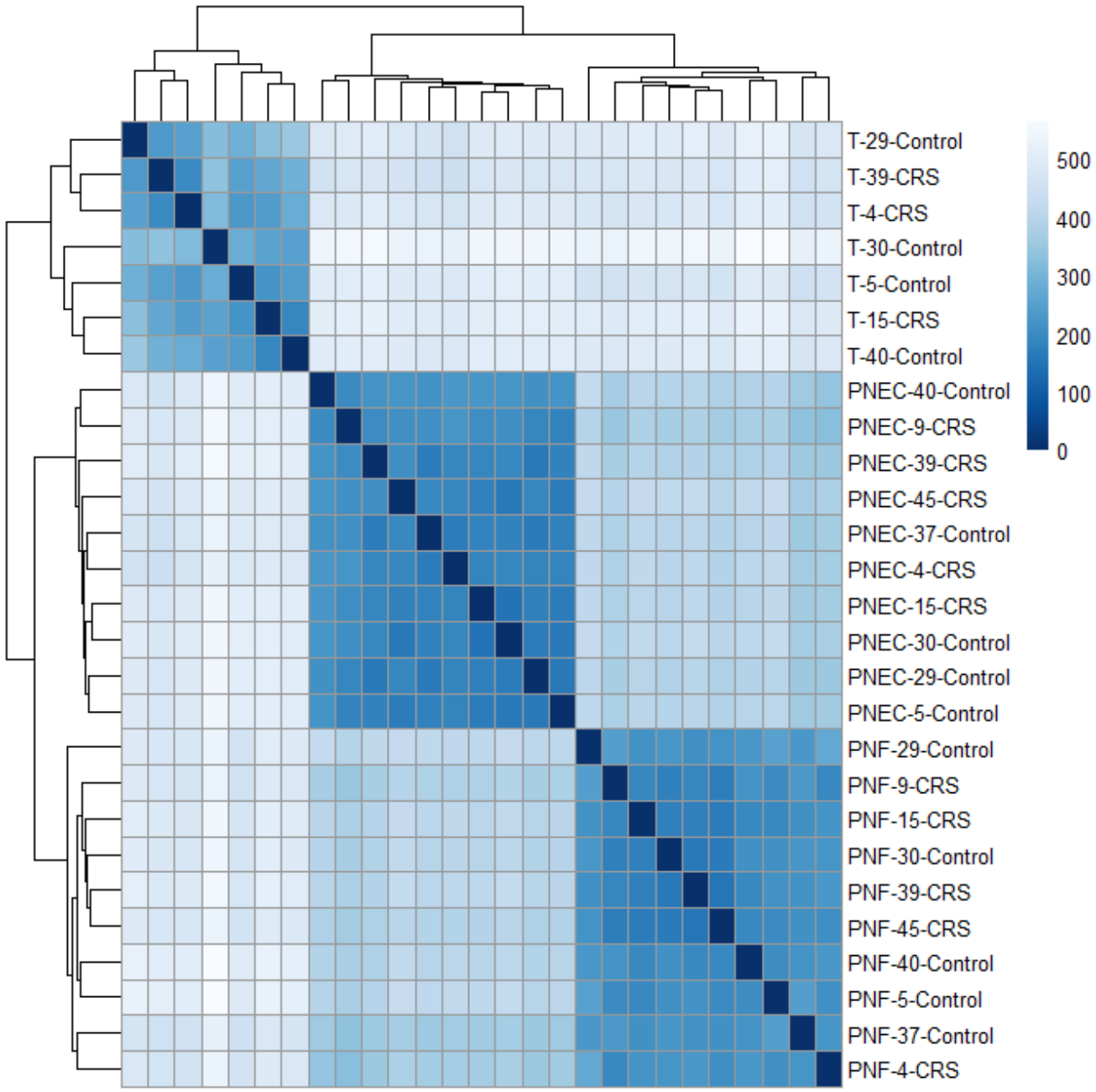

Figure 87. Heat map representation of Euclidian distance data from primary nasal epithelial cell (PNEC), primary nasal fibroblast (PNF) and tissue biopsy (T) samples from both CRSsNP and healthy control cohorts.

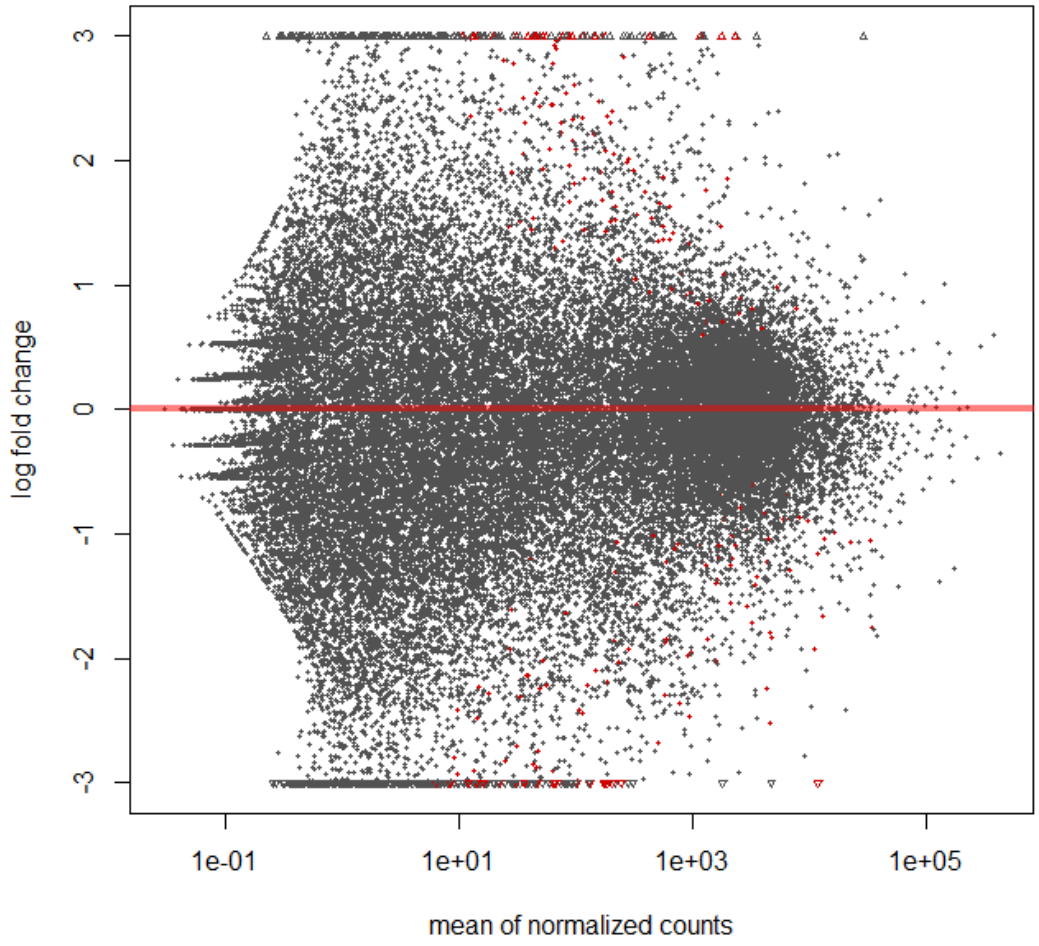

Figure 88. MA plot of RNA sequencing data comparing CRSsNP and control tissue biopsy samples. The log ratios of the two measurements are called 'M' values represented on the vertical axis. The mean average values of the measurements are called 'A' values and are represented on the horizontal axis. Each point represents a single gene and those coloured red (n=239) are significantly differentially expressed between CRSsNP and controls following multiple hypothesis testing correction.

Entrez Gene ID	Associated Gene Name	log2FoldChange	p value	Adjusted p value	Chromosome
NA	IGLV3-1	5.015314	1.79E-06	0.003837	22
931	MS4A1	4.699899	1.64E-08	0.000194	11
93432	MGAM2	4.326691	0.000574	0.078833	7
168620	BHLHA15	4.129225	4.91E-05	0.018631	7
NA	LINC00519	4.077802	0.000666	0.081632	14
643	CXCR5	4.03579	4.75E-07	0.002074	11
10563	CXCL13	4.020391	0.000385	0.063174	4

Table 17. Examples of the most significantly differentially expressed genes between CRSsNP and control tissue samples. A complete list of differentially expressed genes has been included in the appendix.

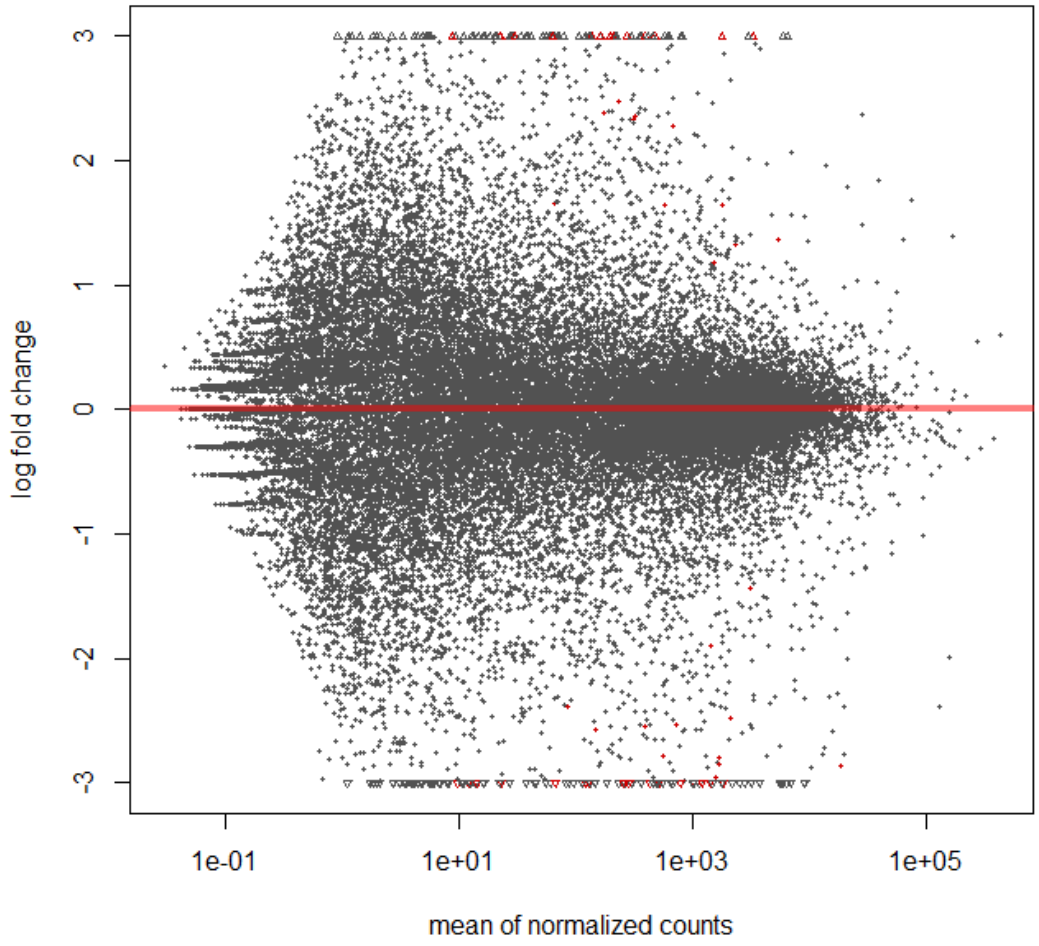

Figure 89. MA plot of RNA sequencing data comparing CRSsNP and control primary nasal fibroblast samples. Each point represents a single gene and those coloured red (n=60) are significantly differentially expressed between CRSsNP and controls following multiple hypothesis testing correction.

Entrez Gene ID	Associated Gene Name	log2FoldChange	P value	Adjusted p value	Chromosome
4316	MMP7	5.748825437	8.63E-06	0.0204119	11
1439	CSF2RB	4.585301446	1.40E-07	0.0016593	22
221476	PI16	4.464623102	6.19E-05	0.0511442	6
4360	MRC1	4.050052797	1.25E-05	0.0229034	10
56253	CRTAM	3.958263575	3.37E-05	0.0437037	11
3553	IL1B	3.946288056	8.95E-05	0.0618933	2
6289	SAA2	3.831654757	0.0001186	0.0669485	11

Table 18. Examples of the most significantly differentially expressed genes between CRSsNP and control fibroblast samples. A complete list of differentially expressed genes has been included in the appendix.

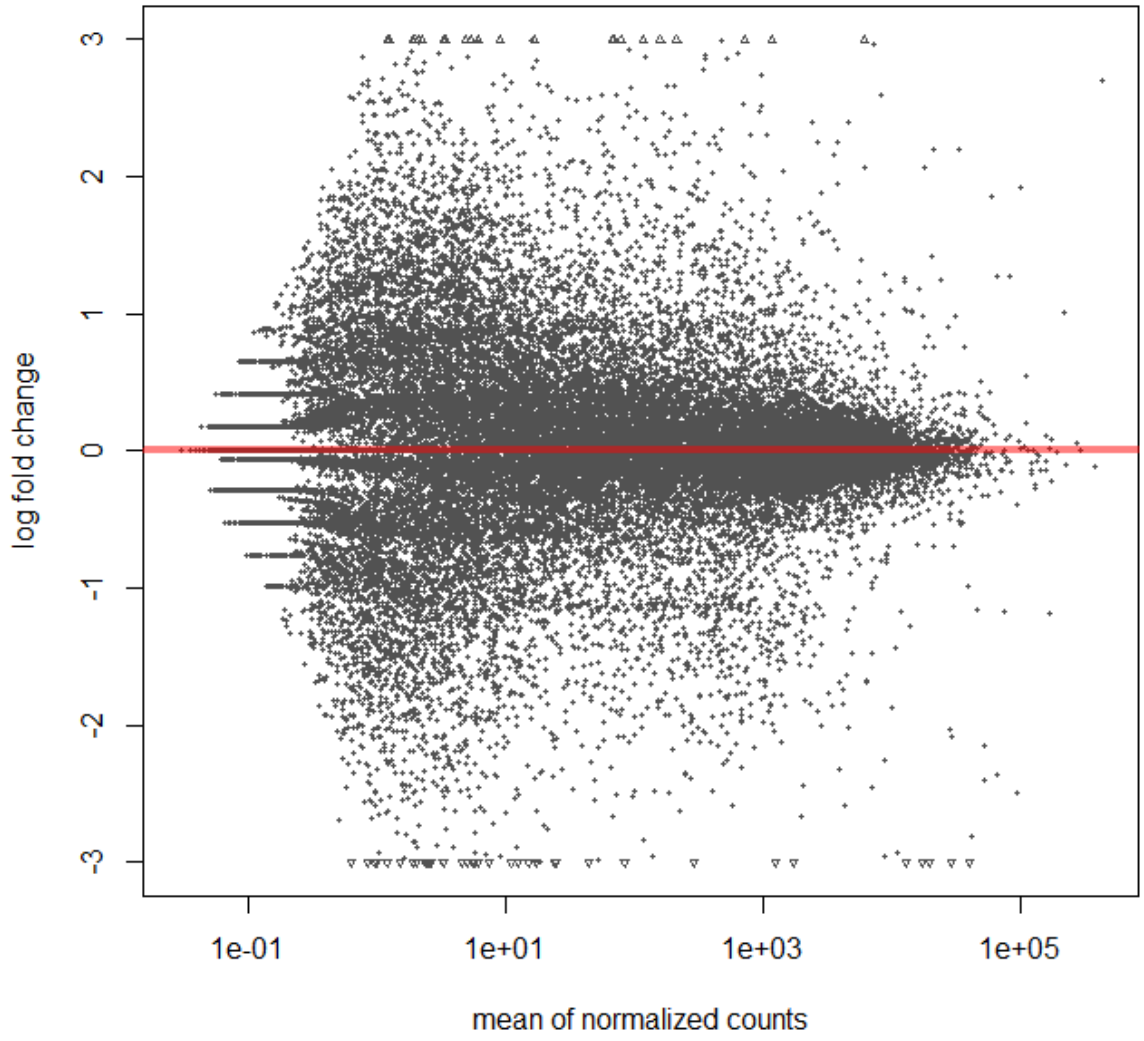

Figure 90. MA plot of RNA sequencing data comparing CRSsNP and control primary nasal epithelial cell samples. Each point on the graph represents a single gene. In this figure no points are coloured red as no significantly differentially expressed genes were identified between CRSsNP and controls following multiple hypothesis testing correction.

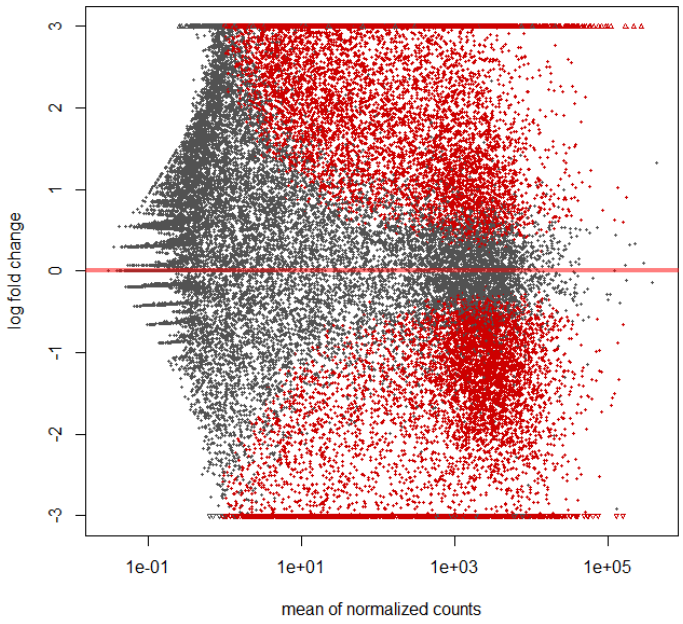

Figure 91. MA plot of RNA sequencing data comparing control tissue samples with their isolated primary nasal epithelial cell samples. Each point represents a single gene and those coloured red are significantly differentially expressed between control tissues and control epithelial cells following multiple hypothesis testing correction (n=18,223).

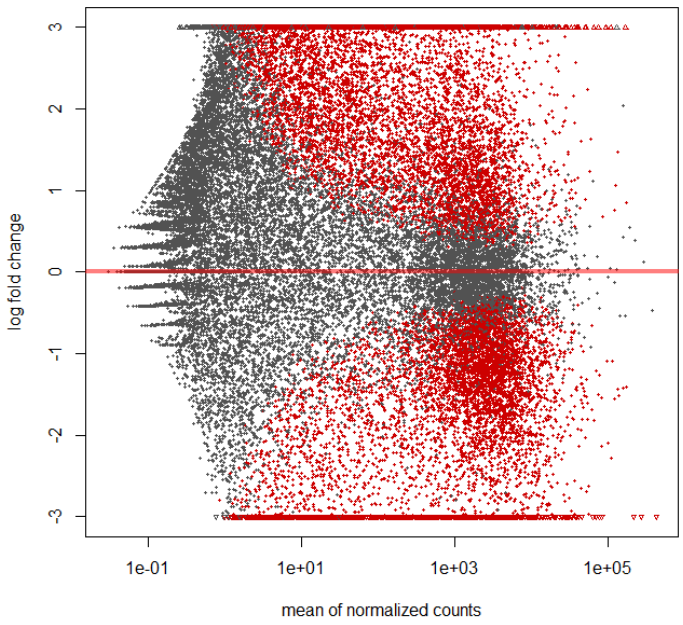

Figure 92. MA plot of RNA sequencing data comparing control tissue samples with their isolated primary nasal fibroblast samples. Each point represents a single gene and those coloured red are significantly differentially expressed between control tissues and control fibroblast cells following multiple hypothesis testing correction (n=20,350).

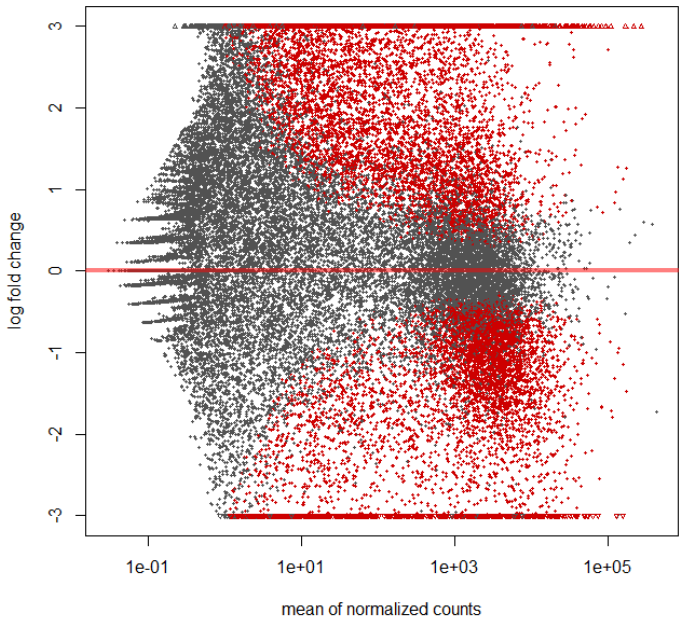

Figure 93. MA plot of RNA sequencing data comparing CRSsNP tissue samples with their isolated primary nasal epithelial cell samples. Each point represents a single gene and those coloured red are significantly differentially expressed between control tissues and control epithelial cells following multiple hypothesis testing correction (n=15,685).

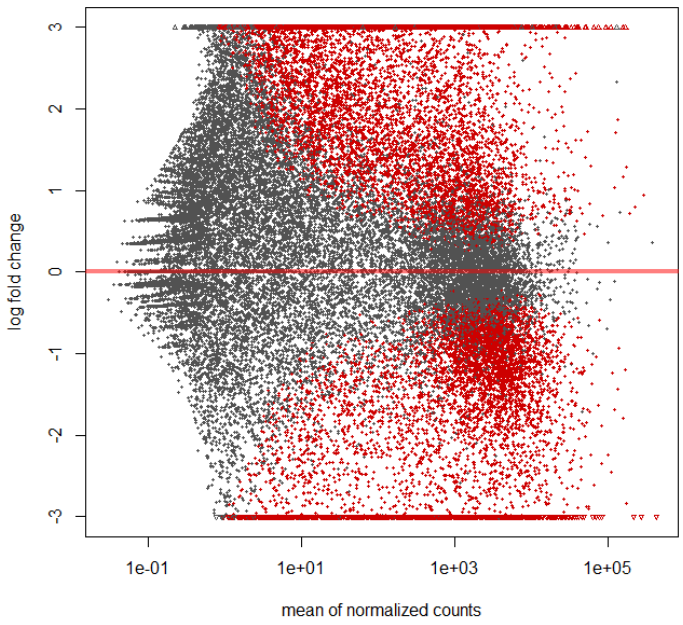

Figure 94. MA plot of RNA sequencing data comparing CRSsNP tissue samples with their isolated primary nasal fibroblast samples. Each point represents a single gene and those coloured red are significantly differentially expressed between control tissues and control epithelial cells following multiple hypothesis testing correction (n=15,952).

5.4.4.2 RNA sequencing pathway analysis

Differential gene expression data was available for tissue biopsy and primary nasal fibroblast samples allowing subsequent pathway analysis to be performed. CRSsNP tissue samples demonstrated 239 and fibroblast samples 60 differentially expressed genes compared to their respective healthy control samples. The differential expression ratios and adjusted p value from multiple hypothesis testing correction were entered into Ingenuity Pathway Analysis with standardised cut off thresholds ($p<0.05$ & fold change >2x) and returned pathway data consisting of:

1. The most significant canonical pathways
2. Associated diseases and biological functions
3. Molecular and cellular functions
4. Physiological System Development and Function

Results for tissue samples and primary nasal fibroblasts are presented in Table 19 and Table 20 respectively. Within tissue biopsy samples the majority of pathways map to inflammatory and immune system functions, whereas isolated fibroblast cell samples appear related to oncological processes.

The top five most significant pathways are presented in Table 19 and Table 20. Networks demonstrating the inter-relationships of the canonical pathways in tissue biopsy and fibroblast samples are presented in Figure 95 and Figure 96). The representative figure for tissue biopsies (Figure 95) shows one main network of 19 inter-related inflammatory and immune pathways and one smaller network of 3 amino acid degradation pathways. The comparative figure for primary nasal fibroblasts consists of three smaller pathways (Figure 96), the largest of which contains 11 inter-related pathways with the most significant results mapped to bladder and ovarian cancer signalling. An additional network of 8 related pathways is identified principally for polysaccharide biosynthesis and a smaller network of 4 pathways regarding antigen presentation and macrophage migration inhibitory factor (MIF) immune regulation roles.

Top Canonical Pathways
Altered T Cell and B Cell Signalling in Rheumatoid Arthritis
Systemic Lupus Erythematosus Signalling
T Cell Receptor Signalling
Tumoricidal Function of Hepatic Natural Killer Cells
Communication between Innate and Adaptive Immune Cells

Top Diseases and Biological Functions
Inflammatory Response
Cancer
Haematological Disease
Immunological Disease
Organismal Injury and Abnormalities

Molecular and Cellular Functions
Cellular Development
Cellular Growth and Proliferation
Cell-To-Cell Signalling and Interaction
Cell Death and Survival
Cell Morphology

Physiological System Development and Function
Haematological System Development and Function
Lymphoid Tissue Structure and Development
Immune Cell Trafficking
Humoral Immune Response
Tissue Morphology

Table 19. Summary pathway analysis tables of differentially expressed CRSsNP tissue samples based on Ingenuity Pathway Analysis. The top 5 canonical pathways, associated diseases and biological functions, molecular functions and physiological system functions are presented.

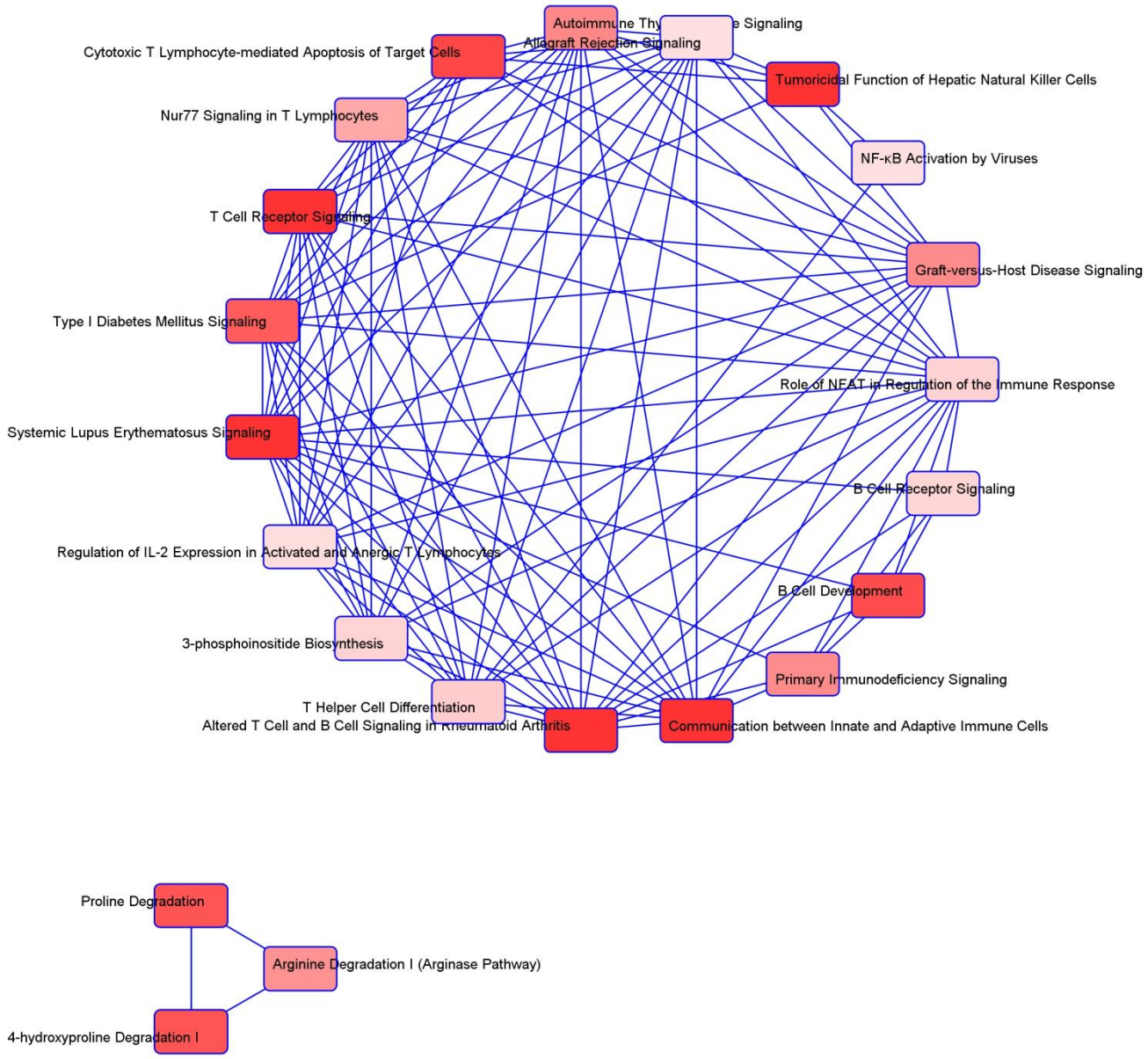

Figure 95. Top networks identified with Ingenuity pathway analysis demonstrating inter-related canonical pathways from CRSsNP tissue samples versus healthy controls. The strongest red colour is associated with the most significantly associated pathways.

Top Canonical Pathways
Bladder Cancer Signalling
Ovarian Cancer Signalling
Antigen Presentation
Axonal Guidance Signalling
HIF1α Signalling

Top Diseases and Biological Functions
Cancer
Organismal Injury and Abnormalities
Reproductive System Disease
Endocrine System Disorders
Gastrointestinal Disease

Molecular and Cellular Functions
Cellular Function and Maintenance
Cellular Movement
Cellular Growth and Proliferation
Cellular Development
Cell Morphology

Physiological System Development and Function
Haematological System Development and Function
Behaviour
Tissue Development
Reproductive System Development and Function
Embryonic Development

Table 20. Summary pathway analysis tables of differentially expressed CRSsNP primary nasal fibroblast samples based on Ingenuity Pathway Analysis. The top 5 canonical pathways, associated diseases and biological functions, molecular functions and physiological system functions are presented.

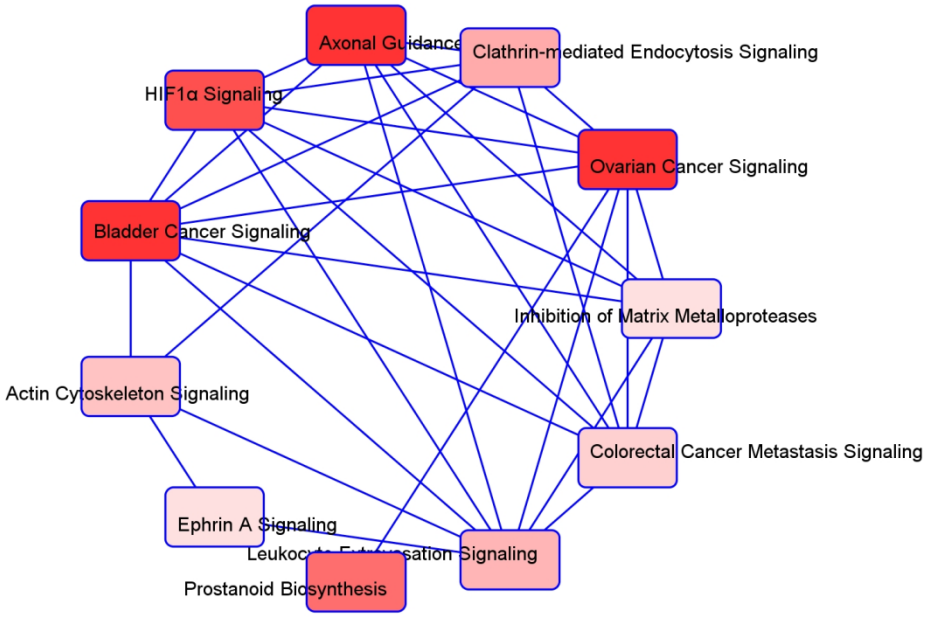

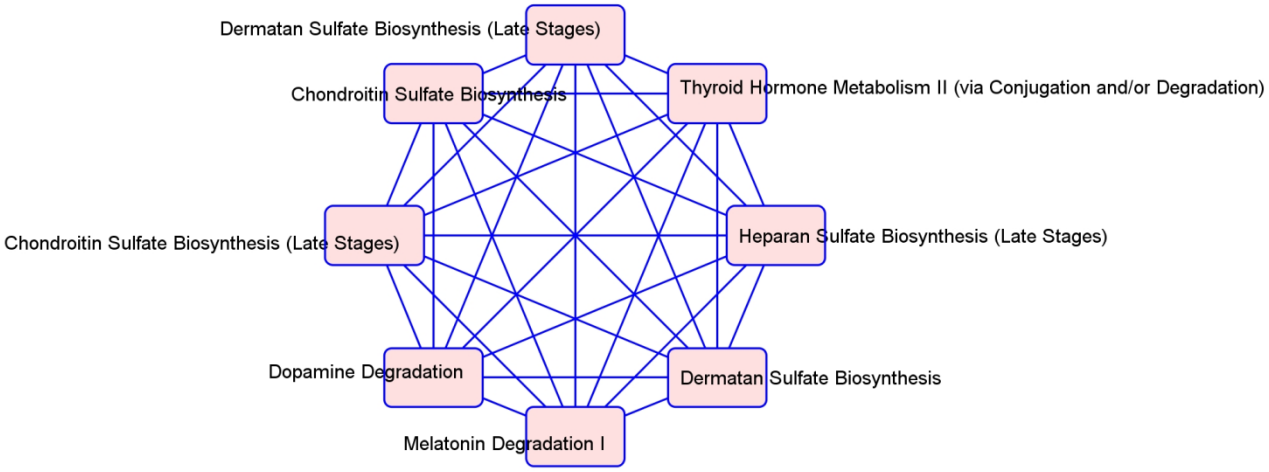

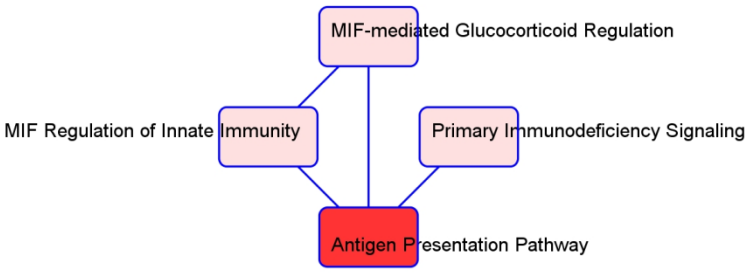

Figure 96. Top networks identified with Ingenuity pathway analysis demonstrating inter-related canonical pathways from CRSsNP primary nasal fibroblast samples versus healthy controls. The strongest red colour is associated with the most significantly associated pathways.

5.5 Discussion

5.5.1 Microarray of epithelial and fibroblast cells

Using the cohorts of carefully phenotyped CRSsNP patients and healthy control isolated cells from chapter 3, a genome wide microarray has been performed to look for differentially expressed CRSsNP genes as candidates for CRSsNP mechanistic studies. Bioinformatics analysis of the microarray data has shown that the transcription factor NFE2L3 was significantly upregulated in component fibroblast cells from CRSsNP patients compared with healthy controls. Somewhat surprisingly there was no significant difference in gene expression between CRSsNP & control epithelial cells (Figure 76 & Figure 77). Quantitative real time RT-PCR replication with a series of candidate genes has replicated and confirmed the findings of the microarray analysis (Figure 83 - Figure 85). Immunohistochemical staining of tissue biopsies for NFE2L3 protein further corroborated the micro array and RT-PCR findings.

Nuclear factor erythroid-derived 2-like 3 (NFE2L3) belongs to the evolutionarily conserved Cap'n'Collar (CNC) protein subgroup of basic region-leucine transcription factors (Sykiotis and Bohmann, 2010). It contains a 43 amino acid CNC domain specific to its DNA binding activity (Toki et al., 1997). Cap'n'Collar transcription factors also contain a basic region leucine zipper motif (bZIP),enhancing DNA binding activity, and a leucine zipper motif for dimerization (Landschulz et al., 1988). Cap'n'Collar transcription factors are obligate heterodimers functionally by forming complexes with jun proteins (Venugopal and Jaiswal, 1998) and small musculoaponeurotic fibrosarcoma (Maf) proteins (Kobayashi et al., 1999, Itoh et al., 1995). NFE2L3 expression has been investigated in a range of tissues, with the highest levels found in placental chorionic villi in the second and third trimester. Expression is also present in heart, lung, brain, kidney, pancreas, thymus, colon, spleen tissues and leukocytes (Kobayashi et al., 1999). Biochemical, fractionation and immunofluorescence studies have identified three differentially migrating forms of NFE2L3; a slow A form found in the endoplasmic reticulum, an intermediate B form mainly found in the cytoplasm and fast C form mainly associated in the nucleus (Nouhi et al., 2007). A hypothetical model has been proposed for the differentially migrating forms of NFE2L3 by Chevillard & Blank (2011) and is shown in Figure 97. In summary, transcription of the NFE2L3 gene is dependent on a stimulus, such as tissue necrosis factor (TNF). NFE2L3 mRNA in the nucleus is then translated into the B form of NFE2L3 in the cytosol. The B form can then translocate to the

endoplasmic reticulum and following N-glycosylation becomes the A form of NFE2L3. The A and B forms are converted into the active C form following cleavage at the N-terminal end which dimerise with Maf proteins to activate transcription at antioxidant response, stress response element and electrophile response element DNA binding sites. The A, B and C forms are then proposed to be degraded through the conventional ubiquitin-proteasome pathway.

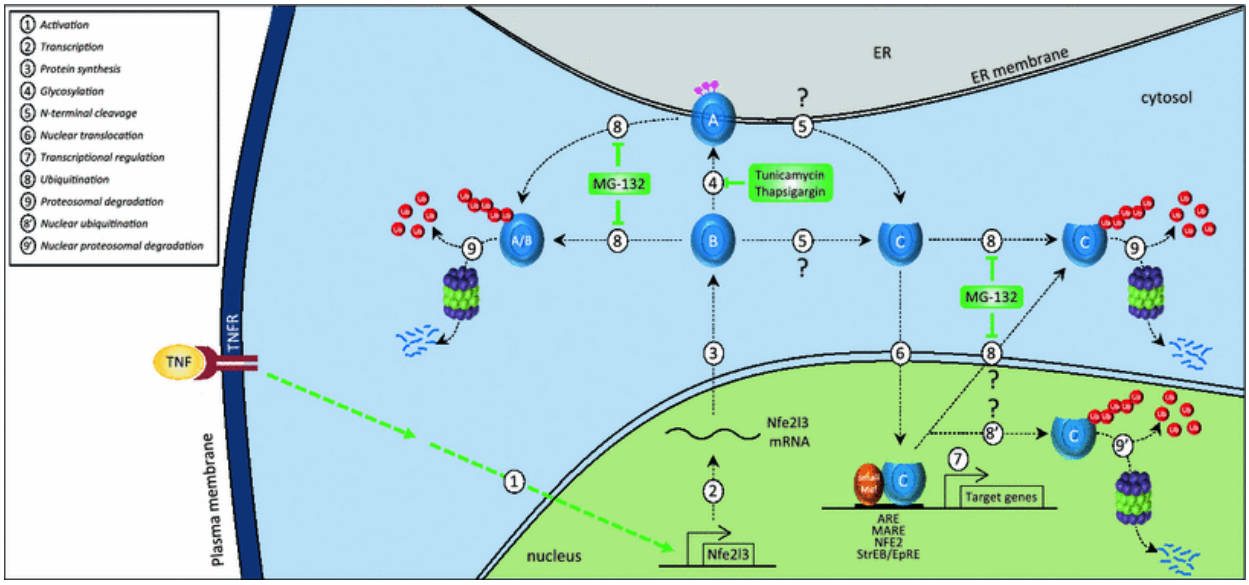

Figure 97. Hypothetical model of NFE2L3 regulation. Adapted from (Chevillard and Blank, 2011).

Attempts have been made to study the physiological role of NFE2L3 in mouse knockout models. Results from two independently generated NFE2L3 knockout models have produced mice that have been shown to grow normally, with no difference in development, blood chemistry, or haematological parameters (Derjuga et al., 2004, Kobayashi et al., 2004). The knock out mice are, however, more susceptible to inflammation (Witschi et al., 1989, Chevillard et al., 2010) and carcinogenesis (Chevillard et al., 2011, Willenbrock et al., 2006, Rhee et al., 2008). NFE2L3 knockout mice are more susceptible to tobacco smoke carcinogen induced lymphomagenesis (Chevillard et al., 2011), from which the authors suggest a potential role of NFE2L3 in T-cell regulation.

There is established evidence for a role of NFE2L3 in inflammation both *in vitro* and *in vivo* and via human genome wide association studies. NFE2L3 is a member of a family of genes

that act as negative regulators of a collection of defensive genes in response to oxidative stress (Sankaranarayanan and Jaiswal, 2004, Jaiswal, 2004, Jaiswal, 2000). Both NFE2L3 protein and mRNA are upregulated in tissue culture by tumour necrosis factor and interferon-γ (Chenais et al., 2005, Kitaya et al., 2007), which are key Th1 cytokines in the pathophysiology of CRSsNP (Van Crombruggen et al., 2011). NFE2L3 has been shown to be an important factor in murine models of oxidative lung injury (Chevillard et al., 2010, Paola and Cuzzocrea, 2007). Genome wide association studies have also identified NFE2L3 being associated with the chronic inflammatory gynaecological condition endometriosis (Painter et al., 2011), obesity and diabetes (Heid et al., 2010). Given the roles discussed it is therefore plausible that the transcription factor NFE2L3 may have a part to play in the complex chronic inflammation seen within the sinonasal cavity, though for this to be determined further work is required.

In spite of the finding of upregulated NFE2L3 within sinonasal fibroblasts it is perhaps surprising that more differentially expressed genes were not identified between CRSsNP patients and healthy controls from primary cultures of their sinonasal epithelial and fibroblast cells. Although the multiple hypothesis testing correction is strict, over 47,000 different human probes were successfully screened for each sample. The answer to this may lie in the patient selection, however as illustrated by the clinical, radiological and histological data in chapter 3 all patients were carefully phenotyped for CRSsNP. The lack of differentially expressed genes may also be related to the fact that the cells studied were in fact quiescent cells grown in sterile tissue culture conditions, removed from the body and the complex environmental stimuli of the sinonasal cavity. All cells were grown in tissue culture conditions, a sterile environment together with growth factors and antibiotics, to aid the successful proliferation of the primary human sinonasal cell lines established. Both cell types used early passage cells of either P0 for epithelial cells and P1 for fibroblast cells rather than those that have undergone multiple cell divisions and trypsinisations in culture (Hughes et al., 2007, Almeida et al., 2016). Within the cell culture, however, the presence of growth factors and antibiotics may have two fold effects. Firstly, the sterile media with supplemental antibiotics removes the normal microenvironment of the sinonasal cavity, be it planktonic bacteria (Lee and Lane, 2011), viral (Hox et al., 2015) or biofilm (Foreman et al., 2012, Aurora et al., 2013, Boase et al., 2013a) microbial stimulation. Secondly the growth medium supplements to promote successful proliferation of primary cells in culture may provide supra-physiological stimulus for growth and cellular activity that over rides any

difference in gene expression between the healthy control and CRSsNP cells. It is also worth commenting that a lack of major differences at the gene and RNA level does not always equate to a lack of difference at the functional level of the gene product i.e. the proteins translated from the individual genes and RNAs.

Microarray technology has been used only relatively recently to study CRS, popularised in part following the suggestions of van Drunen et al. (2008). The majority of published CRS microarray data has been derived from CRSwNP patient tissue biopsy samples. One of the earliest published reports of microarrays in CRS used tissue biopsy samples from two patients with non-eosinophilic CRSwNP and two healthy controls (Payne et al., 2008). From their small sample, 120 differentially expressed genes were identified using the same parameters as my microarray analysis with an absolute fold change cut off >1.5 and $p<0.05$, though no mention of multiple hypothesis testing correction methodology was made. Of the 120 differentially expressed genes, 58 were up-regulated and 62 down-regulated, with the largest clusters of genes upregulated concerned with Gene Ontology biological process categories of cell communication, and cell growth/maintenance. Payne et al. also identified that a number of genes traditionally associated with CRS showed trends of differential expression, but did not reach statistical significance. The same authors also identified upregulation of genes associated with fibrosis and fibroblast migration such as Tenascin-C, a pro-inflammatory extracellular matrix glycoprotein, and stem cell factor. The main limitation of this early report is the small sample size of 2 per group, which is important in a disease with the heterogeneity of CRS. The small sample size was probably in part due to financial constraints since the cost of microarrays was significantly higher at the time Payne's initial exploratory study was carried out.

Subsequently Frączek et al. (2013) published a microarray analysis of 15 cases of CRSwNP and 8 control samples. The microarray technology used in this report was a focused array to investigate a panel of 14,500 genes with 580 genes related to the NF-κB transcription factor. NF-κB (nuclear factor kappa-light-chain-enhancer of activated B cells) is a family of transcription factors involved in regulating many normal physiological processes including immune and inflammatory responses, growth and development. Differential expression analysis between the CRSwNP and control groups identified 25 genes with >2 fold upregulation and 19 genes with decreased expression, although again no mention was made regarding the methodology of multiple hypothesis testing correction. In agreement with

Payne et al., Tenascin-C was found to be upregulated in CRSwNP samples - along with a list of genes without any clear functional relationship, with the exception of 4 chemokines. No functional analysis of the differentially regulated genes was performed such as Gene Ontology biological processes (GO BP), KEGG pathway (Kyoto Encyclopaedia of Genes and Genomes) or wikipathways to explain or hypothesise the consequences of altered expression.

Linke et al. (2013) investigated inferior turbinate and nasal polyp tissue samples from 6 CRSwNP patients using Agilent human genome 44K DNA microarrays to analyse over 43,000 human genes. The DNA microarray was used with the principal aim of evaluating quantitative differences in STAT3 (signal transducer and activator of transcription 3) mRNA between the nasal polyps and inferior turbinates as internal controls. STAT3 was chosen as a phosphokinase with key roles in cell cycle signalling regulation and is responsive to numerous cytokines and ligands. No comparison with external healthy control tissue was made, however. Microarray data was appropriately analysed using the Rosetta Revolver gene differential expression analysis (Weng et al., 2006). The authors reported no quantitative difference in amounts of STAT3 mRNA between turbinate and polyp from matched participants, with a mean fold change of 0.99 (SD 0.23). Unfortunately no mention was made regarding the remainder of the human genome data measured by the microarrays.

In another early CRS microarray study, Orlandi et al (2007) analysed nasal polyp tissue biopsy samples from four patients with allergic fungal sinusitis (defined by - nasal polyposis, eosinophilic mucin, histological or culture based detection of fungus and immunological evidence of type I hypersensitivity) and three patients with eosinophilic mucin rhinosinusitis (defined by - nasal polyposis, eosinophilic mucin and absence of fungus). Microarray analysis was performed using glass based arrays with 6912 specific gene probes. The nasal polyp tissue samples were compared to universal human reference RNA, a commercial product consisting of a mix of 14 cell lines from different human tissues – rather than healthy control nasal tissue. From data within chapter 3 it has been shown that there is only one commercially available nasal cell line which has limited resemblance to primary human cells (Ball et al., 2015), so perhaps the choice of universal reference RNA as a control may not be appropriate.

More recently Liu et al (2015) compared nasal polyp tissue biopsies from 30 CRSwNP patients and tissue biopsies from 16 healthy control patients having a septoplasty procedure due to a bent nasal septum (partition) between the two nostrils. The authors used a SuperArray Bioscience extracellular matrix and adhesion molecule microarray with differential expression levels between polyp tissue and control tissue cut off set at two fold change and $p<0.05$. Following careful reading of the supplementary online technical details however, only tissue biopsies from 2 CRSwNP patients and 2 controls were subject to microarray analysis. A total of 27 differentially expressed genes were identified, with 19 being upregulated and 8 downregulated. Their most significant finding reported was the upregulation of osteopontin, known also as T lymphocyte activation 1. Osteopontin was discovered in bone as a matrix protein (Cantor and Shinohara, 2009) and has also been identified in most immune cells (Shinohara et al., 2006) with numerous roles in the pathogenesis of inflammatory, immune and fibrotic processes. Osteopontin is involved in both Th1 and Th2 pro inflammatory mechanisms (Cho et al., 2009, Konno et al., 2011) and as a result monoclonal blocking antibodies have been developed in an attempt pharmacologically to modify pathological inflammation. The safety, pharmacokinetic and pharmacodynamic data of osteopontin inhibitors was first shown in a cohort of patients with rheumatoid arthritis (Boumans et al., 2012), though it failed to demonstrate significant clinical improvements in arthritis patients. Osteopontin inhibitors have subsequently received attention in the respiratory literature (Gela et al., 2016) and may represent possible future candidates for therapeutic trials in sinonasal and lower respiratory tract disease.

The published literature harnessing microarray experiments in CRS has thus far typically used RNA generated from nasal polyp tissue biopsy samples. The results presented in this chapter are to the best of my knowledge the first study to utilise microarrays to compare the component nasal epithelial and fibroblast cells in CRSsNP and health. The aim of investigating the isolated patient derived epithelial and fibroblast cells was two-fold; firstly to separate the epithelial and fibroblast cells from the recruited immune cells in CRSsNP and secondly to identify clusters of differentially expressed genes that could be used in subsequent future cellular CRS mechanistic studies. Reflecting on the results of the microarray data I have generated it appears that primary patient derived epithelial and fibroblast CRSsNP cells have not shown major differences when compared to healthy controls. This was an unexpected result and prompted a more in depth next generation RNA

sequencing experiment to compare the whole transcriptome between matched tissue, epithelial and fibroblast cells from both CRSsNP and healthy controls.

5.5.2 RNA sequencing of matched biopsy and cellular samples

To investigate the low number of differentially expressed primary nasal epithelial and fibroblast gene targets identified by microarray, a next generation RNA sequencing transcriptome analysis of the parent tissue biopsies and their matched epithelial and fibroblast cells was performed. RNA sequencing, unlike microarrays is not limited by the number of pre-determined probes on an array but instead reads the sequence of RNA present in the samples and maps this to a reference genome. As a result the number of genes that can be measured is significantly greater and similarly the dynamic range of expression levels for which genes can be measured is much larger than microarrays. Moreover, RNA sequencing has been proven to be highly accurate and reproducible compared with quantitative RT-PCR (Nagalakshmi et al., 2008, Mortazavi et al., 2008, Cloonan et al., 2008). Such an analysis generates vast amounts of data requiring extensive analysis which will extend beyond the completion of this thesis. No studies using RNA sequencing have thus far been performed in the published sinonasal literature. The primary RNA sequencing analysis has shown some interesting observations between CRSsNP and control samples. Firstly, in agreement with the microarray and qRT-PCR analysis, no significantly differentially expressed genes have been identified between CRSsNP and control primary nasal epithelial cells. Consistent findings across two different transcriptomics platforms suggest that there is no difference to be found in the transcriptome of my CRSsNP and control primary nasal epithelial cells. In comparison, 239 genes have been found to be significantly differentially expressed between CRSsNP and control tissue biopsy samples (Figure 88). Such variation between epithelial cells and their matched parent tissue biopsies suggests that a difference between CRSsNP and health is not reflected in the primary cultures of epithelial cells. To investigate further how closely patient derived primary nasal cells match their parent tissues a direct comparison was made between primary nasal epithelial cells and their matched parent tissue biopsies. The initial MA plot analyses show extensive numbers (n=15,685-20,350) of significantly differentially expressed genes in both CRSsNP and control tissues with their respective primary epithelial cells (Figure 91 and Figure 93). The combination of findings presented from the microarray and RNA sequencing data in this chapter suggests that in this cohort of patients, isolated primary nasal epithelial cells are not representative of their matched tissue biopsies for studying CRSsNP. Efforts

were made to carefully phenotype and culture primary nasal epithelial cells, for example using only early cultures at P0 without trypsinisations or splitting of cells. However, it appears that in spite of this phenotyping the pathological features of CRSsNP visible in the histological sections in chapter 3 are not reflected in differences in gene expression of isolated epithelial cells. Epithelial cells were grown in submerged culture on laboratory plastic ware with epithelial growth supplements as is standard in laboratory tissue culture. The combination of these factors may well underlie such a loss of differentiation between CRSsNP and health.

In addition to looking at differential expression of genes between CRSsNP and healthy controls it is possible to use the extensive established data available on biological functions to perform functional pathway analysis. Although a list of up or down regulated genes provides very detailed information of molecular changes in the transcriptome it can be difficult to make functional sense of all the RNA changes. Furthermore, most genes typically have many different context-dependent functions and act very differently in isolation compared to within biological pathways and organisms (Werner, 2008). As a result powerful bioinformatics methods have been developed to resolve lists of differentially expressed genes into functionally relevant information. A schematic illustration of such methods is presented in Figure 98.

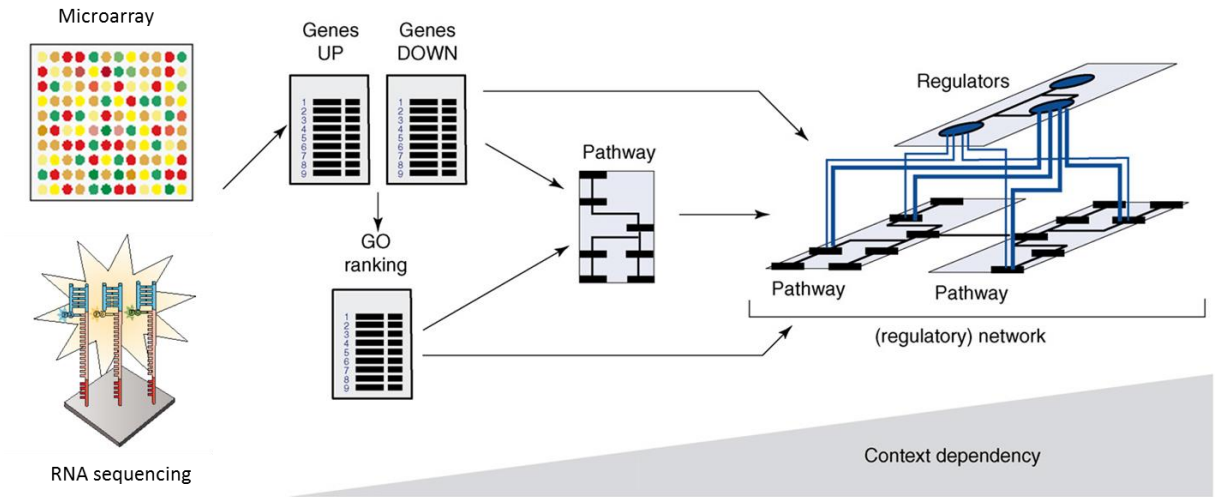

Figure 98. Schematic of how differential expression data from RNA sequencing and microarrays can be used to compile pathways and regulatory networks based on known biological information. Image adapted from (Werner, 2008) and (Goodwin et al., 2016).

For the RNA sequencing presented in this chapter I have used the software package Ingenuity Pathway Analysis as per Kramer et al. (2014). Ingenuity pathway analysis is a web based software package for analysing RNA sequencing data that utilises the vast amount of publically available biological knowledge on genes, proteins, diseases and drugs. In addition to this publically available information such as the Gene Ontology (GO) and KEGG (Kyoto Encyclopaedia of Genes and Genomes) databases, Ingenuity pathway analysis is also continuously updated from published literature by a dedicated team of research scientists. One of the drawbacks of using an alternate database such as KEGG or GOstats is related to how current the biological information is. KEGG became a subscription predominant service from 2011 following a change in its funding structure. As a result the last free release data which supplies many packages including GO stats is approximately five years out of date. Ingenuity pathway analysis has the additional advantage that it is not a command line code based package, but instead uses a windows interface. This makes it much more user friendly, for example than the code written to analyse the microarray data (see appendix).

The use of Ingenuity pathway analysis on my sequencing data has identified a series of functional pathways and networks for both CRSsNP tissue biopsies and primary nasal fibroblasts. Within tissue biopsies the most significant associations are seen in inflammatory and immune functions (Table 19 and Figure 95), similar to the multiplex MSD electrochemiluminescence disease micro-environment findings from chapter 4 and immunohistochemical images in chapter 3. Primary nasal fibroblast samples also generated functional pathways based on their differential expression, although the pathways identified differed significantly from those generated for tissue biopsy samples (Table 20 and Figure 96), with the top two canonical pathways identified as bladder and ovarian cancer signalling. Such a difference in the pathways observed, together with the extensive numbers of significantly differentially expressed genes between tissue biopsy samples and their matched fibroblasts implies that my cohort of primary nasal fibroblasts may not be the optimum model with which to study CRSsNP.

5.6 Conclusion

In conclusion, within this chapter two separate transcriptomics approaches have been utilised in microarrays and RNA sequencing to analyse CRSsNP samples.

- Neither microarrays nor RNA sequencing showed any significant differences between CRSsNP and healthy control primary nasal epithelial cells, therefore it is recommended they should not be utilised in further work to model CRSsNP.
- Primary nasal fibroblasts show some significant differences between CRSsNP and healthy controls although these changes do not appear reflective of those seen in their matched tissue biopsies and their further use to model CRSsNP in their current state is at least questionable.
- Tissue biopsies, when compared with RNA sequencing show the most significant changes between CRSsNP and health. Furthermore, functional pathway analysis shows alteration of predominantly immune and inflammatory pathways consistent with the histological data and disease microenvironment data obtained within this thesis. My further work should and will be directed principally by these tissue biopsy samples and will utilise the additional potential of the RNA sequencing data to obtain the maximal information from this novel resource for CRSsNP pathophysiology.

6 Thesis summary

A detailed discussion of the results presented in this thesis has so far been included within chapters 3, 4 and 5. In this section I shall provide a brief summary of the major findings and conclusions from my thesis and outline my plans for future work.

Chronic rhinosinusitis (CRS) continues to pose a therapeutic challenge for patients and clinicians alike. Our current therapeutic options mean that many patients require surgery when pharmacological treatment fails; however, the relatively high post-surgical recurrence rate further underlines the inadequacy of medical treatments - since CRS remains principally a medical rather than a surgical disease. A more in depth understanding of CRS pathophysiology will ultimately lead to better treatments. In an effort to address this knowledge gap I prospectively recruited a carefully phenotyped cohort of CRS patients without nasal polyps and healthy control participants with their associated clinical symptom scores. My cohorts were subject to a detailed histological assessment of sinonasal tissue biopsy sections using tinctorial stains, immunohistochemistry and electron microscopy to investigate their disease status. I analysed the microbiological environment of the participants' sinonasal cavities with conventional microbiological culture and a microbiome approach. Additionally, I developed a novel non-invasive measure of the sinonasal inflammatory microenvironment. By using a standardised 210mm^2 piece of clinical grade hydrophilic filter paper strip, a mucosal lining fluid sample, has helped obtain information on the inflammatory environment of the nasal mucosa. Placed alongside the sinonasal mucosa it has been used to collect mucosal lining fluid i.e. mucus in continuity with the epithelial mucosa. Characterising this fluid using a panel of human proteins and cytokines, a group of 13 mediators has been shown to discriminate between control and CRS without nasal polyp participants. Such an assay would be valuable in the clinic, improving on our current symptom and endoscopic based assessment. This mucosal lining fluid strip has the potential to give a measure of the 'inflammatory score' of CRS, both as a diagnostic aid and as a means of monitoring disease activity. Additionally, further mucosal lining strip analysis may lead to the development of biomarkers to help stratify patient's therapeutic interventions.

My mucosal lining fluid assay is very much in its infancy, however, and I have identified in this thesis a number of important limitations when it is applied in a heterogeneous condition such as CRS. For this reason, much of the previous work has focussed on CRS with nasal polyposis – but my intention was to tackle the more diverse and even less well understood

non polypoid chronic sinusitis. Only once I have had the opportunity to control for key demographic variables (notably age, gender, cigarette smoking) in both normal and diseased individuals will I be in a position to attempt to stratify different inflammatory subtypes of CRS without nasal polyps.

Despite the constraints of the sample size feasible within a PhD timescale, my results have shown some significant differences in CRS without nasal polyposis in terms of upregulated mucosal chemokines and cytokines, notably MIP-1 alpha, MIP-1beta, MCP-4, TARC, eotaxin 3, IL-6, IL-10 and IL-17. Correlating these discriminant mediators with symptom scores of rhinological disease severity suggests that MIP-1 alpha and MIP-1 beta appear the most promising candidates for CRS disease severity – which can be the initial focus of my future investigations. These studies are very timely, given the increasing emergence of targeted biological therapies in inflammatory conditions of the airways.

In short, the potential of such a measure to help look after patients with sinonasal disease clearly merits further exploration. I intend to seek funding for a more detailed longitudinal study investigating mucosal lining fluid measurements in a much larger cohort of CRS with and without nasal polyp patients and controls. I propose to take measurements longitudinally from diagnosis through disease flare ups, in response to medical treatment, surgical procedures and at different times of the day to investigate the intra individual variability of mucosal lining fluid scores. Such a study will also need careful assessment of the whole respiratory tract including for the presence of respiratory diseases such as asthma and related conditions. The possible use of nasal and respiratory nitric oxide measurements could also be incorporated to complement the mucosal lining fluid measurement.

Throughout the thesis I have sought to compare findings *in vivo* with those in my respective study tissue biopsies and isolated primary cells. My aim was to see if primary patient-derived epithelial and fibroblast cells could be used to model CRS disease in the laboratory. Furthermore, information gained from *in vivo* and tissue biopsy studies could serve to make any *in vitro* cellular studies more representative of the sinonasal environment in health and disease. The present work has highlighted, however, some key deficiencies in my hypotheses. I have discovered that primary patient-derived cells - epithelial cells especially – differ significantly in terms of their inflammatory profile and transcriptome. This may be a reflection of how they are isolated, though I suspect it is more to do with the process of cell culture. Although the cells have been very recently isolated from participants' sinonasal

cavities, rather than being grown in a complex mucosal environment, they are proliferating on laboratory plastic ware with numerous potent primary cell media supplements.

My short term plans therefore do not include continuing investigation with these primary cells. Instead I wish to focus my attention on CRS tissue biopsies to investigate the upregulated inflammatory pathways identified from bioinformatics analysis of the tissue transcriptome data – the first report of RNA sequencing technology in the field. In addition, I shall consider newer, more sophisticated tissue culture systems such as tissue slice or 3D cell culture, where for example a fresh tissue biopsy is sectioned very thinly with an ultramicrotome and bathed in a continuous supply of fresh media to mimic capillary flow. In such a system all the component cells are present to more accurately model the tissue situation *in vivo*. However, one challenge from such a system would be to isolate individual cell types in an effort to determine their precise functions. Bearing this in mind, complimentary laser capture microdissection of tissue sections and subsequent molecular analysis of the dissected cells with quantitative RT-PCR or RNA sequencing data may be useful.

In conclusion, the phenotyped CRS and control samples generated in this thesis have provided a detailed comparison of the histological, disease micro-environment and transcriptome of chronic rhinosinusitis without nasal polyps. Cellular models, both immortalised cell lines and primary patient-derived cells do not convincingly provide representative models of CRS and further work should be directed towards isolated tissue biopsy specimens.

7 Appendix

7.1 Appendix 1 – Publications, presentations and personal development

7.1.1 Publications

- Complications of rhinosinusitis. Ball SL, Carrie S. ***British Medical Journal***. 2016 Feb 26;352:i795.
- The Role of the Fibroblast in Inflammatory Upper Airway Conditions. Ball SL, Mann DA, Wilson JA, Fisher AJ. ***American Journal of Pathology***. 2016 Feb;186(2):225-33. Review.
- Thymoma complicated by deep vein thrombosis of the arm. Ball SL, Cocks HC. ***BMJ Case Rep***. 2015 Dec 21;2015. pii: bcr2015213404
- Pott's puffy tumour: a forgotten diagnosis. Ball SL, Carrie S. ***BMJ Case Rep***. 2015 Sep 29;2015. pii: bcr2015211099.
- How Reliable Are Sino-Nasal Cell Lines for Studying the Pathophysiology of Chronic Rhinosinusitis? Stephen Ball, Monika Suwara, Lee Borthwick, Janet Wilson, Derek Mann & Andrew Fisher. ***Annals of Otology, Rhinology & Laryngology*** 2015.
- The use of phenol as a topical anaesthetic for the tympanic membrane. Ball SL. ***Clinical Otolaryngology***. 2015 Oct;40(5):506..
- Anatomy of a swallow. Ball SL, Arullendran P. ***British Medical Journal***. 2015 Jul 13;351:h3494.
- Pharyngeal angiosarcoma following multimodal treatment for oropharyngeal squamous cell carcinoma. Stephen Ball, Foon Ng Kee Kwong, Fergus Young & Andrew Robson. ***The Annals of the Royal College of Surgeons*** 2014 Mar;96(2):e5-6.
- Complications of Bone Anchored Hearing Aids. Stephen Ball & Ian Johnson. ***The Otolaryngologist*** 2014;7(3)146-50.
- ***Scott Brown's Otolaryngology, Head & Neck Surgery***, 8th Edition. Stephen Ball & Sean Carrie. Text book chapter: Complications of Rhinosinusitis co-authored & in press. CRC press.
- Are pro-inflammatory fibroblasts the driving force in chronic rhinosinusitis? Stephen L Ball, Anthony De Soyza, Andrew Fisher, Derek Mann & Janet A Wilson. (2012) ***Clinical Otolaryngology*** July:37(Suppl.1):1-2.

7.1.2 Prizes

- **European Rhinological Society**. Junior member travelling Fellowship, 2016
- **Royal Society of Medicine, Section of Laryngology & Rhinology**: Ian Mackay Essay prize, 2014. Osteitis – the modern theory of sinusitis.
- **Munro-Black Research Prize.** Northern Region ENT Surgery research prize, 2014.
- **Royal Society of Medicine, Section of Laryngology & Rhinology.** Annual short paper prize, 2013.

7.1.3 Presentations

- **European Rhinology Society** 26th Congress in conjunction with the 35th International Symposium of Infection & Allergy of the Nose, Stockholm June 2016.
- **British Rhinological Society**, Leeds May 2016
- **British Academic Conference in Otolaryngology**, Liverpool 8-10th July 2015
- **British Rhinological Society**, Manchester May 2015
- **European Rhinology Society** 25th Congress in conjunction with the 32nd International Symposium of Infection & Allergy of the Nose, Amsterdam June 2014.

- **British Rhinological Society**, Norwich May 2014
- **European Respiratory Society, Lung Science Conference**, Estoril March 2014.
- **British Society of Academic Otolaryngology** March 2014.
- **Royal Society of Medicine**, Section of Laryngology & Rhinology February 2013.

7.1.4 Papers in submission/preparation

- Transcriptome analysis of tissue biopsies, epithelial and fibroblast cells in Chronic rhinosinusitis.
- Sinonasal mucosal lining fluid analysis – a 'biosignature' for CRS.
- Sinonasal disease- a consequence of autonomic imbalance? Yao A, Wilson JA & Ball SL.
- A Review of Periorbital Cellulitis Protocols in the United Kingdom. Okwonko A, Carrie S & Ball SL.
- 15 years and 100 cases of paediatric intracranial suppuration.

7.1.5 Clinical trials

I am a Principal Investigator on a £745,355 NIHR (National Institute for Health Research) funded phase 3 randomised controlled trial; TOPPITS (Trial Of Proton Pump Inhibitors in Throat Symptoms) www.toppits.co.uk.

7.2 Appendix 2 – R Studio code for microarray analysis

```
library(lumi)
library(affycoretools)
library(arrayQualityMetrics)
library(annotate)
library(lumiHumanAll.db)
library(limma)
library(gplots)

setwd('~/20150219_analysis')

# read the raw microarray data
raw_data = lumiR("SampleProbeProfile.txt")

pheno = read.csv('Micro array data table.csv')
rownames(pheno) = pheno$Illumina.sample.ID

pheno$sample_type = paste(pheno$Cell.type, pheno$Case.vs.Control, sep="_")
pheno$sample_type = as.factor(pheno$sample_type)
pheno = pheno[sampleNames(raw_data),]
pData(raw_data) = pheno

# Transformation & Normalisation
vst_data = lumiT(raw_data, method="vst")
rsn_data = lumiN(vst_data, method="rsn")

plot(rsn_data, what="sampleRelation", method="mds")


#To plot raw & normalised/transformed data vs sample names rather than sentrix IDs
par(cex=0.45)
temp = raw_data
sampleNames(temp) = pheno$Patient.number
plot(temp, what="density")
plot(temp, what="boxplot" )
rm(temp)

temp = rsn_data
sampleNames(temp) = pheno$Patient.number
plot(temp, what="density")
plot(temp, what="boxplot" )
rm(temp)
par(cex=1.0)

## to remove legend# plot(raw_data, what="density", addLegend=FALSE)
##to plot data vs sentrix IDs## plot(rsn_data, what="density")
##to plot data vs sentrix IDs## plot(raw_data, what="boxplot")
##to plot data vs sentrix IDs## plot(rsn_data, what="boxplot")



#Cluster dendrogram
plot(rsn_data, what="sampleRelation")
d = dist(t(exprs(rsn_data)), method="euclidian")
h = hclust(d, method="complete")
h$labels = pData(rsn_data)$Case.vs.Control
plot(h, xlab="", sub="")

as.numeric(pData(rsn_data)$Cell.type)
levels(pData(rsn_data)$Cell.type)
```

```
#Heat map
heatmap.2(as.matrix(d), trace="none", density.info="none", col=redblue(255),
          labRow=pData(rsn_data)$Patient.number, labCol=pData(rsn_data)$Patient.number)


#Principal component analysis
plotPCA(rsn_data, groups=as.numeric(pData(rsn_data)$Cell.type),
        groupnames=levels(pData(rsn_data)$Cell.type))
plotPCA(rsn_data, groups=as.numeric(pData(rsn_data)$Case.vs.Control),
        groupnames=levels(pData(rsn_data)$Case.vs.Control))
plotPCA(rsn_data, groups=as.numeric(pData(rsn_data)$sample_type),
        groupnames=levels(pData(rsn_data)$sample_type))



##Separating raw data for arrays epithelial vs. fibroblast
raw_data_e = raw_data[,pData(raw_data)$Cell.type == 'Epithelial']
raw_data_f = raw_data[,pData(raw_data)$Cell.type == 'Fibroblast']



##### EPITHELIAL #####
vst_data_e = lumiT(raw_data_e, method="vst")
rsn_data_e = lumiN(vst_data_e, method="rsn")

normalised_data_e = lumiQ(rsn_data_e)


#To plot raw & normalised/transformed data vs sample names rather than sentrix IDs
par(cex=0.6)
temp = raw_data_e
sampleNames(temp) = pData(temp)$Patient.number
plot(temp, what="density")
plot(temp, what="boxplot")
rm(temp)

temp = rsn_data_e
sampleNames(temp) = pData(temp)$Patient.number
plot(temp, what="density")
plot(temp, what="boxplot" )
rm(temp)


##to plot data vs sentrix IDs## plot(raw_data_e, what="density")
##to plot data vs sentrix IDs## plot(normalised_data_e, what="density")
##to plot data vs sentrix IDs## plot(raw_data_e, what="boxplot")
##to plot data vs sentrix IDs## plot(normalised_data_e, what="boxplot")


par(cex=1.0)
#Principal component analysis
plotPCA(rsn_data_e, groups=as.numeric(pData(rsn_data_e)$Case.vs.Control),
        groupnames=levels(pData(rsn_data_e)$Case.vs.Control),
        addtext=pData(rsn_data_e)$Patient.number)
```

```
#Cluster dendrogram
plot(rsn_data_e, what="sampleRelation")
d = dist(t(exprs(rsn_data_e)), method="euclidian")
h = hclust(d, method="complete")
h$labels = pData(rsn_data_e)$Case.vs.Control
plot(h, xlab="", sub="")


#Quality control - arrayQualityMetrics (identifies array 5 as an outlier)
# arrayQualityMetrics(rsn_data_e)

#Removing outlier array 5
raw_data_e = raw_data_e[,-5]
vst_data_e = lumiT(raw_data_e, method="vst")
rsn_data_e = lumiN(vst_data_e, method="rsn")


#Array annotation - applying gene names to probe IDs
filtered_data_e = rsn_data_e[detectionCall(rsn_data_e) > 0,]

probe_list = featureNames(filtered_data_e)
nuIDs = IlluminaID2nuID(probe_list)[,"nuID"]
symbol = getSYMBOL(nuIDs, "lumiHumanAll.db")
description = unlist(lookUp(nuIDs, data="lumiHumanAll.db", what="GENENAME"))
anno_df = data.frame(ID=nuIDs, probe_list, symbol, description)


#Differential gene expression
design = model.matrix(~0 + Case.vs.Control, data=pData(rsn_data_e))
colnames(design) = c("Case", "Control")

fit = lmFit(filtered_data_e, design)


#make contrast matrix & apply empirical Bayes statistics
#to derive moderated t-statistics of differential expression for all probes
contrasts = makeContrasts(Case-Control, levels=c("Case", "Control"))
fit2 = contrasts.fit(fit, contrasts=contrasts)
fit2 = eBayes(fit2)
# fit2$genes = anno_df

#Filter by fold change (1.5x)
#Adjusted using Benjamini-Hochberg False Discovery Rate
# tt1 = topTable(fit2, coef="Case - Control", number=Inf,
sort.by="logFC", adjust.method="BH")
# p.adjust(tt1$P.Value, method="BH")

write.table(topTable(fit2, coef="Case - Control", number=Inf),
            file="~/lumi_epithelial_Case-Control_all.txt",
            quote = FALSE, sep="\t", row.names=FALSE)


#Volcano plot of differentially expressed genes
for_volcano_e = topTable(fit2, coef="Case - Control", number=Inf)

plot(x=for_volcano_e$logFC, y=for_volcano_e$adj.P.Val, xlab="log2 Fold Change,
     ylim=c(0,1), ylab="Adjusted PValue")
abline(v=log2(2/3), lty=2, col="gray")
abline(v=log2(3/2), lty=2, col="gray")
abline(h=(0.05), lty=2, col="gray")
```

```
# XY scatter plot

mean_control = apply(exprs(filtered_data_e[,pData(filtered_data_e)
$sample_type=="Epithelial_control"]), 1, mean)
mean_case = apply(exprs(filtered_data_e[,pData(filtered_data_e)
$sample_type=="Epithelial_case"]), 1, mean)

plot(x=mean_control, y=mean_case, pch=20, col=alpha(colour="black", alpha=0.5),
     xlab='Normalised Expression, Controls', ylab='Normalised Expression, Cases')
abline(a=0, b=1, col='green')
abline(a=log2(1.5), b=1, col='red')
abline(a=log2(2/3), b=1, col='red')


#Heat maps - distance plot
heatmap.2(as.matrix(d), trace="none", density.info="none", col=redblue(255),
          labRow=pData(rsn_data_e)$Patient.number, labCol=pData
(rsn_data_e)$Patient.number)


# Genes with linear relationship to SNOT-22
pData(filtered_data_e)$Scaled_SNOT = pData(filtered_data_e)$SNOT_22/110
design = model.matrix(~pData(filtered_data_e)$Scaled_SNOT)
fit = lmFit(filtered_data_e, design=design)
fit = eBayes(fit)
best_genes_snot = topTable(fit, number=Inf, sort.by="logFC")

head(best_genes_snot, 10)[,'DEFINITION']
fit = lmFit(filtered_data_e, design=design)
fit = eBayes(fit)
tt = topTable(fit) #sort.by="logFC"

View(tt)

plot
(x=pData(filtered_data_e)$Scaled_SNOT,
     y=exprs(filtered_data_e)
     [rownames
       (best_genes_snot)[4],],
     xlab="SNOT 22", ylab="Gene Expression (log2)", pch=20)
abline(lm(exprs(filtered_data_e)
          [rownames(best_genes_snot)[4],] ~ pData(filtered_data_e)
$Scaled_SNOT), col='red')



# Genes with linear relationship to Lund-Mackay
pData(filtered_data_e)$Scaled_LM = pData(filtered_data_e)$Lund_Mackay/24
design = model.matrix(~pData(filtered_data_e)$Scaled_LM)
fit = lmFit(filtered_data_e, design=design)
fit = eBayes(fit)
best_genes_lund = topTable(fit, number=Inf, sort.by="logFC")

head(best_genes_lund, 10)[,'DEFINITION']
fit = lmFit(filtered_data_f, design=design)
fit = eBayes(fit)
tt = topTable(fit) #sort.by="logFC"

View(tt)
```

```
plot
(x=pData(filtered_data_e)$Scaled_LN,
     y=exprs(filtered_data_e)
     [rownames(best_genes_lund)[1],],
     xlab="Lund-Mackay", ylab="Gene Expression (log2)", pch=20)
abline(lm(exprs(filtered_data_e)[rownames(best_genes_lund)[1],]
~ pData(filtered_data_e)$Scaled_LN), col='red')


##### FIBROBLASTS #####

#Transformation & Normalisation
vst_data_f = lumiT(raw_data_f, method="vst")
rsn_data_f = lumiN(vst_data_f, method="rsn")

normalised_data_f = lumiQ(rsn_data_f)

par(cex=0.6)
temp = raw_data_f
sampleNames(temp) = pData(temp)$Patient.number
plot(temp, what="density")
plot(temp, what="boxplot" )
rm(temp)

temp = rsn_data_f
sampleNames(temp) = pData(temp)$Patient.number
plot(temp, what="density")
plot(temp, what="boxplot" )
rm(temp)

##to plot data vs sentrix IDs## plot(raw_data_f, what="density")
##to plot data vs sentrix IDs## plot(normalised_data_f, what="density")
##to plot data vs sentrix IDs## plot(raw_data_f, what="boxplot")
##to plot data vs sentrix IDs## plot(normalised_data_f, what="boxplot")

par(cex=1.0)

#Principal component analysis
plotPCA(rsn_data_f, groups=as.numeric(pData(rsn_data_f)$Case.vs.Control),
groupnames=levels(pData(rsn_data_f)$Case.vs.Control),
        addtext=pData(rsn_data_f)$Patient.number)


#Cluster dendrogram
plot(rsn_data_f, what="sampleRelation")
d = dist(t(exprs(rsn_data_f)), method="euclidian")
h = hclust(d, method="complete")
h$labels = pData(rsn_data_f)$Case.vs.Control
plot(h, xlab="", sub="")


#Heat map
heatmap.2(as.matrix(d), trace="none", density.info="none", col=redblue(255),
          labRow=pData(rsn_data_f)$Patient.number,
labCol=pData(rsn_data_f)$Patient.number)

#Quality control with arrayQualityMetrics
# arrayQualityMetrics(rsn_data_f)
```

```
#Array annotation - applying gene names to probe IDs
filtered_data_f = rsn_data_f[detectionCall(rsn_data_f) > 0,]


probe_list = featureNames(filtered_data_f)
nuIDs = IlluminaID2nuID(probe_list)[,"nuID"]
symbol = getSYMBOL(nuIDs, "lumiHumanAll.db")
description = unlist(lookUp(nuIDs, data="lumiHumanAll.db", what="GENENAME"))
anno_df = data.frame(ID=nuIDs, probe_list, symbol, description)


#Differential gene expression
design = model.matrix(~0 + Case.vs.Control, data=pData(rsn_data_f))
colnames(design) = c("Case", "Control")

fit = lmFit(filtered_data_f, design)


#make contrast matrix & apply empirical Bayes statistics
#to derive moderated t-statistics of differential expression for all probes
contrasts = makeContrasts(Case-Control, levels=c("Case", "Control"))
fit2 = contrasts.fit(fit, contrasts=contrasts)
fit2 = eBayes(fit2)
# fit2$genes = anno_df


#Filter by fold change (1.5x) cut off
#Adjusted using Benjamini-Hochberg False Discovery Rate
topTable(fit2, coef="Case - Control", number=100, lfc=log2(1.5))

write.table(topTable(fit2, coef="Case - Control", number=Inf),
            file="~/lumi_fibroblast_Case-Control_all.txt",
quote = FALSE, sep="\t", row.names=FALSE)



#Volcano plot of differentially expressed genes
for_volcano_f = topTable(fit2, coef="Case - Control", number=Inf)

plot(x=for_volcano_f$logFC, y=-log10(for_volcano_f$adj.P.Val),
xlab="log2 Fold Change", ylab="-log10(Adjusted P Value)",      pch=20,
col=ifelse(abs(for_volcano_f$logFC)>log2(1.5)&for_volcano_f$adj.P.Val<0.05,
'red', alpha('black', 0.5)))
abline(v=log2(2/3), lty=2, col="gray")
abline(v=log2(3/2), lty=2, col="gray")
abline(h=-log10(0.05), lty=2, col="gray")

# XY scatter plot
#use apply to run mean over a matrix of Control expression values
mean_control = apply(exprs(filtered_data_f[,pData(filtered_data_f)
$sample_type=="Fibroblast_control"]), 1, mean)
#use apply to run mean over a matrix of Case expression values
mean_case = apply(exprs(filtered_data_f[,pData(filtered_data_f)
$sample_type=="Fibroblast_case"]), 1, mean)

#for colouring
col_bool = names(mean_control) == rownames(for_volcano_f
[for_volcano_f$logFC>log2(1.5)&for_volcano_f$adj.P.Val<0.05,])
```

```
plot(x=mean_control, y=mean_case, pch=20,
col=ifelse(col_bool, "red", alpha(colour="black", alpha=0.5)),
     xlab='Normalised Expression, Controls',
     ylab='Normalised Expression, Cases')
abline(a=0, b=1, col='green')
abline(a=log2(1.5), b=1, col='red')
abline(a=log2(2/3), b=1, col='red')



# Genes with linear relationship to SNOT-22
# standardised_data_f = (exprs(filtered_data_f)
- mean(exprs(filtered_data_f))) / sd(exprs(filtered_data_f))

pData(filtered_data_f)$Scaled_SNOT = pData(filtered_data_f)$SNOT_22/110

#pData(filtered_data_f)$Standardised_SNOT =
(pData(filtered_data_f)$SNOT_22 - mean(pData(filtered_data_f)$SNOT_22))
/ sd(pData(filtered_data_f)$SNOT_22)
design = model.matrix(~pData(filtered_data_f)$Scaled_SNOT)


fit = lmFit(filtered_data_f, design=design)
fit = eBayes(fit)
tt = topTable(fit) #sort.by="logFC"

View(tt)

top_gene = as.numeric(exprs(filtered_data_f[rownames(tt[1,]),]))
scaled_snot = pData(filtered_data_f)$Scaled_SNOT

plot(x=scaled_snot, y=top_gene,
     xlab="SNOT 22", ylab="Gene Expression (log2)", pch=20)
mod = lm(top_gene ~ scaled_snot)
abline(mod, col='red')


# Genes with linear relationship to Lund-Mackay
pData(filtered_data_f)$Scaled_LM = pData(filtered_data_f)$Lund_Mackay/24
design = model.matrix(~pData(filtered_data_f)$Scaled_LM)
fit = lmFit(filtered_data_f, design=design)
fit = eBayes(fit)
tt = topTable(fit)

View(tt)

plot(x=pData(filtered_data_f)$Scaled_LM, y=exprs(filtered_data_f)
[rownames(tt[1,]),], xlab="Lund-Mackay", ylab="Gene Expression (log2)",
pch=20)
abline(lm(exprs(filtered_data_f)[rownames(tt[1,]),]
~ pData(filtered_data_f)$Scaled_LM), col='red')
```

7.3 Appendix 3 – Mucosal lining fluid non-parametric correlations

Correlations

		SNOTRmax35	Eotaxin3	MIP1b	IL10	MIP1a	IL6	IL17	SAA	MCP4	TARC	PIGF	sFlt1	bFGF	VCAM1
Spearman's rho	SNOTRmax35	Correlation Coefficient	.381*	.509**	.351*	.481**	.400*	.417**	.496**	.397*	.341*	.372*	.408**	.368*	.413**
		Sig. (2-tailed)	.015	.001	.027	.002	.011	.007	.001	.011	.031	.018	.009	.020	.008
		N	40	40	40	40	40	40	40	40	40	40	40	40	40
	Eotaxin3	Correlation Coefficient	1.000	.837**	.386*	.807**	.666**	.464**	.638**	.874**	.827**	.572**	.671**	.614**	.648**
		Sig. (2-tailed)	.	.000	.014	.000	.000	.003	.000	.000	.000	.000	.000	.000	.000
		N	40	40	40	40	40	40	40	40	40	40	40	40	40
	MIP1b	Correlation Coefficient	.837**	1.000	.406**	.888**	.765**	.522**	.635**	.801**	.830**	.697**	.751**	.533**	.671**
		Sig. (2-tailed)	.000	.	.009	.000	.000	.001	.000	.000	.000	.000	.000	.000	.000
		N	40	40	40	40	40	40	40	40	40	40	40	40	40
	IL10	Correlation Coefficient	.386*	.406**	1.000	.551**	.598**	.626**	.461**	.457**	.230	.312	.422**	.277	.454**
		Sig. (2-tailed)	.014	.009	.	.000	.000	.000	.003	.003	.153	.050	.007	.083	.003
		N	40	40	40	40	40	40	40	40	40	40	40	40	40
	MIP1a	Correlation Coefficient	.807**	.888**	.551**	1.000	.761**	.619**	.599**	.849**	.719**	.611**	.723**	.535**	.639**
		Sig. (2-tailed)	.000	.000	.000	.	.000	.000	.000	.000	.000	.000	.000	.000	.000
		N	40	40	40	40	40	40	40	40	40	40	40	40	40
	IL6	Correlation Coefficient	.666**	.765**	.598**	.761**	1.000	.629**	.631**	.703**	.647**	.632**	.669**	.477**	.653**
		Sig. (2-tailed)	.000	.000	.000	.000	.	.000	.000	.000	.000	.000	.000	.002	.000
		N	40	40	40	40	40	40	40	40	40	40	40	40	40
	IL17	Correlation Coefficient	.464**	.522**	.626**	.619**	.629**	1.000	.630**	.573**	.483**	.564**	.629**	.616**	.560**
		Sig. (2-tailed)	.003	.001	.000	.000	.000	.	.000	.000	.002	.000	.000	.000	.000
		N	40	40	40	40	40	40	40	40	40	40	40	40	40
	SAA	Correlation Coefficient	.638**	.635**	.461**	.599**	.631**	.630**	1.000	.608**	.639**	.532**	.647**	.674**	.847**
		Sig. (2-tailed)	.000	.000	.003	.000	.000	.000	.	.000	.000	.000	.000	.000	.000
		N	40	40	40	40	40	40	40	40	40	40	40	40	40
	MCP4	Correlation Coefficient	.874**	.801**	.457**	.849**	.703**	.573**	.608**	1.000	.838**	.685**	.741**	.586**	.620**
		Sig. (2-tailed)	.000	.000	.003	.000	.000	.000	.000	.	.000	.000	.000	.000	.000
		N	40	40	40	40	40	40	40	40	40	40	40	40	40
	TARC	Correlation Coefficient	.827**	.830**	.230	.719**	.647**	.483**	.639**	.838**	1.000	.775**	.781**	.610**	.671**
		Sig. (2-tailed)	.000	.000	.153	.000	.000	.002	.000	.000	.	.000	.000	.000	.000
		N	40	40	40	40	40	40	40	40	40	40	40	40	40
	PIGF	Correlation Coefficient	.572**	.697**	.312	.611**	.632**	.564**	.532**	.685**	.775**	1.000	.830**	.521**	.659**
		Sig. (2-tailed)	.000	.000	.050	.000	.000	.000	.000	.000	.000	.	.000	.001	.000
		N	40	40	40	40	40	40	40	40	40	40	40	40	40
	sFlt1	Correlation Coefficient	.671**	.751**	.422**	.723**	.669**	.629**	.647**	.741**	.781**	.830**	1.000	.616**	.707**
		Sig. (2-tailed)	.000	.000	.007	.000	.000	.000	.000	.000	.000	.000	.	.000	.000
		N	40	40	40	40	40	40	40	40	40	40	40	40	40
	bFGF	Correlation Coefficient	.614**	.533**	.277	.535**	.477**	.616**	.674**	.586**	.610**	.521**	.616**	1.000	.675**
		Sig. (2-tailed)	.000	.000	.083	.000	.002	.000	.000	.000	.000	.001	.000	.	.000
		N	40	40	40	40	40	40	40	40	40	40	40	40	40
	VCAM1	Correlation Coefficient	.648**	.671**	.454**	.639**	.653**	.560**	.847**	.620**	.671**	.659**	.707**	.675**	1.000
		Sig. (2-tailed)	.000	.000	.003	.000	.000	.000	.000	.000	.000	.000	.000	.000	.
		N	40	40	40	40	40	40	40	40	40	40	40	40	40

*. Correlation is significant at the 0.05 level (2-tailed).

**. Correlation is significant at the 0.01 level (2-tailed).

Table showing significant non-parametric correlations among all differentially expressed mucosal lining fluid markers and SNOT-22 rhinological sub-scale symptom scores.

Correlations

			SNOTRmax35	MIP1b	Eotaxin3	IL10	MIP1a	IL6	IL17	SAA	MCP4	TARC	PIGF	sFlt1	bFGF	VCAM1
Spearman's rho	SNOTRmax35	Correlation Coefficient	1.000	.455*	.344	.249	.424*	.366	.289	.420	.278	.318	.257	.453*	.095	.498*
		Sig. (2-tailed)	.	.033	.117	.263	.049	.094	.192	.052	.210	.149	.248	.034	.675	.018
		N	22	22	22	22	22	22	22	22	22	22	22	22	22	22
	MIP1b	Correlation Coefficient	.455*	1.000	.768**	.243	.852**	.781**	.431*	.484*	.744**	.745**	.623**	.633**	.368	.591**
		Sig. (2-tailed)	.033	.	.000	.277	.000	.000	.045	.022	.000	.000	.002	.002	.092	.004
		N	22	22	22	22	22	22	22	22	22	22	22	22	22	22
	Eotaxin3	Correlation Coefficient	.344	.768**	1.000	.126	.604**	.586**	.302	.589**	.819**	.888**	.411	.457*	.504*	.561**
		Sig. (2-tailed)	.117	.000	.	.576	.003	.004	.172	.004	.000	.000	.058	.033	.017	.007
		N	22	22	22	22	22	22	22	22	22	22	22	22	22	22
	IL10	Correlation Coefficient	.249	.243	.126	1.000	.495*	.512*	.829**	.358	.361	.091	.255	.227	.185	.319
		Sig. (2-tailed)	.263	.277	.576	.	.019	.015	.000	.102	.099	.687	.252	.310	.410	.147
		N	22	22	22	22	22	22	22	22	22	22	22	22	22	22
	MIP1a	Correlation Coefficient	.424*	.852**	.604**	.495*	1.000	.804**	.609**	.318	.619**	.503*	.470*	.449*	.234	.406
		Sig. (2-tailed)	.049	.000	.003	.019	.	.000	.003	.149	.002	.017	.027	.036	.294	.061
		N	22	22	22	22	22	22	22	22	22	22	22	22	22	22
	IL6	Correlation Coefficient	.366	.781**	.586**	.512*	.804**	1.000	.631**	.350	.762**	.647**	.686**	.618**	.275	.403
		Sig. (2-tailed)	.094	.000	.004	.015	.000	.	.002	.111	.000	.001	.000	.002	.216	.063
		N	22	22	22	22	22	22	22	22	22	22	22	22	22	22
	IL17	Correlation Coefficient	.289	.431*	.302	.829**	.609**	.631**	1.000	.546**	.476*	.299	.400	.456*	.471*	.506*
		Sig. (2-tailed)	.192	.045	.172	.000	.003	.002	.	.009	.025	.177	.065	.033	.027	.016
		N	22	22	22	22	22	22	22	22	22	22	22	22	22	22
	SAA	Correlation Coefficient	.420	.484*	.589**	.358	.318	.350	.546**	1.000	.502*	.601**	.387	.561**	.588**	.916**
		Sig. (2-tailed)	.052	.022	.004	.102	.149	.111	.009	.	.017	.003	.075	.007	.004	.000
		N	22	22	22	22	22	22	22	22	22	22	22	22	22	22
	MCP4	Correlation Coefficient	.278	.744**	.819**	.361	.619**	.762**	.476*	.502*	1.000	.859**	.589**	.466*	.390	.486*
		Sig. (2-tailed)	.210	.000	.000	.099	.002	.000	.025	.017	.	.000	.004	.029	.073	.022
		N	22	22	22	22	22	22	22	22	22	22	22	22	22	22
	TARC	Correlation Coefficient	.318	.745**	.888**	.091	.503*	.647**	.299	.601**	.859**	1.000	.587**	.570**	.488*	.582**
		Sig. (2-tailed)	.149	.000	.000	.687	.017	.001	.177	.003	.000	.	.004	.006	.021	.004
		N	22	22	22	22	22	22	22	22	22	22	22	22	22	22
	PIGF	Correlation Coefficient	.257	.623**	.411	.255	.470*	.686**	.400	.387	.589**	.587**	1.000	.767**	.242	.540**
		Sig. (2-tailed)	.248	.002	.058	.252	.027	.000	.065	.075	.004	.004	.	.000	.277	.009
		N	22	22	22	22	22	22	22	22	22	22	22	22	22	22
	sFlt1	Correlation Coefficient	.453*	.633**	.457*	.227	.449*	.618**	.456*	.561**	.466*	.570**	.767**	1.000	.466*	.658**
		Sig. (2-tailed)	.034	.002	.033	.310	.036	.002	.033	.007	.029	.006	.000	.	.029	.001
		N	22	22	22	22	22	22	22	22	22	22	22	22	22	22
	bFGF	Correlation Coefficient	.095	.368	.504*	.185	.234	.275	.471*	.588**	.390	.488*	.242	.466*	1.000	.579**
		Sig. (2-tailed)	.675	.092	.017	.410	.294	.216	.027	.004	.073	.021	.277	.029	.	.005
		N	22	22	22	22	22	22	22	22	22	22	22	22	22	22
	VCAM1	Correlation Coefficient	.498*	.591**	.561**	.319	.406	.403	.506*	.916**	.486*	.582**	.540**	.658**	.579**	1.000
		Sig. (2-tailed)	.018	.004	.007	.147	.061	.063	.016	.000	.022	.004	.009	.001	.005	.
		N	22	22	22	22	22	22	22	22	22	22	22	22	22	22

*. Correlation is significant at the 0.05 level (2-tailed).

**. Correlation is significant at the 0.01 level (2-tailed).

Table showing significant non-parametric correlations in CRSsNP participants in all differentially expressed mucosal lining fluid markers and SNOT-22 rhinological sub-scale symptom scores.

7.4 Appendix 4 - Sino-Nasal Outcome Test-22 Questionnaire v4

Below you will find a list of symptoms and social/emotional consequences of your nasal disorder. We would like to know more about these problems and would appreciate you answering the following question to the best of your ability. There are no right or wrong answers, and only you can provide us with this information. Please rate your problems, as they have been over the past two weeks. Thank you for your participation.

Considering how severe the problem is when you experience it and how frequently it happens, please rate each item below	**No problem**	**Very mild problem**	**Mild or slight problem**	**Moderate problem**	**Severe problem**	**Problem as bad as it can be**
1. Need to blow nose	0	1	2	3	4	5
2. Sneezing	0	1	2	3	4	5
3. Runny nose	0	1	2	3	4	5
4. Cough	0	1	2	3	4	5
5. Post nasal discharge (dripping at the back of your nose)	0	1	2	3	4	5
6. Thick nasal discharge	0	1	2	3	4	5
7. Ear fullness	0	1	2	3	4	5
8. Dizziness	0	1	2	3	4	5
9. Ear pain/pressure	0	1	2	3	4	5
10. Facial pain/pressure	0	1	2	3	4	5
11. Difficulty falling asleep	0	1	2	3	4	5
12. Waking up at night	0	1	2	3	4	5
13. Lack of a good night's sleep	0	1	2	3	4	5
14. Waking up tired	0	1	2	3	4	5
15. Fatigue during the day	0	1	2	3	4	5
16. Reduced productivity	0	1	2	3	4	5
17. Reduced concentration	0	1	2	3	4	5
18. Frustrated/restless/irritable	0	1	2	3	4	5
19. Sad	0	1	2	3	4	5
20. Embarrassed	0	1	2	3	4	5
21. Sense of taste/smell	0	1	2	3	4	5
22. Blockage/congestion of nose	0	1	2	3	4	5

7.5 Appendix 5 – Sample Patient information sheet

The Newcastle upon Tyne Hospitals NHS Trust

Freeman Hospital
High Heaton
Newcastle upon Tyne
NE7 7DN

Patient Information Sheet and Consent Form – non - sinusitis surgery patients

Study Code:

Patient Initials: **Subject Number:**

Study Title: **Studying the nasal & sinus cells in rhinosinusitis**

Name of Researchers: Professor Janet Wilson, Professor Andrew Fisher, Professor Derek Mann & Dr Stephen Ball

You are being invited to take part in a research study. Before you decide it is important for you to understand why the research is being done and what it will involve. Please take time to read the following information carefully. Talk to others about the study if you wish.

Ask us if there is anything that is not clear or if you would like more information. Take time to decide whether or not you wish to take part.

Thank you for reading this.

What is the background and purpose of the study?
Sinusitis is a common disease of the nose and sinuses. It is caused by swelling of the nasal passages from infection or inflammation. For some people it is very severe and up to 15 000 patients per year have surgery for sinusitis in the UK. The exact causes for severe or prolonged sinusitis are not well known. As a result our treatments for sinusitis do not always work. We aim to understand sinusitis better so hopefully we can develop more non-surgical treatments. To do this we would like to analyse samples from the nose and blood in the laboratory in both people who suffer from sinusitis and those who do not.

We propose to take small samples of the nasal lining from patients undergoing routine nasal surgery either for sinusitis or nose operations other than sinusitis, at the Newcastle Hospitals to allow us to do research into this condition. Patients who want to take part will sign a consent form and complete questionnaires about problems they have with their nose & sinuses called SNOT-22 (Sino-Nasal Outcome Test version 22), a fatigue and sleep questionnaire before any tissue samples are taken. Involvement in the study is over once the operation has been performed and the tissue samples taken. Taking part in the study will not change your hospital treatment or lengthen your hospital stay.

What would normally happen to the tissue being used for research?

We wish to collect part of the tissue removed as part of your procedure that would normally be thrown away. In addition to this we would like to collect some additional research samples – see below.

Why have I been chosen?

You have been asked to consider taking part in this study because you are having an operation on your nasal passages typically not for sinusitis. For example you may be having surgery to straighten your nasal septum (the central wall between the two nasal passages) or pituitary surgery, as the nasal passages are used to access the gland. By comparing samples from sinusitis patients and non-sinusitis patients we hope to understand the disease better.

Do I have to take part?

No. It is up to you to decide whether or not to take part. If you do, you will be given this information sheet to keep and be asked to sign a consent form. You are still free to withdraw at any time and without giving a reason. A decision to withdraw at any time, or a decision not to take part, will not affect the standard of care you receive.

What will happen to me if I take part?

Following the discussion and consent for the study, when you will be given opportunity to ask questions you will be asked to complete two questionnaires about any nasal problems or fatigue you have. The questionnaires, which will take about 10 minutes to do, will tell us more about how you are feeling and about your nose and sinus problems. You will have your operation as normal. As part of your procedure we would like to collect small research nasal samples. These may include:

1. tissue removed that would normally be thrown away in the hospital waste. If no suitable tissue is removed we may consider a small (few millimetre) nasal lining biopsy for research purposes
2. a small brush sample of the nasal lining to collect a few tiny nasal cells and
3. a sample of the nasal secretions. .
4. You may also be asked about giving a blood sample which can often be taken whilst you are asleep under anaesthetic if you prefer.
5. You may also be asked about optional allergy skin prick tests as allergy sometimes complicates sinusitis.

What do I have to do?

Come to hospital for your operation as normal and we will provide the consent form and questionnaires if you decide to take part. Unfortunately, due to logistical reasons, not everyone who receives this letter will actually be approached by the research team on admission.

What are the side effects of any study procedures?

The side effects of any study procedures are exactly the same as those of your operation as discussed by your surgeon. Collecting small research samples should not cause any additional side effects.

What are the other possible disadvantages and risks of taking part?

If you have private medical insurance you should let the insurers know that you intend to take part in a research study. They will be able to tell you if this will affect your medical insurance. If during the study you were found to have a new medical condition, the condition would be dealt with following normal clinical practice.

What are the possible benefits of taking part?

There is no direct benefit to your treatment in taking part in the study. It is hoped that the information we get will help our understanding of sinusitis and improve the treatment of people with sinusitis in the future.

What happens when the research study stops?

At the end of the study we will stop looking at the nasal tissue samples and write our findings in a report. Your treatment will not be any different if you take part in the study. The end of the research study will not affect your treatment in any way. We hope to use the results of this study to work towards new treatments for sinusitis.

What if there is a problem?

If you have a concern about any aspect of this study, you should ask to speak with the researchers who will do their best to answer your questions (see contact details section below). If you remain unhappy and wish to complain formally, you can do this through the NHS Complaints Procedure. Details can be found on our hospital web site www.newcastle-hospitals.org.uk or by contacting the Patient Relations Department on 0191 223 1382.

Will my taking part in the study be kept confidential?

By agreeing to take part in this study you are consenting to the study staff collecting personal data about you, including the following:

- Your date of birth
- Your sex
- Details of your medical condition e.g. reason for the operation on the nose, previous treatment of nose problems etc.

The data will be collected and entered onto a secure database stored in a locked office only available to your doctors and the research staff. All data stored on computer will be coded, your name will not appear – you will be given a unique study number under which all data and test results will be entered.

All the information about your participation in this study will be kept confidential.

We will not notify your GP that you are taking part in the study as your hospital treatment will not be any different if you take part in the study. Participation in the study will be noted in your hospital records so that anyone who treats you will be aware that you are taking part in the study.

How will my data and tissue be stored and for how long?

Your tissue, blood sample and the data from all the patients taking part in this study, will be analysed so we can better understand the mechanism of sinusitis. Typically the tissue will only be useful for 6 weeks, when it will normally have been used up in our experiments. It is possible that in the future new tests become available that will help identify causes of sinusitis. Some samples of your nasal tissue and blood may be stored so that future testing can be done. The blood sample will be used to see if there is a body wide response in sinusitis. These samples will be coded so that there will be no direct link back to you. The tissue will be stored as part of a tissue bank in accordance with The Human Tissue Act. The tissue will be retained for up to 10 years.

What will happen if I don't want to carry on with the study?

Participation in any research study is completely voluntary and you can decide to withdraw from the study at any time. If you do withdraw from the study any information collected may still be used. If there is any stored tissue samples that can still be identified as yours they will be destroyed if you wish.
Withdrawing from the study will not affect the level of care that you get from your doctors.

What if something goes wrong?

In the event that something does go wrong and you are harmed during the research study there are no special compensation arrangements. If you are harmed and this is due to someone's negligence then you may have grounds for a legal action for compensation against Newcastle upon Tyne Hospitals NHS Trust. The normal National Health Service complaints mechanisms will still be available to you.

What will happen to the results of the research study?

The results of this study will be published in a medical journal which will be read by doctors and scientists with an interest in this area but your identity will not be revealed.

Who is organising and funding the research?

The study is funded by research grants from The Wellcome Trust and Royal College of Surgeons of England.
This study will be overseen by the Newcastle upon Tyne Hospitals NHS Trust.

Who has reviewed the study?

This study has been reviewed by the National Research Ethics Service - Sunderland Research Ethics Committee.
Contact Details:
For further information about the study you can speak to the consultant ENT surgeon in charge, Professor Janet Wilson. Please state that this is the 2013 Prof Wilson/Dr Ball sinusitis study.

Tel: 0191 2231086

Thank you for taking the time to read this information sheet.
If you decide you would like to take part in this study, you will be given a copy of this information sheet and a signed consent form to keep.

7.6 Appendix 6 – Sample participant consent form

The Newcastle upon Tyne Hospitals NHS Trust

Freeman Hospital
High Heaton
Newcastle upon Tyne
NE7 7DN

Patient Consent Form

Study Code:

Patient Initials: **Subject Number:**

Study Title: **Studying the nasal & sinus cells in rhinosinusitis**

Lead Investigator: Professor Janet Wilson (ENT surgeon)
Name of Researchers: Dr Stephen Ball

Please initial in the box

1. I confirm that I have read and understand the information sheet dated 4th April 2013 for the above study. I have had the opportunity to consider the information, ask questions and have had these answered satisfactorily. ☐
2. I understand that my participation is voluntary and that I am free to withdraw at any time, without giving any reason, without my medical care or legal rights being affected. ☐
3. I understand that relevant sections of any of my medical notes and data collected during the study, may be looked at by responsible individuals from the research team and regulatory authorities or from the NHS Trust, where it is relevant to my taking part in this research. I give permission for these individuals to have access to my records. ☐
4. I agree to biopsy & blood samples being taken and retained for future testing and understand they will be stored as part of a Tissue Bank in accordance with The Human Tissue Act and be stored for up to 10 years. ☐
5. If appropriate, and one has not already been done, I agree to being contacted about a further allergy skin prick test. ☐
6. I agree to take part in the above study ☐

Name of Patient	Signature	Date
Name of Person taking consent	Signature	Date

When completed, 1 for patient; 1 for researcher site file (original); 1 to be kept in medical notes.

7.7 Appendix 7 – Participant look up sheet

Study identifier	Patient identifier

7.8 Appendix 8 – Ethical approval

NHS
Health Research Authority

NRES Committee North East - Sunderland
Room 002
TEDCO Business Centre
Viking Business Park
Jarrow
Tyne & Wear
NE32 3DT

Telephone: 0191 4283563
Facsimile: 0191 4283432

26 April 2013

Professor Janet Wilson
Professor of Otolaryngology
Newcastle upon Tyne Hospitals NHS Trust & University of Newcastle
Department of ENT
Freeman Hospital
Freeman Road
Newcastle upon Tyne NE7 7DN

Dear Professor Wilson

Study title:	**Studying the nasal & sinus cells in rhinosinusitis**
REC reference:	**13/NE/0099**
Protocol number:	**1**
IRAS project ID:	**122939**

Thank you for your letter of 4 April 2013, responding to the Committee's request for further information on the above research [and submitting revised documentation].

The further information has been considered on behalf of the Committee by myself as Chair.

We plan to publish your research summary wording for the above study on the NRES website, together with your contact details, unless you expressly withhold permission to do so. Publication will be no earlier than three months from the date of this favourable opinion letter. Should you wish to provide a substitute contact point, require further information, or wish to withhold permission to publish, please contact the Co-ordinator Mrs Helen M Wilson, nrescommittee.northeast-sunderland@nhs.net.

Confirmation of ethical opinion

On behalf of the Committee, I am pleased to confirm a **favourable ethical opinion** for the above research on the basis described in the application form, protocol and supporting documentation [as revised], subject to the conditions specified below.

Ethical review of research sites

NHS sites

The favourable opinion applies to all NHS sites taking part in the study, subject to management permission being obtained from the NHS/HSC R&D office prior to the start of the study (see "Conditions of the favourable opinion" below).

Conditions of the favourable opinion

The favourable opinion is subject to the following conditions being met prior to the start of the study.

Management permission or approval must be obtained from each host organisation prior to the start of the study at the site concerned.

Management permission ("R&D approval") should be sought from all NHS organisations involved in the study in accordance with NHS research governance arrangements.

Guidance on applying for NHS permission for research is available in the Integrated Research Application System or at http://www.rdforum.nhs.uk.

Where a NHS organisation's role in the study is limited to identifying and referring potential participants to research sites ("participant identification centre"), guidance should be sought from the R&D office on the information it requires to give permission for this activity.

For non-NHS sites, site management permission should be obtained in accordance with the procedures of the relevant host organisation.

Sponsors are not required to notify the Committee of approvals from host organisations

It is the responsibility of the sponsor to ensure that all the conditions are complied with before the start of the study or its initiation at a particular site (as applicable).

Approved documents

The final list of documents reviewed and approved by the Committee is as follows:

Document	*Version*	*Date*
Covering Letter		04 March 2013
Covering Letter		04 April 2013
Evidence of insurance or indemnity		06 July 2012
Investigator CV	Professor Janet Wilson	21 December 2012
Letter from Sponsor	NUTH	28 January 2013
Letter of invitation to participant	Nasal surgery, Version 1.0	22 February 2013
Letter of invitation to participant	Outpatients, Version 1.0	22 February 2013
Other: CV	Stephen Ball	12 February 2013
Other: CV	Derek Mann	07 February 2013

Other: CV	Andrew Fisher	07 February 2013
Other: Letter from funder	Confirmation of funding	22 February 2013
Other: Study participant look up sheet	Version 1.0	25 January 2013
Participant Consent Form: Sinusitis surgery	Version 2.0	04 April 2013
Participant Consent Form: Non-sinusitis surgery	Version 2.0	04 April 2013
Participant Consent Form: Non-surgery	Version 2.0	04 April 2013
Participant Information Sheet: Sinusitis surgery	Version 2.0	04 April 2013
Participant Information Sheet: Non-sinusitis surgery	Version 2.0	04 April 2013
Participant Information Sheet: Non-surgery	Version 2.0	04 April 2013
Protocol	Version 1.0	25 March 2013
REC application	Version 3.4	04 March 2013
Response to Request for Further Information		

Statement of compliance

The Committee is constituted in accordance with the Governance Arrangements for Research Ethics Committees and complies fully with the Standard Operating Procedures for Research Ethics Committees in the UK.

After ethical review

Reporting requirements

The attached document *"After ethical review – guidance for researchers"* gives detailed guidance on reporting requirements for studies with a favourable opinion, including:

- Notifying substantial amendments
- Adding new sites and investigators
- Notification of serious breaches of the protocol
- Progress and safety reports
- Notifying the end of the study

The NRES website also provides guidance on these topics, which is updated in the light of changes in reporting requirements or procedures.

Feedback

You are invited to give your view of the service that you have received from the National Research Ethics Service and the application procedure. If you wish to make your views known please use the feedback form available on the website.

Further information is available at National Research Ethics Service website > After Review

13/NE/0099	**Please quote this number on all correspondence**

We are pleased to welcome researchers and R & D staff at our NRES committee members' training days – see details at http://www.hra.nhs.uk/hra-training/

With the Committee's best wishes for the success of this project.

Yours sincerely

pp 

Mr Paddy Stevenson
Chair

Email: nrescommittee.northeast-sunderland@nhs.net

Enclosures: "After ethical review – guidance for researchers"

Copy to: Jillian Peacock, Newcastle upon Tyne Hospitals NHS Foundation Trust

7.9 Appendix 9 – Newcastle Hospitals NHS Trust R&D Approvals

The Newcastle upon Tyne Hospitals NHS
NHS Foundation Trust

Royal Victoria Infirmary
Queen Victoria Road
Newcastle upon Tyne
NE1 4LP

Tel: 0191 233 6161
Fax: 0191 201 0155
www.newcastle-hospitals.nhs.uk

AJ/MC

1st May 2013

Professor Janet Wilson
Professor of Otolaryngology
The Newcastle upon Tyne Hospitals NHS Foundation Trust
Department of ENT
Freeman Hospital

Dear Professor Wilson

Trust R&D Project:	**6487**
Title of Project:	***Studying the nasal & sinus cells in rhinosinusitis***
Principal Investigator:	**Professor Janet Wilson**
Number of patients:	**180**
Funder (proposed):	**Wellcome Trust and Newcastle University Translational Fellowship Scheme / Royal College of Surgeons England**
Sponsor (proposed):	**The Newcastle Upon Tyne Hospitals NHS Foundation Trust**
REC number:	**13/NE/0099**
CLRN ID:	**122939**

Having carried out the necessary risk and site assessment for the above research project, Newcastle upon Tyne Hospitals NHS Foundation Trust grants NHS Permission for this research to take place at this Trust dependent upon:

(i) you, as Principal Investigator, agreeing to comply with the Department of Health's Research Governance Framework for Health and Social Care, and confirming your understanding of the responsibilities and duties of Principal Investigators by signing the Investigator Responsibilities Document. A copy of this document will be kept on file within the Joint Research Office.

(ii) you, as Principal Investigator, ensuring compliance of the project with all other legislation and guidelines including Caldicott Guardian approvals and compliance with the Data Protection Act 1998, Health and Safety at Work Act 1974, any requirements of the MHRA (*eg* CTA, EudraCT registration), and any other relevant UK/European guidelines or legislation (*eg* reporting of suspected adverse incidents).

(iii) where applicable, you, as Principal Investigator, should also adhere to the GMC supplementary guidance *Good practice in research* and *Consent to research* which sets out the good practice principles that doctors are expected to understand and follow if they are involved in research – see http://www.gmc-uk.org/guidance/ethical_guidance/5991.asp

Sponsorship

The Newcastle upon Tyne Hospitals NHS Foundation Trust will act as Sponsor for this project, under the Department of Health's guidelines for research in health and social care.

In addition, the Trust has a Research Governance Implementation Plan, agreed with the Department of Health, in order to fully comply with Research Governance and fulfil the responsibility of a Sponsor.

1

As the Trust is acting as Sponsor for the research and where some of the research is taking place outside of Newcastle upon Tyne, then all costs must be met for research governance audit visits to those sites. It is the responsibility of the PI to provide confirmation to the Trust of who will pay these costs. Audit is required under the Research Governance Framework for Health and Social Care. (Please note that the Trust randomly audits 10% of approved research projects annually.)

NHS Permission applies to the research described in the protocol and related documentation as listed on the favourable ethical opinion(s) from North East - Sunderland Research Ethics Committee, dated 26th April 2013. Specifically, the following versions of the key documents are approved:

Document	Version	Date
Protocol	Version 1.0	25th March 2013
Participant Information Sheet: Sinusitis surgery	Version 2.0	4th April 2013
Participant Information Sheet: Non-sinusitis surgery	Version 2.0	4th April 2013
Participant Information Sheet: Non-surgery	Version 2.0	4th April 2013
Participant Consent Form: Sinusitis surgery	Version 2.0	4th April 2013
Participant Consent Form: Non-sinusitis surgery	Version 2.0	4th April 2013
Participant Consent Form: Non-surgery	Version 2.0	4th April 2013
Letter of invitation to participant	Nasal Surgery, Version 1.0	22nd February 2013
Letter of invitation to participant	Outpatients, Version 1.0	22nd February 2013
Other: Study participant look up sheet	Version 1.0	25th January 2013

Any changes to these documents, or any other amendments to the study must be submitted to the Research Ethics Committee and MHRA (if relevant) for review – see http://www.nres.npsa.nhs.uk/applications/after-ethical-review/amendments/ for guidance). All amendments must be submitted to the R&D office for review in parallel with ethical and regulatory review so that implications of the amendment can be assessed. You must send a copy of all amendment documents to the R&D office and if the changes or amendments to the study have implications for costs or use of resources, you must also submit details of these changes.

It is the Principal Investigator's responsibility to ensure that all staff involved in the research have Honorary Research Contracts or the necessary Letters of Access. These must be issued prior to commencing the research.

In addition, unless otherwise agreed with the Trust, the research will be covered for negligence under the CNST (Clinical Negligence Scheme for Trusts), however cover for no-fault harm is the responsibility of the Principal Investigator to arrange if required.

Please also note that for any NHS employee who generates Intellectual Property *in the normal course of their duties*, it is recognised that the Intellectual Property Rights remain with the employer and not the employee.

Yours sincerely

Andrew Johnston
Research Management & Governance (RM&G) Manager

CC: Finance Department, Room 203, Cheviot Court, Freeman Hospital
Mr Philip Yates, Clinical Director
Dr Stephen Ball, Trial Coordinator

8 References

AKDIS, C. A., BACHERT, C., CINGI, C., DYKEWICZ, M. S., HELLINGS, P. W., NACLERIO, R. M., SCHLEIMER, R. P. & LEDFORD, D. 2013. Endotypes and phenotypes of chronic rhinosinusitis: a PRACTALL document of the European Academy of Allergy and Clinical Immunology and the American Academy of Allergy, Asthma & Immunology. *J Allergy Clin Immunol,* 131**,** 1479-90.

ALEXANDER, E. H. & HUDSON, M. C. 2001. Factors influencing the internalization of Staphylococcus aureus and impacts on the course of infections in humans. *Appl Microbiol Biotechnol,* 56**,** 361-6.

ALMEIDA, J. L., COLE, K. D. & PLANT, A. L. 2016. Standards for Cell Line Authentication and Beyond. *PLoS Biol,* 14**,** e1002476.

ANDERS, S., PYL, P. T. & HUBER, W. 2015. HTSeq--a Python framework to work with high-throughput sequencing data. *Bioinformatics,* 31**,** 166-9.

ARAL, M., KELES, E. & KAYGUSUZ, I. 2003. The microbiology of ethmoid and maxillary sinuses in patients with chronic sinusitis. *Am J Otolaryngol,* 24**,** 163-8.

AURORA, R., CHATTERJEE, D., HENTZLEMAN, J., PRASAD, G., SINDWANI, R. & SANFORD, T. 2013. Contrasting the microbiomes from healthy volunteers and patients with chronic rhinosinusitis. *JAMA Otolaryngol Head Neck Surg,* 139**,** 1328-38.

BACHERT, C., GEVAERT, P., HOLTAPPELS, G., CUVELIER, C. & VAN CAUWENBERGE, P. 2000. Nasal polyposis: from cytokines to growth. *Am J Rhinol,* 14**,** 279-90.

BACHERT, C., MANNENT, L., NACLERIO, R. M., MULLOL, J., FERGUSON, B. J., GEVAERT, P., HELLINGS, P., JIAO, L., WANG, L., EVANS, R. R., PIROZZI, G., GRAHAM, N. M., SWANSON, B., HAMILTON, J. D., RADIN, A., GANDHI, N. A., STAHL, N., YANCOPOULOS, G. D. & SUTHERLAND, E. R. 2016. Effect of Subcutaneous Dupilumab on Nasal Polyp Burden in Patients With Chronic Sinusitis and Nasal Polyposis: A Randomized Clinical Trial. *JAMA,* 315**,** 469-79.

BACHERT, C., VAN ZELE, T., GEVAERT, P., DE SCHRIJVER, L. & VAN CAUWENBERGE, P. 2003. Superantigens and nasal polyps. *Curr Allergy Asthma Rep,* 3**,** 523-31.

BACHERT, C., ZHANG, N., VAN ZELE, T., GEVAERT, P., PATOU, J. & VAN CAUWENBERGE, P. 2007. Staphylococcus aureus enterotoxins as immune stimulants in chronic rhinosinusitis. *Clin Allergy Immunol,* 20**,** 163-75.

BALL, S. L., MANN, D. A., WILSON, J. A. & FISHER, A. J. 2016. The Role of the Fibroblast in Inflammatory Upper Airway Conditions. *Am J Pathol,* 186**,** 225-33.

BALL, S. L., SUWARA, M. I., BORTHWICK, L. A., WILSON, J. A., MANN, D. A. & FISHER, A. J. 2015. How reliable are sino-nasal cell lines for studying the pathophysiology of chronic rhinosinusitis? *Ann Otol Rhinol Laryngol,* 124**,** 437-42.

BASSIOUNI, A., CHEN, P. G. & WORMALD, P. J. 2013. Mucosal remodeling and reversibility in chronic rhinosinusitis. *Curr Opin Allergy Clin Immunol,* 13**,** 4-12.

BASSIOUNI, A., NAIDOO, Y. & WORMALD, P. J. 2012. Does mucosal remodeling in chronic rhinosinusitis result in irreversible mucosal disease? *Laryngoscope,* 122**,** 225-9.

BENJAMINI, Y. & HOCHBERG, Y. 1995. Controlling the False Discovery Rate: A Practical and Powerful Approach to Multiple Testing. *Journal of the Royal Statistical Society. Series B (Methodological),* 57**,** 289-300.

BENNINGER, M. S., SINDWANI, R., HOLY, C. E. & HOPKINS, C. 2015. Early versus delayed endoscopic sinus surgery in patients with chronic rhinosinusitis: impact on health care utilization. *Otolaryngol Head Neck Surg,* 152**,** 546-52.

BEWICK, J., AHMED, S., CARRIE, S., HOPKINS, C., SAMA, A., SUNKARANENI, V., WOODS, J., MORRIS, S., ERSKINE, S. & PHILPOTT, C. 2016. The value of a Feasibility Study into long-term Macrolide therapy in Chronic Rhinosinusitis. *Clin Otolaryngol*.

BISGAARD, H., ROBINSON, C., ROMELING, F., MYGIND, N., CHURCH, M. & HOLGATE, S. T. 1988. Leukotriene C4 and histamine in early allergic reaction in the nose. *Allergy,* 43**,** 219-27.

BOASE, S., FOREMAN, A., CLELAND, E., TAN, L., MELTON-KREFT, R., PANT, H., HU, F. Z., EHRLICH, G. D. & WORMALD, P. J. 2013a. The microbiome of chronic rhinosinusitis: culture, molecular diagnostics and biofilm detection. *BMC Infect Dis,* 13**,** 210.

BOASE, S., JERVIS-BARDY, J., CLELAND, E., PANT, H., TAN, L. & WORMALD, P. J. 2013b. Bacterial-induced epithelial damage promotes fungal biofilm formation in a sheep model of sinusitis. *Int Forum Allergy Rhinol,* 3**,** 341-8.

BOUMANS, M. J., HOUBIERS, J. G., VERSCHUEREN, P., ISHIKURA, H., WESTHOVENS, R., BROUWER, E., ROJKOVICH, B., KELLY, S., DEN ADEL, M., ISAACS, J., JACOBS, H., GOMEZ-REINO, J., HOLTKAMP, G. M., HASTINGS, A., GERLAG, D. M. & TAK, P. P. 2012. Safety, tolerability, pharmacokinetics, pharmacodynamics and efficacy of the monoclonal antibody ASK8007 blocking osteopontin in patients with rheumatoid arthritis: a randomised, placebo controlled, proof-of-concept study. *Ann Rheum Dis,* 71**,** 180-5.

BRAZMA, A., HINGAMP, P., QUACKENBUSH, J., SHERLOCK, G., SPELLMAN, P., STOECKERT, C., AACH, J., ANSORGE, W., BALL, C. A., CAUSTON, H. C., GAASTERLAND, T., GLENISSON, P., HOLSTEGE, F. C., KIM, I. F., MARKOWITZ, V., MATESE, J. C., PARKINSON, H., ROBINSON, A., SARKANS, U., SCHULZE-KREMER, S., STEWART, J., TAYLOR, R., VILO, J. & VINGRON, M. 2001. Minimum information about a microarray experiment (MIAME)-toward standards for microarray data. *Nat Genet,* 29**,** 365-71.

BROOK, I. 1981. The importance of lactic acid levels in body fluids in the detection of bacterial infections. *Rev Infect Dis,* 3**,** 470-8.

BROOK, I. 2005. Bacteriology of acute and chronic ethmoid sinusitis. *J Clin Microbiol,* 43**,** 3479-80.

BROOK, I., YOCUM, P. & FRAZIER, E. H. 1996. Bacteriology and beta-lactamase activity in acute and chronic maxillary sinusitis. *Arch Otolaryngol Head Neck Surg,* 122**,** 418-22; discussion 423.

BROWNE, J. P., HOPKINS, C., SLACK, R. & CANO, S. J. 2007. The Sino-Nasal Outcome Test (SNOT): can we make it more clinically meaningful? *Otolaryngol Head Neck Surg,* 136**,** 736-41.

BRUNO, A., GERBINO, S., FERRARO, M., SIENA, L., BONURA, A., COLOMBO, P., LA GRUTTA, S., GALLINA, S., BALLACCHINO, A., GIAMMANCO, M., GJOMARKAJ, M. & PACE, E. 2014. Fluticasone furoate maintains epithelial homeostasis via leptin/leptin receptor pathway in nasal cells. *Mol Cell Biochem,* 396**,** 55-65.

BURUIANA, F. E., SOLA, I. & ALONSO-COELLO, P. 2010. Recombinant human interleukin 10 for induction of remission in Crohn's disease. *Cochrane Database Syst Rev***,** CD005109.

CANTOR, H. & SHINOHARA, M. L. 2009. Regulation of T-helper-cell lineage development by osteopontin: the inside story. *Nat Rev Immunol,* 9**,** 137-41.

CASTANO, R., BOSSE, Y., ENDAM, L. M. & DESROSIERS, M. 2009. Evidence of association of interleukin-1 receptor-like 1 gene polymorphisms with chronic rhinosinusitis. *Am J Rhinol Allergy,* 23**,** 377-84.

CATTELL, R. B. 1966. The Scree Test For The Number Of Factors. *Multivariate Behavioral Research,* 1**,** 245-276.

CAUNA, N., MANZETTI, G. W., HINDERER, K. H. & SWANSON, E. W. 1972. Fine structure of nasal polyps. *Ann Otol Rhinol Laryngol,* 81**,** 41-58.

CHABAUD, M., DURAND, J. M., BUCHS, N., FOSSIEZ, F., PAGE, G., FRAPPART, L. & MIOSSEC, P. 1999. Human interleukin-17: A T cell-derived proinflammatory cytokine produced by the rheumatoid synovium. *Arthritis Rheum,* 42**,** 963-70.

CHALERMWATANACHAI, T., VELASQUEZ, L. C. & BACHERT, C. 2015. The microbiome of the upper airways: focus on chronic rhinosinusitis. *World Allergy Organ J,* 8**,** 3.

CHAWES, B. L., EDWARDS, M. J., SHAMJI, B., WALKER, C., NICHOLSON, G. C., TAN, A. J., FOLSGAARD, N. V., BONNELYKKE, K., BISGAARD, H. & HANSEL, T. T. 2010. A novel method for assessing unchallenged levels of mediators in nasal epithelial lining fluid. *J Allergy Clin Immunol,* 125**,** 1387-1389 e3.

CHENAIS, B., DERJUGA, A., MASSRIEH, W., RED-HORSE, K., BELLINGARD, V., FISHER, S. J. & BLANK, V. 2005. Functional and placental expression analysis of the human NRF3 transcription factor. *Mol Endocrinol,* 19**,** 125-37.

CHEVILLARD, G. & BLANK, V. 2011. NFE2L3 (NRF3): the Cinderella of the Cap'n'Collar transcription factors. *Cell Mol Life Sci,* 68**,** 3337-48.

CHEVILLARD, G., NOUHI, Z., ANNA, D., PAQUET, M. & BLANK, V. 2010. Nrf3-deficient mice are not protected against acute lung and adipose tissue damages induced by butylated hydroxytoluene. *FEBS Lett,* 584**,** 923-8.

CHEVILLARD, G., PAQUET, M. & BLANK, V. 2011. Nfe2l3 (Nrf3) deficiency predisposes mice to T-cell lymphoblastic lymphoma. *Blood,* 117**,** 2005-8.

CHO, G. S., MOON, B. J., LEE, B. J., GONG, C. H., KIM, N. H., KIM, Y. S., KIM, H. S. & JANG, Y. J. 2013. High rates of detection of respiratory viruses in the nasal washes and mucosae of patients with chronic rhinosinusitis. *J Clin Microbiol,* 51**,** 979-84.

CHO, H. J., CHO, H. J. & KIM, H. S. 2009. Osteopontin: a multifunctional protein at the crossroads of inflammation, atherosclerosis, and vascular calcification. *Curr Atheroscler Rep,* 11**,** 206-13.

CHONG, L. Y., HEAD, K., HOPKINS, C., PHILPOTT, C., GLEW, S., SCADDING, G., BURTON, M. J. & SCHILDER, A. G. 2016. Saline irrigation for chronic rhinosinusitis. *Cochrane Database Syst Rev,* 4**,** CD011995.

CHUNG, T. F., SIPE, J. D., MCKEE, A., FINE, R. E., SCHREIBER, B. M., LIANG, J. S. & JOHNSON, R. J. 2000. Serum amyloid A in Alzheimer's disease brain is predominantly localized to myelin sheaths and axonal membrane. *Amyloid,* 7**,** 105-10.

CLOONAN, N., FORREST, A. R., KOLLE, G., GARDINER, B. B., FAULKNER, G. J., BROWN, M. K., TAYLOR, D. F., STEPTOE, A. L., WANI, S., BETHEL, G., ROBERTSON, A. J., PERKINS, A. C., BRUCE, S. J., LEE, C. C., RANADE, S. S., PECKHAM, H. E., MANNING, J. M., MCKERNAN, K. J. & GRIMMOND, S. M. 2008. Stem cell transcriptome profiling via massive-scale mRNA sequencing. *Nat Methods,* 5**,** 613-9.

COHEN, N. A. 2006. Sinonasal mucociliary clearance in health and disease. *Ann Otol Rhinol Laryngol Suppl,* 196**,** 20-6.

CONRAD, M., ANGELI, J. P., VANDENABEELE, P. & STOCKWELL, B. R. 2016. Regulated necrosis: disease relevance and therapeutic opportunities. *Nat Rev Drug Discov,* 15**,** 348-66.

CORMIER, C., BOSSE, Y., MFUNA, L., HUDSON, T. J. & DESROSIERS, M. 2009. Polymorphisms in the tumour necrosis factor alpha-induced protein 3 (TNFAIP3) gene are associated with chronic rhinosinusitis. *J Otolaryngol Head Neck Surg,* 38**,** 133-41.

COSTABEL, U. & TESCHLER, H. 1997. Biochemical changes in sarcoidosis. *Clin Chest Med,* 18**,** 827-42.

D'SOUZA, G., KREIMER, A. R., VISCIDI, R., PAWLITA, M., FAKHRY, C., KOCH, W. M., WESTRA, W. H. & GILLISON, M. L. 2007. Case-control study of human papillomavirus and oropharyngeal cancer. *N Engl J Med,* 356**,** 1944-56.

DALGORF, D. M. & HARVEY, R. J. 2013. Chapter 1: Sinonasal anatomy and function. *Am J Rhinol Allergy,* 27 Suppl 1**,** S3-6.

DAVIS, M. P., VAN DONGEN, S., ABREU-GOODGER, C., BARTONICEK, N. & ENRIGHT, A. J. 2013. Kraken: a set of tools for quality control and analysis of high-throughput sequence data. *Methods,* 63**,** 41-9.

DE OLIVEIRA, S., ROSOWSKI, E. E. & HUTTENLOCHER, A. 2016. Neutrophil migration in infection and wound repair: going forward in reverse. *Nat Rev Immunol,* 16**,** 378-91.

DERJUGA, A., GOURLEY, T. S., HOLM, T. M., HENG, H. H., SHIVDASANI, R. A., AHMED, R., ANDREWS, N. C. & BLANK, V. 2004. Complexity of CNC transcription factors as revealed by gene targeting of the Nrf3 locus. *Mol Cell Biol,* 24**,** 3286-94.

DEROEE, A. F., NARAGHI, M., SONTOU, A. F., EBRAHIMKHANI, M. R. & DEHPOUR, A. R. 2009. Nitric oxide metabolites as biomarkers for follow-up after chronic rhinosinusitis surgery. *Am J Rhinol Allergy,* 23**,** 159-61.

DERYCKE, L., EYERICH, S., VAN CROMBRUGGEN, K., PEREZ-NOVO, C., HOLTAPPELS, G., DERUYCK, N., GEVAERT, P. & BACHERT, C. 2014. Mixed T helper cell signatures in chronic rhinosinusitis with and without polyps. *PLoS One,* 9**,** e97581.

DIABETESUK. 2015. *https://www.diabetes.org.uk/About_us/What-we-say/Statistics/diabetes-prevalence-2015/* [Online]. Diabetes UK. Available: https://www.diabetes.org.uk/About_us/What-we-say/Statistics/diabetes-prevalence-2015/ [Accessed 23/08/16.

DISCOVERY, M. S. 2016. *Electrochemiluminescence* [Online]. Available: https://www.mesoscale.com/en/technical_resources/our_technology/ecl [Accessed 18/07/2016 2016].

DIVEKAR, R. D., SAMANT, S., RANK, M. A., HAGAN, J., LAL, D., O'BRIEN, E. K. & KITA, H. 2015. Immunological profiling in chronic rhinosinusitis with nasal polyps reveals distinct VEGF and GM-CSF signatures during symptomatic exacerbations. *Clin Exp Allergy,* 45**,** 767-78.

DRAKE, R., VOGL, A W, MITCHELL, A.W 2014. *Gray's Anatomy for Students: With student consult online access*, Churchill Livingstone.

DU, P. & GANG FENG, W. A. K., SIMON LIN. 2016. *Using lumi, a package processing Illumina Microarray* [Online]. Available: http://www.bioconductor.org/packages/release/bioc/vignettes/lumi/inst/doc/lumi.pdf [Accessed 17/08/2016 2016].

DU, P., KIBBE, W. A. & LIN, S. M. 2008. lumi: a pipeline for processing Illumina microarray. *Bioinformatics,* 24**,** 1547-8.

DUBIN, M. G., LIU, C., LIN, S. Y. & SENIOR, B. A. 2007. American Rhinologic Society member survey on "maximal medical therapy" for chronic rhinosinusitis. *Am J Rhinol,* 21**,** 483-8.

EARLY, S. B., HISE, K., HAN, J. K., BORISH, L. & STEINKE, J. W. 2007. Hypoxia stimulates inflammatory and fibrotic responses from nasal-polyp derived fibroblasts. *Laryngoscope,* 117**,** 511-5.

ENSEMBL. 2016. *Human assembly and gene annotation* [Online]. Available: http://www.ensembl.org/Homo_sapiens/Info/Annotation [Accessed 06/09/2016 2016].

FALCON, S. & GENTLEMAN, R. 2007. Using GOstats to test gene lists for GO term association. *Bioinformatics,* 23**,** 257-8.

FERENCE, E. H., TAN, B. K., HULSE, K. E., CHANDRA, R. K., SMITH, S. B., KERN, R. C., CONLEY, D. B. & SMITH, S. S. 2015. Commentary on gender differences in prevalence,

treatment, and quality of life of patients with chronic rhinosinusitis. *Allergy Rhinol (Providence),* 6**,** 82-8.

FOKKENS, W. J., LUND, V. J., MULLOL, J., BACHERT, C., ALOBID, I., BAROODY, F., COHEN, N., CERVIN, A., DOUGLAS, R., GEVAERT, P., GEORGALAS, C., GOOSSENS, H., HARVEY, R., HELLINGS, P., HOPKINS, C., JONES, N., JOOS, G., KALOGJERA, L., KERN, B., KOWALSKI, M., PRICE, D., RIECHELMANN, H., SCHLOSSER, R., SENIOR, B., THOMAS, M., TOSKALA, E., VOEGELS, R., WANG DE, Y. & WORMALD, P. J. 2012. European Position Paper on Rhinosinusitis and Nasal Polyps 2012. *Rhinol Suppl***,** 3 p preceding table of contents, 1-298.

FOREMAN, A., BOASE, S., PSALTIS, A. & WORMALD, P. J. 2012. Role of bacterial and fungal biofilms in chronic rhinosinusitis. *Curr Allergy Asthma Rep,* 12**,** 127-35.

FRACZEK, M., ROSTKOWSKA-NADOLSKA, B., KAPRAL, M., SZOTA, J., KRECICKI, T. & MAZUREK, U. 2013. Microarray analysis of NF-kappaB-dependent genes in chronic rhinosinusitis with nasal polyps. *Adv Clin Exp Med,* 22**,** 209-17.

GELA, A., KASETTY, G., MORGELIN, M., BERGQVIST, A., ERJEFALT, J. S., PEASE, J. E. & EGESTEN, A. 2016. Osteopontin binds and modulates functions of eosinophil-recruiting chemokines. *Allergy,* 71**,** 58-67.

GENTLEMAN, R. C., CAREY, V. J., BATES, D. M., BOLSTAD, B., DETTLING, M., DUDOIT, S., ELLIS, B., GAUTIER, L., GE, Y., GENTRY, J., HORNIK, K., HOTHORN, T., HUBER, W., IACUS, S., IRIZARRY, R., LEISCH, F., LI, C., MAECHLER, M., ROSSINI, A. J., SAWITZKI, G., SMITH, C., SMYTH, G., TIERNEY, L., YANG, J. Y. & ZHANG, J. 2004. Bioconductor: open software development for computational biology and bioinformatics. *Genome Biol,* 5**,** R80.

GEORGALAS, C., VIDELER, W., FRELING, N. & FOKKENS, W. 2010. Global Osteitis Scoring Scale and chronic rhinosinusitis: a marker of revision surgery. *Clin Otolaryngol,* 35**,** 455-61.

GEVAERT, P., CALUS, L., VAN ZELE, T., BLOMME, K., DE RUYCK, N., BAUTERS, W., HELLINGS, P., BRUSSELLE, G., DE BACQUER, D., VAN CAUWENBERGE, P. & BACHERT, C. 2013. Omalizumab is effective in allergic and nonallergic patients with nasal polyps and asthma. *J Allergy Clin Immunol,* 131**,** 110-6 e1.

GEVAERT, P., VAN BRUAENE, N., CATTAERT, T., VAN STEEN, K., VAN ZELE, T., ACKE, F., DE RUYCK, N., BLOMME, K., SOUSA, A. R., MARSHALL, R. P. & BACHERT, C. 2011. Mepolizumab, a humanized anti-IL-5 mAb, as a treatment option for severe nasal polyposis. *J Allergy Clin Immunol,* 128**,** 989-95 e1-8.

GIAVINA-BIANCHI, P., AUN, M. V., TAKEJIMA, P., KALIL, J. & AGONDI, R. C. 2016. United airway disease: current perspectives. *J Asthma Allergy,* 9**,** 93-100.

GOODWIN, S., MCPHERSON, J. D. & MCCOMBIE, W. R. 2016. Coming of age: ten years of next-generation sequencing technologies. *Nat Rev Genet,* 17**,** 333-51.

GREGORY R. WARNES, B. B., LODEWIJK BONEBAKKER, ROBERT, GENTLEMAN, W. H. A. L., THOMAS LUMLEY, MARTIN, MAECHLER, A. M., STEFFEN MOELLER, MARC SCHWARTZ, BILL & VENABLES. 2016. *Package 'gplots'* [Online]. Available: https://cran.r-project.org/web/packages/gplots/gplots.pdf [Accessed 08/08/2016.

GROBLER, A., WEITZEL, E. K., BUELE, A., JARDELEZA, C., CHEONG, Y. C., FIELD, J. & WORMALD, P. J. 2008. Pre- and postoperative sinus penetration of nasal irrigation. *Laryngoscope,* 118**,** 2078-81.

GROGER, M., BERNT, A., WOLF, M., MACK, B., PFROGNER, E., BECKER, S. & KRAMER, M. F. 2013. Eosinophils and mast cells: a comparison of nasal mucosa histology and cytology to markers in nasal discharge in patients with chronic sino-nasal diseases. *Eur Arch Otorhinolaryngol,* 270**,** 2667-76.

GUO, T., EISELE, D. W. & FAKHRY, C. 2016. The potential impact of prophylactic human papillomavirus vaccination on oropharyngeal cancer. *Cancer*.

HAMILOS, D. L. & LUND, V. J. 2004. Etiology of chronic rhinosinusitis: the role of fungus. *Ann Otol Rhinol Laryngol Suppl,* 193**,** 27-31.

HARVEY, R. J., GODDARD, J. C., WISE, S. K. & SCHLOSSER, R. J. 2008. Effects of endoscopic sinus surgery and delivery device on cadaver sinus irrigation. *Otolaryngol Head Neck Surg,* 139**,** 137-42.

HASTAN, D., FOKKENS, W. J., BACHERT, C., NEWSON, R. B., BISLIMOVSKA, J., BOCKELBRINK, A., BOUSQUET, P. J., BROZEK, G., BRUNO, A., DAHLEN, S. E., FORSBERG, B., GUNNBJORNSDOTTIR, M., KASPER, L., KRAMER, U., KOWALSKI, M. L., LANGE, B., LUNDBACK, B., SALAGEAN, E., TODO-BOM, A., TOMASSEN, P., TOSKALA, E., VAN DRUNEN, C. M., BOUSQUET, J., ZUBERBIER, T., JARVIS, D. & BURNEY, P. 2011. Chronic rhinosinusitis in Europe--an underestimated disease. A GA(2)LEN study. *Allergy,* 66**,** 1216-23.

HAWRYLOWICZ, C. M. & O'GARRA, A. 2005. Potential role of interleukin-10-secreting regulatory T cells in allergy and asthma. *Nat Rev Immunol,* 5**,** 271-83.

HEAD, K., CHONG, L. Y., PIROMCHAI, P., HOPKINS, C., PHILPOTT, C., SCHILDER, A. G. & BURTON, M. J. 2016. Systemic and topical antibiotics for chronic rhinosinusitis. *Cochrane Database Syst Rev,* 4**,** CD011994.

HEID, I. M., JACKSON, A. U., RANDALL, J. C., WINKLER, T. W., QI, L., STEINTHORSDOTTIR, V., THORLEIFSSON, G., ZILLIKENS, M. C., SPELIOTES, E. K., MAGI, R., WORKALEMAHU, T., WHITE, C. C., BOUATIA-NAJI, N., HARRIS, T. B., BERNDT, S. I., INGELSSON, E., WILLER, C. J., WEEDON, M. N., LUAN, J., VEDANTAM, S., ESKO, T., KILPELAINEN, T. O., KUTALIK, Z., LI, S., MONDA, K. L., DIXON, A. L., HOLMES, C. C., KAPLAN, L. M., LIANG, L., MIN, J. L., MOFFATT, M. F., MOLONY, C., NICHOLSON, G., SCHADT, E. E., ZONDERVAN, K. T., FEITOSA, M. F., FERREIRA, T., LANGO ALLEN, H., WEYANT, R. J., WHEELER, E., WOOD, A. R., MAGIC, ESTRADA, K., GODDARD, M. E., LETTRE, G., MANGINO, M., NYHOLT, D. R., PURCELL, S., SMITH, A. V., VISSCHER, P. M., YANG, J., MCCARROLL, S. A., NEMESH, J., VOIGHT, B. F., ABSHER, D., AMIN, N., ASPELUND, T., COIN, L., GLAZER, N. L., HAYWARD, C., HEARD-COSTA, N. L., HOTTENGA, J. J., JOHANSSON, A., JOHNSON, T., KAAKINEN, M., KAPUR, K., KETKAR, S., KNOWLES, J. W., KRAFT, P., KRAJA, A. T., LAMINA, C., LEITZMANN, M. F., MCKNIGHT, B., MORRIS, A. P., ONG, K. K., PERRY, J. R., PETERS, M. J., POLASEK, O., PROKOPENKO, I., RAYNER, N. W., RIPATTI, S., RIVADENEIRA, F., ROBERTSON, N. R., SANNA, S., SOVIO, U., SURAKKA, I., TEUMER, A., VAN WINGERDEN, S., VITART, V., ZHAO, J. H., CAVALCANTI-PROENCA, C., CHINES, P. S., FISHER, E., KULZER, J. R., LECOEUR, C., NARISU, N., SANDHOLT, C., SCOTT, L. J., SILANDER, K., STARK, K., et al. 2010. Meta-analysis identifies 13 new loci associated with waist-hip ratio and reveals sexual dimorphism in the genetic basis of fat distribution. *Nat Genet,* 42**,** 949-60.

HESONLINE. 2015. *Hospital Episode Statistics [Online]* [Online]. Available: http://digital.nhs.uk/hesdata [Accessed 23/08/16.

HIRANO, T. 2014. Revisiting the 1986 molecular cloning of interleukin 6. *Front Immunol,* 5**,** 456.

HOLLBORN, M., TENCKHOFF, S., SEIFERT, M., KOHLER, S., WIEDEMANN, P., BRINGMANN, A. & KOHEN, L. 2006. Human retinal epithelium produces and responds to placenta growth factor. *Graefes Arch Clin Exp Ophthalmol,* 244**,** 732-41.

HOPKINS, C., ANDREWS, P. & HOLY, C. E. 2015a. Does time to endoscopic sinus surgery impact outcomes in chronic rhinosinusitis? Retrospective analysis using the UK clinical practice research data. *Rhinology,* 53**,** 18-24.

HOPKINS, C., GILLETT, S., SLACK, R., LUND, V. J. & BROWNE, J. P. 2009a. Psychometric validity of the 22-item Sinonasal Outcome Test. *Clin Otolaryngol,* 34**,** 447-54.

HOPKINS, C., RIMMER, J. & LUND, V. J. 2015b. Does time to endoscopic sinus surgery impact outcomes in Chronic Rhinosinusitis? Prospective findings from the National Comparative Audit of Surgery for Nasal Polyposis and Chronic Rhinosinusitis. *Rhinology,* 53**,** 10-7.

HOPKINS, C., SLACK, R., LUND, V., BROWN, P., COPLEY, L. & BROWNE, J. 2009b. Long-term outcomes from the English national comparative audit of surgery for nasal polyposis and chronic rhinosinusitis. *Laryngoscope,* 119**,** 2459-65.

HOX, V., MAES, T., HUVENNE, W., VAN DRUNEN, C., VANOIRBEEK, J. A., JOOS, G., BACHERT, C., FOKKENS, W., CEUPPENS, J. L., NEMERY, B. & HELLINGS, P. W. 2015. A chest physician's guide to mechanisms of sinonasal disease. *Thorax,* 70**,** 353-8.

HUGHES, P., MARSHALL, D., REID, Y., PARKES, H. & GELBER, C. 2007. The costs of using unauthenticated, over-passaged cell lines: how much more data do we need? *Biotechniques,* 43**,** 575, 577-8, 581-2 passim.

HUNTER, C. A. & JONES, S. A. 2015. IL-6 as a keystone cytokine in health and disease. *Nat Immunol,* 16**,** 448-57.

ILLUMINA. 2016. *Illumina microarray solutions* [Online]. Available: http://www.illumina.com/techniques/microarrays.html [Accessed 03/08/2016 2016].

IMAI, T., BABA, M., NISHIMURA, M., KAKIZAKI, M., TAKAGI, S. & YOSHIE, O. 1997. The T cell-directed CC chemokine TARC is a highly specific biological ligand for CC chemokine receptor 4. *J Biol Chem,* 272**,** 15036-42.

ITOH, K., IGARASHI, K., HAYASHI, N., NISHIZAWA, M. & YAMAMOTO, M. 1995. Cloning and characterization of a novel erythroid cell-derived CNC family transcription factor heterodimerizing with the small Maf family proteins. *Mol Cell Biol,* 15**,** 4184-93.

JAISWAL, A. K. 2000. Regulation of genes encoding NAD(P)H:quinone oxidoreductases. *Free Radic Biol Med,* 29**,** 254-62.

JAISWAL, A. K. 2004. Regulation of antioxidant response element-dependent induction of detoxifying enzyme synthesis. *Methods Enzymol,* 378**,** 221-38.

JANG, Y. J., KWON, H. J., PARK, H. W. & LEE, B. J. 2006. Detection of rhinovirus in turbinate epithelial cells of chronic sinusitis. *Am J Rhinol,* 20**,** 634-6.

JARDELEZA, C., MILJKOVIC, D., BAKER, L., BOASE, S., TAN, N. C., KOBLAR, S. A., ZALEWSKI, P., RISCHMUELLER, M., LESTER, S., DRILLING, A., JONES, D., TAN, L. W., WORMALD, P. J. & VREUGDE, S. 2013. Inflammasome gene expression alterations in Staphylococcus aureus biofilm-associated chronic rhinosinusitis. *Rhinology,* 51**,** 315-22.

JONES, S. A. 2005. Directing transition from innate to acquired immunity: defining a role for IL-6. *J Immunol,* 175**,** 3463-8.

JORDANA M, D. J., OHNO I, FINOTTO S, DENBURG J 1995. *Nasal Polyposis: A model for chronic inflammation.,* Boston, Blackwell Scientific Publications.

KAISER, H. 1974. An index of factorial simplicity. *Psychometrika,* 39**,** 31-36.

KALLENBERG, C. G., HEERINGA, P. & STEGEMAN, C. A. 2006. Mechanisms of Disease: pathogenesis and treatment of ANCA-associated vasculitides. *Nat Clin Pract Rheumatol,* 2**,** 661-70.

KARA, C. O. 2004. Animal models of sinusitis: relevance to human disease. *Curr Allergy Asthma Rep,* 4**,** 496-9.

KAROSI, T., CSOMOR, P. & SZIKLAI, I. 2012. Tumor necrosis factor-alpha receptor expression correlates with mucosal changes and biofilm presence in chronic rhinosinusitis with nasal polyposis. *Laryngoscope,* 122**,** 504-10.

KAY, R. R., LANGRIDGE, P., TRAYNOR, D. & HOELLER, O. 2008. Changing directions in the study of chemotaxis. *Nat Rev Mol Cell Biol,* 9**,** 455-63.

KENNEDY, D. W., SENIOR, B. A., GANNON, F. H., MONTONE, K. T., HWANG, P. & LANZA, D. C. 1998. Histology and histomorphometry of ethmoid bone in chronic rhinosinusitis. *Laryngoscope,* 108**,** 502-7.

KERN, R. C., CONLEY, D. B., WALSH, W., CHANDRA, R., KATO, A., TRIPATHI-PETERS, A., GRAMMER, L. C. & SCHLEIMER, R. P. 2008. Perspectives on the etiology of chronic rhinosinusitis: an immune barrier hypothesis. *Am J Rhinol,* 22**,** 549-59.

KIM, D., SALZBERG, S. & TRAPNELL, C. 2016. *TopHat - A spliced read mapper for RNA-Seq* [Online]. Center for Computational Biology at Johns Hopkins University. Available: https://ccb.jhu.edu/software/tophat/index.shtml [Accessed 06/09/16 2016].

KIM, Y. M., JIN, J., CHOI, J. A., CHO, S. N., LIM, Y. J., LEE, J. H., SEO, J. Y., CHEN, H. Y., RHA, K. S. & SONG, C. H. 2014. Staphylococcus aureus enterotoxin B-induced endoplasmic reticulum stress response is associated with chronic rhinosinusitis with nasal polyposis. *Clin Biochem,* 47**,** 96-103.

KIMBALL, A. B., KAWAMURA, T., TEJURA, K., BOSS, C., HANCOX, A. R., VOGEL, J. C., STEINBERG, S. M., TURNER, M. L. & BLAUVELT, A. 2002. Clinical and immunologic assessment of patients with psoriasis in a randomized, double-blind, placebo-controlled trial using recombinant human interleukin 10. *Arch Dermatol,* 138**,** 1341-6.

KING, V. L., THOMPSON, J. & TANNOCK, L. R. 2011. Serum amyloid A in atherosclerosis. *Curr Opin Lipidol,* 22**,** 302-7.

KITAYA, K., YASUO, T., YAMAGUCHI, T., FUSHIKI, S. & HONJO, H. 2007. Genes regulated by interferon-gamma in human uterine microvascular endothelial cells. *Int J Mol Med,* 20**,** 689-97.

KOBAYASHI, A., ITO, E., TOKI, T., KOGAME, K., TAKAHASHI, S., IGARASHI, K., HAYASHI, N. & YAMAMOTO, M. 1999. Molecular cloning and functional characterization of a new Cap'n' collar family transcription factor Nrf3. *J Biol Chem,* 274**,** 6443-52.

KOBAYASHI, A., OHTA, T. & YAMAMOTO, M. 2004. Unique function of the Nrf2-Keap1 pathway in the inducible expression of antioxidant and detoxifying enzymes. *Methods Enzymol,* 378**,** 273-86.

KOMATSU, N., OKAMOTO, K., SAWA, S., NAKASHIMA, T., OH-HORA, M., KODAMA, T., TANAKA, S., BLUESTONE, J. A. & TAKAYANAGI, H. 2014. Pathogenic conversion of Foxp3+ T cells into TH17 cells in autoimmune arthritis. *Nat Med,* 20**,** 62-8.

KONNO, S., KUROKAWA, M., UEDE, T., NISHIMURA, M. & HUANG, S. K. 2011. Role of osteopontin, a multifunctional protein, in allergy and asthma. *Clin Exp Allergy,* 41**,** 1360-6.

KONO, H., ONDA, A. & YANAGIDA, T. 2014. Molecular determinants of sterile inflammation. *Curr Opin Immunol,* 26**,** 147-56.

KORECKA, J. A., VAN KESTEREN, R. E., BLAAS, E., SPITZER, S. O., KAMSTRA, J. H., SMIT, A. B., SWAAB, D. F., VERHAAGEN, J. & BOSSERS, K. 2013. Phenotypic characterization of retinoic acid differentiated SH-SY5Y cells by transcriptional profiling. *PLoS One,* 8**,** e63862.

KOU, W., HU, G. H., YAO, H. B., WANG, X. Q., SHEN, Y., KANG, H. Y. & HONG, S. L. 2012. Regulation of transforming growth factor-beta1 activation and expression in the tissue remodeling involved in chronic rhinosinusitis. *ORL J Otorhinolaryngol Relat Spec,* 74**,** 172-8.

KOUZAKI, H., SENO, S., FUKUI, J., OWAKI, S. & SHIMIZU, T. 2009. Role of platelet-derived growth factor in airway remodeling in rhinosinusitis. *Am J Rhinol Allergy,* 23**,** 273-80.

KRAMER, A., GREEN, J., POLLARD, J., JR. & TUGENDREICH, S. 2014. Causal analysis approaches in Ingenuity Pathway Analysis. *Bioinformatics,* 30**,** 523-30.

KRUEGER, J. G. 2012. Hiding under the skin: A welcome surprise in psoriasis. *Nat Med,* 18**,** 1750-1.
KUDOH, S., AZUMA, A., YAMAMOTO, M., IZUMI, T. & ANDO, M. 1998. Improvement of survival in patients with diffuse panbronchiolitis treated with low-dose erythromycin. *Am J Respir Crit Care Med,* 157**,** 1829-32.
KUEHNEMUND, M., ISMAIL, C., BRIEGER, J., SCHAEFER, D. & MANN, W. J. 2004. Untreated chronic rhinosinusitis: a comparison of symptoms and mediator profiles. *Laryngoscope,* 114**,** 561-5.
KUHN, K., BAKER, S. C., CHUDIN, E., LIEU, M. H., OESER, S., BENNETT, H., RIGAULT, P., BARKER, D., MCDANIEL, T. K. & CHEE, M. S. 2004. A novel, high-performance random array platform for quantitative gene expression profiling. *Genome Res,* 14**,** 2347-56.
KUMAR, M., SEEGER, W. & VOSWINCKEL, R. 2014. Senescence-associated secretory phenotype and its possible role in chronic obstructive pulmonary disease. *Am J Respir Cell Mol Biol,* 51**,** 323-33.
LAL, D., SCIANNA, J. M. & STANKIEWICZ, J. A. 2009. Efficacy of targeted medical therapy in chronic rhinosinusitis, and predictors of failure. *Am J Rhinol Allergy,* 23**,** 396-400.
LANDSCHULZ, W. H., JOHNSON, P. F. & MCKNIGHT, S. L. 1988. The leucine zipper: a hypothetical structure common to a new class of DNA binding proteins. *Science,* 240**,** 1759-64.
LANE, A. P. 2009. The role of innate immunity in the pathogenesis of chronic rhinosinusitis. *Curr Allergy Asthma Rep,* 9**,** 205-12.
LAZARUS, S. C. 2006. Mild persistent asthma: is any treatment needed? *J Allergy Clin Immunol,* 118**,** 805-8.
LEE, S. & LANE, A. P. 2011. Chronic rhinosinusitis as a multifactorial inflammatory disorder. *Curr Infect Dis Rep,* 13**,** 159-68.
LENGTH, R. V. 2000. *Two sample size practices that I don't reccomend* [Online]. University of Iowa, Department of Statistics. Available: http://homepage.divms.uiowa.edu/~rlenth/Power/2badHabits.pdf 2016].
LEUNG, N., MAWBY, T. A., TURNER, H. & QUREISHI, A. 2016. Osteitis and chronic rhinosinusitis: a review of the current literature. *Eur Arch Otorhinolaryngol,* 273**,** 2917-23.
LIN, R. Y., NAHAL, A., LEE, M. & MENIKOFF, H. 2001. Cytologic distinctions between clinical groups using curette-probe compared to cytology brush. *Ann Allergy Asthma Immunol,* 86**,** 226-31.
LIN, S. M., DU, P., HUBER, W. & KIBBE, W. A. 2008. Model-based variance-stabilizing transformation for Illumina microarray data. *Nucleic Acids Res,* 36**,** e11.
LINKE, R., PRIES, R., KONNECKE, M., BRUCHHAGE, K. L., BOSCKE, R., GEBHARD, M. & WOLLENBERG, B. 2013. Increased activation and differentiated localization of native and phosphorylated STAT3 in nasal polyps. *Int Arch Allergy Immunol,* 162**,** 290-8.
LIU, W. L., ZHANG, H., ZHENG, Y., WANG, H. T., CHEN, F. H., XU, L., WEI, Y., SUN, Y. Q., SHI, J. B. & LI, H. B. 2015. Expression and regulation of osteopontin in chronic rhinosinusitis with nasal polyps. *Clin Exp Allergy,* 45**,** 414-22.
LOOMIS-KING, H., FLAHERTY, K. R. & MOORE, B. B. 2013. Pathogenesis, current treatments and future directions for idiopathic pulmonary fibrosis. *Curr Opin Pharmacol,* 13**,** 377-85.
LOVE, M. I., HUBER, W. & ANDERS, S. 2014. Moderated estimation of fold change and dispersion for RNA-seq data with DESeq2. *Genome Biol,* 15**,** 550.
LUND, V. J. & MACKAY, I. S. 1993. Staging in rhinosinusitus. *Rhinology,* 31**,** 183-4.

LUTTUN, A., TJWA, M., MOONS, L., WU, Y., ANGELILLO-SCHERRER, A., LIAO, F., NAGY, J. A., HOOPER, A., PRILLER, J., DE KLERCK, B., COMPERNOLLE, V., DACI, E., BOHLEN, P., DEWERCHIN, M., HERBERT, J. M., FAVA, R., MATTHYS, P., CARMELIET, G., COLLEN, D., DVORAK, H. F., HICKLIN, D. J. & CARMELIET, P. 2002. Revascularization of ischemic tissues by PlGF treatment, and inhibition of tumor angiogenesis, arthritis and atherosclerosis by anti-Flt1. *Nat Med,* 8**,** 831-40.

MACHADO-CARVALHO, L., ROCA-FERRER, J. & PICADO, C. 2014. Prostaglandin E2 receptors in asthma and in chronic rhinosinusitis/nasal polyps with and without aspirin hypersensitivity. *Respir Res,* 15**,** 100.

MAGLIONE, D., GUERRIERO, V., VIGLIETTO, G., DELLI-BOVI, P. & PERSICO, M. G. 1991. Isolation of a human placenta cDNA coding for a protein related to the vascular permeability factor. *Proc Natl Acad Sci U S A,* 88**,** 9267-71.

MAUNE, S., BERNER, I., STICHERLING, M., KULKE, R., BARTELS, J. & SCHRODER, J. M. 1996. Fibroblasts but not epithelial cells obtained from human nasal mucosa produce the chemokine RANTES. *Rhinology,* 34**,** 210-4.

MAVRODI, A. & PARASKEVAS, G. 2013. Evolution of the paranasal sinuses' anatomy through the ages. *Anat Cell Biol,* 46**,** 235-8.

MCCAIG, L. F. & HUGHES, J. M. 1995. Trends in antimicrobial drug prescribing among office-based physicians in the United States. *JAMA,* 273**,** 214-9.

MELTZER, E. O., HAMILOS, D. L., HADLEY, J. A., LANZA, D. C., MARPLE, B. F., NICKLAS, R. A., BACHERT, C., BARANIUK, J., BAROODY, F. M., BENNINGER, M. S., BROOK, I., CHOWDHURY, B. A., DRUCE, H. M., DURHAM, S., FERGUSON, B., GWALTNEY, J. M., KALINER, M., KENNEDY, D. W., LUND, V., NACLERIO, R., PAWANKAR, R., PICCIRILLO, J. F., ROHANE, P., SIMON, R., SLAVIN, R. G., TOGIAS, A., WALD, E. R., ZINREICH, S. J., AMERICAN ACADEMY OF ALLERGY, A., IMMUNOLOGY, AMERICAN ACADEMY OF OTOLARYNGIC, A., AMERICAN ACADEMY OF, O.-H., NECK, S., AMERICAN COLLEGE OF ALLERGY, A., IMMUNOLOGY & AMERICAN RHINOLOGIC, S. 2004. Rhinosinusitis: establishing definitions for clinical research and patient care. *J Allergy Clin Immunol,* 114**,** 155-212.

MENTEN, P., WUYTS, A. & VAN DAMME, J. 2002. Macrophage inflammatory protein-1. *Cytokine Growth Factor Rev,* 13**,** 455-81.

MERKLE, H. P., DITZINGER, G., LANG, S. R., PETER, H. & SCHMIDT, M. C. 1998. In vitro cell models to study nasal mucosal permeability and metabolism. *Adv Drug Deliv Rev,* 29**,** 51-79.

MERTENS, M. & SINGH, J. A. 2009. Anakinra for rheumatoid arthritis. *Cochrane Database Syst Rev***,** CD005121.

MESSERKLINGER, W. 1980. [Diagnosis and endoscopic surgery of the nose and its adjoining structures]. *Acta Otorhinolaryngol Belg,* 34**,** 170-6.

MFUNA-ENDAM, L., ZHANG, Y. & DESROSIERS, M. Y. 2011. Genetics of rhinosinusitis. *Curr Allergy Asthma Rep,* 11**,** 236-46.

MFUNA ENDAM, L., CORMIER, C., BOSSE, Y., FILALI-MOUHIM, A. & DESROSIERS, M. 2010. Association of IL1A, IL1B, and TNF gene polymorphisms with chronic rhinosinusitis with and without nasal polyposis: A replication study. *Arch Otolaryngol Head Neck Surg,* 136**,** 187-92.

MILJKOVIC, D., BASSIOUNI, A., COOKSLEY, C., OU, J., HAUBEN, E., WORMALD, P. J. & VREUGDE, S. 2014. Association between group 2 innate lymphoid cells enrichment, nasal polyps and allergy in chronic rhinosinusitis. *Allergy,* 69**,** 1154-61.

MOHAMMED, K. A., NASREEN, N., TEPPER, R. S. & ANTONY, V. B. 2007. Cyclic stretch induces PlGF expression in bronchial airway epithelial cells via nitric oxide release. *Am J Physiol Lung Cell Mol Physiol,* 292**,** L559-66.

MOLL, R., KREPLER, R. & FRANKE, W. W. 1983. Complex cytokeratin polypeptide patterns observed in certain human carcinomas. *Differentiation,* 23**,** 256-69.

MOORE, G. E. & SANDBERG, A. A. 1964. Studies of a Human Tumor Cell Line with a Diploid Karyotype. *Cancer,* 17**,** 170-5.

MOORE, K. W., DE WAAL MALEFYT, R., COFFMAN, R. L. & O'GARRA, A. 2001. Interleukin-10 and the interleukin-10 receptor. *Annu Rev Immunol,* 19**,** 683-765.

MOORHEAD, P. S. 1965. Human tumor cell line with a quasi-diploid karyotype (RPMI 2650). *Exp Cell Res,* 39**,** 190-6.

MORLEY, A. D. & SHARP, H. R. 2006. A review of sinonasal outcome scoring systems - which is best? *Clin Otolaryngol,* 31**,** 103-9.

MORTAZAVI, A., WILLIAMS, B. A., MCCUE, K., SCHAEFFER, L. & WOLD, B. 2008. Mapping and quantifying mammalian transcriptomes by RNA-Seq. *Nat Methods,* 5**,** 621-8.

MULLER, L., BRIGHTON, L. E., CARSON, J. L., FISCHER, W. A., 2ND & JASPERS, I. 2013. Culturing of human nasal epithelial cells at the air liquid interface. *J Vis Exp*.

MULLOL, J., LOPEZ, E., ROCA-FERRER, J., XAUBET, A., PUJOLS, L., FERNANDEZ-MORATA, J. C., FABRA, J. M. & PICADO, C. 1997. Effects of topical anti-inflammatory drugs on eosinophil survival primed by epithelial cells. Additive effect of glucocorticoids and nedocromil sodium. *Clin Exp Allergy,* 27**,** 1432-41.

MULLOL, J., ROCA-FERRER, J., XAUBET, A., RASERRA, J. & PICADO, C. 2000. Inhibition of GM-CSF secretion by topical corticosteroids and nedocromil sodium. A comparison study using nasal polyp epithelial cells. *Respir Med,* 94**,** 428-31.

MULLOL, J., XAUBET, A., LOPEZ, E., ROCA-FERRER, J. & PICADO, C. 1995. Comparative study of the effects of different glucocorticosteroids on eosinophil survival primed by cultured epithelial cell supernatants obtained from nasal mucosa and nasal polyps. *Thorax,* 50**,** 270-4.

MUNOZ-ESPIN, D. & SERRANO, M. 2014. Cellular senescence: from physiology to pathology. *Nat Rev Mol Cell Biol,* 15**,** 482-96.

NAGAI, H., SHISHIDO, H., YONEDA, R., YAMAGUCHI, E., TAMURA, A. & KURASHIMA, A. 1991. Long-term low-dose administration of erythromycin to patients with diffuse panbronchiolitis. *Respiration,* 58**,** 145-9.

NAGALAKSHMI, U., WANG, Z., WAERN, K., SHOU, C., RAHA, D., GERSTEIN, M. & SNYDER, M. 2008. The transcriptional landscape of the yeast genome defined by RNA sequencing. *Science,* 320**,** 1344-9.

NAYLOR, A. J., FILER, A. & BUCKLEY, C. D. 2013. The role of stromal cells in the persistence of chronic inflammation. *Clin Exp Immunol,* 171**,** 30-5.

NCBI. 2015. *Gene Expression Omnibus* [Online]. Available: http://www.ncbi.nlm.nih.gov/geo.

NICHOLSON, G. C., KARIYAWASAM, H. H., TAN, A. J., HOHLFELD, J. M., QUINN, D., WALKER, C., RODMAN, D., WESTWICK, J., JURCEVIC, S., KON, O. M., BARNES, P. J., KRUG, N. & HANSEL, T. T. 2011. The effects of an anti-IL-13 mAb on cytokine levels and nasal symptoms following nasal allergen challenge. *J Allergy Clin Immunol,* 128**,** 800-807 e9.

NONAKA, M., FUKUMOTO, A., OGIHARA, N., PAWANKAR, R., SAKANUSHI, A. & YAGI, T. 2007. Expression of MCP-4 by TLR ligand-stimulated nasal polyp fibroblasts. *Acta Otolaryngol,* 127**,** 1304-9.

NONAKA, M., FUKUMOTO, A., OGIHARA, N., SAKANUSHI, A., PAWANKAR, R. & YAGI, T. 2010a. Synergistic induction of thymic stromal lymphopoietin by tumor necrosis

factor alpha and Th2 cytokine in nasal polyp fibroblasts. *Am J Rhinol Allergy,* 24**,** e14-8.

NONAKA, M., NONAKA, R., WOOLLEY, K., ADELROTH, E., MIURA, K., OKHAWARA, Y., GLIBETIC, M., NAKANO, K., O'BYRNE, P., DOLOVICH, J. & ET AL. 1995. Distinct immunohistochemical localization of IL-4 in human inflamed airway tissues. IL-4 is localized to eosinophils in vivo and is released by peripheral blood eosinophils. *J Immunol,* 155**,** 3234-44.

NONAKA, M., OGIHARA, N., FUKUMOTO, A., SAKANUSHI, A., KUSAMA, K., PAWANKAR, R. & YAGI, T. 2010b. Combined stimulation with Poly(I:C), TNF-alpha and Th2 cytokines induces TARC production by human fibroblasts from the nose, bronchioles and lungs. *Int Arch Allergy Immunol,* 152**,** 327-41.

NONAKA, M., OGIHARA, N., FUKUMOTO, A., SAKANUSHI, A., KUSAMA, K., PAWANKAR, R. & YAGI, T. 2010c. Nasal polyp fibroblasts produce MIP-3alpha in response to toll-like receptor ligands and cytokine stimulation. *Rhinology,* 48**,** 41-6.

NONAKA, M., PAWANKAR, R., SAJI, F. & YAGI, T. 1999. Distinct expression of RANTES and GM-CSF by lipopolysaccharide in human nasal fibroblasts but not in other airway fibroblasts. *Int Arch Allergy Immunol,* 119**,** 314-21.

NOUHI, Z., CHEVILLARD, G., DERJUGA, A. & BLANK, V. 2007. Endoplasmic reticulum association and N-linked glycosylation of the human Nrf3 transcription factor. *FEBS Lett,* 581**,** 5401-6.

O'HARA, R., MURPHY, E. P., WHITEHEAD, A. S., FITZGERALD, O. & BRESNIHAN, B. 2000. Acute-phase serum amyloid A production by rheumatoid arthritis synovial tissue. *Arthritis Res,* 2**,** 142-4.

ODORISIO, T., CIANFARANI, F., FAILLA, C. M. & ZAMBRUNO, G. 2006. The placenta growth factor in skin angiogenesis. *J Dermatol Sci,* 41**,** 11-9.

OHLRICH, E. J., CULLINAN, M. P. & SEYMOUR, G. J. 2009. The immunopathogenesis of periodontal disease. *Aust Dent J,* 54 Suppl 1**,** S2-10.

ONG, H. X., JACKSON, C. L., COLE, J. L., LACKIE, P. M., TRAINI, D., YOUNG, P. M., LUCAS, J. & CONWAY, J. 2016. Primary Air-Liquid Interface Culture of Nasal Epithelium for Nasal Drug Delivery. *Mol Pharm*.

ONUORA, S. 2012. Rheumatoid arthritis: RF levels predict RA risk in the general population. *Nat Rev Rheumatol,* 8**,** 562.

OOI, E. H., WORMALD, P. J. & TAN, L. W. 2008. Innate immunity in the paranasal sinuses: a review of nasal host defenses. *Am J Rhinol,* 22**,** 13-9.

ORLANDI, R. R., THIBEAULT, S. L. & FERGUSON, B. J. 2007. Microarray analysis of allergic fungal sinusitis and eosinophilic mucin rhinosinusitis. *Otolaryngol Head Neck Surg,* 136**,** 707-13.

ORNITZ, D. M. & ITOH, N. 2001. Fibroblast growth factors. *Genome Biol,* 2**,** REVIEWS3005.

OWINGS, M. F. & KOZAK, L. J. 1998. Ambulatory and inpatient procedures in the United States, 1996. *Vital Health Stat 13***,** 1-119.

OYER, S. L., NAGEL, W. & MULLIGAN, J. K. 2013. Differential expression of adhesion molecules by sinonasal fibroblasts among control and chronic rhinosinusitis patients. *Am J Rhinol Allergy,* 27**,** 381-6.

PACE, E., FERRARO, M., DI VINCENZO, S., GERBINO, S., BRUNO, A., LANATA, L. & GJOMARKAJ, M. 2014. Oxidative stress and innate immunity responses in cigarette smoke stimulated nasal epithelial cells. *Toxicol In Vitro,* 28**,** 292-9.

PAINTER, J. N., ANDERSON, C. A., NYHOLT, D. R., MACGREGOR, S., LIN, J., LEE, S. H., LAMBERT, A., ZHAO, Z. Z., ROSEMAN, F., GUO, Q., GORDON, S. D., WALLACE, L., HENDERS, A. K., VISSCHER, P. M., KRAFT, P., MARTIN, N. G., MORRIS, A. P., TRELOAR,

S. A., KENNEDY, S. H., MISSMER, S. A., MONTGOMERY, G. W. & ZONDERVAN, K. T. 2011. Genome-wide association study identifies a locus at 7p15.2 associated with endometriosis. *Nat Genet,* 43**,** 51-4.

PAOLA, R. D. & CUZZOCREA, S. 2007. Peroxisome proliferator-activated receptors and acute lung injury. *PPAR Res,* 2007**,** 63745.

PARK, C. S., PARK, Y. S., PARK, Y. J., CHO, J. H., KANG, J. M. & KIM, S. Y. 2007. The inhibitory effects of macrolide antibiotics on bone remodeling in chronic rhinosinusitis. *Otolaryngol Head Neck Surg,* 137**,** 274-9.

PAUWELS, B., JONSTAM, K. & BACHERT, C. 2015. Emerging biologics for the treatment of chronic rhinosinusitis. *Expert Rev Clin Immunol,* 11**,** 349-61.

PAWANKAR, R. & NONAKA, M. 2007. Inflammatory mechanisms and remodeling in chronic rhinosinusitis and nasal polyps. *Curr Allergy Asthma Rep,* 7**,** 202-8.

PAYNE, S. C., HAN, J. K., HUYETT, P., NEGRI, J., KROPF, E. Z., BORISH, L. & STEINKE, J. W. 2008. Microarray analysis of distinct gene transcription profiles in non-eosinophilic chronic sinusitis with nasal polyps. *Am J Rhinol,* 22**,** 568-81.

PENNEBAKER, J. W. 1976. *The Psychology of Physical Symptoms*, Springer-Verlag.

PEREZ-NOVO, C. A., WATELET, J. B., CLAEYS, C., VAN CAUWENBERGE, P. & BACHERT, C. 2005. Prostaglandin, leukotriene, and lipoxin balance in chronic rhinosinusitis with and without nasal polyposis. *J Allergy Clin Immunol,* 115**,** 1189-96.

PICCININI, A. M. & MIDWOOD, K. S. 2010. DAMPening inflammation by modulating TLR signalling. *Mediators Inflamm,* 2010.

PICCIRILLO, J. F., MERRITT, M. G., JR. & RICHARDS, M. L. 2002. Psychometric and clinimetric validity of the 20-Item Sino-Nasal Outcome Test (SNOT-20). *Otolaryngol Head Neck Surg,* 126**,** 41-7.

POLYAK, K. & WEINBERG, R. A. 2009. Transitions between epithelial and mesenchymal states: acquisition of malignant and stem cell traits. *Nat Rev Cancer,* 9**,** 265-73.

PONIKAU, J. U., SHERRIS, D. A., KERN, E. B., HOMBURGER, H. A., FRIGAS, E., GAFFEY, T. A. & ROBERTS, G. D. 1999. The diagnosis and incidence of allergic fungal sinusitis. *Mayo Clin Proc,* 74**,** 877-84.

PREVETE, N., SALZANO, F. A., ROSSI, F. W., RIVELLESE, F., DELLEPIANE, M., GUASTINI, L., MORA, R., MARONE, G., SALAMI, A. & DE PAULIS, A. 2011. Role(s) of formyl-peptide receptors expressed in nasal epithelial cells. *J Biol Regul Homeost Agents,* 25**,** 553-64.

PROUDFOOT, A. E. 2002. Chemokine receptors: multifaceted therapeutic targets. *Nat Rev Immunol,* 2**,** 106-15.

RAMAKRISHNAN, V. R., FEAZEL, L. M., GITOMER, S. A., IR, D., ROBERTSON, C. E. & FRANK, D. N. 2013. The microbiome of the middle meatus in healthy adults. *PLoS One,* 8**,** e85507.

RAMAKRISHNAN, V. R., HAUSER, L. J. & FRANK, D. N. 2016. The sinonasal bacterial microbiome in health and disease. *Curr Opin Otolaryngol Head Neck Surg,* 24**,** 20-5.

RAMANATHAN, M., JR., LEE, W. K., DUBIN, M. G., LIN, S., SPANNHAKE, E. W. & LANE, A. P. 2007. Sinonasal epithelial cell expression of toll-like receptor 9 is decreased in chronic rhinosinusitis with polyps. *Am J Rhinol,* 21**,** 110-6.

RAMESH, S., BRODSKY, L., AFSHANI, E., PIZZUTO, M., ISHMAN, M., HELM, J. & BALLOW, M. 1997. Open trial of intravenous immune serum globulin for chronic sinusitis in children. *Ann Allergy Asthma Immunol,* 79**,** 119-24.

RAY, N. F., BARANIUK, J. N., THAMER, M., RINEHART, C. S., GERGEN, P. J., KALINER, M., JOSEPHS, S. & PUNG, Y. H. 1999. Healthcare expenditures for sinusitis in 1996: contributions of asthma, rhinitis, and other airway disorders. *J Allergy Clin Immunol,* 103**,** 408-14.

RHEE, D. K., PARK, S. H. & JANG, Y. K. 2008. Molecular signatures associated with transformation and progression to breast cancer in the isogenic MCF10 model. *Genomics,* 92**,** 419-28.

RIECHELMANN, H., DEUTSCHLE, T., ROZSASI, A., KECK, T., POLZEHL, D. & BURNER, H. 2005. Nasal biomarker profiles in acute and chronic rhinosinusitis. *Clin Exp Allergy,* 35**,** 1186-91.

ROMAGNANI, S. 2002. Cytokines and chemoattractants in allergic inflammation. *Mol Immunol,* 38**,** 881-5.

RUDACK, C., HERMANN, W., EBLE, J. & SCHROEDER, J. M. 2002. Neutrophil chemokines in cultured nasal fibroblasts. *Allergy,* 57**,** 1159-64.

SACKS, P. L., SNIDVONGS, K., ROM, D., EARLS, P., SACKS, R. & HARVEY, R. J. 2013. The impact of neo-osteogenesis on disease control in chronic rhinosinusitis after primary surgery. *Int Forum Allergy Rhinol,* 3**,** 823-7.

SAID, E. A., DUPUY, F. P., TRAUTMANN, L., ZHANG, Y., SHI, Y., EL-FAR, M., HILL, B. J., NOTO, A., ANCUTA, P., PERETZ, Y., FONSECA, S. G., VAN GREVENYNGHE, J., BOULASSEL, M. R., BRUNEAU, J., SHOUKRY, N. H., ROUTY, J. P., DOUEK, D. C., HADDAD, E. K. & SEKALY, R. P. 2010. Programmed death-1-induced interleukin-10 production by monocytes impairs CD4+ T cell activation during HIV infection. *Nat Med,* 16**,** 452-9.

SALIB, R. J., LAU, L. C. & HOWARTH, P. H. 2005. The novel use of the human nasal epithelial cell line RPMI 2650 as an in vitro model to study the influence of allergens and cytokines on transforming growth factor-beta gene expression and protein release. *Clin Exp Allergy,* 35**,** 811-9.

SAMTOOLS. 2016. *Samtools -a suite of programs for interacting with high-throughput sequencing data.* [Online]. Available: http://www.htslib.org/ [Accessed 06/09/2016 2016].

SANCHEZ-SEGURA, A., BRIEVA, J. A. & RODRIGUEZ, C. 1998. T lymphocytes that infiltrate nasal polyps have a specialized phenotype and produce a mixed TH1/TH2 pattern of cytokines. *J Allergy Clin Immunol,* 102**,** 953-60.

SANGER, F., NICKLEN, S. & COULSON, A. R. 1977. DNA sequencing with chain-terminating inhibitors. *Proc Natl Acad Sci U S A,* 74**,** 5463-7.

SANKARANARAYANAN, K. & JAISWAL, A. K. 2004. Nrf3 negatively regulates antioxidant-response element-mediated expression and antioxidant induction of NAD(P)H:quinone oxidoreductase1 gene. *J Biol Chem,* 279**,** 50810-7.

SASAMA, J., SHERRIS, D. A., SHIN, S. H., KEPHART, G. M., KERN, E. B. & PONIKAU, J. U. 2005. New paradigm for the roles of fungi and eosinophils in chronic rhinosinusitis. *Curr Opin Otolaryngol Head Neck Surg,* 13**,** 2-8.

SCHETT, G., DAYER, J. M. & MANGER, B. 2016. Interleukin-1 function and role in rheumatic disease. *Nat Rev Rheumatol,* 12**,** 14-24.

SHAN, X., CHEN, L., CAO, M., XU, L. & ZHANG, S. 2006. Effects of human soluble BAFF synthesized in Escherichia coli on CD4+ and CD8+ T lymphocytes as well as NK cells in mice. *Physiol Res,* 55**,** 301-7.

SHINOHARA, M. L., LU, L., BU, J., WERNECK, M. B., KOBAYASHI, K. S., GLIMCHER, L. H. & CANTOR, H. 2006. Osteopontin expression is essential for interferon-alpha production by plasmacytoid dendritic cells. *Nat Immunol,* 7**,** 498-506.

SHUN, C. T., LIN, S. K., HONG, C. Y., HUANG, H. M. & LIU, C. M. 2011. Hypoxia induces cysteine-rich 61, vascular endothelial growth factor, and interleukin-8 expressions in human nasal polyp fibroblasts: An implication of neutrophils in the pathogenesis of nasal polyposis. *Am J Rhinol Allergy,* 25**,** 15-8.

SINGH, J. A., HOSSAIN, A., TANJONG GHOGOMU, E., KOTB, A., CHRISTENSEN, R., MUDANO, A. S., MAXWELL, L. J., SHAH, N. P., TUGWELL, P. & WELLS, G. A. 2016. Biologics or tofacitinib for rheumatoid arthritis in incomplete responders to methotrexate or other traditional disease-modifying anti-rheumatic drugs: a systematic review and network meta-analysis. *Cochrane Database Syst Rev*, CD012183.

SMITH, K. A., ORLANDI, R. R. & RUDMIK, L. 2015. Cost of adult chronic rhinosinusitis: A systematic review. *Laryngoscope,* 125, 1547-56.

SNIDVONGS, K., EARLS, P., DALGORF, D., SACKS, R., PRATT, E. & HARVEY, R. J. 2014. Osteitis is a misnomer: a histopathology study in primary chronic rhinosinusitis. *Int Forum Allergy Rhinol,* 4, 390-6.

SOLER, Z. M., WITTENBERG, E., SCHLOSSER, R. J., MACE, J. C. & SMITH, T. L. 2011. Health state utility values in patients undergoing endoscopic sinus surgery. *Laryngoscope,* 121, 2672-8.

STEINKE, J. W., CROUSE, C. D., BRADLEY, D., HISE, K., LYNCH, K., KOUNTAKIS, S. E. & BORISH, L. 2004. Characterization of interleukin-4-stimulated nasal polyp fibroblasts. *Am J Respir Cell Mol Biol,* 30, 212-9.

SUH, J. D. & KENNEDY, D. W. 2011. Treatment options for chronic rhinosinusitis. *Proc Am Thorac Soc,* 8, 132-40.

SUN, D., MATSUNE, S., OHORI, J., FUKUIWA, T., USHIKAI, M. & KURONO, Y. 2005. TNF-alpha and endotoxin increase hypoxia-induced VEGF production by cultured human nasal fibroblasts in synergistic fashion. *Auris Nasus Larynx,* 32, 243-9.

SUWARA, M. I., GREEN, N. J., BORTHWICK, L. A., MANN, J., MAYER-BARBER, K. D., BARRON, L., CORRIS, P. A., FARROW, S. N., WYNN, T. A., FISHER, A. J. & MANN, D. A. 2014. IL-1alpha released from damaged epithelial cells is sufficient and essential to trigger inflammatory responses in human lung fibroblasts. *Mucosal Immunol,* 7, 684-93.

SYKIOTIS, G. P. & BOHMANN, D. 2010. Stress-activated cap'n'collar transcription factors in aging and human disease. *Sci Signal,* 3, re3.

TAKAHASHI, N., YAMADA, T., NARITA, N. & FUJIEDA, S. 2006. Double-stranded RNA induces production of RANTES and IL-8 by human nasal fibroblasts. *Clin Immunol,* 118, 51-8.

TAKEUCHI, O. & AKIRA, S. 2010. Pattern recognition receptors and inflammation. *Cell,* 140, 805-20.

TANDE, A. J. & PATEL, R. 2014. Prosthetic joint infection. *Clin Microbiol Rev,* 27, 302-45.

TAUB, D. D., CONLON, K., LLOYD, A. R., OPPENHEIM, J. J. & KELVIN, D. J. 1993. Preferential migration of activated CD4+ and CD8+ T cells in response to MIP-1 alpha and MIP-1 beta. *Science,* 260, 355-8.

TCHKONIA, T., ZHU, Y., VAN DEURSEN, J., CAMPISI, J. & KIRKLAND, J. L. 2013. Cellular senescence and the senescent secretory phenotype: therapeutic opportunities. *J Clin Invest,* 123, 966-72.

THAI, L. H., CHARLES, P., RESCHE-RIGON, M., DESSEAUX, K. & GUILLEVIN, L. 2014. Are anti-proteinase-3 ANCA a useful marker of granulomatosis with polyangiitis (Wegener's) relapses? Results of a retrospective study on 126 patients. *Autoimmun Rev,* 13, 313-8.

THURSTONE, L. 1948. Thurstone, L. L. Multiple-factor analysis. Chicago: University of Chicago Press, 1947, pp. 535. $7.50. *Journal of Clinical Psychology,* 4, 224-224.

TOKI, T., ITOH, J., KITAZAWA, J., ARAI, K., HATAKEYAMA, K., AKASAKA, J., IGARASHI, K., NOMURA, N., YOKOYAMA, M., YAMAMOTO, M. & ITO, E. 1997. Human small Maf proteins form heterodimers with CNC family transcription factors and recognize the NF-E2 motif. *Oncogene,* 14, 1901-10.

TOMA, S. & HOPKINS, C. 2016. Stratification of SNOT-22 scores into mild, moderate or severe and relationship with other subjective instruments. *Rhinology,* 54**,** 129-33.

TOMASSEN, P., VANDEPLAS, G., VAN ZELE, T., CARDELL, L. O., AREBRO, J., OLZE, H., FORSTER-RUHRMANN, U., KOWALSKI, M. L., OLSZEWSKA-ZIABER, A., HOLTAPPELS, G., DE RUYCK, N., WANG, X., VAN DRUNEN, C., MULLOL, J., HELLINGS, P., HOX, V., TOSKALA, E., SCADDING, G., LUND, V., ZHANG, L., FOKKENS, W. & BACHERT, C. 2016. Inflammatory endotypes of chronic rhinosinusitis based on cluster analysis of biomarkers. *J Allergy Clin Immunol,* 137**,** 1449-1456 e4.

TREMBLAY GM, J. M., GAULDIE J, SARNSTRAND B. 1995. *Fibroblasts as effector cells in fibrosis.,* New York, Marcel Dekker.

VAN BRUAENE, N., C, P. N., VAN CROMBRUGGEN, K., DE RUYCK, N., HOLTAPPELS, G., VAN CAUWENBERGE, P., GEVAERT, P. & BACHERT, C. 2012. Inflammation and remodelling patterns in early stage chronic rhinosinusitis. *Clin Exp Allergy,* 42**,** 883-90.

VAN BRUAENE, N., DERYCKE, L., PEREZ-NOVO, C. A., GEVAERT, P., HOLTAPPELS, G., DE RUYCK, N., CUVELIER, C., VAN CAUWENBERGE, P. & BACHERT, C. 2009. TGF-beta signaling and collagen deposition in chronic rhinosinusitis. *J Allergy Clin Immunol,* 124**,** 253-9, 259 e1-2.

VAN BUUL, J. D., KANTERS, E. & HORDIJK, P. L. 2007. Endothelial signaling by Ig-like cell adhesion molecules. *Arterioscler Thromb Vasc Biol,* 27**,** 1870-6.

VAN CROMBRUGGEN, K., HOLTAPPELS, G., DE RUYCK, N., DERYCKE, L., TOMASSEN, P. & BACHERT, C. 2012. RAGE processing in chronic airway conditions: involvement of Staphylococcus aureus and ECP. *J Allergy Clin Immunol,* 129**,** 1515-21 e8.

VAN CROMBRUGGEN, K., JACOB, F., ZHANG, N. & BACHERT, C. 2013. Damage-associated molecular patterns and their receptors in upper airway pathologies. *Cell Mol Life Sci,* 70**,** 4307-21.

VAN CROMBRUGGEN, K., ZHANG, N., GEVAERT, P., TOMASSEN, P. & BACHERT, C. 2011. Pathogenesis of chronic rhinosinusitis: inflammation. *J Allergy Clin Immunol,* 128**,** 728-32.

VAN DRUNEN, C. M., MJOSBERG, J. M., SEGBOER, C. L., CORNET, M. E. & FOKKENS, W. J. 2012. Role of innate immunity in the pathogenesis of chronic rhinosinusitis: progress and new avenues. *Curr Allergy Asthma Rep,* 12**,** 120-6.

VAN DRUNEN, C. M., VROLING, A. B., RINIA, A. B. & FOKKENS, W. J. 2008. Considerations on the application of microarray analysis in rhinology. *Rhinology,* 46**,** 259-66.

VAN ROON, J., WIJNGAARDEN, S., LAFEBER, F. P., DAMEN, C., VAN DE WINKEL, J. & BIJLSMA, J. W. 2003. Interleukin 10 treatment of patients with rheumatoid arthritis enhances Fc gamma receptor expression on monocytes and responsiveness to immune complex stimulation. *J Rheumatol,* 30**,** 648-51.

VANDERMEER, J., SHA, Q., LANE, A. P. & SCHLEIMER, R. P. 2004. Innate immunity of the sinonasal cavity: expression of messenger RNA for complement cascade components and toll-like receptors. *Arch Otolaryngol Head Neck Surg,* 130**,** 1374-80.

VENUGOPAL, R. & JAISWAL, A. K. 1998. Nrf2 and Nrf1 in association with Jun proteins regulate antioxidant response element-mediated expression and coordinated induction of genes encoding detoxifying enzymes. *Oncogene,* 17**,** 3145-56.

VESTWEBER, D. 2015. How leukocytes cross the vascular endothelium. *Nat Rev Immunol,* 15**,** 692-704.

VIDELER, W. J., GEORGALAS, C., MENGER, D. J., FRELING, N. J., VAN DRUNEN, C. M. & FOKKENS, W. J. 2011. Osteitic bone in recalcitrant chronic rhinosinusitis. *Rhinology,* 49**,** 139-47.

WANG, J., DUNCAN, D., SHI, Z. & ZHANG, B. 2013. WEB-based GEne SeT AnaLysis Toolkit (WebGestalt): update 2013. *Nucleic Acids Res,* 41**,** W77-83.

WANG, M., WANG, X., ZHANG, N., WANG, H., LI, Y., FAN, E., ZHANG, L., ZHANG, L. & BACHERT, C. 2015. Association of periostin expression with eosinophilic inflammation in nasal polyps. *J Allergy Clin Immunol,* 136**,** 1700-3 e1-9.

WENG, L., DAI, H., ZHAN, Y., HE, Y., STEPANIANTS, S. B. & BASSETT, D. E. 2006. Rosetta error model for gene expression analysis. *Bioinformatics,* 22**,** 1111-21.

WENGST, A. & REICHL, S. 2010. RPMI 2650 epithelial model and three-dimensional reconstructed human nasal mucosa as in vitro models for nasal permeation studies. *Eur J Pharm Biopharm,* 74**,** 290-7.

WERNER, T. 2008. Bioinformatics applications for pathway analysis of microarray data. *Curr Opin Biotechnol,* 19**,** 50-4.

WILLENBROCK, K., KUPPERS, R., RENNE, C., BRUNE, V., ECKERLE, S., WEIDMANN, E., BRAUNINGER, A. & HANSMANN, M. L. 2006. Common features and differences in the transcriptome of large cell anaplastic lymphoma and classical Hodgkin's lymphoma. *Haematologica,* 91**,** 596-604.

WILSON, M. T. & HAMILOS, D. L. 2014. The nasal and sinus microbiome in health and disease. *Curr Allergy Asthma Rep,* 14**,** 485.

WITSCHI, H., MALKINSON, A. M. & THOMPSON, J. A. 1989. Metabolism and pulmonary toxicity of butylated hydroxytoluene (BHT). *Pharmacol Ther,* 42**,** 89-113.

WOLPE, S. D., DAVATELIS, G., SHERRY, B., BEUTLER, B., HESSE, D. G., NGUYEN, H. T., MOLDAWER, L. L., NATHAN, C. F., LOWRY, S. F. & CERAMI, A. 1988. Macrophages secrete a novel heparin-binding protein with inflammatory and neutrophil chemokinetic properties. *J Exp Med,* 167**,** 570-81.

WOOD, A. J., ANTOSZEWSKA, H., FRASER, J. & DOUGLAS, R. G. 2011. Is chronic rhinosinusitis caused by persistent respiratory virus infection? *Int Forum Allergy Rhinol,* 1**,** 95-100.

XAUBET, A., MULLOL, J., ROCA-FERRER, J., PUJOLS, L., FUENTES, M., PEREZ, M., FABRA, J. M. & PICADO, C. 2001. Effect of budesonide and nedocromil sodium on IL-6 and IL-8 release from human nasal mucosa and polyp epithelial cells. *Respir Med,* 95**,** 408-14.

XIA, J., GILL, E. E. & HANCOCK, R. E. 2015. NetworkAnalyst for statistical, visual and network-based meta-analysis of gene expression data. *Nat Protoc,* 10**,** 823-44.

YAMADA, T., LIZHONG, S., TAKAHASHI, N., KUBO, S., NARITA, N., SUZUKI, D., TAKABAYASHI, T., KIMURA, Y. & FUJIEDA, S. 2010. Poly(I:C) induces BLyS-expression of airway fibroblasts through phosphatidylinositol 3-kinase. *Cytokine,* 50**,** 163-9.

YOSHIMURA, T., MATSUSHIMA, K., TANAKA, S., ROBINSON, E. A., APPELLA, E., OPPENHEIM, J. J. & LEONARD, E. J. 1987. Purification of a human monocyte-derived neutrophil chemotactic factor that has peptide sequence similarity to other host defense cytokines. *Proc Natl Acad Sci U S A,* 84**,** 9233-7.

ZHANG, B., KIROV, S. & SNODDY, J. 2005. WebGestalt: an integrated system for exploring gene sets in various biological contexts. *Nucleic Acids Res,* 33**,** W741-8.

ZHANG, Q., WANG, C. S., HAN, D. M., SY, C., HUANG, Q., SUN, Y., FAN, E. Z., LI, Y. & ZHOU, B. 2013. Differential expression of Toll-like receptor pathway genes in chronic rhinosinusitis with or without nasal polyps. *Acta Otolaryngol,* 133**,** 165-73.

ZIPFEL, P. F., BALKE, J., IRVING, S. G., KELLY, K. & SIEBENLIST, U. 1989. Mitogenic activation of human T cells induces two closely related genes which share structural similarities with a new family of secreted factors. *J Immunol,* 142**,** 1582-90.

ZLOTNIK, A. & YOSHIE, O. 2000. Chemokines: a new classification system and their role in immunity. *Immunity,* 12**,** 121-7.